Trinity College Dublin
Coláiste na Tríonóide, Baile Átha Cliath
The University of Dublin

Ph.D. Surgery

September 2025

Investigating the therapeutic utility of targeting the chemokine fractalkine and the suitability of Natural Killer cell therapy in Oesophageal Adenocarcinoma

Caroline Dalal Marie Marion

Submitted to Trinity College Dublin for the degree of Doctor of Philosophy

Primary Supervisor: Dr. Melissa Conroy

Secondary Supervisor: Prof. Joanne Lysaght

Declaration

I declare that this thesis has not been submitted as an exercise for a degree at this or any other university and it is entirely my own work.

I agree to deposit this thesis in the University's open access institutional repository or allow the Library to do so on my behalf, subject to Irish Copyright Legislation and Trinity College Library conditions of use and acknowledgement.

I consent to the examiner retaining a copy of the thesis beyond the examining period, should they so wish (EU GDPR May 2018).

Abstract

Oesophageal adenocarcinoma (OAC) arises in a background of chronic inflammation and is characterised by an aggressive phenotype and poor prognosis, with a five-year survival rate of less than 25%. Current response rates to chemotherapy and/or radiotherapy are only ~30% and most patients present with advanced-stage disease, underscoring the urgent need for a deeper understanding of mechanisms driving tumour progression and the identification of novel therapeutic strategies.

Immunotherapy efficacy rates for OAC have also been disappointing so far, standing below 25%. It is well established that the immune infiltrate in solid tumours can be a strong prognostic factor in cancer patients and higher intratumoural frequencies of $CD8^+$ T cells and natural killer (NK) cells are often associated with improved survival and better response to immunotherapy. Our group have shown that OAC patients with higher visceral obesity have the lowest numbers of intratumoural NK cells, contributing to 'immune-excluded' tumours in this poor prognosis malignancy. We have previously shown that the pro-inflammatory chemokine fractalkine plays a role in the disruption of anti-tumour immunity in OAC via the erroneous recruitment of NK and $CD8^+$ T cells to the visceral adipose tissue (VAT), at the expense of effective tumour infiltration. Furthermore, we have reported that modulation of the fractalkine receptor CX3CR1 with the modulator E6130 can prevent NK cell migration towards the soluble chemotactic cues of the VAT and redirect them towards the tumour. Thus, we propose that E6130 holds potential alone and in combination with other immunotherapies to re-invigorate their infiltration and killing of OAC tumours. Other groups have reported the direct pro-tumourigenic effects of fractalkine in cancers of the stomach, lung, pancreatic and prostate and have demonstrated that targeting CX3CR1 can attenuate these effects. Therefore, this study aims to elucidate 1) the direct biological effects of fractalkine on OAC tumour progression and 2) the additional anti-tumour utility of E6130 in OAC, beyond NK cell migration. We propose that fractalkine may directly promote OAC tumour survival, progression and metastasis and that E6130, a CX3CR1 modulator, can attenuate such effects. Finally, this study evaluated the potential utility of KHYG-1 cell therapy in OAC, investigating whether they were susceptible to the chemotactic cues of the VAT and if this could be overcome using E6130.

Our data demonstrate that fractalkine significantly increases OAC cell line survival, proliferation and migration and that E6130 can reverse these pro-tumourigenic effects. In addition, the data presented here demonstrate the utility of E6130 in treatment-resistant OAC tumour cell lines. The tumouricidal activity of E6130 was validated in *ex vivo* OAC patient tumour samples further highlighting the anti-cancer therapeutic potential of this drug in OAC. Moreover, our data uncovered associations between CX3CR1 expression in OAC tumour cells and stemness and metastatic potential suggesting that CX3CR1 expression confers a survival advantage and might hold prognostic utility. Our findings also show that E6130 elicits no detrimental effects on NK cell phenotype and function, further strengthening its therapeutic potential. Finally, this study revealed that while KHYG-1 cell therapy are from distinct blood-derived NK cells in phenotype, they exhibit similar preferential migration towards the VAT and this cannot be reduced using E6130. Interestingly, KHYG-1 migration towards OAC tumour can be enhanced by remodelling the TME with the chemokine IP-10.

In conclusion, this study uncovers the pro-tumourigenic role of fractalkine and additional therapeutic potential of E6130 in OAC. Moreover, if E6130 was selected as a combination strategy with NK cell therapy, our data suggest that blood-derived NK cells would be more amenable to its effects than KHYG-1 cell therapy. Ultimately, this project uncovers novel data on the therapeutic utility of E6130 in OAC, which holds promise to promote tumour eradication via its reversal of fractalkine's direct and indirect pro-tumourigenic effects.

Acknowledgments

A PhD is an incredible but challenging experience, and I was so fortunate to be supported and helped by many people throughout.

I must firstly thank my truly amazing supervisor, Dr. Melissa Conroy. I'll never forget my first job interview I had with you Melissa, which was also the first time I met you, and I remember my mum saying to me "It sounded like you really got along with her, she seems so nice!" and little did I know 6 months later I would be starting this 3-year journey with you. I still question to this day how you picked me for this project, I didn't have a lot of experience, and I wasn't even sure I wanted to do a PhD, but I'm so glad I did. I'm so thankful for the unlimited amount of support, time, and advice you give to your students. You always reassure me, and even though I always left your office with more work than when I entered, I also always left feeling instantly better, with a smile on my face and boosted confidence. Thank you for trusting me with this project which I know is so important to you, for letting me become an independent scientist but also always helping me when I needed it, and for believing in my abilities. I'm delighted I get to continue to work with you on a new project!

I also would like to thank my co-supervisor, Prof. Joanne Lysaght. Thank you so much for integrating me in your group in TTMI, it was always a bit strange to not have my main supervisor in the same building, but you were always there when I needed help and support every week at your meetings. I'm extremely grateful for all your feedback on my work, presentations and posters, and you always gave a more "external" point of view which was so helpful and Melissa is right when she says "Joanne is always right!".

Thank you to all the clinical staff at St James Hospital for procuring samples throughout this project and importantly, thank you to all the patients who so generously donated their samples for our research, even though they are going through the most difficult time of their lives, this project would be impossible without them. Thank you to the PIs in the Department of Surgery, Prof. Stephen Maher, Dr Niamh Lynam-Lennon, and Prof. Jacintha O' Sullivan for all your advice and feedback at lab meetings, which has helped this project to expand and flourish.

I want to thank everyone at Breakthrough Cancer Research, in particular Orla Dolan, Eoghan O'Sullivan, and Frances Drummond for their support on this project. I truly enjoyed participating to all the events, getting to know patient representatives and sponsors and I was so honoured be an ambassador for Breakthrough Cancer Research over the last 3 years.

Thank you for to all the PhD students, research assistants, biobank managers, MD students, and postdocs I have encountered and worked with over the last 3 years. Thank you to Simone Marcone, Andrew Sheppard, Jason McGrath, Fiona Crotty, Neil Kearney, Cillian O'Donovan, Nick Schellenberg, Cian Gargan, Sarah Crean, Yashna Chabria, Adele Connor, Omar Hadidi, Oana Deac, James Phelan, Laoighse Geoghegan, Raquel Santamaria, and Marina Zaki. Thank you to Brendan Moran, Nicola Raftery, Jenny Cox, Georgia Richard and Ellen Walsh for taking bloods for me, we don't know what we do without you!

A special thank you to the wonderful postdocs Aisling Heeran, Aoife Kilgallon and Aisling Ui Mhaonaigh who were always there when I needed help and advice, especially Aoife Killgallon, I would have been lost without your expert knowledge on flow cytometry! Thank you to Maria Davern who would always reply to all my questions with such patience. Thank you to Aisling Heeran and Rebecca O'Brien for all your help and friendship during your time in the department and after, I'm so grateful to have you both as my friends.

A huge thanks to Eimear Mylod for your endless help and training, the first year of my PhD would have been a lot harder if it wasn't for you! You were always so nice and patient with me, and I'm so grateful that you shared your expertise with me. Thank you to Laura Kane and Fiona O'Connell for welcoming me to the department and always helping me out, for making Saturdays in the lab less sad! Thank you to the Biobank Managers Christine Butler, Niamh O'Connor and especially Meghana Menon, this project would not be possible without you and I am so grateful for your patience and all the late evenings you had to wait for samples.

There are so many people in TTMI that I would like to thank, but I will specifically mention the lunch crew (past, present and to all the new ones since I've submitted) Matt McElheron, Arlena Carney, Tara Murphy, Jordan O'Keefe, Jack Mitchell, Jordy Smith, Julie David, Isabella Batten, Daniel Hang Chu, Taylor Smith, Eabha O'Sullivan and many more, you made my days so much better and I'm so grateful I got to know you all. Thank you to Martin Barr for all the chats, always made my day better! Thank you to Prof Derek Doherty for sharing his love of science with me when I was an undergraduate student, I wouldn't be here without you.

Then of course I have to thank the basement crew, Christina Cahill, Rebecca Lyons, David Hackett, Lorraine Smith, Maitiú Ó Murchú, Kirstan Murphy, Xuehua Lin, Samuel Cahill, Volga Saini and Joyce Barry. Thank you for the coffee breaks, all the laughter, for the movie nights, the drinks at the pub, and for your constant help, friendship and support. I really couldn't have done it without such a supportive group of friends. I think we all went a bit insane in that basement but I have so many great memories in there. A special thanks to Lorraine Smith who I'm so glad I got to know you better these last 3 years, to Joyce Barry who I could share all my problems and troubles with, to Rebecca Lyons for being the sweetest friend, and to Christina Cahill for your endless help and support.

Thank you to me previous flatmate and close friend Maddie Comtois for all your support and always asking me "how are your cells today?". Thank you to my current flatmate Liz Dunne Sheil for looking out for me, for being my constant support these last months, and for listening to my daily complaints. Thank you to all my friends Maire Fergusson, Julia Piaskowy, Sophia Leonard, Paula Klavina, Libby Nelson, Nathan Simoncini, Eabha O'Sullivan, Roisin Fox, Cian Horneck, Morgan Hurley O'Dwyer, Nicolas Johnston, Alfie Cavaliero, and Sean Clarke who helped me enjoy life outside of work and who have been so supportive. Thank you to all my high school friends for constantly encouraging me in this journey, especially Nora Aubry, Edith Roger, Marion Botte and Anne-Claude Baran. Thank you Eamonn Daly for your constant support and for always believing in me more than I would believe in myself.

Thank you to my mum Zeina, for encouraging me every single day of my life. You are the reason I was able to do a PhD, and you have always been my constant support. Thank

you to Alain, you have always believed in me and you have always been the most supportive step-dad I could ask for. Thank you Yasmine for your encouragements and for always being there for me. I am so grateful to have such a supportive family. I lastly want to thank my grandparents, my Teita and Jiddo, who have always taught me the importance of education, and how lucky we are to be able to pursue the careers that we want. I'm truly grateful for the opportunity and the privilege of being able to do a PhD.

Publications – Accepted

Authored

- Real-time *ex vivo* monitoring of NK cell migration toward obesity-associated oesophageal adenocarcinoma following modulation of CX3CR1. Authors: Eimear Mylod, Fiona O'Connell, Noel E. Donlon, Maria Davern, **Caroline Marion**, Christine Butler, John V. Reynolds, Joanne Lysaght, Melissa J. Conroy. *Scientific Reports, 2024*.
- Investigating the Effects of Olaparib on the Susceptibility of Glioblastoma Multiforme Tumour Cells to Natural Killer Cell-Mediated Responses. Authors: Jennifer Moran, Eimear Mylod, Laura E. Kane, **Caroline Marion**, Emily Keenan, Marianna Mekhaeil, Joanne Lysaght, Kumlesh K. Dev, Jacintha O'Sullivan, Melissa J. Conroy. *Pharmaceutics, 2023*.

Publications – Under Revision/Preparation

First author

- Enhancement of IP-10 signaling augments KHYG-1 cell therapy homing towards the tumor microenvironment in obesity-associated cancer. **Caroline Marion**, Joyce C. Barry, Eimear Mylod, Lorraine Smith, Meghana Menon, Niamh O'Connor, Christine Butler, Oana M. Deac, Claire L. Donohoe, Jessie A. Elliot, Maeve Lowery, John V. Reynolds, Joanne Lysaght, Melissa J. Conroy. Submitted to *the Journal of Leukocyte Biology*.
- Fractalkine: a pro-inflammatory chemokine with protumourigenic effects in oesophageal adenocarcinoma that can be attenuated by CX3CR1 modulation. **Caroline Marion**, Lorraine Smith, Meghana Menon, Niamh O'Connor, Becky A. S. Bibby, Niamh Lynam-Lennon, Stephen G. Maher, John V. Reynolds, Joanne Lysaght, Melissa J. Conroy.

Authored

- Chemokine receptor antagonism as a potential therapy to attenuate metastasis in oesophageal adenocarcinoma. Maria Davern, Katelynn Cahill, Noel E. Donlon, Eimear Mylod, Fiona O' Connell, **Caroline Marion**, Anshul Bhardwaj, Andrew D.

Sheppard, Mohammad Habash, Jasmine Yun-Tong Kung, Ashanty M. Melo, Meghana Menon, Dara Bracken-Clarke, Christine Butler, Klaudia Majcher, Narayanasamy Ravi, Claire L. Donohoe, John V. Reynolds, Melissa J. Conroy, Joanne Lysaght.

Oral presentations

- **Trinity St James Cancer Institute research day**, Dublin, 2024. Title: Fractalkine: a chemokine with pro-tumourigenic effects in oesophageal adenocarcinoma that can be attenuated by CX3CR1 modulation with E6130
- **Trinity Translational Medicine Institute research day**, Dublin, 2024. Title: Fractalkine: a key player in NK cell dysfunction and tumour growth in oesophageal cancer
- **School of Medicine Research Blitz**, Dublin 2024. Title: Fractalkine: a key player in NK cell dysfunction and tumour growth in oesophageal cancer
- **Trinity St James Cancer Institute research blitz**, Dublin, 2023. Title: Fractalkine: a key player in NK cell dysfunction and tumour growth in oesophageal cancer
- **Trinity Translational Medicine Institute research day**, Dublin, 2023. Title: Fractalkine: a key player in NK cell dysfunction and tumour growth in oesophageal cancer
- **School of Medicine Research Blitz**, Dublin 2023. Title: Fractalkine: a key player in NK cell dysfunction and tumour growth in oesophageal cancer
- **Ma thèse en 180 secondes**, Dublin, 2023. Presentation of my thesis in 180 secondes in French at Dublin City University

Poster presentations:

- **European Conference of Immunology**, Dublin, 2024. Poster 1: Fractalkine: a chemokine with protumourigenic effects in oesophageal adenocarcinoma that can be attenuated by CX3CR1 modulation with E6130. Poster 2: Investigating the applicability of KHYG-1 cell therapy for obesity-associated cancer
- **Chemotactic cytokines, Gordon Research Conference**, Portland, Maine, 2024. Title: Modulation of the chemokine receptor CX3CR1 with E6130 ameliorates the pro- tumourigenic effects of fractalkine in oesophageal adenocarcinoma

- **EACR-AACR-IACR, Basic and Translational Research Conference**, Dublin 2024. Title: CX3CR1 modulation can attenuate fractalkine-induced pro-tumourigenic effects in oesophageal adenocarcinoma
- **Annual Congress of the European Association for Cancer Research**, Torino, 2023. Title: CX3CR1 antagonism holds therapeutic utility to reverse the pro-tumourigenic effects of fractalkine in oesophageal adenocarcinoma
- **Irish Association for Cancer Research**, Athlone, 2023. Title: Investigating the anti-proliferative and anti-metastatic potential of CX3CR1 antagonism in oesophageal adenocarcinoma
- **Trinity Translational Medicine Institute cancer conference,** Dublin 2022. Title: Investigating the role of fractalkine in oesophageal adenocarcinoma tumour growth and epithelial mesenchymal transition.
- **Irish Society of Immunology Annual Meeting**, Maynooth, 2022. Title: Elucidating the pro-tumourigenic effects of fractalkine in oesophageal adenocarcinoma

Awards:

- Immunotools Special Award (2024)
- Why Research Matters 2023, Union of Students in Ireland and Irish Research Council (2023). Poster to illustrate to a lay audience why your research matters, 2nd prize.

Table of contents

List of Figures

Chapter 1

Chapter 2

Chapter 3

Chapter 4

Chapter 6:

List of Tables:

Chapter 1:

Chapter 2:

Chapter 5:

Abbreviations

ACM	Adipose Tissue Conditioned Media
ADAM	ADAM metallopeptidase domain
ANOVA	Analysis Of Variance
BCA	Bicinchoninic acid assay
BMI	Body Mass Index
BO	Barrett's Oesophagus
BSA	Bovine Serum Albumin
CAF	Cancer-associated fibroblast
CAR	Chimeric Antigen Receptor
CCK-8	Cell Counting Kit-8
CCL	Chemokine (C-C motif) Ligand
cDMEM	Complete Dulbecco's Modified Eagle Medium
CROSS	Chemoradiotherapy for Oesophageal Cancer followed by Surgery Study
cRPMI	Complete Roswell Parks Memorial Institute
DNA	Deoxyribonucleic acid
DMSO	Dimethyl sulfoxide
E6130	[(3S,4R)-1-[2-Chloro-6-(trifluoromethyl)benzyl]-3-4-methylpyrrolidin-3-yl]acetic acid (2S)-hydroxy(phenyl)acetate
ECM	Extracellular Matrix
ELISA	Enzyme-Linked Immunosorbent Assay
EMT	Epithelial to Mesenchymal Transition
FACS	Fluorescent Activated Cell Sorting
FBS	Foetal Bovine Serum
FLOT	Chemotherapy regimen which includes 5-FU, leucovorin, oxaliplatin and docetaxel
FMI	Forward Migration Index
GAC	Gastric adenocarcinoma
GORD	Gastro-Oesophageal Reflux Disease
GPCR	G-Protein Coupled Receptor

HBSS	Hanks' Balanced Salt Solution
HIF	Hypoxia Inducible Factor
IBD	Inflammatory Bowel Disease
IL	Interleukin
IFN	Interferon
JAK/STAT	Janus Kinase/Signal Transducers and Activators of Transcription
LCM	Liver Conditioned Media
LDH	Lactate Dehydrogenase assay
LNCM	Lymph Node Conditioned Media
MAPK	Mitogen Activate Protein Kinase
MDSC	Myeloid Derived Suppressor Cells
MHC	Major Histocompatibility Complex
MMP	Matrix Metalloproteinase
NK-$_k$B	Nuclear Factor-kappa B
NGCM	Normal Gastric Conditioned Media
NK cell	Natural Killer Cell
NKG2A	Natural Killer Group 2a
NKG2D	Natural Killer Group 2d
NOCM	Normal Oesophageal Conditioned Media
OAC	Oesophageal Adenocarcinoma
OC	Oesophageal Cancer
OSCC	Oesophageal Squamous Cell Carcinoma
PBMC	Peripheral Blood Mononuclear Cell
PBS	Phosphate Buffer Saline
PD-1	Programmed Cell Death Protein-1
PI3K	Phosphoinositide 3-Kinase
RA	Rheumatoid Arthritis
RFU	Relative Fluorescence Unit
RLU	Relative Luminescence Unit
SD	Standard Deviation

SOC	Standard of Care
TAM	Tumour-Associated Macrophages
TCM	Tumour Conditioned Media
TGF-β	Tumour Growth Factor β
Th cell	T helper cell
TIGIT	T Cell Immunoreceptor with Ig and ITIM Domains
TLR	Toll Like Receptor
TNF-α	Tumour necrosis factor α
TME	Tumour Microenvironment
TRAIL	TNF-Related Apoptosis-Inducing Ligand
Treg cell	T regulatory cell
TRG	Tumour Regression Grade
VAT	Visceral Adipose Tissue
VFA	Visceral Fat Area
5-FU	5-Fluorouracil

Chapter 1- Introduction

1.1 Oesophageal Adenocarcinoma

1.1.1 Clinical challenges

Oesophageal Adenocarcinoma (OAC) is a subtype of oesophageal cancer (OC) that develops in the lower region of the oesophagus and is characterised by differentiation of squamous epithelium into columnar glandular cells [1, 2]. In Ireland, there are more than 500 cases of OC every year, which is one of the highest rates in Europe [3, 4]. Globally, OC accounts for ~544,000 deaths, placing it as the 6th most common cause of cancer related death [3-8]. Patients often exhibit advanced disease at the time of diagnosis, with symptoms such as dysphagia, weight loss, and chest pain [4, 9, 10]. Unfortunately, OAC remains a poor prognosis cancer with a 5-year survival rate of less than 25%, which is largely due to late-stage diagnosis and response rates to current standard-of-care therapies of only ~30%, which comprises surgery, chemotherapy, and radiotherapy [7, 10, 11]. For OAC patients with progressive metastatic disease, survival rates fall to less than 6% [5, 7]. OAC's high rates of recurrence and resistance to conventional treatments underscore the need for improved strategies in early detection, risk stratification, management and new therapies.

1.1.2 Risk factors

OAC is regarded as an inflammation-driven cancer with identifiable risk factors for this malignancy including smoking, alcohol consumption, obesity, gastro-oesophageal reflux disease (GORD) and Barrett's oesophagus (BO) [9].

1.1.2.1 GORD and Barrett's oesophagus

GORD is a chronic condition in which stomach acid and digestive enzymes flow back into the oesophagus, causing irritation and inflammation [12-15]. This occurs due to dysfunction of the lower oesophageal sphincter, a muscular valve that normally prevents reflux [14, 15]. Symptoms may include heartburn, acid regurgitation, dysphagia, chronic cough, sore throat and chest pain [14-16]. The risk of GORD consequently increases with increasing obesity rates worldwide, as obesity induces elevated abdominal pressure, forces caustic stomach and bile acids into the distal portion of the oesophagus [12-17]. Chronic GORD creates conditions that promote BO, a precursor to OAC and BO is involved in the replacement of squamous epithelium with metaplastic columnar

epithelium due to prolonged acid and bile reflux [18-22]. Its prevalence in Ireland is rising alongside GORD and obesity [13, 23, 24]. Patients undergo endoscopic surveillance to track progression from non-dysplastic BO to invasive adenocarcinoma, though transformation rates vary [19, 21, 22]. Management includes risk stratification based on endoscopic and histopathological findings, with treatment ranging from surveillance for low-risk cases to endoscopic resection and ablation for high-risk lesions [19, 24, 25]. Obesity is another important risk factor for BO, and individuals with obesity, particularly visceral obesity, are twice as likely to develop BO [21, 24].

1.1.2.2 Obesity

Obesity is a burgeoning global health problem whose prevalence has tripled worldwide since 1975 [26]. It is estimated that 1 billion people are obese worldwide and at risk of obesity-associated disease [26]. Over the past decade, the worldwide prevalence of overweight or obesity has increased and now affects more than 25% of adults and 45% of children [27]. Obesity is a state of chronic low-grade inflammation with associated pathologies including diabetes, liver disease, cardiovascular disease, and cancer [26, 28]. Of all cancers, OAC has one of the highest associations with obesity [29, 30]. Men typically exhibit greater visceral obesity, a key risk factor for OAC, which may explain its higher prevalence in men compared to women, with reported ratios ranging from 3:1 to 9:1 [21, 31, 32].

Visceral adipose tissue (VAT), which is the intra-abdominal fat, is found to be one of the main initiators of chronic and systemic inflammation in obesity [31]. This persistent low-grade inflammation contributes to oxidative stress, DNA damage, and a body-wide immune dysfunction conducive to malignant transformation [33]. Increased intra-abdominal pressure due to excessive VAT promotes GORD and exacerbates reflux, leading to chronic acid and bile exposure that induces metaplastic and dysplastic changes in the oesophageal epithelium [17, 34, 35]. Additionally, obesity-induced immune dysfunction compromises tumour surveillance, as alterations in the tumour microenvironment (TME), including increased myeloid-derived suppressor cells (MDSCs) and regulatory T cells, suppress anti-tumour immune responses, thus facilitating neoplastic growth [36]. Our group has reported that the obese condition in OAC patients contributes to tumour cell proliferation, migration, and metastatic phenotype [37, 38].

Furthermore, our group has shown that the largest depot of VAT in humans known as the omentum is the source of many soluble mediators in this dysregulation, with T cells and Natural Killer (NK) cells being recruited to this tissue compartment, where they undergo phenotypical and functional alterations, that likely contribute to local and systemic inflammation while undermining effective anti-tumour immunity [33, 39-41]. Considering these findings, identifying and targeting key drivers of obesity-associated inflammation, immune dysfunction, and tumourigenesis in OAC is a desirable therapeutic concept.

1.1.3 Current therapies

Current standard-of-care (SOC) treatment for locally advanced stages (defined as stage II and stage III) of OAC is surgical resection and neo-adjuvant chemotherapy or chemoradiotherapy with common regimens consisting of the CROSS (Chemoradiotherapy for Oesophageal Cancer followed by Surgery Study) and FLOT regimens in the clinical setting in Ireland [42-44].CROSS chemoradiotherapy regimen is administered neoadjuvantly and includes paclitaxel and carboplatin in combination with radiation while FLOT chemotherapy regimen includes 5-FU, leucovorin, oxaliplatin and docetaxel and is given peri-operatively [42, 43, 45]. Recent clinical trials such as the ESOPEC (NCT02509286) or TOPGEAR (NCT01924819) trials have demonstrated statistically significant overall benefit of pre-operative chemotherapy compared to pre-operative chemo-radiotherapy, and although both pre-operative strategies remain standard in European and American countries, the FLOT regimen has mainly been recommended in Ireland for the treatment of OAC [44, 46, 47]. Currently, two immune checkpoint inhibitors (ICI), nivolumab and pembrolizumab, are approved as a first-line therapy for patients with advanced metastatic disease, who are not eligible for SOC treatment, and in the second- and third-line treatments for OAC patients who do not respond to first-line therapies [5, 42, 48-51]. Combined positive score or CPS is used to identify patients who are most likely to benefit from ICIs [52, 53]. However, current efficacy rates for these ICIs stand at less than 25% for OAC and further studies are needed to ascertain how their efficacy can be improved and how to optimise their sequenced timing with SOC [54]. Most trials assessing the efficacy of ICIs have concluded that cancer patients require an inflamed TME to benefit from this therapy, further suggesting that

immune landscape of the TME must be characterised to maximise the efficacy of immunotherapies in OAC patients. In 2024, after successful results from the SPOTLIGHT (NCT03504397) and GLOW (NCT03653507) trials, the European Medicines Agency (EMA) has recommended and approved zolbetuximab, a monoclonal antibody targeting Claudin-18.2 tight junction molecule, for the treatment of Claudin 18.2 positive, HER2 negative and locally advanced or metastatic gastric or gastro-oesophageal junction adenocarcinoma, in combination with chemotherapy [55-57].

1.2 Immune responses in OAC

1.2.1 Immune dysfunction in OAC

OAC is characterised by many features of immune dysfunction, which facilitates tumour progression. Locally, the sequence from BO to OAC is underpinned by several significant shifts in oesophageal immune infiltrates. In BO, a T helper (Th)2-type immune response predominates, marked by elevated interleukin (IL)-4 producing and IL-10 levels. However, during OAC progression, this shifts toward a more pro-inflammatory Th1-type response, with increased interferon-γ (IFN-γ), IL-2, IL-1β, and IL-8 expression [58, 59]. Our group has further validated this transition, showing that BO tissue exhibits higher $CD4^+$ T cell expression of IL-4 and increased IL-6 levels, whereas OAC tissue presents both pro-inflammatory (IL-1β, tumour necrosis factor α (TNF-α), IL-2) and anti-inflammatory (IL-6, IL-10) cytokine profiles [60].

NK cells, crucial for early tumour immunity, induce cytotoxicity via perforin/granzyme release, death ligands (Fas-L, TRAIL), and IFN-γ and TNF-α production [61]. Additionally, IL-17 secreted by $CD4^+Foxp3^-$ Th17 cells enhances NK cell recruitment by stimulating OC cells to produce chemokines CXCL9 and CXCL10. IL-17 also promotes NK cell activation by increasing TNF-α, IFN-γ, granzyme B, perforin production, and the expression of activating receptors, including NKp46, NKp44, and NKG2D [62, 63]. However, upon tumour infiltration, NK cells often lose effector function, adopt a tissue-resident phenotype, and experience mitochondrial dysfunction, leading to metabolic impairment [64, 65]. In OC, NK cell infiltration in the TME correlates with improved overall survival and postoperative prognosis [62, 66]. NK cells contribute to anti-tumour immunity by recognizing and killing tumour cells via the NKp30/B7-H6 pathway [66, 67]. However, our

group demonstrated that NK cells in the OAC TME exhibit significantly lower expression of activation markers NKp30, NKp46, and NKG2D compared to circulating NK cells. However, intratumoural NK cells show higher expression of death receptor ligands TRAIL and FasL, suggesting that upon infiltration into the TME, their death receptors are activated—potentially by IFN-γ, IL-2, and IL-15—enhancing their cytotoxic activity [60, 68, 69]. Furthermore, our group has previously demonstrated that the cisplatin-resistant OAC cell line OE33CisR, developed by our department [70], exhibits lower expression of activating NKR ligands (B7-H6, MICA/B, ULBP-3) compared to its parental counterpart, OE33CisP. Additionally, NK cells cultured in OE33CisR supernatants showed decreased frequencies of $NKp30^+$ and $NKp46^+$ NK cells, a trend also observed in poor treatment responders among OAC patients, suggesting that treatment resistance is marked by reduced NK cell activation in the TME [71]. Notably, FLOT chemotherapy induces B7-H6 shedding in OAC tumour cells which is paralleled by reduced $NKp30^+$ NK cell frequencies in patient tumour samples [71]. These findings highlight the direct impact of first-line OAC treatment on NK cell phenotype and function along with the features of chemo-resistant tumours that might present challenges for NK cell therapies.

T cells play a key role in initiating OAC-associated inflammation, as demonstrated in a reflux-induced rat model where T cells were the first immune cells to infiltrate the submucosal layer; however, their functions become impaired in OAC [72]. Similarly, cytotoxic T lymphocytes (CTLs) play an important role in anti-tumour functions as they recognise tumour antigens via MHC class I proteins presented by antigen-presenting cells (APCs), including dendritic cells (DCs). Once activated, CTLs upregulate inhibitory receptors such as CTLA-4 and PD-1 to prevent excessive cytotoxicity [73]. DCs play a pivotal role in priming cytotoxic responses by activating NK cells, $CD8^+$ T cells, and Th1 cells through IL-12 secretion, which promotes pro-inflammatory cytokine production [74]. However, DCs can also adopt an immunosuppressive immature phenotype, characterized by diminished phagocytic activity, impaired antigen presentation, and reduced expression of costimulatory molecules [74]. OAC tumours have been shown by our group to be enriched with cytotoxic $CD8^+$T cells, as high expression of CD107a was also observed in these tumour samples [75]. Moreover, our lab's previous data revealed reduced $CD45RO^+$ and $CD69^+CD4^+$ T cells in OAC suggesting that the TME suppresses

immune activation [60]. Additionally, secreted factors within the OAC tumour tissue microenvironment can lead to lower proportions of activated T-cells such as TNF-α^+ and IFN-γ^+CD8^- and $CD8^+$ T cells, altered cytokine expression as described above, and may have a detrimental impact on T-cell mediated anti-tumour immunity [60]. Furthermore, our group has shown that the FLOT and CROSS chemotherapy reduced CD27 and increased CD69 expression on tumour-infiltrating and circulating T cells, with similar effects observed in T cells exposed to supernatants from treated oesophagogastric junctional adenocarcinoma (OGJ) cell lines and *ex vivo* biopsies [76]. Additionally, these chemotherapy regimens enhanced the cytotoxic potential of healthy donor and patient-derived T cells, suggesting their immunostimulatory properties could be leveraged in combination with immunotherapy and how 1st line treatment can alter T cell phenotype and function [76].

In OAC, NK and T cells exhibit altered phenotypes and profiles within the TME, highlighting the need for new therapeutic strategies that enhance their anti-tumour activity.

1.2.2 Pro-tumourigenic immune responses in OAC

It is well established that impaired immune surveillance, weakened anti-tumour immune responses, and microenvironments that recruit and activate pro-tumour immune cell subsets facilitate tumour progression across cancer types. In the setting of OAC, the cytokine shift observed from BO to OAC enables tumour cells to interact with pro-inflammatory immune components, including tumour-associated macrophages (TAMs), while also promoting cancer-associated fibroblasts (CAFs) and regulatory T cells (Tregs) [77-79].

MDSCs in tumours are expanded and activated by pro-inflammatory cytokines (IL-6, PGE-2, IL-1β, and vascular endothelial growth factor (VEGF)), secreted from tumour and immunosuppressive cells [80], enabling immune suppression in the TME by inhibiting NK and T cell activity through IL-4, IL-10, TGF-β, and PD-L1 expression, thereby facilitating tumour progression and metastasis [81, 82]. Notably, patients with OAC exhibit significantly elevated frequencies of Tregs and MDSCs compared to non-cancer controls, reinforcing the immunosuppressive role of MDSCs in OAC [79]. Furthermore, MDSCs with

high CD38 expression ($CD38^{high}$MDSCs) demonstrate enhanced suppression of activated T cells, thereby promoting tumour growth, potentially due to increased production of inducible nitric oxide synthase (iNOS), which inhibits T cell responses and contributes to immune evasion [83]. Indeed, Daratumumab, an anti-CD38 monoclonal antibody used in multiple myeloma treatment, was shown to restrict tumour growth *in vitro* and *in vivo* in OAC models [83].

The OAC microenvironment is characterized by elevated expression of immunosuppressive factors, including cyclooxygenase-2 (COX-2), VEGF, and IL-8 [84]. COX-2 has been implicated in multiple oncogenic processes, including cancer stemness, apoptotic resistance, angiogenesis, metastasis, and immunosuppression. Its expression is elevated in BO and OAC epithelial cells and is further induced by bile acid exposure due to reflux, making it a potential therapeutic target [85, 86]. Tregs ($CD25^{+}FoxP3^{+}CD4^{+}$) suppress anti-tumour immune responses by inhibiting APC maturation, thereby reducing cytokine secretion and CTL activity [87]. In OC, Tregs downregulate IL-2 expression while upregulating CTLA-4 and CD25 via FoxP3, which may be used as a prognostic marker [88-90].

Tumour cells can evade anti-tumourigenic mechanisms by overexpressing PD-L1, PD-L2, and VISTA, thereby inhibiting T cell function and cytokine production [91]. Although gastric-oesophageal tumours are enriched with CTLs, their function is often impaired due to an immunosuppressive TME driven by pro-tumour immune cells [75, 92]. Our previous research has shown that higher-grade tumours and poorer responses to neoadjuvant treatment in OAC patients were associated with increased immune checkpoint expression on T cells, which was further modulated by first-line chemotherapy, leading to upregulation of PD-1, A2aR, KLRG-1, PD-L1, PD-L2, and CD160 while reducing TIM-3 and lymphocyte activation gene-3 (LAG-3), supporting the rationale for combining ICI with first-line chemotherapy to improve efficacy [93]. NK cells in OAC also express elevated levels of immune checkpoints TIM-3 and PD-1, leading to reduced cytotoxicity and functional exhaustion [94, 95]. Notably, increased intratumoural $TIM\text{-}3^{+}$ NK cell levels correlate with advanced tumour stage and higher invasion, suggesting its potential as a prognostic biomarker in OAC [94]. This was further confirmed by research in our group which demonstrated higher frequencies of intratumoural $PD\text{-}1^{+}$NK cells compared to

circulating NK cells in OAC patients [68]. Additionally, LAG-3 is expressed in 10.5% of OAC tumours and is associated with T cell exhaustion and impaired anti-tumour immunity [96, 97]. This highlights the critical role of immune suppression in OAC progression and the potential for immunotherapies in this malignancy.

Moreover, BO has been identified as a precursor to the TME alterations observed in OAC, particularly by inducing tissue hypoxia [98]. In solid tumours such as OAC, cancer cells have an increased oxygen demand, but tumour growth, blood vessel compression, and vascular damage limit oxygen availability. While normal cells are adversely affected by hypoxia, cancer cells exploit this condition to sustain proliferation [99]. Chronic inflammation, oxidative stress, and hypoxia contribute to genetic instability and defective DNA repair, leading to the accumulation of mutations in tumour suppressor genes such as *TP53* [100, 101]. Hypoxia also shifts cancer cell metabolism from oxidative phosphorylation to glycolysis, a process regulated by hypoxia-inducible factor 1 (HIF-1)[102]. This metabolic reprogramming increases lactic acid production, causing intracellular pH imbalances and activating proton transport mechanisms to restore homeostasis [103]. Notably, high expression of carbonic anhydrase IX (CAIX), a key regulator of pH under hypoxic conditions, correlates with shorter survival rates and greater tumour aggressiveness in oesophageal and gastric adenocarcinomas [104]. Our group has previously shown that hypoxia and nutrient deprivation can influence immune checkpoint expression of PD-1, CTLA-4, A2aR, PD-L1 and PD-L2 on circulating T cells derived from OAC patients, but also increase secretion of PD-L1 and PD-L2 on the OE33 OAC cell line when co-cultured with these T cells [105]. Similarly, acidosis was shown by our group to increase TIM-3, LAG-3 and CTLA-4 expression on T cells derived from OAC patients, further demonstrating how the harsh TME of solid tumours can upregulate immune checkpoints on T cells and potentially contribute to immune-evasion and disease progression in OAC [106].

1.2.3 Obesity associated-inflammation in OAC

The progression of obesity-associated cancer is influenced by profound changes in immune mediators, cytokines, and adipokines. Obesity induces chronic low-grade inflammation through alterations in adipose tissue endocrine function and immune cell profiles and function [30, 31, 33]. In obese VAT, leptin becomes the dominant adipokine,

amplifying the pro-inflammatory response [36, 107, 108]. Elevated leptin levels in BO patients, where it regulates energy homeostasis and immune function, correlate with an increased risk of OAC and are further upregulated in the malignancy [107, 109]. Leptin also inhibits apoptotic pathways, including Akt, mitogen-activated protein kinase (MAPK), and STAT, thereby promoting cancer cell proliferation [107].

Chronic acid and bile reflux sustain the activation of inflammatory pathways, including nuclear factor kappa-light-chain-enhancer of activated B cells (NF-κB) and signal transducer and activator of transcription 3 (STAT3) signalling cascades, which promote epithelial proliferation and inhibit apoptosis [23, 110, 111]. Persistent epithelial injury recruits immune cells—neutrophils, NK cells, and T cells—that secrete pro-inflammatory cytokines such as IL-1β, IL-6, IL-8, TGF-β, and TNF-α, reinforcing chronic inflammation and tissue damage [108, 111, 112]. These cytokines further activate NF-κB and STAT3, establishing a pro-tumorigenic feedback loop [80, 113].

Chronic inflammation in obesity at both local and distant tissue sites, contributes to carcinogenesis [33]. The VAT is a complex, highly metabolically active tissue compartment that comprises of adipocytes but is also enriched of innate and adaptive immune cells, fibroblasts, endothelial cells, pericytes, and progenitor cells [35, 114]. Obesity-induced fluctuations significantly alter the homeostatic balance of immune cell populations in VAT and the liver [115]. Adipose tissue expansion disrupts energy storage and endocrine function while promoting pro-inflammatory signalling [36]. Specifically, the transition from lean adipose tissue to obese adipose tissue reduces anti-inflammatory Treg cells and Th2, which normally mitigate adipose tissue inflammation [36]. This shift is accompanied by an increase in Th1 and $CD8^+$ T cells and a polarization of macrophages from the anti-inflammatory M2 phenotype to the pro-inflammatory M1 phenotype [115]. Additionally, systemic inflammation is exacerbated by the release of cytokines such as IFN-γ, TNF-α, IL-6, and IL-1β [36, 40].

Oxidative stress resulting from chronic inflammation leads to excessive reactive oxygen species (ROS) production. While ROS are normally generated during oxidative phosphorylation and T cell activation [116, 117], their excessive accumulation in OAC—due to low pH exposure and recurrent DNA breaks—induces DNA damage, depletes antioxidant glutathione, and promotes genetic instability, facilitating malignant

transformation [34, 118, 119]. Additionally, ROS upregulate platelet-derived growth factor receptor (PDGFR) and epidermal growth factor receptors (EGFR), further driving tumour progression [120, 121].

Overall, obesity is a significant risk factor for OAC and drives its tumour development and progression via several pathways [17, 122, 123].

1.2.4. Obesity-associated immune dysfunction in OAC

The local and systemic inflammatory microenvironment in OAC is driven by persistent GORD, obesity-associated inflammation, and immune dysfunction [23, 40, 72, 80, 110]. Our group and others have uncovered several ways obesity can contribute to severe immune dysfunction and inflammation in OAC patients, identifying macrophage- and T cell-rich environments that modulate inflammatory processes not only in the VAT but also in the liver of these cohorts [124, 125]. The omentum of OAC patients exhibits an enrichment of $CD4^+$ and $CD8^+$ T cells, with elevated expression of activation markers CD69 and pro-inflammatory cytokines IFN-γ, TNF-α, and IL-17 [124, 126], whereas NK cells in OAC omentum exhibit diminished expression of activation receptors NKG2D, NKp30, and NKp46, reduced TNF-α, Fas-L and TRAIL , and increased IL-10 and CD27 expression [39, 68, 69, 127]. The omentum of OAC patients recruits and activates NK and T cells via [60, 110, 128]. Specifically, the pro-inflammatory chemokine fractalkine was demonstrated as a driver of $CD8^+$T cells and NK cells to the omentum as it in present in abundance in this compartment, however, frequencies of NK cells are significantly lower in the omentum of OAC patients compared to circulating NK cells, suggesting soluble factors in the omentum [39, 127, 129].

Furthermore, adipose-conditioned media (ACM) generated from OAC omental tissue alters immune checkpoint expression TIGIT on $CD4^+$ and $CD8^+$ T cells and promotes a Th1/Th17 phenotype, and downregulating PD-1, TIGIT, CTLA-4, and PD-L1 in Th1/Th17 subsets. These findings suggest potential therapeutic targets for enhancing ICI efficacy in OAC [130].

Importantly, our group has shown significant differences in the TME of OAC patients with obesity compared to those patients without obesity. Indeed, OAC tumour-conditioned media (TCM) from patients with obesity enhanced IFN-γ, TNF-α, and IL-10 production by

NK cells from healthy donor blood, while significantly reducing degranulation marker CD107a, reinforcing a pro-inflammatory yet less cytotoxic NK cell state [68]. Furthermore, lower intratumoural NK cell frequencies in OAC patients correlate with increased visceral obesity, suggesting that NK cell infiltration declines with rising visceral adiposity, potentially due to their migration to and apoptosis within the omentum [127].

These findings underscore inflammation and immune dysfunction as a key driver of OAC, highlighting the need for targeted anti-inflammatory interventions in disease prevention and treatment. The exact mechanisms whereby the distal VAT affects the tumour in OAC patients with obesity are relatively unknown but crucially need to be addressed to improve anti-tumour immunity and immunotherapy efficacy in this malignancy.

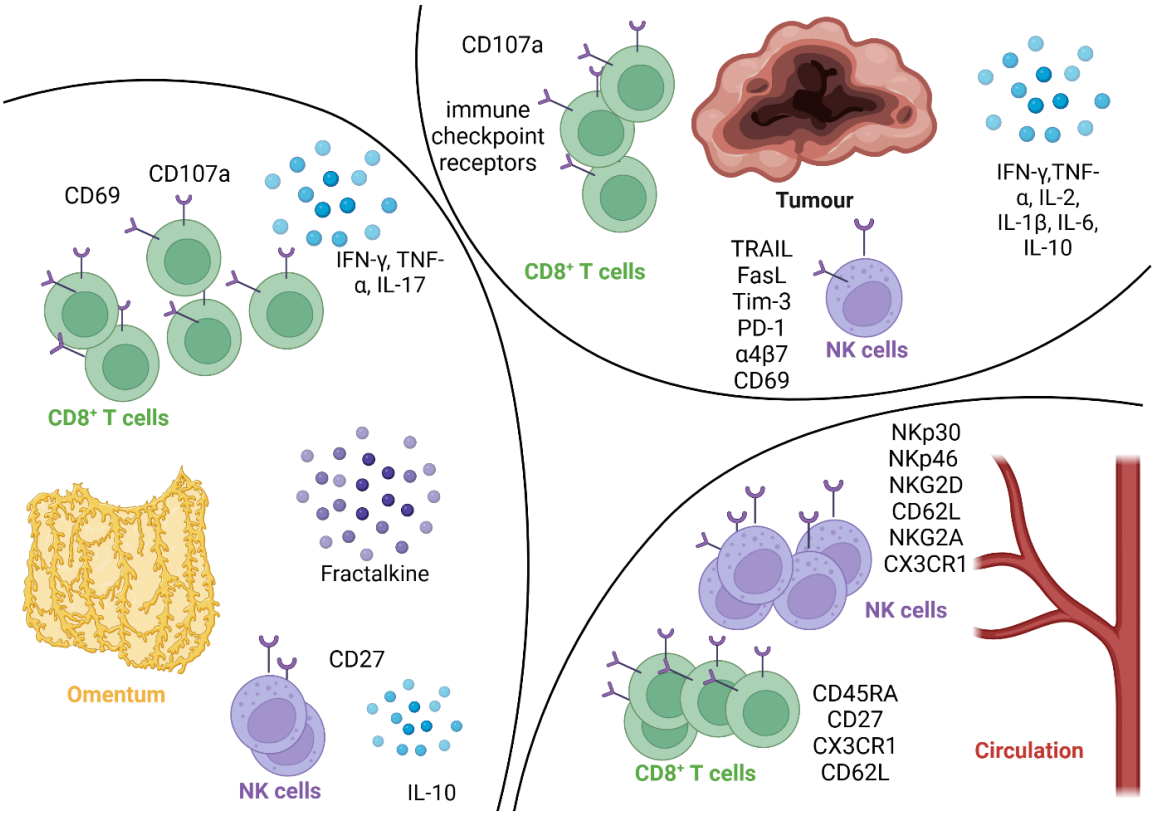

Figure 1.1: Immune dysfunction in OAC

Overview of the immune dysfunction in OAC. In the **omentum**, there are high frequencies of CD8⁺T cells, which express CD69 and CD107a, and produce high levels of IFN-γ, TNF-α and IL-17 whereas NK cell numbers are low in the omentum, CD27 receptor is elevated on their surface and they express high levels of IL-10. Fractalkine is abundant in the omentum. The **oesophageal tumour site** presents with high levels of CD8⁺ T cells which express high CD107a, however they also have increased expression of ICI such as PD-1, TIGIT and CTLA-4. NK cells are diminished in the OAC tumour and death receptor ligands TRAIL and FasL, Tim-3 and PD-1, α4β7 and CD69 receptors are elevated. There are high levels of IFN-γ, TNF-α, IL-2, IL-1β, IL-6 and IL-10 in the OAC TME. In the **circulation**, there are higher levels of NK cells and CD8⁺ T cells compared to the omentum and tumour, with NK cells expressing high frequencies of activation markers NKp30, NKp46 and NKG2D, but also NKG2A, and CD8+T cells express high CD45RA and CD27 while both subsets of immune cells express higher levels of CD62L and CX3CR1 on their surface. Created with Biorender.com

1.3 The role of Fractalkine in inflammation and cancer

1.3.1 Chemokines in health and disease

Chemokines, or chemotactic cytokines, are small proteins (8-12kDa) that regulate immune cell function and direct their migration to sites of infection or disease [131]. They are categorised into four families—C, C-C, C-X-C, and C-X3-C—based on N-terminal cysteine motifs, with corresponding receptors designated CR, CCR, CXCR, and CX3CR [132] **[Table 1.1]**. Chemokine receptors, members of the class A rhodopsin-like G protein-coupled receptor (GPCR) family, trigger intracellular signalling cascades upon ligand binding, facilitating the movement of leukocytes, allowing for the precise spatial and temporal organisation of immune cells [133, 134]. Although all chemokine receptors are seven-membrane GPCRs, they differ in their ligand specificity, expression patterns, signalling pathways and functional specialisation [**Table 1.1**]. The differential expression of chemokines receptors and ligands by immune cells or non-hematopoietic cells maintains homeostasis and ensures appropriate immune cell trafficking during inflammation [135]. Atypical chemokine receptors, a distinct subfamily, do not engage in conventional G protein signalling but regulate chemokine availability and activity, thereby modulating immune responses and physiological processes [136]. Chemokines play essential roles in embryonic development, immune cell trafficking, and homeostasis [137-141].

In immunity, chemokines regulate both innate and adaptive responses. CXCL8 and CXCL1, signalling through CXCR1/CXCR2, mediate neutrophil recruitment, while CCL27 attracts keratinocyte precursors to accelerate wound healing [142]. Adaptive immunity relies on CCL19 (MIP-3β), CCL2 (MCP-1), and CXCL12 (SDF-1), which guide T cells and DCs to secondary lymphoid organs via CCR7 and CXCR4, promoting antigen presentation [143]. Dysregulated chemokine signalling contributes to chronic inflammation in autoimmune diseases, as seen with CCL5 (RANTES)/CCR5 in rheumatoid arthritis [144], and can be exploited by viruses such as HIV, which utilises CCR5 and CXCR4 for entry [145]. Given their pivotal role in immune regulation, chemokines and their receptors represent promising therapeutic targets in inflammatory and infectious diseases.

Table 1.1: Chemokines and their receptors

X = any amino acid residue

Chemokine Subfamily	Receptor Class	Cysteine Motif	Receptors	Principal Expression	Functional Role
CXC	CXCR	C-X-C	CXCR1-6	Neutrophils, lymphocytes, endothelial cells	Acute inflammation, angiogenesis, stem cell trafficking
CC	CCR	C-C	CCR1-10	Monocyte, T-cell, dendritic cell, eosinophils	chronic inflammatory diseases, cancer metastasis and HIV entry
CX3C	CX3CR	C-X-X-X-C	CX3CR1	Leukocytes, microglia	Adhesion, neuron-immune interaction
C	XCR	Single cysteine	XCR1	Dendritic cell and T cell	Antigen cross-presentation, cytotoxic T cell priming

1.3.2 Chemokines in inflammation and cancer

1.3.2.1 Chemokines in inflammation

Chemokines orchestrate the movement of immune cells via their chemokine receptors found on immune cells by attracting bone-marrow derived cells. In chronic inflammatory conditions, dysregulated chemokine signalling sustains immune cell infiltration, contributing to tissue damage and disease progression.

For instance, the chemokine CCL2 and its receptor CCR2 play a pivotal role in monocyte recruitment, driving macrophage accumulation in inflamed tissues and promoting the persistence of inflammatory responses [146]. Similarly, CXCL8 facilitates neutrophil migration and activation, exacerbating inflammatory damage in diseases such as rheumatoid arthritis and chronic obstructive pulmonary disease [147]. CXCR3 is expressed on various immune cells, facilitating a Th1-mediated response by recruiting NK cells, $CD4^+$ Th1 cells, and $CD8^+$ CTLs to the tumour site, thereby inhibiting disease progression [148, 149]. These recruited immune cells produce IFN-γ, which induces the expression of CXCL9 (MIG), CXCL10 (IP-10), and CXCL11 (I-TAC), further enhancing effector cell recruitment through CXCR3 binding [148, 149]. CCR5 and CXCR3 are key mediators of lymphocyte and macrophage recruitment to the liver, and obesity-associated inflammation is characterized by increased chemokine secretion, with elevated levels of CCL2 and CCL5 contributing to adipose tissue macrophage infiltration and systemic metabolic dysfunction [150, 151]. Given their central role in inflammatory processes, chemokines represent promising therapeutic targets for controlling chronic inflammation, immune dysregulation, and associated pathologies.

1.3.2.2 Chemokines in cancer

In cancer-related inflammation, chemokines not only recruit immune cells but they can facilitate cancer progression by promoting angiogenesis and metastasis [135]. However, some chemokines exhibit anti-tumour properties, making them potential therapeutic targets. Modulating chemokine expression - either enhancing or inhibiting their activity - remains a promising yet challenging strategy in cancer treatment.

The chemokine receptor CXCR4 is widely implicated in cancer progression, with overexpression reported in more than 23 cancer types, including breast, lung, ovarian,

pancreatic, colorectal, and oesophageal cancers [132, 134, 152]. CXCR4 plays a key role in metastasis, as evidenced in breast, ovarian, prostate, and lung cancers, as well as in glioblastoma and pancreatic cancer stem cells [153-155]. Through binding to its sole ligand, CXCL12, CXCR4 promotes tumour survival, growth, and metastasis [154]. CXCR4 is overexpressed in oesophageal squamous cell carcinoma (OSCC) and gastric cancer, suggesting its potential as a therapeutic target in OAC, where it contributes to tumour metastasis and TAM recruitment [134, 156].

CCL2 is mostly associated with a pro-tumourigenic role as it recruits monocytes, neutrophils and MDSCs to the tumour site which facilitates the transition of monocytes and neutrophils into TAMs and tumour-associated neutrophils (TANs) [157, 158]. Among the first chemokines identified as a cancer promoter, CCL2 was shown to drive metastasis and NF-κB activation in a lymphoma mouse model [159]. In gastric cancer, CCL2 promotes drug resistance by inhibiting autophagy, a process that can be reversed through forced autophagy or CCL2 knockdown [160].

Recent studies suggest that CXCR3 suppresses cancer cell expansion by modulating peripheral rather than intratumoural T cell movement in pancreatic cancer [161]. While CXCR3 appears to have anti-tumourigenic properties, it has also been implicated in tumour growth, metastasis, and angiogenesis [162]. Elevated CXCR3 expression has been linked to increased metastasis in ovarian, gastric, colon, and prostate cancers [162]. Additionally, CXCL11 influences CXCR3 by activating FOXp3^{-}IL-10-^{high} CD4^{+} Treg cells, complicating its potential as a therapeutic target [163].

CCL3 (MIP-1α), CCL4 (MIP-1β), and CCL5 contribute to cancer metastasis and the recruitment of DCs and MDSCs in colorectal, ovarian cancer, and glioblastoma [164-166]. Our group has investigated the role of chemokines in shaping immune cell migration in OAC, particularly in the liver and visceral adipose tissue (VAT). Our previous research demonstrated impaired T cell migration in oesophageal cancer tissue, with reduced CXCR3^{+} Th1 and CCR6^{+} Th17 populations [110]. Although CCL5 and CCL3 are enriched in OAC tumour tissue, T cells expressing their respective receptors are scarce, indicating compromised recruitment to the tumour site [110]. Additionally, CCL2, CCL3, CXCL8 (IL-8), CXCL10 and CCL13 (MCP-4) are significantly elevated in the omentum of OAC patients, while CCL2, CCL3, and CXCL8 show higher levels in the liver compared to serum

[128]. Notably, $CCR5^+$ $CD4^+$ and $CD8^+$ T cells are more prevalent in the omentum and liver than in circulation and CCR5 expression can be enhanced with clinically relevant doses of irradiation on T cells [128, 167]. These findings highlight the potential of targeting T cell migration to mitigate immune cell infiltration into the inflamed omentum and liver in OAC and augment their homing to tumour.

The CCR4 chemokine receptor plays a critical role in immune regulation within the tumour microenvironment and is implicated in several solid malignancies, including gastric and breast cancer [168]. Its ligands, CCL17 and CCL22, recruit Treg cells, which suppress cytotoxic immune responses, facilitating tumour immune evasion by inhibiting key effector cells such as NK cells [168]. Targeting these chemokines could reduce Treg infiltration, promote anti-tumorigenic immune cells such as DCs, cytotoxic T cells, and NK cells, and inhibit cancer metastasis. Our group has shown that in OAC, CCR4 antagonism on T cells should be implemented at the pre-neoplastic stage, as it reduces migration toward BO but not OAC tissue-derived conditioned media [110]. This aligns with previous findings highlighting the predominant Th2 immune profile in BO [60].

Overall, targeting chemokine receptors and their ligands represents a promising strategy in cancer therapy, particularly for difficult-to-treat malignancies such as OAC. Leveraging their functions to enhance anti-tumour immune responses may offer a viable approach for improving treatment outcomes.

1.3.3 Biological functions of fractalkine

Fractalkine, also known as CX3CL1, is a unique chemokine protein that functions as both a chemoattractant and an adhesion molecule [169]. It is the sole member of the CX3C chemokine family and possesses a distinctive structure with a transmembrane domain anchoring the molecule to the cell membrane, an extracellular N-terminal ligand-binding domain conferring receptor binding specificity and initiating downstream signalling, a mucin-like stalk, which allows it to be expressed as a membrane-bound protein on the surface of certain cells, such as endothelial cells, epithelial cells and neurons, and a cytoplasmic tail [170]. Upon activation, which can be induced by inflammatory cytokines such as TNF-α, IL-1β, and IFN-γ, the extracellular portion of fractalkine is cleaved: during homeostatic conditions by ADAM metallopeptidase domain 10 (ADAM10) but in

response to inflammation by ADAM17, yielding its soluble form [171]. The latter can attract and bind to its sole receptor, CX3CR1, predominantly found on immune cells such monocytes, $CD8^+$ T cells and NK cells and becomes a chemotactic cytokine [172, 173]. CX3CR1 is a GPCR that contains an extracellular N-terminus with a ligand-binding pocket, seven transmembrane α-helices, forming a helical bundle critical for G-protein interaction and conformational changes upon ligand binding and intracellular C-terminal domains that couple to Gi proteins, triggering downstream signalling cascades [174]. In steady-state conditions, the fractalkine:CX3CR1 axis supports monocytes and tissue-resident macrophages, contributing to tissue integrity and non-inflammatory clearance of apoptotic cells. In the central nervous system, fractalkine:CX3CR1 interactions regulate microglial quiescence, synaptic pruning, and neuroimmune homeostasis [174]. While fractalkine has a sole receptor, its receptor CX3CR1 has another ligand CCL26 (Eotaxin-3), with studies showing that both fractalkine and CCL26 can recruit NK cells to allergic nasal tissue [175, 176]. The CCL26-CX3CR1 axis plays a key role in resolving allergic lung inflammation by activating $CX3CR1^+$ macrophages, which facilitate eosinophil clearance [177]. Additionally, in hepatocellular carcinoma, HIF-1α induces CCL26 expression in cancer cells, attracting $CX3CR1^+$ MDSCs to the tumour site [178]. Therefore, CCL26 should also be considered when therapeutically targeting the Fractalkine-CX3CR1 axis.

1.3.4 Fractalkine in inflammation

Binding of fractalkine to its receptor CX3CR1 can lead to the inhibition of adenylate cyclase, or the mobilisation of intracellular $Ca2^+$, however it can also activate many pro-inflammatory pathways, including NF-κB which regulates the expression of cytokines and chemokines, Janus kinase signal transducer and activator of transcription protein (JAKSTAT) modulating the immune system, regulating cellular proliferation, and maintaining tissue homeostasis, MAPK which regulates inflammation, cell proliferation and immune cell activation, the PI3K/Akt pathway, involved in cell survival, growth and migration, contributing to the pro-inflammatory response, but also Toll like receptor (TLR), Wnt/β-catenin and others [179-181]. Fractalkine has been reported to be implicated in multiple inflammatory diseases, such as rheumatoid arthritis (RA), Crohn's disease, atherosclerosis, and certain neurodegenerative disorders [182, 183]. In RA, fractalkine was found to impact the differentiation of human peripheral blood monocytes

and monocytes-derived DCs into osteoclasts, which promote bone destruction [183]. Fractalkine binding to its receptor in Crohn's disease induces chronic inflammation and the ligand has been shown to be upregulated in inflamed lesions [170]. Defects in the fractalkine:CX3CR1 signalling pathway have been shown to promote neuroinflammation by altering demyelination in mice microglia [182]. More recently, it was found that fractalkine may play a role in acute kidney injury through Wnt/β-catenin signalling pathway by aggravating the activation of LPS-induced macrophages, as when both fractalkine and Wnt/β-catenin signalling pathway were inhibited, murine mice models of acute kidney injury improved [184]. CX3CR1 modulator E6130 ([(3S,4R)-1-[2-Chloro-6-(trifluoromethyl)benzyl]-3-4-methylpyrrolidin-3-yl]acetic acid (2S)-hydroxy(phenyl)acetate) has been shown as a promising way of reducing inflammation in a mouse model of inflammatory bowel disease (IBD) as it blocked the migration of $CX3CR1^+$ immune cells to the gut mucosal membrane [185].

1.3.5 Fractalkine in cancer

Fractalkine plays both pro- and anti-tumorigenic roles across various cancers. Its anti-tumour effects stem from its ability to recruit $CX3CR1^+$ immune cells, such as cytotoxic T cells and NK cells, to the TME, enhancing cancer cell recognition and elimination [172, 186]. Studies have linked high fractalkine levels from gastric and colorectal cancer patient tumour tissue with increased immune cell infiltration and improved outcomes [187, 188] However, conflicting evidence suggests that CX3CR1 overexpression can also enhance tumour survival, proliferation, and metastasis, as observed in gastric cancer tissues from patients [189]. In breast cancer, results on fractalkine's anti-tumour role are also disputed: one study has shown that higher expression levels of the chemokine on cancer cells increase cell infiltration of DCs, NK cells and T cells, and corresponded to the patients without lymph node metastasis, while Tsang *et al.* demonstrated that higher fractalkine expression correlated with poorer patient clinical outcomes [190, 191]. Fractalkine has therefore also been demonstrated as a promoter of tumour development by stimulating cancer cell proliferation, migration, and invasion, fostering tumour aggressiveness [69, 127, 129, 173, 179, 192-195]. In the context of immune cell recruitment, fractalkine has been shown to mediate TAMs recruitment to the TME via IL-10, which upregulates CX3CR1 expression on lung cancer cell lines. Genetic ablation of fractalkine and CCL2

shifted TAMs from a tumour-promoting M2 phenotype to an M1 phenotype *in vivo*, suggesting a potential therapeutic strategy [196]. Furthermore, tumour expressing fractalkine in mice were found to mediate the recruitment of MDSCs expressing high levels of CX3CR1 via $p16^{Ink4}$ and $p21^{Cip1/Waf1}$ activation [197]. In neuroblastoma, TGF-β1 release downregulates CX3CR1 while upregulating CXCR4 and CXCR3 on NK cells, potentially sequestering them in the bone marrow and impairing immune surveillance [198]. Reversing this effect could offer therapeutic benefits [198]. However, in a mouse model of glioblastoma, CX3CR1 deletion had no impact on tumour growth or immune cell infiltration, suggesting a limited role in this cancer type [199] **[Table 1.2].**

Beyond its chemotactic properties, fractalkine also directly contributes to tumour cell survival in breast, gastric, prostate, pancreatic, and lung cancers [192-195]. In prostate cancer cell lines, it enhances EMT via the TACE/TGF-α/EGFR pathway, promoting metastasis [192, 193]. In lung cancer patient samples, higher levels of fractalkine expression were associated with higher tumour stage and lymph node metastasis, and fractalkine knockdown on lung cancer cell lines reduced activation of JNK and MMP-2/MMP-9, while also decreasing cell migration and invasion [200]. In ovarian cancer, despite recruiting $CX3CR1^{+}$ T cells to the tumour site, high fractalkine expression correlates with poor prognosis in patients and may interfere with PARP inhibitor efficacy [201] **[Table 1.2].**

In pancreatic ductal adenocarcinoma (PDAC) patients, fractalkine and CX3CR1 overexpression are associated with poor prognosis [202]. In PDAC cell lines, fractalkine promotes cancer cell growth and migration via the JAK/STAT pathway and enhances resistance to TRAIL by recruiting inflammatory cells [203, 204]. It also induces HIF-1α expression through PI3K/Akt and MAPK pathways, increasing glucose uptake and supporting tumour growth [205]. Notably, fractalkine inhibition reduced cancer cell viability and motility, highlighting the fractalkine-CX3CR1 axis as a potential therapeutic target [203]**[Table 1.2].**

1.3.6 Fractalkine in obesity and obesity-associated cancer

In the setting of obesity, fractalkine facilitates the recruitment of immune cells, particularly monocytes and macrophages into adipose tissue, where they contribute to

chronic low-grade inflammation, as fractalkine:CX3CR1 interaction modifies monocyte adhesion to adipocytes and correlates with obesity [206]. In the context of obesity-associated cancer OAC, our group has previously shown the chemotactic force of abundant levels of fractalkine in the VAT. Our earlier reports demonstrate fractalkine's ability to recruit $CD8^+$ T cells and NK cells to the omentum, where they undergo alterations and in the case of NK cells, exhibit hindered migratory capacity towards tumour [68, 127, 129]. Recruitment of NK cells to the omentum and exposure to fractalkine alters their phenotype by altering their CD27 expression, and elevating their TNF-α and IFN-γ production [127]. Therefore, these studies show that fractalkine could be a potential and interesting target to explore in the context of OAC, to reverse inflammation in the adipose tissue and to boost anti-tumour immunity **[Table 1.2].**

Overall, fractalkine is a potent inflammatory chemokine with diverse biological effects and its therapeutic utility has been under investigation in multiple disease settings including cancer. Its role in misguided anti-tumour NK and T cell migration towards the VAT in OAC likely occurs at the expense of anti-tumour immunity, placing it as a potential therapeutic target in OAC. Furthermore, its role in tumourigenic processes in OAC has not been fully elucidated and warrants further investigation.

Table 1.2: Fractalkine's role in pro- and anti-tumourigenic processes in cancer

Type of cancer	Pro-tumourigenic effects	Anti-tumourigenic effects	References
Breast cancer	Higher fractalkine expression correlates with poorer patient clinical outcome Fractalkine promotes tumour survival	High fractalkine levels from patient tumour tissue increases DC, NK and T cell infiltration High levels of fractalkine correlate with patients without lymph node metastasis	[190, 191]
Colorectal cancer	High levels of fractalkine in plasma are associated with increased mortality CX3CR1 upregulation in TAMs correlates with a poor prognosis	High fractalkine levels from patient tumour tissue increases immune infiltration and improves incomes Fractalkine increases TIL infiltration	[188, 207-210]
Lung cancer	Fractalkine facilitates recruitment of TAMs to the TME in lung cancer cell lines Fractalkine promotes tumour survival Higher levels of fractalkine in patient tumour samples are associated with higher tumour stage and lymph node metastasis	Elevated mRNA expression of fractalkine in tumour samples correlates with a good prognosis	[170, 195, 196, 211]
Neuroblastoma	TGF-β1 release downregulates CX3CR1 while upregulating CXCR4 and CXCR3 on NK cells, potentially sequestering them in the bone marrow and impairing immune surveillance		[198]

Hepatocellular cancer		High fractalkine levels on patient tumour samples correlates with good prognosis Fractalkine increases $CD4^+$ and $CD8^+$T cell recruitment in mouse models	[212, 213]
Gastric cancer	CX3CR1 overexpression on gastric tumour tissues enhance tumour survival, proliferation and metastasis	High fractalkine levels from patient tumour tissue increases immune infiltration and improves incomes	[187, 189, 214]
Melanoma	Higher levels of fractalkine in the bone marrow and in tumour cells correlates with worse prognosis		[215]
Pancreatic cancer	Fractalkine and CX3CR1 overexpression are associated with poor prognosis Fractalkine promotes cancer cell line growth and migration via the JAK/STAT pathway and enhances resistance to TRAIL by recruiting inflammatory cells Fractalkine induces HIF-1α expression through PI3K/Akt and MAPK pathways, increasing glucose uptake and supporting cancer cell line growth		[194, 202-204, 216, 217]
Ovarian cancer	Fractalkine promotes tumour survival High fractalkine expression in patient tumour samples correlates	Fractalkine recruits $CX3CR1^+$T cells to the tumour site	[201, 218, 219]

	with a poor prognosis and may interfere with PARP inhibitor efficacy Fractalkine enhances proliferation of cancer cell lines through AKT activation		
Leukaemia	Increased CX3CR1 expression in leukaemia cells increases pro-tumourigenic processes		[220]
Renal carcinoma	CX3CR1 expression is associated with the process of cellular migration *in vitro* and tumour metastasis *in vivo*		[221]
Prostate cancer	Fractalkine promotes tumour survival Fractalkine enhances EMT via TACE/TGF-α/EGFR pathway and promotes metastasis		[192, 193, 222, 223]
Oesophageal cancer	Fractalkine attracts $CD8^+$T cells and NK cells to the omentum, induces CX3CR1 receptor endocytosis and affects their phenotype and function Fractalkine drives erroneous migration of NK cells to the omentum over the oesophageal tumour		[68, 69, 127, 129]

1.4 Novel immunotherapies for the treatment of OAC

1.4.1 Chemokine-targeted therapies in OAC

Chemokines are essential for directing immune cells to the TME [36, 133, 134, 224] and represent a promising immunotherapeutic target for reshaping the immune landscape to enhance tumour eradication [225, 226]. Chemokine-targeted therapies also hold potential to hinder cancer metastasis. Despite multiple trials, chemokine-based therapies have yet to achieve clinical success in cancer treatment. We propose that their multifunctionality in the processes underpinning tumour development contribute to this along with their inherent redundancy. Furthermore, more thorough investigation of the biological effects of chemokines on immune cells and tumour cells is warranted to delineate their complex role in tumour progression prior to clinical trials.

In OAC, CXCR4 antagonists remain the only chemokine-targeting therapy evaluated in clinical trials (NCT03281369), though preclinical investigations continue to explore additional therapeutic avenues. Plerixafor, a CXCR4 antagonist, is approved for mobilizing hematopoietic stem cells in multiple myeloma (NCT04552743) and is now being repurposed in clinical trials for ovarian, gastric, pancreatic, and oesophageal cancers alongside BL-8040, another CXCR4 antagonist (NCT02179970, NCT03281369) [226]. Preclinical studies in a xenograft mouse model of gastro-oesophageal junctional adenocarcinoma demonstrated that CXCR4 antagonist CTCE-9908 reduced tumour burden by over 50% [227], while AMD3100, another CXCR4 antagonist, showed promising anti-proliferative effects in OSCC in both *in vitro* and *in vivo* models[228] **[Table 1.3].**

The combination of chemokine antagonists with approved therapies is under investigation in colorectal cancer. The CXCR2 antagonist MK-7123, in combination with the anti-PD-1 inhibitor pembrolizumab, is currently in clinical trials (NCT03473925), and CCR5 antagonism combined with chemotherapy has achieved a partial response in 60% of patients with refractory colorectal cancer, with an additional 20% exhibiting stable disease [229]. However, targeting certain chemokines remains challenging due to their dual roles in tumour biology. For example, CCL2 inhibition has been ineffective in clinical trials despite promising preclinical findings. The human monoclonal antibody carlumab

failed to suppress CCL2 in phase I clinical trial in solid tumours (NCT00537368) and phase II trials in metastatic prostate cancer (NCT00992186)[230, 231]. Preclinical studies demonstrated that CCL2 blockade could prevent metastasis in breast cancer, but withdrawal of treatment led to enhanced metastasis, underscoring the complexity of chemokine signalling [232] **[Table 1.3].**

Despite promising preclinical data, the clinical translation of chemokine-targeted therapies remains challenging due to the complex and often redundant roles of chemokines in the TME. While CXCR2 is generally associated with pro-tumourigenic effects, its role in OAC remains unclear. The CXCR2 antagonist SB332235 reduced OAC cell invasiveness *in vitro* but had no significant impact on cancer cell proliferation [233]. In contrast, CXCR2 blockade in OSCC inhibited MAPK phosphorylation and reduced tumour growth in mice [234] **[Table 1.3].**

CCR5 inhibitors, including maraviroc, have shown promise in modulating immune cell infiltration and suppressing metastasis. In a gastric cancer model, CCR5 inhibition improved anti-PD-1 efficacy by reducing MDSCs and Treg accumulation at the tumour site, leading to a 53% reduction in tumour growth [235]. The CCR5 small-molecule inhibitor OB-002 is currently in clinical trials for metastatic colorectal, pancreatic, gastric, urothelial, and breast cancers (NCT05940844) [236]. Our group previously demonstrated that targeting the CCL3 ligand via CCR1 and CCR5 antagonism could modulate T cell chemotaxis in OAC. Specifically, CCR1 antagonism reduced T cell migration toward omentum- and liver-derived soluble factors, while CCR5 blockade impaired migration toward omentum-derived factors only [128]. Additionally, our recent findings suggest that combining the CCR5 antagonist maraviroc with clinically relevant doses of irradiation enhanced T cell responses, increasing IFN-γ expression in $CD4^+$ T cells and promoting $CD8^+$ T cell migration toward irradiated OAC patient tumour sample-derived conditioned media [167]. We have also explored the potential of CX3CR1 modulation using E6130 in combination with NK cells, utilizing an *ex vivo* model to assess immune cell migration. This study demonstrated that E6130 redirected NK cells toward tumour-derived soluble factors while preventing their attraction to the fractalkine-rich omentum [68] **[Table 1.3].**

A deeper understanding of chemokine receptor signalling in OAC is crucial for refining therapeutic strategies and identifying patient subgroups most likely to benefit from these

interventions. Despite existing challenges in clinical translation, chemokine-targeted therapies remain a promising avenue in OAC treatment.

1.4.2 NK cell immunotherapies in OAC

Engineered T and NK cell therapies have been extensively studied as strategies to restore immune function in 'cold' tumours. However, unlike their success in haematological malignancies, these approaches have shown limited efficacy in solid tumours [237, 238]. NK cells, a key component of the innate immune response, play a crucial role in anti-tumour immunity [61, 239, 240]. However, their dysfunction or reduced presence within the TME impairs their cytotoxic activity, facilitating immune evasion and tumour progression [241, 242].

As aforementioned, our group has previously demonstrated that in OAC, NK cells are diverted away from the tumour toward the omentum by fractalkine [39, 127]. In OAC patients with obesity, NK cell frequencies are significantly reduced and exhibit impaired cytotoxic function [39, 69, 127]. Importantly, NK cell infiltration in tumours has been correlated with improved patient outcomes [243, 244]. Given their ability to eliminate tumour cells without requiring antigen recognition or MHC restriction, NK cells represent a promising alternative to T cell-based therapies. Furthermore, NK cells have demonstrated superior safety profiles in clinical studies, positioning them as a potential off-the-shelf immunotherapy option [239, 245].

Over the past decade, immune cell therapies have significantly advanced, improving survival outcomes in cancers with poor prognoses [246-250]. However, their application in solid tumours remains challenging due to difficulties in tumour targeting and the immunosuppressive nature of the TME [241]. Addressing these barriers will be critical for the successful translation of NK cell-based therapies into clinical practice.

1.4.2.1 Adoptive NK cell therapy: CAR-NK cells

Advances in genetic engineering have facilitated the modification of NK cells to express chimeric antigen receptors (CARs) or tumour-specific receptors, enhancing their ability to recognise and eliminate cancer cells [241, 242, 245, 251]. NK cell-based therapies have been investigated in obesity-associated cancers, with NK cells sourced from peripheral blood, cord blood, clonal NK cell lines, or induced pluripotent stem cells. Among these,

the clonal NK cell line NK-92 has emerged as a promising immunotherapeutic agent and is already in clinical development [252-254]. Due to their potent anti-tumour activity and favourable safety profile, NK-92 cells are the most extensively studied NK cell line in clinical trials across multiple malignancies, including colorectal, pancreatic, breast, and gastric cancers [242, 252]. KHYG-1 cells, another NK cell line, has demonstrated superior cytotoxicity compared to NK-92 [255]. It was derived from a patient with NK cell leukaemia and has been shown to effectively kill target cells such as K562, but also EM2, EM3 and HL60 leukaemia cell lines [255, 256].

A key advantage of NK cell lines is their immediate availability and potential for genetic modification. However, as they are derived from malignant sources, they must be irradiated before infusion to prevent *in vivo* proliferation, necessitating multiple infusions to maintain effective NK cell numbers. This requirement increases treatment costs and potential complications [257]. In obesity-associated cancers, a major challenge for NK cell therapies is mounting effective tumour infiltration and killing, which demands large numbers of functional NK cells [251, 258]. Therefore, the development of more personalized and effective NK cell therapies is crucial to improving current treatment strategies.

Currently, no CAR-NK cell therapies are in clinical trials for OAC, whereas over ten clinical trials are evaluating CAR-T cell therapies for OAC, including CAR-T cells targeting intraperitoneal mesothelin (NCT06623396) and claudin 18.2 (NCT06353152). Several CAR-NK cell therapies have demonstrated preclinical efficacy in obesity-associated solid cancers, suggesting their potential utility in OAC treatment. For instance, CAR-NK cells targeting HER2, which is frequently overexpressed in certain malignancies, have been shown *in vitro* and *in vivo* to lyse $HER2^+$ gastric cancer cells, coinciding with increased TNF-α and IFN-γ expression [259]. HER2-targeted CAR-NK cells are now being evaluated in clinical trials for glioblastoma and various solid tumours (NCT03383978, NCT04143711, NCT04319757, NCT05678205). Notably, a recent study identified a correlation between HER2 positivity and lower NK cell infiltration in OAC, highlighting HER2-directed CAR-NK cells as a potential therapeutic avenue [260].

Additionally, CAR-NK cells can be engineered to enhance the expression of key activation receptors, such as NKG2D, which has demonstrated promising *in vitro* and *in vivo* results

by increasing NK cell cytotoxicity and reducing tumour burden in colorectal and ovarian cancer models [261, 262]. Clinical trials are currently evaluating NKG2D-enhanced CAR-NK cells for these malignancies (NCT05213195, NCT05776355). Another promising approach involves engineering NK-92 cells to express the extracellular domain of the death receptor ligand TRAIL, a key mediator of NK cell cytotoxicity that selectively induces apoptosis in TRAIL-sensitive tumour cells while sparing normal cells [263]. In colorectal cancer cell lines and mice models, TRAIL-expressing NK-92 cells have exhibited high TRAIL expression and enhanced tumour cell lysis [264].

KHYG-1 cells exhibit high expression of key activating receptors, including NKp44 and NKG2D, which contribute to their potent anti-tumour activity [255, 256]. Genetic engineering strategies have been explored to enhance their therapeutic potential, such as the introduction of a folate receptor 1 (FOLR1)-specific CAR to target gastric cancer cells. Given that FOLR1 is overexpressed in over one-third of gastric cancer cases, FOLR1-CAR-KHYG-1 cells have demonstrated the ability to induce cytotoxic cytokine release and cancer cell death in gastric cell lines [265]. Similarly, KHYG-1 cells engineered to target c-Met, FOLR1, or AXL have shown promising efficacy against glioblastoma, effectively lysing glioblastoma cells *in vitro* [266]. In ovarian cancer, a modified KHYG-1 variant expressing a DR5-specific TRAIL ligand significantly reduced the viability of the OVCAR-3 cell line but had no effect on SKOV-3 cells, suggesting the presence of intrinsic TRAIL resistance mechanisms in certain ovarian cancer subtypes [267].

These findings underscore the potential of CAR-NK cell therapies in targeting OAC and other solid tumours.

1.4.2.2 Immune checkpoint and inhibitory receptors

Pembrolizumab and nivolumab have been approved for OAC treatment, but their efficacy remains limited, necessitating strategies to enhance their effectiveness and identify responsive patient cohorts. While ICI are primarily associated with T cells, NK cells also influence ICI outcomes. In gastrointestinal cancers, elevated PD-1 expression on NK cells at the tumour site or periphery correlates with poorer survival and impaired NK cell function [95, 268, 269]. Consequently, studies have explored PD-1 inhibition on NK cells to restore their anti-tumour activity [270].

A phase II clinical trial is currently evaluating NK cell therapy targeting PD-L1 in gastric and head and neck cancers, with promising results (NCT04847466). TIGIT blockade has also been investigated to prevent NK cell exhaustion and enhance cytotoxicity [271]. Another inhibitory NK cell receptor, NKG2A, binds to HLA-E, which is overexpressed in various gastrointestinal cancers and associated with poor prognosis [272-277]. The anti-NKG2A monoclonal antibody Monalizumab showed disease stabilisation in ovarian cancer patients and demonstrated improved NK cell-mediated tumour suppression when combined with PD-L1 blockade in preclinical models [278, 279]. A phase I/II trial combining Monalizumab with Durvalumab (anti-PD-L1) in solid tumours has shown safety and a modest 10% response rate in non-small cell lung cancer (NCT02671435) [280].

1.4.2.3 Cytokine based NK cell therapies

Enhancing NK cell activation *in vivo* is essential for improving NK cell therapy efficacy. Strategies primarily focus on cytokines such as IL-2, IL-15, and IL-18 [281-283]. IL-2 stimulates NK cell proliferation but also promotes Treg expansion, potentially dampening immune responses. High-dose IL-2 therapy has been linked to severe toxicity, including heart failure and liver injury [284-286]. Despite this, IL-2 immunotherapy is FDA-approved for metastatic renal cell carcinoma and melanoma due to its survival benefits [287]. To mitigate toxicity, NK-92Mi and NK-92CI cell lines have been engineered to express human IL-2 (hIL-2) to sustain activation without exogenous IL-2 administration [288]. Additionally, encapsulating IL-2 mRNA in NK-92, KHYG-1, and peripheral blood-derived NK cells enhances their longevity and activation without external cytokine support [289]. IL-15 has gained attention for its ability to stimulate NK and $CD8^+$T cells while maintaining disease stability. Subcutaneous IL-15 infusion has shown promise in solid tumour patients [290], and a clinical trial is currently evaluating IL-15-transduced cord blood-derived NK cells in advanced solid tumours (NCT06066424). Another trial is assessing the combination of recombinant IL-15 with nivolumab and ipilimumab in refractory cancers (NCT03388632).

Other avenues recently explored in the context of NK cell therapies are cytokine induced memory-like (CIML) NK cells, which possess memory-like characteristics. They are activated by IL-12, IL-15 and IL-18 cytokines and exhibit enhanced resistance,

proliferation, and cytokine production [291]. TGF-β may further support their metabolic and epigenetic reprogramming, improving persistence in immunotherapy settings [292]. This imprinting could be a strategy for improving the persistence and memory response of NK cells in immunotherapy settings. A clinical trial is currently evaluating the safety of CIML NK cells with low-dose IL-2 in high-grade ovarian cancer (NCT06321484).

1.4.3 Combining chemokines and immune cells for cancer treatment

Genetic engineering of NK cells to express specific chemokine receptors has emerged as a promising strategy to enhance tumour infiltration and improve their tumour-homing capacity. Transfection of chemokine receptor mRNA into human NK cells has been shown to preserve their viability, function, and phenotype while enhancing migration and cytotoxicity [293-295]. Wennerberg *et al.* demonstrated that upregulating CXCR3 expression on NK cells *ex vivo* increased their migration towards the TME in xenograft models of melanoma while also elevating CXCL10 secretion in the TME, facilitating NK cell infiltration and reducing tumour burden *in vivo* [296]. Similarly, CXCR2-engineered NK cells exhibited improved migration and cytotoxicity in renal cell carcinoma mice models [293]. Electroporation-mediated overexpression of CXCR1 and NKG2D in NK cells enhanced migration towards solid tumours in murine peritoneal xenografts without compromising cytotoxic functions [297]. Genetic engineering of NK-92 and primary NK cells to overexpress CCR4 and CCR2B enabled migration toward their respective chemokine ligands, CCL22 and CCL2, while preserving NK cell function, suggesting a potential avenue for enhancing NK cell-based therapies for solid tumours [298]. Furthermore, CX3CR1 transduction in T cells facilitated migration toward fractalkine-high colorectal tumours and suppressed tumour growth in murine models [207]. NK cell modification can also be achieved without genetic engineering. For example, cationic nanoparticle treatment induced CCR4 and CXCR4 expression, enhancing NK cell activation, tumour recognition, and breast cancer cell cytotoxicity *in vivo* [299]. Additionally, transient CCR7 expression via trogocytosis significantly increased NK cell migration toward CCL19 and CCL21, leading to a 144% increase in lymph node homing in a murine model [300]. Collectively, these findings underscore the potential of leveraging chemokine receptor engineering to enhance NK cell-mediated immune responses against solid malignancies, offering novel therapeutic strategies **[Table 1.3].**

Remodelling the TME to facilitate NK cell infiltration and convert immunologically "cold" tumours into "hot" ones represents an alternative strategy to enhance immune cell entry. Various approaches have been explored, including the use of oncolytic viruses to modify NK cells. For instance, oncolytic virus-mediated enhancement of $CCR5^{+}$NK cell migration improved anti-tumour responses in a mouse model of colon cancer [301]. Additionally, an NK-cell-recruiting protein-conjugated antibody (NRP-body) was engineered to release CXCL16 upon interaction with pancreatic cancer cells, promoting NK cell infiltration, suppressing tumour growth, and improving overall survival in mice [302]. Moon *et al.* demonstrated in mice that an oncolytic vaccinia virus genetically modified to express CXCL11 increased CXCL11 levels at the tumour site, thereby increasing intratumoural $CXCR3^{+}$T cell recruitment and enhancing the efficacy of adoptive T cell transfer [303]. Similarly, Del Rio *et al.* utilized 3D poly(ethylene) glycol (PEG) hydrogels with heparin-loaded CCL21 to mimic the extracellular matrix (ECM) of lymph nodes, leading to improved human $CD4^{+}$T cell expansion, which could enhance adoptive T cell therapy [304]. Furthermore, our group recently demonstrated in an *ex vivo* OAC model that modulating tumour-derived soluble factors, specifically by spiking it with CCL3 and CCL5, enhanced NK cell migration while preventing their attraction to chemotactic cues from the omentum [68]. These early findings show promising ways of manipulating the TME to enhance immune cell recruitment into solid tumours **[Table 1.3].**

Table 1.3: Chemokine based therapies *in vitro*, *in vivo* and in clinical trials in obesity-associated cancers

Target	Agent	Cancer type	*In vitro*	*In vivo*	Clinical trial	Reference
Chemokine targets						
CXCR4	Plerixafor	Pancreatic, ovarian			NCT02179970	
		Colorectal			Phase 1 trial	
	BL-8040	Oesophageal,			NCT03281369	
	CTCE-9908	Gastric, Gastro-oesophageal		Reduced tumour burden by over 50%	Phase 1/2 trial	[227]
	AMD3100	OSCC		Reduced tumour volume by 50%		
	LY2510924	Pancreatic		44.4% stable disease		[228]
CXCR4 + PD-1 ICI	+ durvalumab					[305]
CXCR2	SB332235	Oesophageal		Reduced invasiveness but no impact on cancer proliferation		[233]
		OSCC	Inhibited MAPK phosphorylation	Reduced tumour growth		[234]
CXCR2 + PD-1 ICI	MK-7123+ pembrolizumab	Colorectal			NCT03473925 Phase 2 trial	
CXCL1	Metformin	OSCC		Decrease in MDSC recruitment		[306]
Multiple chemokines		Breast			NCT03599453 Phase 1 trial	
	UNBS5162	OSCC	Decrease in cell viability			[307]

CCR5	Maraviroc	Colorectal		60% partial response + 20% stable disease		[164]
		Oesophageal	Reduce T cell migration towards omentum			[128]
	OB-002	Metastatic Colorectal, Pancreatic, Gastric, Urothelial, Breast			NCT05940844	
	Maraviroc + radiation	Oesophageal	Enhanced T cell responses and promoted $CD8^+$ T cell migration towards the tumour site			[167]
CCR5 + PD-1	CCR5 inhibition + anti-PD-1	Gastric		53% reduction in tumour growth		[235]
CX3CR1	E6130	Oesophageal	Redirect NK cells towards tumour site, prevent their migration toward omentum			[68, 69]
CCR1	CCX9588 CCX354	Oesophageal	Reduce T cell migration towards omentum and liver			[128]
Chemokine targets in combination with NK cell therapies						
$CXCR1^+$ $NKG2D^+$NK cells	Overexpressing CXCR1 and NKG2D on NK cells	Solid tumours		Increased NK cell migration without compromising with their cytotoxicity		[297]

CCR4$^+$ CCR2B$^+$NK cells	Overexpressing CCR4 and CCR2B on NK cells		Increased migration towards CCL22 and CCL2, preserved NK cell function		[298]
CCR4$^+$ CXCR4$^+$NK cells	Overexpressing CCR4 and CXCR4 on NK cells	Breast		Increased NK cell activation, cytotoxicity and tumour recognition	[299]
CCR7$^+$NK cells	Overexpressing CCR7 on NK cells			144% increase in NK cell lymph node homing	[300]
CCR5$^+$NK cells	Oncolytic virus to increase CCL5 at the tumour site	Colorectal	Enhanced CCR5$^+$ NK cell migration	Enhanced CCR5$^+$ NK cell infiltration and decreased tumour growth	[301]
CXCR6$^+$NK cells	NRP-body release of CXCL16 upon interaction with cancer cells	Pancreatic		Increased NK cell infiltration, reduced tumour growth, improving survival	[302]
CCR1$^+$CCR5$^+$ NK cells	Spiking tumour conditioned media with CCL3 and CCL5	Oesophageal	Increased NK cell migration towards tumour conditioned media and prevented migration towards soluble factors of adipose tissue		[68]

1.4.4 Challenges for future therapies for OAC

Despite the promise of immunotherapies in OAC, significant challenges remain, particularly for chemokine-targeted and NK cell-based strategies. The highly immunosuppressive TME, exacerbated by obesity-related factors, impairs NK cell recruitment and function through dysregulated chemokine signalling [222, 229]. A comprehensive understanding of the TME, including cellular interactions, cytokines, and chemokines, is essential for developing novel immunotherapies aimed at enhancing immune cell infiltration. A key limitation of NK cell therapies, compared to the greater clinical success of T cell-based approaches, is the limited persistence of CAR-NK cells post-infusion, whereas CAR-T cells have demonstrated sustained efficacy for over a decade [308]. Additionally, the metabolic constraints of the hypoxic, nutrient-deprived TME further hinder NK cell persistence and cytotoxicity. Chemokine modulation represents a promising strategy to overcome these barriers by reshaping the immune landscape and enhancing NK cell infiltration and efficacy [225, 226].

Addressing these challenges will require combinatorial approaches integrating chemokine-targeted therapies with ICI, metabolic reprogramming, and advanced gene-editing techniques to optimise NK cell function. Future research should focus on identifying patient subgroups most likely to benefit from chemokine-modulating strategies through comprehensive profiling of chemokine signatures in OAC. Our group has investigated cytokine and chemokine patterns in BO and OAC to understand the limitations of current therapies, examining not only the TME but also adjacent tissues and potential metastatic targets [39, 60, 69, 110, 126, 130]. This approach is critical for uncovering immunosuppressive and immune escape mechanisms, providing essential insights for the development of NK cell and chemokine-targeted therapies.

1.5 Conclusions

Fractalkine has been shown to promote tumour growth both directly and indirectly, with CX3CR1 antagonism emerging as a promising strategy to inhibit breast and pancreatic cancer metastasis. Our preliminary data suggested that CX3CR1 antagonism with AZD8797 can impede OAC tumour growth and EMT (unpublished), while fractalkine levels in VAT correlate with nodal status in OAC patients [68]. Additionally, CX3CR1

modulation with E6130 has been shown to reduce NK cell migration to the omentum while enhancing their recruitment to tumours in an *ex vivo* model [68, 69, 127].

Therefore, in this study, fractalkine was investigated to determine its pro-tumourigenic and pro-metastatic effects in OAC. Given the limited response of most OAC patients to chemotherapy and radiotherapy, and the implication of fractalkine in treatment resistance in other malignancies [7, 10, 194], the effect of fractalkine was also assessed in treatment resistant OAC cell lines. Furthermore, as E6130 effectively redirects NK cells towards tumour, its impact on OAC cancer cell lines and patient samples was assessed to determine potential therapeutic benefits and adverse effects. Our group has previously reported that fractalkine recruits NK cells to the omentum of OAC patients, where they undergo phenotypic alterations and apoptosis [69, 127]. Therefore, this study also evaluated the therapeutic potential of the NK cell therapy KHYG-1 in OAC, comparing its functionality to blood-derived NK cells. Overall, this investigation aimed to determine whether combining chemokine-targeted therapy with NK cell-based strategies represents a viable therapeutic approach for OAC.

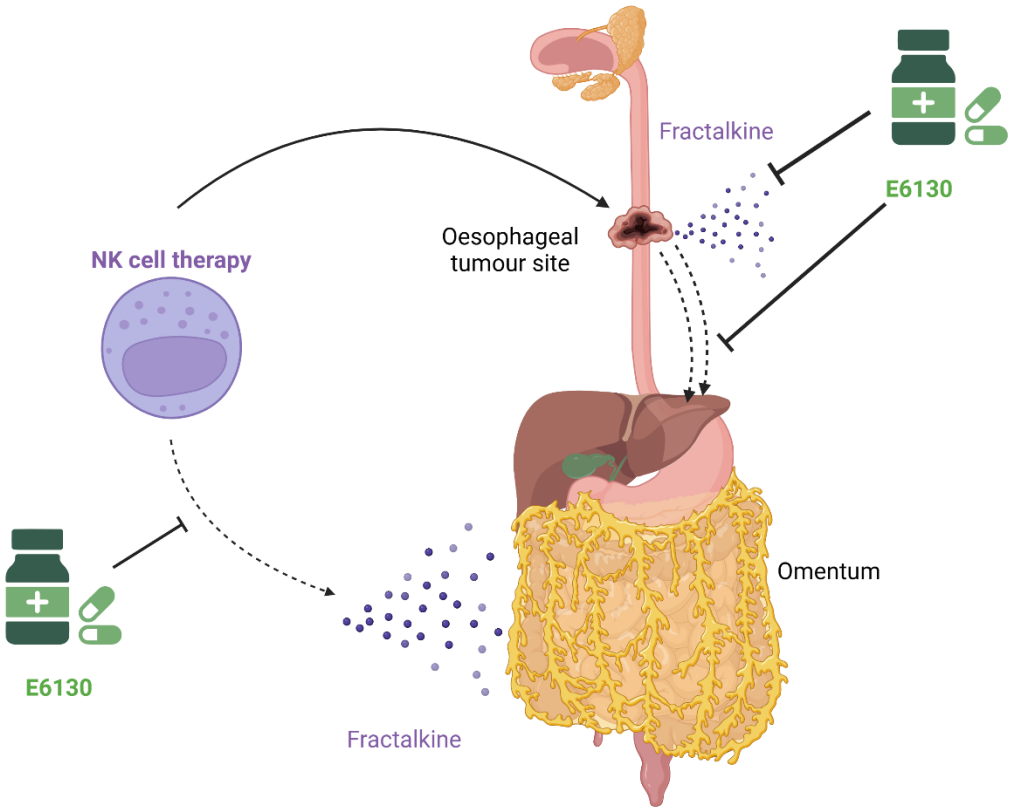

Figure 1.2: Hypothesis for this study

CX3CR1 modulator E6130 can prevent migration of NK cell therapy to the omentum and redirect them towards the oesophageal tumour site. Fractalkine increases OAC tumour growth and metastasis but E6130 can attenuate these effects. Combining NK cell therapy with E6130 can boost immune cell infiltration to the tumour site while directly reducing OAC tumour growth and metastasis. Created with Biorender.com

1.6 Hypotheses and Aims

Hypothesis: Fractalkine elicits pro-tumourigenic and pro-metastatic effects in OAC, which can be overcome with CX3CR1 modulator E6130.

The specific hypotheses and aims for this study are as follows:

Hypothesis 1: Fractalkine drives tumourigenic processes in OAC which can be reversed using the CX3CR1 modulator E6130.

Aims:

- Assess the surface expression of the fractalkine receptor CX3CR1 on OAC cell lines and soluble fractalkine levels in OAC cell line supernatants
- Elucidate the effects of fractalkine on OAC cell viability and proliferation and the potential of E6130 to reduce such effects.
- Explore whether the physiological conditions of the tumour microenvironment (acidosis, nutrient deprivation and hypoxia) impact CX3CR1 expression and elucidate the effect of fractalkine on OAC cell lines under such conditions.

Hypothesis 2: Fractalkine drives metastatic processes in OAC and the CX3CR1 modulator E6130 can limit such detrimental effects.

Aims:

- Investigate the effects of fractalkine and E6130 on FLO-1 cell cycle distribution
- Elucidate the effects of fractalkine and E6130 on FLO-1 cell invasion and epithelial-mesenchymal transition
- Assess CX3CR1 surface expression patterns on FLO-1 cells and its association with viability
- Investigate if CX3CR1 expression on FLO-1 cells relates to stemness and metastatic potential

Hypothesis 3: The CX3CR1 modulator E6130 elicits anti-tumour effects in OAC patient samples.

Aims:

- Investigate if E6130 alters LDH release and tumour cell viability in OAC patient tumour samples
- Evaluate fractalkine as a biomarker of tumour stage and treatment response in OAC serum and patient tissues
- Assess if E6130 alters NK cell activation, inhibition and cytotoxic markers in healthy donor blood and OAC patient blood
- Assess if E6130 alters NK cell activation, inhibition and cytotoxic markers in intratumoural NK cells from OAC patients

Hypothesis 4: NK cell therapy KHYG-1 holds potential for OAC but may be susceptible to the chemotactic cues of OAC omentum and immunosuppressive mechanisms of the OAC TME.

Aims:

- Compare phenotypical and functional markers of KHYG-1 cells to healthy donor blood-derived NK cells
- Assess migration of KHYG-1 cells towards visceral adipose and tumour conditioned media from OAC patients
- Investigate the effects of the soluble visceral adipose tissue and tumour microenvironment of OAC patients with or without obesity on KHYG-1 cell phenotype and function
- Evaluate if E6130 or AMG487 can block KHYG-1 cell migration to the adipose tissue conditioned media of OAC patients and whether the supplementation of IP-10 to the tumour conditioned media can increase KHYG-1 cell migration

Chapter 2 - Materials and Methods

2.1 Materials

Table 2.1: Table of reagents for media and buffers

Media	**Ingredients**
Complete Roswell Park Memorial Institute 1640 (cRPMI) media	500ml RPMI 1640 (Gibco, UK) supplemented with: -10% (v/v) Foetal Bovine Serum (FBS) (Sigma-Aldrich, USA) -1% (v/v) Penicillin-streptomycin (Lonza, Switzerland)
Complete Dulbecco's Modified Eagle's medium (cDMEM)	500ml DMEM (Gibco, UK) supplemented with: -10% (v/v) FBS (Sigma-Aldrich, USA) -1% (v/v) Penicillin-streptomycin (Lonza, Switzerland)
Media for conditioned media generation	500ml M199 (Gibco, UK), supplemented with: -500µl Gentamycin (Lonza, Switzerland)
KHYG-1 cell media	500ml RPMI 1640 (Gibco, UK) supplemented with: -10% FBS (Sigma-Aldrich, USA) -1% Penicillin-streptomycin (Lonza, Switzerland) -10ng/ml IL-2 (MedChemExpress, USA)
Buffers	**Ingredients**
Fluorescence-activated sorting (FACS) Buffer	500ml phosphate buffered saline (Gibco, UK) supplemented with: -2% foetal bovine serum (FBS) (Gibco, UK), -0.01% sodium azide (Sigma Aldrich, USA).
FACS Blocking Buffer	50% FACS Buffer 50% FBS (Sigma-Aldrich, USA)

Tumour Collagenase Buffer	5ml Hank's balanced salt solution (HBSS) (GE, USA), supplemented with: -4% BSA (Sigma, USA) -43µl collagenase type IV (1mg/ml) (Sigma, USA)
Lactate Dehydrogenase (LDH) storage buffer	200mM Tris-HCl 10% Glycerol 1% Bovine Serum Albumin (BSA)
Lysis Buffer for biopsy	Distilled H_2O, supplemented with: -200mM Tris HCL pH 8.0 -0.1% Triton X-100 -10% glycerol

Table 2.2: Table of reagents and kits used

Reagent	Vendor	Catalog number
Recombinant human fractalkine (CX3CL1)	Peprotech, UK	300-31-20G
E6130 (CX3CR1 modulator)	Medchem Express, USA	HY-107456
Recombinant human IP-10 (CXCL10)	R&D systems, USA	266-IP-010
AMG487 (CXCR3 antagonist)	Tocris Bioscience, UK	4487/10
Recombinant human IL-2	MedChemExpress, USA	HY-P7037-10ug
Recombinant human IL-12	Immunotools, Germany	11349123
Recombinant human IL-15	Peprotech, UK	200-15-10UG
Brefeldin A	Sigma, USA	B7651-5MG
Ficoll-Paque	GE, USA	17144003
Dimethyl Sulfoxide (DMSO)	Sigma Aldrich, USA	472301-100ML
FIX&PERM Cell Fixation and Permeabilization Kit	Nordic MUBio, Netherlands	GAS-002
eBioscience Foxp3 Staining Buffer Set	Fisher Scientific, USA	11500597

CountBright™ Absolute Counting Beads, for flow cytometry	ThermoFisher Scientific, USA	C36950
QCM ECMatrix Cell Invasion Assay, 96-well (8 µm), fluorimetric, 1 plate	Sigma Aldrich, USA	ECM555
Cell proliferation ELISA, BrdU (Colorimetric)	Sigma Aldrich, USA	11647229001
Cell Counting Kit 8 for quantification	Sigma Aldrich, USA	96992-500TESTS-F
LDH-Glo™ Cytotoxicity Assay	Promega, USA	J2380

2.2 Cell culture

2.2.1 Cell lines

2.2.1.1 OE33, OE33P, OE33R, OE33CisP and OE33CisR

The OE33 cell line was derived from a human Caucasian oesophageal carcinoma cell line and is cultured in cRPMI. This cell line was acquired from the European collection of cell cultures and was established from a 73-year-old female patient from the adenocarcinoma of the lower oesophagus. The tumour stage was IIA and was poorly differentiated.

The OE33 parental radiosensitive (OE33P) and OE33 radiosensitive (OE33R) cell lines were generated from the OE33 cell line by our department as previously described [309, 310]. OE33R cells were generated by irradiation at fractioned doses of 2 Gy X-Ray radiation, cumulative to 50Gy, to induce radio resistance, while OE33 cells were mock irradiated to maintain an age- and passaged-matched control. OE33 parental cisplatin sensitive (OE33CisP) and OE33 cisplatin resistant (OE33CisR) were generated from the OE33 cell line by our department as previously described [70, 310]. OE33CisR were generated by treating them with a metronomic dosing of cisplatin following cell splitting, while an age- and passaged-matched OE33 flask was mock treated. The OE33, OE33P, OE33R, OE33CisP and OE33CisR cell lines were cultured in cRPMI and were cultured in 75cm2 (T-75) filtered culture flasks (Thermo Scientific) as a monolayer, at 37°C in a 5% CO_2 humidified incubator (Thermo Forma, Steri-cycle, CO_2, incubator, Hepafilter). When cells

reached 70 to 80% confluency, they were sub-cultured. Growth medium was removed, and the cells were washed with 3ml of sterile phosphate buffer saline (PBS, Gibco, UK). Adherent cells were then lifted by adding 3ml of trypsin (Gibco, UK) and incubating the cells for 3 minutes at 37°C. A volume of 6ml of cRPMI was added to neutralise trypsin. The cell suspension was then transferred to a 15ml tube and centrifuged at 1400RPM for 3 minutes. The cell pellet was then resuspended and diluted at a ratio of 1:3 to 1:10, depending on their confluency. A volume of 1ml of cell suspension was then added to a fresh T-75 flask containing 9ml of cRPMI and the cells were maintained at 37°C in a 5% CO_2 humidified incubator.

2.2.1.2 FLO-1 and FLO-1^{LM} cell line

The FLO-1 cell line was derived from a primary distal oesophageal adenocarcinoma in a 68-year-old male patient, with many known mutations. The FLO-1^{LM} (Liver metastasis) cell line was established from the parental FLO-1 line after injecting FLO-1 cell line into mice, as described in the paper by David S. Liu *et al.* [311]. The cells were gifted to our department by Dr. Nicholas Clemons (Tumourigenesis and cancer therapeutics Lab, Peter MacCallum Institute, East Melbourne, Australia). FLO-1 and FLO-1^{LM} cell line were cultured in cDMEM. The same method was used to culture FLO-1 and FLO-1^{LM} cells as described previously for OE33 cells.

2.2.1.3 KHYG-1 cell line

The KHYG-1 cell line is derived from the peripheral blood of a 45-year-old woman with aggressive Natural Killer (NK) cell leukaemia and carry a point mutation in exon 7 of the TP53 (p53 gene). The cell line was acquired from DSMZ-German Collection of Microorganisms and cell cultures GmbH. The KHYG-1 cells were cultured in the KHYG-1 media detailed in table 2.1, with IL-2 added separately every time. The KHYG-1 cells were cultured in suspension in T-25 flasks (standing up) or 6 well plates at 37°C in a 5% CO2 humidified incubator. When cells reached 70 to 80% confluency, cells were sub-cultured by splitting them at a ratio of 1:3 to 1:4 every two to three days. For cell counting, the cells were centrifuged at 210xg for 5 minutes and supernatant was discarded.

2.3 Ethical approval and patient samples

2.3.1 Ethical approval

This study was carried out in accordance with the declaration of Helsinki ethical guidelines for medical research involving human subjects. St James's Hospital/Tallaght University Hospital joint research ethics committee has given full ethical approval for this study. All samples and data were collected and stored in accordance with Good Clinical Practise (GCP) and General Data Protection Regulations (GDPR).

All patients consented prior to sample collection and were informed that their participation was strictly voluntary and that they may withdraw from the study at any time. All patients consented to the use of their clinical data for this study.

Healthy donors provided informed consent prior to peripheral blood collection. Samples were anonymised as per our ethical approval and in accordance with GDPR. This study had full ethical approval from the Faculty of Health Sciences Ethics Committee at Trinity College Dublin.

2.3.2 Patient samples

Omental, liver, normal oesophageal, and normal gastric tissue were collected at the time of surgical resection. Peripheral venous blood and tumour biopsies were collected at the time of surgical resection or re-staging endoscopy from consenting patients, undergoing oesophagectomy or gastrectomy at St. James's Hospital, Dublin.

A total of 48 samples were collected for this study from patients with confirmed cases of oesophageal adenocarcinoma (OAC), gastric carcinoma (GC), or oesophago-gastric junctional adenocarcinoma (OGJ) between 2019 and 2024. OAC patient serum samples were obtained from the upper GI biobank within the Department of Surgery. The full demographics of patient samples used in chapter 5 and 6 are described in **[Table 2.3]**. All samples were given a pseudo-anonymised code by the biobank manager within the Department of Surgery as per GDPR guidelines. The biobank manager provided clinical data on tumour stage, treatment regiment, treatment response, age, sex and BMI for all pseudonymised patient samples. The study cohort comprised 35 males and 13 females, reflecting the higher prevalence of OAC in males. The mean age of the cohort was 66 years. The majority of patients presented with disease at stage T2 or T3, and 66% were

nodal positive. The mean body mass index (BMI) at the time of surgery was 26.8 kg/m², with 62% of patients classified as overweight or with obesity. Neo-adjuvant chemoradiotherapy (CRT) was administered to 79% of patients, and 58% received the FLOT chemotherapy regimen, consisting of 5-fluorouracil, leucovorin, oxaliplatin, and docetaxel. Among patients for whom tumour regression grade (TRG) data were available, 78% exhibited a low or poor response to neo-adjuvant therapy (TRG 3–5).

Table 2.3: Demographics information for patient samples in Chapter 5 and Chapter 6

Mean age (years)	66
Sex ratio (M: F)	35:13
Diagnosis (n° of patients)	
OAC [a]	22
OGJ [b]	14
Gastric	12
Tumour Stage [c] (n° of patients)	
T0	2
T1	4
T2	11
T3	23
T4	6
Nodal status[d] (n° of patients)	
Positive	29
Negative	15
BMI [e] (n° of patients)	
Mean BMI (kg/m^2) *	26.8
Underweight (BMI<19.9)	1
Normal Weight (BMI 20-24.9)	16
Overweight (BMI 25-29.9)	18
Obese (BMI >30)	10
Received Neoadjuvant CRT	38
Treatment received [g]	

FLOT	28
CROSS	9
FOLFOX	1
Naïve	10
Tumour regression grade [h]	
TRG 1-2	8
TRG 3-5	28
Evidence of recurrence [i]	
Patients who developed recurrence (primary or metastatic disease)	15
Patients who show no evidence of disease recurrence	33
Patient survival [i]	
Alive	42
Deceased	6

[a] Oesophageal adenocarcinoma, [b] Oesophageal-gastric junctional adenocarcinoma, [c] stage unavailable for 2 patients, [d] nodal status unavailable for 4 patients. [e] BMI unavailable for 3 patients. [g] FLOT (5-fluorouracil, leucovorin, oxaliplatin and docetaxel), CROSS (paclitaxel, carboplatin, radiotherapy), FOLFOX (5-fluorouracil, leucovorin, oxaliplatin). [h] Tumour regression grade unavailable for 2 eligible patients. [i] Patient data last updated on the 25/07/2025.

2.3.3 Serum collection

Whole blood was collected in 9ml red top vacutainer tubes suitable for collecting serum (BD Biosciences, USA). Blood was centrifuged at 10000RPM for 10 minutes. The upper layer consisting of the serum was pipetted into labelled cryovials and stored at -70°C for future use.

2.3.4 Healthy donor blood

Healthy donor blood was taken fresh (on the day) from consenting donors using 9ml red top vacutainer tubes suitable for peripheral blood (BD Biosciences, USA).

2.3.5 Conditioned media generation

Visceral adipose tissue (VAT) from the omentum and liver were sampled from OAC, GC and OGJ patients at the beginning of surgery. Adipose conditioned media (ACM) was generated by weighing the VAT and chopping it into approximately 0.5g pieces using sterile scissors in a petri dish. Fresh media at a ratio of 1g in 2ml of serum-free M199 media (Gibco, UK) supplemented with 500µl gentamycin (Lonza, Switzerland) was then added to the chopped tissue. The VAT was cultured at 37°C and 5% CO_2 for 72 hours. The ACM was then filtered through a 70µm mesh filter (Corning, USA) and the media was collected and stored at -70°C. Liver conditioned media (LCM) was generated by weighing the liver and chopping into the well of a 24 well plate using sterile scissors. A volume of 350µl of serum-free M199 media (Gibco, UK) supplemented with 500µl gentamycin (Lonza, Switzerland) were added to the chopped pieces of liver in the well and they were incubated at 37°C and 5% CO_2 for 72 hours. The LCM was then collected from the plate in labelled cryovials and stored at -70°C. Tumour tissue conditioned media (TCM), Normal Oesophageal tissue Conditioned Media (NOCM) and Normal Gastric tissue Conditioned Media (NGCM) was generated by culturing tissue in 1ml of serum-free M199 media (Gibco, UK) supplemented with 500µl gentamycin (Lonza, Switzerland)) in a 24 well plate at 37°C and 5% CO_2 for 24 hours. Following a 24-hour incubation, the conditioned media was collected into labelled cryovials, and tissue was snap frozen for subsequent protein quantification. Snap frozen biopsies and conditioned media were stored at -70°C **[Figure 2.1].**

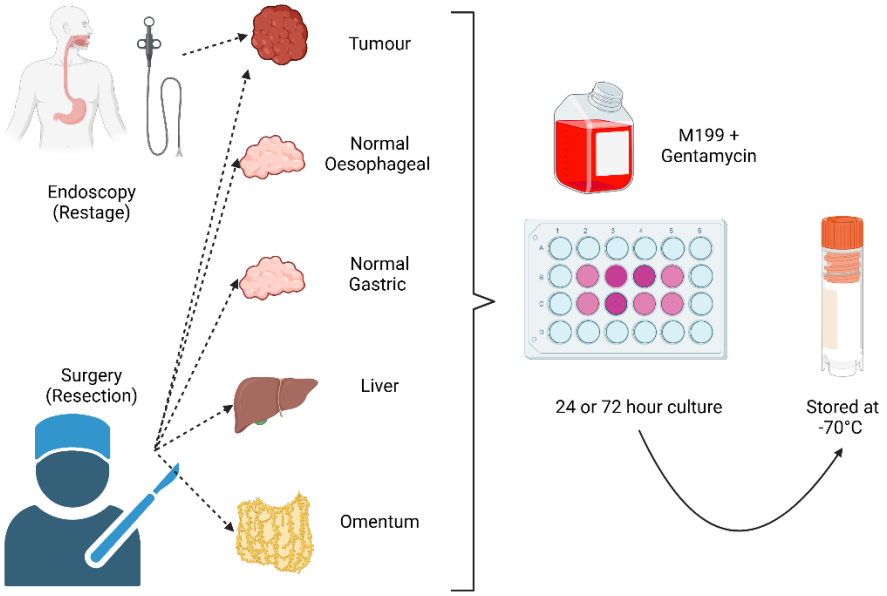

Figure 2.1: Generation of conditioned media from OAC, GC and OGJ patient-derived tissues

Left: Schematic representation of collection of VAT from the omentum, liver, normal gastric and oesophageal and tumour from surgery or endoscopy at the time of resection or restage. **Right:** Tissues are subsequently cultured in M199 media supplemented with gentamycin for 24 hours (tumour, normal oesophageal and gastric samples) or 72 hours (VAT and liver). Media is then collected, and samples are stored for long term storage at -70°C. Created with Biorender.com

2.3.6 Surface phenotyping of patient-derived tumour

2.3.6.1 Enzymatic digestion of tumour

Tumour biopsies were sampled from OAC, GC and OGJ patients at the time of restaging or surgical resection. Tissues were enzymatically digested to generate a mixed single cell suspension of tumour cells and intratumoural immune cells.

First, the tissue biopsy was divided into 2 equal parts and placed in 1ml of serum-free M199 media (Gibco, UK) supplemented with 500µl gentamycin (Lonza, Switzerland)) in a 24 well plate. The first piece of tissue was treated with 4.9nM E6130 and the second was treated with 0.01% DMSO (vehicle control for E6130) for 24 hours at 37°C and 5% CO_2. Following a 24-hour incubation, the pieces of tumour biopsy were teased apart using sterile tweezers and scalpel. Tumour collagenase buffer consisting of 5ml Hanks' Balanced Salt solution (HBSS) (GE, USA), supplemented with 4% bovine serum albumin (Sigma, USA) and 43µl collagenase Type IV (1mg/ml, Sigma, USA) was added to each biopsy in a 50ml tube and incubated for 30 minutes in a shaking incubator at maximum agitation at 37˚C (Thermofisher, UK). The digested biopsy sample was filtered using a 40µm filter (BD, USA) to remove debris. The filtered sample was then resuspended in 5ml of PBS and centrifuged for 3 minutes at 1400RPM. Following centrifugation, the supernatant was poured off and the pellet was resuspended in 1ml of PBS for subsequent cell counting.

2.3.6.2 Phenotypic analysis of tumour and intratumoural immune cells by flow cytometry

To assess the effects of E6130 on cell viability and phenotype, the single cell suspension from the tumour samples were analysed by flow cytometry. First, cells were stained for cell viability using zombie aqua staining described in section 2.5.3.2. Cells were washed in 500µl of FACS buffer and then centrifuged at 1400RPM for 3 minutes. The supernatant was discarded, and this last step was repeated once more. Cells were then incubated for 5 minutes at room temperature in the dark in 500µl of FACS blocking buffer. Cells were then washed twice in FACS buffer as described previously. Following cell resuspension in 100µl of FACS buffer, cells were stained with antibodies against the extracellular markers listed in **Table 2.2** at 4°C for 30 minutes in the dark. The cells were then washed twice with FACS buffer as described previously and resuspended in 200µl of FACS Buffer. Cells

were acquired immediately using BD FACs CANTO II (Becton, Dickinson and Company, New Jersey, United States).

Table 2.4: Fluorochrome conjugated flow cytometry antibody panels for intratumoural studies

Antibody	Volume (µl)	Manufacturer	Clone
CD56-FITC Viobright	1	Miltenyi Biotec	REA196
CX3CR1-PE	1	Miltenyi Biotec	REA385
CD3-APC-Cy7	1	Biolegend	HIT3a
PD-1-PerCP-Cy5	2	Biolegend	ETH12.2H7
TRAIL-PE-Cy7	1	Biolegend	RIK-2
NKp30-PerCP-Cy5.5	1	Biolegend	P30-15
CD45-APC	1	Biolegend	2D1
CD31-Pacific Blue	1	Biolegend	WM59
Zombie Aqua (Dye)	1 in 1000	Biolegend	N/A

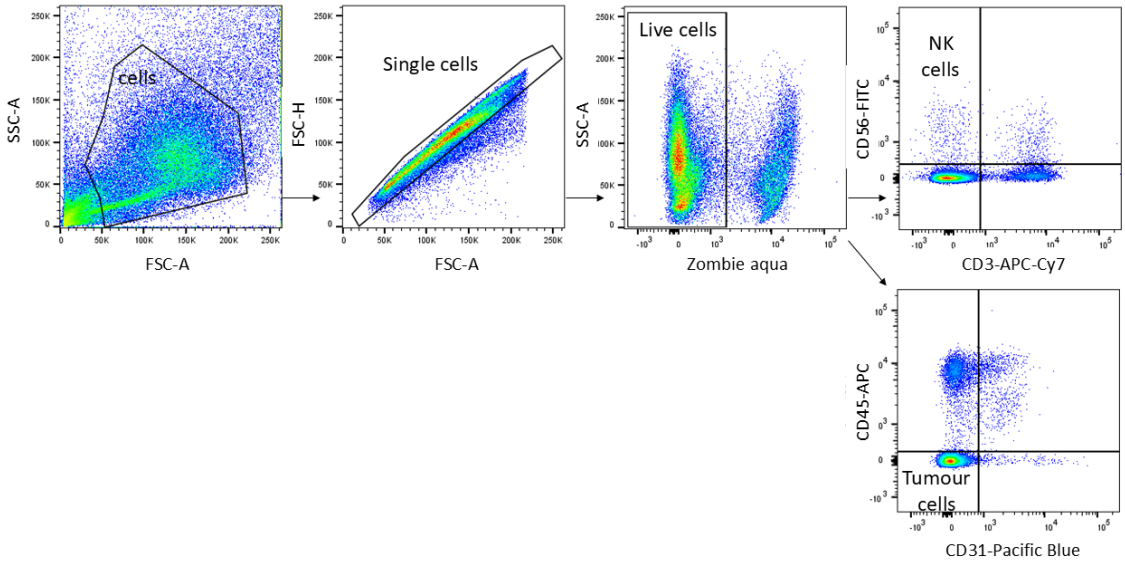

Figure 2.2: Representative dot plots showing gating in tumour samples.

The cell population was first gated based on size and granularity using FSC-A and SSC-A (left). Following this, cells were gated using FSC-H and FSC-A to exclude doublets (centre left). Live cells were gated using Zombie Aqua (centre right). Intratumoural NK cells were gated as $CD56^{+}CD3^{-}$ cells within this gate (top right). Tumour cells were gated as $CD31^{-}CD45^{-}$ cells within the live cell gate (bottom right).

2.3.7 Preparation of peripheral blood mononuclear cells

Isolation of peripheral blood mononuclear cells (PBMC) was performed under sterile conditions within a laminar flow hood, utilising density gradient centrifugation. Blood samples were diluted at a 1:2 ratio with PBS. Using a Pasteur pipette, 35ml of the diluted blood was gently layered onto 15ml of Ficoll-Paque (GE, USA) in a 50ml tube **[Figure 2.3].** The samples were then centrifuged at 400xg for 25 minutes without brakes. Following centrifugation, the buffy coat layer (white and cloudy) located beneath the plasma was carefully collected with a Pasteur pipette and transferred to a new 50ml tube, which was subsequently filled to 50ml with PBS **[Figure 2.3]**. The cells were centrifuged at 800xg for 5 minutes. The PBS supernatant was discarded by inverting the tube, and the remaining pellet was vortexed briefly. Another 50ml of fresh PBS was added, and the cells were centrifuged again at 400xg for 3 minutes. The supernatant was removed by inverting the tube, and the pellet was vortexed once more **[Figure 2.3]**. Finally, the pellet was resuspended in 1ml of cRPMI, and the cell count was determined according to the protocol described in section 2.4.

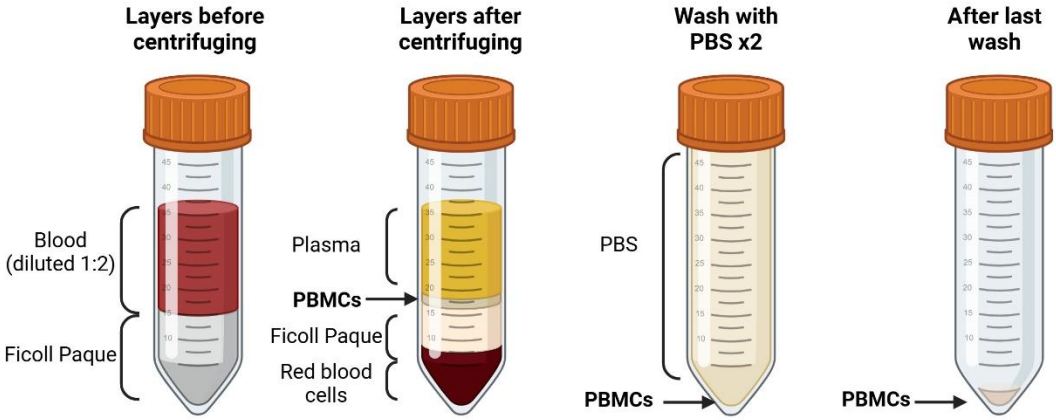

Figure 2.3: Peripheral Blood Mononuclear Cell isolation using density gradient centrifugation.

Schematic representation of PBMC isolation with Ficoll Paque. Following centrifugation, blood is separated into different layers according to their densities, this allows to isolate the PBMC layer, which is subsequently washed with PBS. Created with Biorender.com

2.4 Cell Counting

Cells were counted using trypan blue (Sigma-Aldrich, USA) and a haemocytometer (Neubauer glass haemocytometer 0.01mm depth, Marienfeld-Superior). Cells were resuspended in 1ml of media and 10µl of this cell suspension was mixed thoroughly with 90µl of trypan blue. A volume of 10µl of this cell solution was added on the haemocytometer and viable cells with a non-permeable membrane (unstained) were counted under a 20X magnification light microscope (Nikon Eclipse E200 and Inverso TC100 from Scientific Laboratory supplies). Cells in the four corners of the haemocytometer were counted and the final number of cells was calculated using this formula:

$$Average\ number\ of\ cells * dilution\ factor\ X10^4 = number\ of\ cells/ml$$

2.5 Methods for OAC cell line assays

2.5.1 Cell treatments

2.5.1.1 Treatment of OAC cell lines with recombinant fractalkine for subsequent analysis of cell viability and cell proliferation

To determine the effects of fractalkine on OAC cell viability and proliferation, OAC cell lines OE33, OE33P, OE33R, OE33CisP, OE33CisR, FLO-1 and FLO-1^{LM} were cultured as outlined in section 2.2.1. OE33, OE33P, OE33R OE33CisP and OE33CisR cell line were passaged, counted, and seeded at a density of $0.15x10^6$ cells/ml of cRPMI in a 96 well plate and FLO-1 and FLO-1^{LM} were passaged, counted, and seeded at a density of $0.18x10^6$ cells/ml of cDMEM in a 96 well plate left to adhere overnight. Cells were either left untreated, treated with 0.1% water (vehicle control for fractalkine) or 0.1, 0.5, 1, 5, 10, 50, 100, 200ng/ml of recombinant fractalkine (Peprotech, UK) at 37°C in a 5% CO_2 humidified incubator for 24 hours.

2.5.1.2 Treatment of OAC cell lines with E6130 for subsequent cell viability and cell proliferation assay

To ascertain whether modulation of CX3CR1 could reverse any fractalkine-elicited effects, OAC cell lines OE33, OE33P, OE33R, OE33CisP, OE33CisR, FLO-1 and FLO-1^{LM} were cultured and seeded as outlined in section 2.2.1 and 2.5.1.1. Cells were either pre-treated for an hour with 0.01% DMSO (vehicle control for E6130) or with 0.1, 1, 4.9, 10, 100 and

100nM of E6130 (CX3CR1 modulator) (Medchem express, USA) followed by 24-hour treatment with 100 and 200ng/ml of recombinant fractalkine for OE33 cells, or 10 and 100ng/ml of recombinant FLO-1 and FLO-1^{LM} cells or 10, 100 and 200ng/ml for OE33P, OE33R, OE33CisP and OE33CisR cells at 37°C in a 5% CO_2 humidified incubator for 24 hours. Cells were also treated with 0.1% water alone, 0.01% DMSO alone, 4.9nM E6130 alone, 10, 100 or 200ng/ml of recombinant fractalkine alone or left untreated at 37°C in a 5% CO_2 humidified incubator for 24 hours.

2.5.1.3 Assessing the effects of cell culture under conditions of nutrient deprivation, hypoxia and acidic pH on CX3CR1 surface expression by OAC cell lines

OE33, OE33P, OE33R, OE33CisP, OE33CisR, FLO-1 and FLO-1^{LM} were seeded as described in section 2.5.1.1 in 12 well plates and left to adhere overnight. To mimic some of the conditions of the tumour microenvironment to induce stress on cells, cells were cultured for 24 hours with either cRPMI or cDMEM, cultured with cRPMI or cDMEM with different ranges of FBS (0%, 0.5%, 5%), cultured with glucose-free cRPMI or cDMEM, cultured with cRPMI or cDMEM at increasing levels of acidity (pH 6.6 and 5.5) or cultured in cRPMI or cDMEM under hypoxic conditions (0.5% O_2) using the H35 Don Whitley Hypoxystation (Don Whitley Scientific, UK). The acidity was altered using concentrated hydrochloric acid (1M, Sigma Aldrich, USA) and a pH meter (Accumet AB150, Fisher Scientific, USA). Following the 24-hour treatment, cells were stained for flow cytometry analysis as indicated in section 2.5.3.2 and 2.5.3.3.

To assess the effects of recombinant fractalkine and E6130 treatment on FLO-1 cells under the conditions of nutrient deprivation, hypoxic conditions and acidic pH treatment, FLO-1 cells were seeded as described in section 2.5.2.1 and were left to adhere overnight in a 96 well plate. Cells were cultured for 24 hours with cDMEM, or 0% FBS cDMEM, or cDMEM pH6.6, or cDMEM under hypoxic conditions (0.5% O2). Cells were then treated with recombinant fractalkine and/or E6130 as described in section 2.5.2.1 and 2.5.2.2 for 24 hours. Cell viability was assessed following 24-hour treatment as described in section 2.5.2.1.

2.5.2 Cell assays

2.5.2.1 Cell viability assay

The cell counting Kit-8 (CCK-8) assay (Sigma Aldrich, USA) was used to assess the viability of OAC cell lines following fractalkine and/or E6130 treatment. Cells were treated for 24 hours as described in section 2.5.1.1 and 2.5.1.2 and 2.5.1.3 for FLO-1 cell line CCK8 assay with TME conditions. Following the 24-hour treatments, growth medium was changed and 5µl/well of CCK-8 solution was added to each well. The 96 well plate was then incubated at 37°C in a 5% CO2 humidified incubator in the dark for a duration between 1.5 hours and 3.5 hours, depending on the number of cells present in the wells. The optical density was measured twice (at 2.5 hours and 3.5 hours for OE33, OE33P, OE33R, OE33CisP and OE33CisR cells and at 1.5 hours and 2.5 hours for FLO-1 and FLO-1^{LM} cells) at 450nm using the GloMax explorer multimode microplate reader (Nan-Luc Technology, Promega, USA). Wells with no cells and just growth media with 5µl of CCK-8 solution acted as a blank and the value obtained was subtracted from all other values. Experiments were carried out in triplicate i.e. 3 technical replicates and viability was expressed as a percentage relative to the untreated OAC cells. Cell viability rates were calculated using the following formula: [(T – B) / (NT – B)] x 100 where T is the absorbance of the treated cells, B is the absorbance of the blank sample containing complete medium without cells, and NT is the absorbance of the non-treated cells.

2.5.2.2 Cell proliferation assay

The cell proliferation ELISA, Bromodeoxyuridine (BrdU) colorimetric assay (Sigma Aldrich, USA) was used to assess the proliferation of OAC cell lines following fractalkine and/or E6130 treatment. Cells were treated as described in section 2.5.1.1 and 2.5.1.2. BrdU labelling solution was added to the cells at 10µl/well, 2 hours following the second treatment with recombinant fractalkine, and the cells were incubated at 37°C in a 5% CO_2 humidified incubator. Following 24 hours of fractalkine treatment, medium was removed by tapping and cells were dried for 15 minutes using a hair dryer. FixDenat was added at 200µl/well and cells were incubated for 30 minutes at room temperature. The FixDenat solution was removed by tapping off and 100µl/well of anti-BrdU-POD working solution was added for 90 minutes at room temperature. The anti-BrdU-POD solution was removed by tapping off and the cells were rinsed three times by adding 200µl/well of

washing solution and tapping off the washing solution. A volume of 100µl/well of substrate solution was added and cells were incubated until colorimetric detection was sufficient, for approximately 5 to 10 minutes. Stop solution was added at 25µl/well and cells were incubated for 1 minute on a shaker at 300RPM The optical density was measured at 450nm using the GloMax explorer multimode microplate reader (Nan-Luc Technology, Promega, USA). Wells with no cells/BrdU labelling solution/anti-BrdU-POD acted as a blank and the value obtained was subtracted from all other values. Wells with cells/no BrdU labelling solution/anti-BrdU-POD, no cells/no BrdU labelling solution/anti-BrdU-POD, cells/BrdU labelling solution/no anti-BrdU-POD and no cells/BrdU labelling solution/ no anti-BrdU-POD were used as controls. Each experiment was carried out in triplicate i.e. 3 technical replicates and viability was expressed as a percentage relative to the untreated OAC cells. Cell proliferation rates were calculated using the same formula used for CCK8 assays described in section 2.5.2.1.

2.5.2.3 QCM 96-well cell invasion and migration assay.

The QCM 96-Well Cell Invasion Assay (Fluorometric) (ECM555, EMD Millipore Corp., USA) was used to investigate the effect of fractalkine and/or E6130 on the migration of FLO-1 cells towards either recombinant fractalkine or FLO-1^{LM} cell supernatants (to simulate the soluble cues of the metastatic liver microenvironment) according to the manufacturer's instructions. FLO-1 cells were starved overnight in serum-free media (RPMI + 1% penicillin/streptavidin). Following 16 hours, FLO-1 cells were passaged, counted, left untreated or pretreated with 0.01% DMSO or 4.9nM E6130 for 1 hour. The collagen layer was rehydrated by adding 100µl of pre-warmed serum free media to the inserts for 30 minutes at room temperature. A volume of 75µl of the media in the inserts was carefully removed to not disturb the membrane. For fractalkine treatment wells, cells were either treated with 0.1% water or 100ng of recombinant human fractalkine. Cells were seeded at a density of $0.8x10^6$ cells/ml in a volume of 100µl in each insert. In the lower chambers of the plate, serum free media was added to act as a negative control and media containing 20% FBS was added to act as a positive control. The other wells contained either serum-free media with 100ng of fractalkine, or FLO-1^{LM} cell supernatant (collected from a confluent flask of FLO-1^{LM} cells). cDMEM was also added to some wells to act as a control for the FLO-1^{LM} supernatants. The inserts were then carefully placed on top of

the lower chambers, in direct contact with the media below. The plate was incubated for 24 hours at 37°C, 5% CO_2.

Following 24-hour incubation, cells and media remaining in the upper compartment of the insert were gently removed. A volume of 150µl of pre-warmed cell detachment solution was added to each well of a new 96 well plate. The inserts were placed in the cell detachment solution and incubated for 30 minutes at 37°C in a 5% CO_2 humidified incubator. During that time, the inserts were gently tilted 3-4 times to dislodge the cells from the bottom of the membrane. To detect cells that migrated towards media, 50µl of CyQuant GR dye diluted at a ratio of 1:75 in 4X lysis buffer was added to the wells. The cells were incubated for 15 minutes at room temperature in the dark. A volume of 100µl from each well was transferred to a 96 well plate suitable for fluorescence reading. The relative fluorescence unit (RFU) was measured at 480/520nm using the GloMax explorer multimode microplate reader (Nan-Luc Technology, Promega, USA). Wells containing no cells with cell detachment buffer, CyQuant dye and lysis buffer acted as a blank and the value obtained was subtracted from all other values.

Percentage of cells were determined by running a fluorescent cell dose curve. FLO-1 cells were seeded at different volumes in cell detachment buffer. A volume of 150µl of this cell detachment buffer was mixed with 50µl of CyQuant GR dye diluted at a ratio of 1:75 in 4X lysis buffer. The RFU was measured as described above.

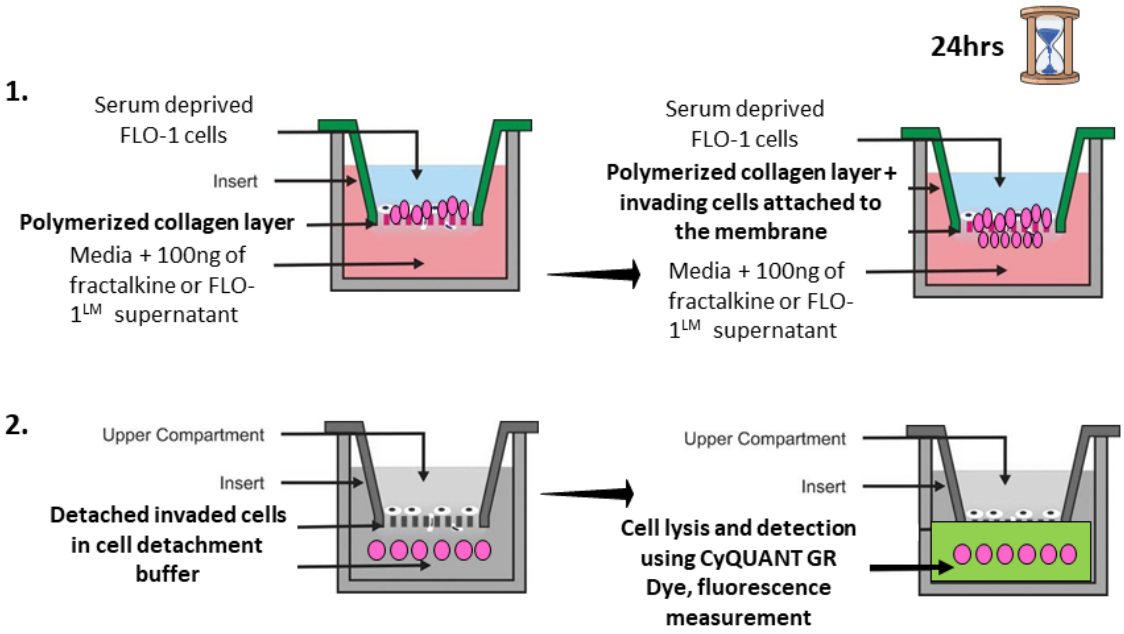

Figure 2.4: Schematic workflow assessing OAC collagen-based cell invasion towards fractalkine or FLO-1^{LM} cell conditioned media

(1) Serum-deprived cells were gently added to the insert, composed of a polymerized collagen layer to allow them to invade to lower chamber, containing media (RPMI) + 100ng of fractalkine or FLO-1^{LM} cell supernatant. Cells were incubated at 37°C in a 5% CO_2 humidified incubator for 24 hours. **(2)** To detach cells from the collagen layer, they were incubated in cell detachment buffer and subsequently lysed and detected by CyQuant GR Dye. Their fluorescence was measured using a plate reader.

2.5.3 Flow cytometric analysis of OAC cell cycle, surface marker expression and transcription factor expression

Unstained controls were subject to the same protocols as their stained counterparts, except for the addition of flow cytometry antibodies.

2.5.3.1 Cell cycle

FLO-1 cells were seeded as described in section 2.5.1.1 in a 6 well plate and left overnight to adhere. Cells were treated with E6130 +/- fractalkine, their respective controls or left untreated as described in section 2.5.1.2 for 24 hours. Cells were trypsinised then washed twice with PBS and resuspended in 1ml of PBS. Cells were fixed by adding 2.5ml of 90% ice cold ethanol (v/v in deionised water) dropwise while vortexing to prevent cell clumping. Cells were incubated for 30 minutes in the dark at room temperature. Cells were washed, resuspended in 1ml of PBS and stored at 4°C overnight until staining. Cells were stained with 250µl of PI stain ((PBS/PI (0.025mg/mL)/RNAase A (0.1mg/mL)/Triton X-100 (0.1%)) for 30 minutes at 37°C, in the dark. Cells were acquired using BD FACs CANTO II (BD Biosciences) and FACS Diva software (BD, USA) and analysed using FlowJo Version 10 software (BD, USA).

2.5.3.2 Zombie aqua staining

To assess for viable cells, cells were first washed by resuspending in 500µl of PBS and centrifuging at 1400RPM for 3 minutes. This process was repeated twice. Cells were resuspended in 100µl of PBS and stained with 1 in 1000 dilution of Zombie Aqua viability stain (Biolegend, USA) for 15 minutes at room temperature in the dark. The next staining steps were continued.

2.5.3.3 Surface staining of OAC cell lines for flow cytometric analysis

Following the 24-hour treatment described in section 2.5.1.1 and/or 2.5.1.2 or 2.5.1.3 or following no treatment, all OAC cell lines were lifted using 200µl of trypsin per well, neutralised with 300µl of cRPMI or cDMEM and transferred to FACS tubes. Following cell staining for viability described in section 2.5.3.2, cells were washed in 500µl of FACS buffer and the cells were then centrifuged at 1400RPM for 3 minutes. The supernatant was discarded, and this last step was repeated once more. After resuspending cells in 100µl of FACS buffer, all OAC cell lines were stained with CX3CR1-PE (Miltenyi Biotec), to assess

CX3CR1 expression on OAC cell lines. FLO-1 cells were stained with CD24-BV421, CD34-FITC, CD44-APC, CD71-PE-Cy7 and CD98-APC-Cy7 (Biolegend, USA) to assess stem cell marker and metabolism marker expression. Cells were stained for 30 minutes at 4°C in the dark. The cells were then washed twice with FACS buffer as described previously and resuspended in 200µl of FACS Buffer. If not analysed immediately, cells were fixed with 1% paraformaldehyde (ChemCruz, USA) solution. Cells were resuspended in 1% paraformaldehyde for 15 minutes in the dark at room temperature. Cells were resuspended in FACS buffer and then centrifuged at 1400RPM for 3 minutes. The supernatants were removed and cells were resuspended in 200µl of FACS buffer. Fixed cells were stored at 4°C until acquired. Unstained controls were subject to the same protocols as their stained counterparts, except for the addition of flow cytometry antibodies. Cells were acquired using BD FACs CANTO II (BD Biosciences) and FACS Diva software (BD, USA) and analysed using FlowJo Version 10 software (BD, USA).

2.5.3.4 Transcription factor staining for FLO-1 cells to assess expression of epithelial-mesenchymal transition markers.

To assess expression of epithelial-mesenchymal transition (EMT) markers on FLO-1 cells treated with recombinant fractalkine and E6130 as described in section 2.5.1.1 and 2.5.1.2, cells were first stained with Zombie Aqua viability dye as described in section 2.5.3.2. Following two FACS buffer washes as described previously, FLO-1 cells were stained for extracellular markers CD324 (E-cadherin)-VB FITC and CX3CR1-BV421 (Miltenyi Biotec, Germany) for 30 minutes at 4°C in the dark. Cells were then washed with FACS buffer as described previously. Cells were then stained for transcription factor staining according to manufacturer's instruction using FoxP3 staining kit (eBioscience, USA). A volume of 500µl of FoxP3 Fixation/Permeabilization working solution (diluting 1 part Fixation/Permeabilization concentrate with 3 parts Fixation/Permeabilization diluent) was added to each tube and cells were incubated for 60 minutes at room temperature in the dark. A volume of 1ml of 1X Permeabilization Buffer (10X Permeabilization Buffer diluted with distilled water) was added to each tube and centrifuged at 600xg for 5 minutes. The supernatant was discarded, and the pellet was resuspended. Cells were then resuspended and stained immediately with SLUG-PE and Vimentin-APC (Miltenyi Biotec, Germany) for 30 minutes at room temperature in the dark. 1ml of 1X Permeabilization Buffer was

added to each tube, and they were subsequently centrifuged at 600xg for 5 minutes. The supernatant was discarded, and cells were resuspended in 200µl of FACS. Cells were acquired using BD FACs CANTO II (BD Biosciences) and FACS Diva software (BD, USA).

2.5.3.5 Cell sorting of FLO-1 cells

FLO-1 cells reaching 80 to 90% confluency were scraped in PBS. Cells were then washed once by adding 1ml of PBS and centrifuging at 1400RPM for 3 minutes. This process was then repeated with FACS buffer. Cells were stained with CX3CR1-PE (Miltenyi Biotech) for 30 minutes at 4°C in the dark. The cells were then washed twice with FACS buffer as described before and resuspended in 1ml of FACS buffer. $CX3CR1^-$ and $CX3CR1^+$ cells were immediately sorted using BD FACS Aria Fusion High Performance Cell Sorter housed in a Class II Type A2 biosafety cabinet and following gating in **[Figure 2.5]**. Cells were subsequently washed with cDMEM, counted, and seeded at a density of 8 $x10^4$ cells/ml in cDMEM in a 24 well plate for 4 days to allow cells to recover. To act as a control, cells that were used for an unstained control to gate on $CX3CR1^-$ and $CX3CR1^+$ cells during cell sorting process were also washed and seeded in cDMEM at the same cell density as $CX3CR1^-$ and $CX3CR1^+$ cells. Half of the cells were treated with 100ng/ml of fractalkine, and the others were treated with 0.1% water for 24 hours and viability was assessed by CCK8 assay as described in section 2.5.2.1. Following the CCK8 assay, cells were immediately lifted with 100µl of trypsin, neutralised with 200µl of cDMEM and subsequently washed twice with PBS as described before. Cells were stained with Zombie Aqua viability dye (Biolegend, USA) as described in section 2.5.3.2. Cells were then washed twice with FACS buffer as described before and were then stained with CX3CR1-PE (Miltenyi Biotec) as described in section 2.5.3.3. Cells were then washed twice with FACS buffer and resuspended with 200µl of FACS Buffer for cells to be acquired using BD FACs CANTO II (BD Biosciences). This flow staining process was also performed 4 days and 6 days following cell sorting on $CX3CR1^-$ cells and control cells only as they were too few $CX3CR1^+$ cells. Cell sorting was performed by Orlaith Walsh in the School of Biochemistry and Immunology at the Flow Cytometry facility in the Trinity Biomedical Sciences Institute (TBSI).

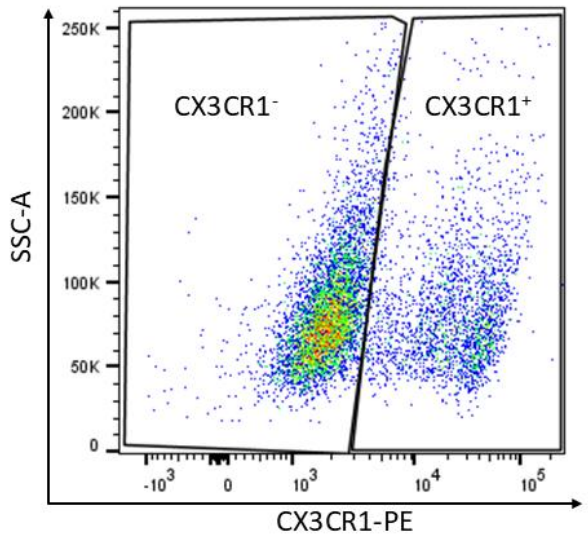

Figure 2.5: Representative dot plot showing flow cytometry gating strategy for FLO-1 cell sorting by CX3CR1$^-$ and CX3CR1$^+$ population

FLO-1 cell population were first gated using gating showed in **[Figure 2.6]** and CX3CR1$^-$ and CX3CR1$^+$ cells were gated based on SSC-A and CX3CR1-PE. An unstained control was used to create the CX3CR1$^+$ gate.

Table 2.5: Fluorochrome conjugated flow cytometry antibody panels for OAC cell line studies

Antibody	Volume (µl)	Manufacturer	Clone
Extracellular staining			
CD324 (E-cadherin) - Vio Bright FITC	1	Miltenyi Biotec	REA811
CX3CR1-PE	1	Miltenyi Biotec	REA385
CX3CR1-BV421	1	Biolegend	2A9-1
CD24-BV421	1	Biolegend	ML5
CD34-FITC	1	Biolegend	581
CD44-APC	1	Biolegend	C44Mab-5
CD71-PECy7	1	Biolegend	CY1G4
CD98- APC/Cy7	1	Biolegend	MEM-108
Transcription factor staining			
Vimentin-APC	1	Miltenyi Biotec	REA409
SLUG-PE	1	Miltenyi Biotec	REA404
Viability staining			
Zombie Aqua (Dye)	1 in 1000	Biolegend	N/A

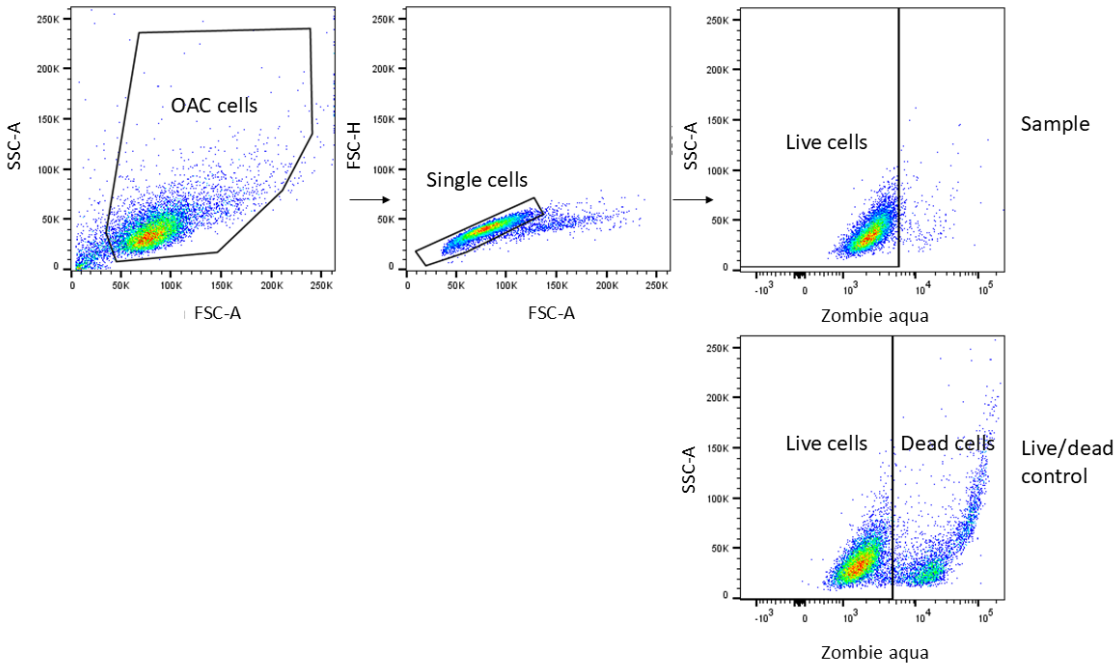

Figure 2.6: Representative dot plots showing flow cytometry gating strategy for OAC cells

The cell population was first gated based on size and granularity using FSC-A and SSC-A (left). Following this, cells were gated using FSC-H and FSC-A to exclude doublets (centre left). Live cells were gated using Zombie Aqua (centre right). A live/dead cell control was used to gate on live cells only (bottom right).

2.6 Assessing the effects of E6130 on healthy donor and OAC patient-derived PBMC

2.6.1 Healthy donor and OAC patient PBMC cell treatments

2.6.1.1 Assessing the effects of E6130 and fractalkine treatment on healthy NK cells.

Following PBMC preparation and counting as described in section 2.3.7, PBMC were seeded at a density of $1x10^6$ cells/ml of cRPMI supplemented with 10ng/ml IL-2 (MedChemExpress, USA) in a 24 well plate. PBMC were either left non-treated, treated with 100ng/ml of fractalkine, its vehicle control 0.1% water, treated with 4.9nM of E6130, or treated with its vehicle control 0.01% DMSO, treated with 0.01% DMSO and 100ng/ml of fractalkine, or treated with 4.9nM of E6130 and 100ng/ml of fractalkine for 24 hours 37°C in a 5% CO_2 humidified incubator. Cells were subsequently stained with extracellular and intracellular markers as described in section 2.6.2 and **[Table 2.6]**

2.6.1.2 Assessing the effects of the soluble tumour microenvironment on healthy donor blood-derived NK cells in the presence and absence of E6130 treatment

Following PBMC preparation and counting as described in section 2.3.7, PBMC were seeded at a density of $1x10^6$ cells/ml of cRPMI and 10ng/ml IL-2 (MedChemExpress, USA) in a 24 well plate. PBMC were either treated with 20% M199 (Gibco, UK), treated with TCM previously treated with 0.01% DMSO or treated with TCM previously treated with E6130 as described in section 2.3.5 for 24 hours 37°C in a 5% CO_2 humidified incubator. Cells were subsequently stained with extracellular and intracellular markers as described in section 2.6.2 and **[Table 2.6].**

2.6.1.3 Assessing NK cell cytotoxic potential using degranulation assay

Following PBMC preparation and counting as described in section 2.3.7, PBMC were seeded at a density of $1x10^6$ cells/ml of cRPMI and 10ng/ml IL-2 (MedChemExpress, USA) in a 24 well plate. Cells were either treated as described in section 2.6.1.1, 2.6.1.2 or 2.6.1.3 or left untreated and 6 hours later, cells were stimulated with 30ng/ml of IL-12 (Immunotools, Germany) and 100ng/ml of IL-15 (Peprotech, USA), for 18 hours in total. Following this, after 14 hours, 1µl of CD107a-PE-Cy7 (BioLegend, USA) was added and one hour later, 10µg/ml of brefeldin A (Sigma, USA) was added for the remaining 3 hours. Cells were subsequently stained for viability staining, (section 2.6.2.1), extracellular staining (section 2.6.2.2) and intracellular staining (2.6.2.3) **[Table 2.6].**

2.6.2 Flow cytometry staining of PBMC.

2.6.2.1 Zombie aqua staining for viable PBMC

Cells were stained for viability as described in section 2.5.3.2.

2.6.2.2 Extracellular staining for PBMC

Following treatment or no treatment, cells were stained for viability as described in section 2.6.2.1. Cells co-cultured with TCM had an added blocking step using FACS blocking buffer as described in section 2.3.6.2. Cells were washed in 500µl of FACS buffer and stained as described in section 2.5.3.3 with extracellular makers described in **[Table 2.6]**. Unstained controls were subject to the same protocols as their stained counterparts, except for the addition of flow cytometry antibodies.

2.6.2.3 Intracellular staining for PBMC

Following extracellular staining, the supernatant was poured off and the pellet was resuspended in FACS buffer and centrifuged at 1400RPM for 3 minutes. Supernatants were removed and cells were incubated with 50µl of fix buffer (Nordic MUBio, Netherlands) at room temperature for 15 minutes. Cells were subsequently washed in FACS buffer and centrifuged at 1400RPM for 3 minutes. Supernatants were removed and cells were incubated for 15 minutes with 50µl of perm buffer (Nordic MUBio, Netherlands) and intracellular antibodies, as described in **[Table 2.6].** Cells were washed twice with FACS buffer and centrifuged at 1400RPM for 3 minutes. The supernatant was poured off and cells were resuspended in 200µl of FACS buffer and acquired using BD FACs CANTO II (BD Biosciences).

2.7 Investigating the effects of the soluble tumour and adipose tissue microenvironments on KHYG-1 cell phenotype, function and migration

2.7.1 Boyden chamber chemotaxis assay

2.7.1.1 Optimisation of KHYG-1 cell activation for chemotaxis

Confluent KHYG-1 cells were centrifuged at 210xg for 5 minutes. Supernatant was discarded, resuspended and sub-cultured with cRPMI. Some cells were treated with 10ng/ml of IL-2 (Medchem express, USA) +/- 100ng/ml of IL-15 (Peprotech, UK) for 2 or 24 hours prior chemotaxis assay. A 24-hour treatment with IL-2 elicited the highest levels

of chemotaxis towards 20% FBS (positive control) and was therefore, also assessed in subsequent chemotaxis experiments.

2.7.1.2 Pre-treatment with chemokine receptor antagonist/modulator

Following a 24-hour boost with 10ng/ml IL-2 (Medchem express, USA) described in section 2.7.1.1, or leaving the cells non-treated, confluent KHYG-1 cells were centrifuged at 210xg for 5 minutes. Supernatant was discarded and cells were resuspended to be counted and seeded in 96 round-bottom plate at a density of $0.2x10^6$ cells/100µl in serum-free RPMI supplemented with 10ng/ml IL-2 (Medchem express, USA). Cells were either pre-treated for 1 hour with 0.01% DMSO, 4.9nM E6130 (CX3CR1 modulator) (Medchem express, USA) or 8.2nM AMG487 (CXCR3 antagonist) (Tocris Bioscience, UK).

2.7.1.3 Measuring KHYG-1 cell migration towards ACM or TCM using Boyden chamber assay

To assess migration of KHYG-1 cells, following the treatments described above, KHYG-1 cells were subsequently added to a 5µm pore Boyden chamber at a density of $0.2x10^6$ cells/100µl in RPMI (Corning Inc, USA). TCM or ACM was diluted 1 in 4 with M199 to a final volume of 600µl and added to the lower chamber of a 24 well plate. To assess if IP-10 increases KHYG-1 cell migration towards TCM, lower chambers containing diluted TCM were supplemented with 10ng/ml of recombinant human IP-10 (CXCL10, R&D systems, USA). M199 media was used as a negative control and M199 supplemented with 20% FBS (Gibco, UK) was used as a positive control. This plate was incubated for 2 hours at 37°C, 5% CO2. The Boyden chamber inserts were gently removed and cells were collected from the lower chamber and washed with FACS buffer twice and resuspended in 200µl of FACS Buffer for flow cytometric analysis. CountBright beads (ThermoFisher, USA) were used to enumerate the migrated KHYG-1s cells by first vortexing the beads, then adding 10 µl of beads to each tube before acquisition. Cells were acquired using the FACS CANTO II (BD Bioscience). The frequency of migrated cells was calculated with this formula:

$$\frac{\text{Number of beads per 10µl x Number of cells acquired}}{\text{Volume of cells acquired x Number of beads acquired}}$$

2.7.2 KHYG-1 cell culture in adipose or tumour conditioned media

To assess the effect of ACM or TCM on KHYG-1s, cells were seeded at a density of 200,000 cells/100µl of cRPMI supplemented with 10ng/ml IL-2 (Medchem express, USA) in a 24 well plate in a final volume of 600µl. Cells were either left in cRPMI, cRPMI with 20% well volume of M199, 20% well volume of ACM or 20% well volume of TCM. Cells were then assessed for degranulation as described in section 2.6.1.3. Cells were subsequently stained for viability (section 2.7.2.1), extracellular marker expression (section 2.7.2.2) and intracellular cytokine production (2.7.2.3) **[Table 2.6].**

2.7.3 Flow cytometry staining for KHYG-1 cells.

Dead KHYG-1 cells were stained using the same methods described in section 2.5.3.2. Extracellular staining for KHYG-1 cells described in section 2.5.3.3 was applied using antibodies from **[Table 2.6].** Cells co-cultured with ACM or TCM had an added blocking step using FACS blocking buffer as described in section 2.3.6.2. Unstained controls were subject to the same protocols as their stained counterparts, except for the addition of flow cytometry antibodies. Intracellular staining for KHYG-1 cells described in section 2.6.3.3 was applied using antibodies from **[Table 2.6].**

Table 2.6: Fluorochrome conjugated flow cytometry antibody panels for PBMC and KHYG-1 studies

Antibody	Volume (µl)	Manufacturer	Clone
Extracellular staining			
CD56-FITC Viobright	1	Miltenyi Biotec	REA196
CX3CR1-PE	1	Miltenyi Biotec	REA385
CD3-APC-Cy7	1	Biolegend	HIT3a
PD-1-PE-Cy7	2	Biolegend	EH12.2H7
TRAIL-APC	1	Biolegend	RIK-2
TRAIL-PE-CY7	1	Biolegend	RIK-2
NKp30-BV421	1	Biolegend	P30-15
NKp30-PerCP-Cy5.5	1	Biolegend	P30-15
NKG2D-PerCP-Cy5.5	2	Biolegend	1D11

NKp46-PE-Cy7	1	Biolegend	9E2
NKG2A-APC	1	Biolegend	S19004C
NKp44-APC-Cy7	1	Biolegend	P44-8
TIGIT-PerCP-Cy5.5	2	Biolegend	A15153G
FasL-Brilliant Violet 421	1	Biolegend	NOK-1
CD69-PE	1	Biolegend	FN50
CD16-PE	1	Biolegend	B73.1
CD54-Pacific Blue	1	BioLegend	HA58
CD27-APC	1	BioLegend	O323
CCR2-APC	1	Miltenyi Biotec	N/A
CCR3-APC-Cy7	1	Biolegend	5E8
CCR5-APC-Cy7	1	Biolegend	J418F1
CCR6-APC	1	Miltenyi Biotec	N/A
CXCR3-PE	1	Miltenyi Biotec	N/A
Intracellular staining			
IFNγ-PerCP-Cy5.5	1	Biolegend	4S.B3
CD107a-PE-Cy7	1	Biolegend	H4A3
TNFα-APC	1	Biolegend	Mab11
IL-10-Brilliant Violet 421	1	Biolegend	JES3-9D7
Viability staining			
Zombie Aqua (Dye)	1 in 1000	Biolegend	N/A

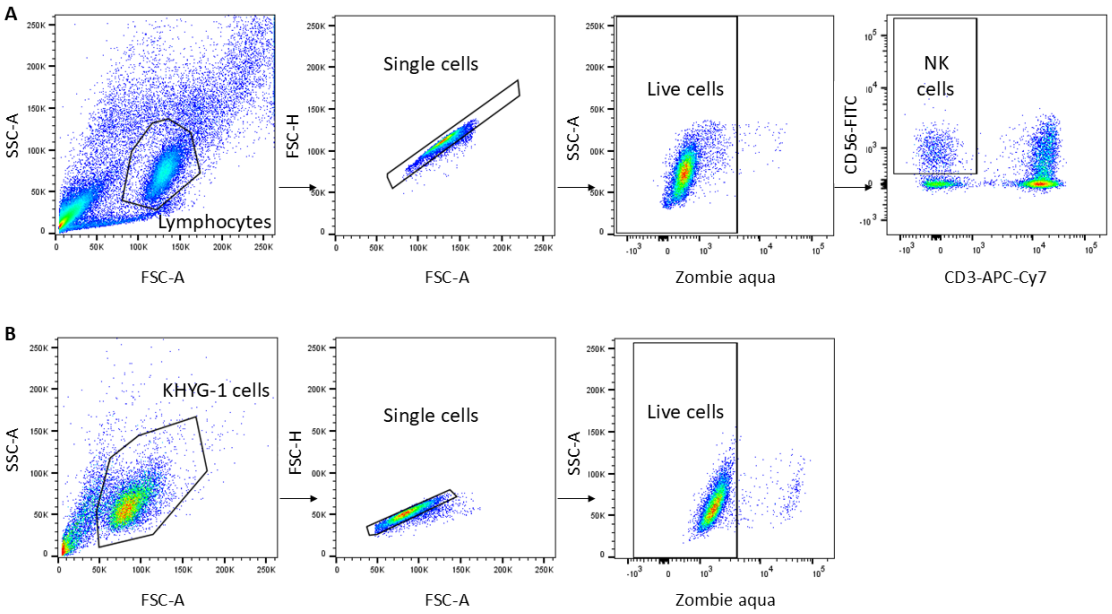

Figure 2.7: Representative dot plots showing flow cytometry gating strategy for PBMC and KHYG-1 cells.

(A) PBMC: The lymphocyte population was first gated based on size and granularity using FSC-A and SSC-A (left). Following this, cells were gated using FSC-H and FSC-A to exclude doublets (centre left). Live cells were gated using Zombie Aqua (centre right). NK cells were gated as $CD56^{+}CD3^{-}$ cells within this gate (right).

(B) KHYG-1 cell population was first gated based on size and granularity using FSC-A and SSC-A (left). Following this, cells were gated using FSC-H and FSC-A to exclude doublets (centre left). Live cells were gated using Zombie Aqua (centre right).

2.8 Flow cytometry analysis

Results were analysed using the FACS Diva software and FlowJo Version 10 software (BD, USA). The gating strategy is outlined in figure 2.2, 2.5 and 2.6. The OAC cell population and KHYG-1 cell populations were gated using the SSC-A and FSC-A. Following this to remove doublets single cells were gated on within FSC-H and FSC-A. Viable cells were gated as Zombie aqua^{-}. The different markers of interest were then gated using SSC-A and the antibody of interest. The lymphocyte population was gated on using the SSC-A and FSC-A. Following this to remove doublets single cells were gated on within FSC-H and FSC-A. Viable cells were gated as Zombie aqua^{-}. NK cells were gated as CD56^{+}CD3^{-} cells within this gate. Cells from tumour biopsies were gated using the SSC-A and FSC-A. Following this to remove doublets single cells were gated on within FSC-H and FSC-A. Viable cells were gated as Zombie aqua^{-}. Tumour cell population was gated as CD31^{-} CD45^{-} within this gate. Unstained controls were used to differentiate positive and negative populations. Compensation beads (Miltenyi Biotec, Invitrogen and BD) were used to compensate for spectral overlap as per manufacturer's instructions on the BD FACS CANTO II.

2.9 Lactate Dehydrogenase (LDH) assay

To validate the cell line data on the utility of E6130 and determine if this CX3CR1 modulator is tumouricidal to tumour samples, the Lactate Dehydrogenase (LDH) activity of OAC tumour samples was measured using the LDH-GloTM Cytotoxicity Assay (J2380, Promega, USA).

2.9.1 Sample preparation

Tumour tissue conditioned media (TCM), Normal Oesophageal tissue Conditioned Media (NOCM) and Normal Gastric tissue Conditioned Media (NGCM) was generated as described in section 2.3.5, however for conditioned media generated for LDH assays, 20 minutes after biopsies were cultured in media, 100µl of media was taken of each sample to establish initial LDH release (timepoint 1, TP1). Then, each sample was either not treated (NT), treated with 0.01% DMSO (vehicle control for E6130) and 4.9nM E6130 for 24 hours (timepoint 2, TP2). Following a 24-hour incubation, conditioned media was taken from each well, tissue was snap frozen and stored at -70°C. For timepoint 3 (TP3),

snap frozen biopsies were lysed using an LDH compatible buffer (200mM Tris HCL, 10% glycerol, 0.1% TritonX100). To lyse the tissue, the tissue lyser was set to 25 agitations per second for 2 minutes with a 5mm stainless steel bead added to each tube to aid homogenisation. Tubes were then centrifuged for 20 minutes at 13000RPM at 4°C. The conditioned media were diluted 1 in 1000 in LDH storage buffer.

2.9.2 LDH assay procedure

A volume of 50µl of the diluted samples at the three different timepoints was added to each well of a 96 well plate suitable for fluorescence reading. A volume of 50µl of LDH Detection reagent (25µl of Reductase substrate mixed with 5ml LDH Detection Enzyme Mix) was added to each well. The plate was incubated for 30 minutes to 60 minutes at room temperature in the dark. The luminescence was measured after 30 minutes, 45 minutes and 60 minutes using the GloMax explorer multimode microplate reader (Nan-Luc Technology, Promega, USA). Experiments were carried out in triplicate i.e. 3 technical replicates. Wells containing M199 alone acted as a blank and the value obtained was subtracted from all other values. A titration curve was generated to establish a linear range of the assay.

LDH release was calculated as follows:

The three timepoints described were measured to assess for total LDH release from each sample using this formula: Total LDH release = TP1 + TP2 + TP3 = 100%.

LDH % from each timepoint could then be calculated (ex: TP1 % = $(\frac{TP1}{Total\ LDH})$ x 100) and the real LDH release from each timepoint was defined by TP2% - TP1%.

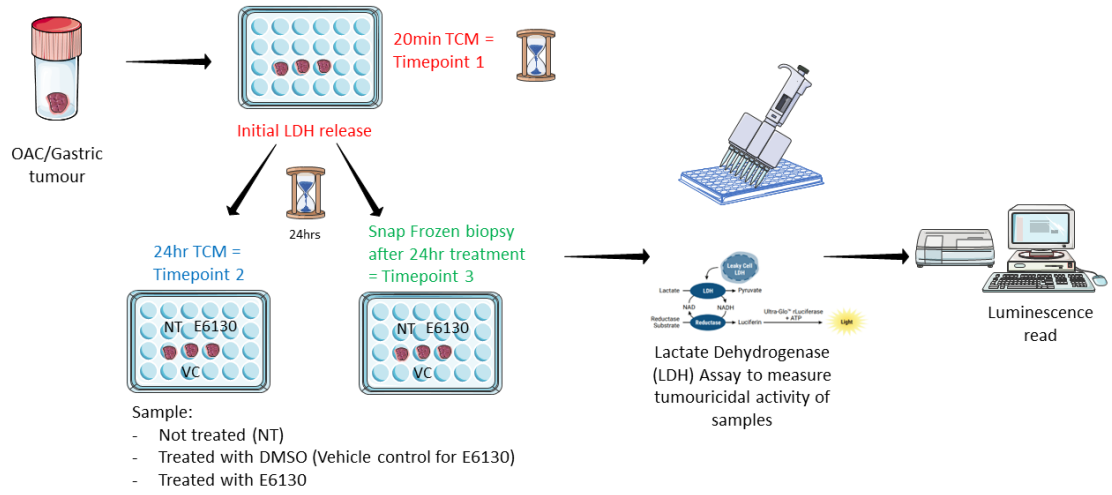

Timepoint 1 + Timepoint 2 + Timepoint 3 = Total LDH release from the sample
Timepoint 1 + Timepoint 2 + Timepoint 3 = 100%
→ Can then calculate % of LDH release of each time point.

Figure 2.8: Schematic workflow assessing tumouricidal activity of tissue samples from OAC/Gastric cancer patients using a Lactate Dehydrogenase assay.

Samples collected at the time of surgical resection or re-staging endoscopy were incubated for 24 hours with serum free media (M199) supplemented with 500µl gentamycin to create tumour conditioned media (TCM) and either not treated, treated with 0.01% DMSO or treated with 4.9nM E6130. Lactate Dehydrogenase (LDH) was measured on the three different timepoints using a LDH cytotoxicity assay. LDH release was measured using a fluorescent plate reader. Created with Smart.Servier.com

2.10 ELISA analysis

Human Fractalkine, human IFN-γ, human TNF-α, human IL-2 and human IL-15 ELISAs (Assay Genie, Ireland) were carried out according to the manufacturer's protocol on OAC cell line supernatants and OAC patient-derived ACM, LCM, TCM, NOCM, NGCM and serum. Fractalkine concentrations were measured in ACM, LCM, TCM, NOCM and NGCM. IFN-γ, TNF-α, IL-2 and IL-15 concentrations were measured in TCM previously treated with 0.01% DMSO and 4.9nM E6130. For analysis by ELISA of IFN-γ, TNF-α, IL-2, IL-15 and fractalkine, the following supernatants were collected following OAC cell treatment described in section 2.5.1 and 2.5.2 and were used in this manner:

Table 2.7: ELISAs

Treatment of OAC cell lines	Target	Product Number
No treatment (baseline)	Fractalkine	HUFI00126
0.1% Water or 100ng of fractalkine	IFN-γ TNF-α IL-2 IL-15	HUFI00147 HUFI00262 HUFI00168 HUDL01469
0.01% DMSO or 4.9nM E6130	Fractalkine	HUFI00126

2.11 Statistical analysis

Data were analysed on GraphPad Prism 10 Software (GraphPad Software, USA). The statistical test used is indicated in the figure legend of all result graphs and data is presented as Mean ± SEM. Paired-t-test, unpaired-t-test, Wilcoxon test or Mann-Whitney test were used to compare between two groups. Parametric one-way ANOVA with Tukey's multiple comparisons test, Kruskal-Wallis or Friedman tests with post-hoc Dunn's test were used to compare three or more groups were used to compare between three or more groups. Spearman correlations were performed to analyse correlations. A p-value of $p<0.05$ was considered statistically significant.

Chapter 3 - Fractalkine elicits pro-tumourigenic effects on Oesophageal Adenocarcinoma cell lines which can be reversed with the CX3CR1 modulator E6130

3.1 Introduction

Oesophageal adenocarcinoma (OAC) is an aggressive inflammation-driven malignancy with poor survival rates and limited therapeutic options [5, 7, 10, 11, 42]. Current standard-of-care (SOC) treatment for OAC is surgical resection and chemoradiotherapy with common regimens consisting of the CROSS and FLOT regimens in Ireland, and with only 30% of patients responding to these treatments [7, 10, 42, 43, 312, 313]. In addition, two immunotherapies that target programmed cell death protein 1 (PD-1) have been approved for the treatment of OAC i.e. the immune checkpoint inhibitors (ICI) nivolumab and pembrolizumab [5, 42, 48-50]. However, current efficacy rates for these ICI stands are low for OAC and further studies are needed to ascertain how their efficacy can be enhanced, to optimise immunotherapy sequenced timing with SOC, and to develop novel and more effective treatment combinations for this poor prognosis malignancy [313].

The tumour microenvironment (TME) plays a pivotal role in driving tumour progression, immune evasion, and therapeutic resistance in cancer [314-317]. The TME is a dynamic and complex ecosystem composed of cancer cells, stromal cells, immune cells, extracellular matrix (ECM) and soluble factors, all of which interact to shape tumour growth [314-327]. This study explores the role of the chemokine fractalkine in the OAC TME and how it influences tumour growth. Chemokines, a class of small cytokine-like proteins, are critical regulators of the TME, mostly understood in their role of modulating immune cell migration through G protein-coupled receptors. However, their influence over tumourigenic processes such as angiogenesis and metastasis has placed them as desirable therapeutic targets [143, 328]. In solid cancers, aberrant chemokine signalling can both contribute to tumour progression by promoting cancer cell invasion, angiogenesis, and immune evasion or inhibit detrimental pro-tumourigenic effects [133, 143, 226, 328, 329]. Consequently, chemokine-based therapies have garnered significant interest for their potential in treating solid cancers [132, 224, 226, 329, 330]. These therapies aim to modulate chemokine signalling to inhibit tumour-promoting activities or enhance anti-tumour immune responses. Approaches under investigation include chemokine receptor antagonists, neutralizing antibodies and engineered chemokines designed to redirect immune cells to the tumour site [132, 224, 226, 329, 330].

Fractalkine is a unique chemokine protein that functions as both a chemoattractant and an adhesion molecule [169]. Soluble fractalkine can attract and bind to its sole receptor, CX3CR1, predominantly found on immune cells such as monocytes, $CD8^+$ T cells and Natural Killer (NK) cells and serves as a chemotactic cytokine [172, 173]. Fractalkine has been reported to be implicated in multiple inflammatory diseases, such as rheumatoid arthritis, atherosclerosis and certain neurodegenerative disorders [182, 183]. In the setting of obesity-associated cancer, our group have shown that fractalkine is a key driver of T and NK cell migration towards the visceral adipose tissue (VAT) of OAC patients where they are polarised towards a pro-inflammatory profile, likely contributing to local and systemic inflammation [127, 129]. In fact, highest fractalkine levels are seen in the OAC patients with the highest systemic CRP levels thus solidifying its pro-inflammatory role in OAC [129]. Beyond its role in inflammation in OAC, fractalkine has been shown to have pro- and anti-tumour roles in several cancers. High fractalkine levels have been previously shown to correlate with increased anti-tumour immune cell infiltration in gastric, breast and colorectal cancer patients [172, 186, 188, 190]. In the setting of OAC, our group have shown that fractalkine is pivotal in the movement of key immune cells towards VAT at the expense of effective infiltration of the tumour. In addition, studies by others have shown that overexpression of CX3CR1 increased gastric cancer cell survival, proliferation and metastasis [189]. Similarly, higher levels of fractalkine in lung and pancreatic tumours are associated with poorer patient outcomes [196, 202]. Fractalkine's role as a promoter of tumour development via its stimulation of cancer cell proliferation, migration, and invasion has been reported so far [69, 127, 129, 173, 179, 192-195]. In this research study, the direct pro-tumourigenic effects of fractalkine on OAC tumour cells were assessed.

Inhibition of fractalkine in pancreatic cancer showed promising results as it reduced cell viability and motility induced by the chemokine [203]. Moreover, pilot data from our group has shown that CX3CR1 antagonist AZD8797 can impede OAC tumour growth and epithelial-mesenchymal transition (unpublished results). E6130, a highly selective and orally available CX3CR1 modulator, has been shown by our group to restore NK cell migration towards OAC tumour following ACM-induced hindrance of this migration and can even redirect NK cells to tumour-derived signals over VAT-derived signals in an *ex*

vivo model [68, 127, 185]. Using a panel of OAC *in vitro* models, the CX3CR1 modulator E6130, which has been shown to counteract the negative effects of fractalkine on NK cell migration [68, 69, 185], was investigated to evaluate if it can also be used to impede any of fractalkine's direct pro-tumourigenic effects on OAC tumour cells.

It is now appreciated that the physiological conditions of hypoxia, nutrient deprivation and acidosis within the TME have a profound effect on tumour growth [318, 321, 324, 325, 327, 331]. Furthermore, cytokine and chemokine release are altered by the physiological conditions of the TME, perpetuating tumourigenic inflammation. Rapidly proliferating tumour cells deplete many essential nutrients within their microenvironment to meet their bioenergetic demands contributing to a nutrient poor TME. For instance, breast cancer cells that were cultured in serum-free media for 24 hours were found to have significantly decreased cell migration, however, after 72 hours, cell migration was significantly higher and transcription markers associated with migration, such as vimentin or ICAM-1 were upregulated [332]. While recapitulation of acidosis *in vitro* has been shown to induce changes on the expression of chemokines such as increase CXCL8 production and reduce CXCL10 (IP-10) production in breast cancer and OSCC studies [333], there are no reports on the impact of nutrient deprivation and acidic conditions on fractalkine signalling in cancer, to our knowledge. Hypoxia is a common feature of the TME due to low supply caused by the inadequate vasculature and high demand by both tumour and stromal cells [334, 335]. Hypoxia exerts its effects through Hypoxia-Inducible Factor-1α (HIF-1α), which is expressed both by tumour cells and infiltrating immune cells. Li *et al.* showed in a pan-cancer study that HIF-1α expression in tumour cells, in particular gastric adenocarcinoma cells, positively correlated with higher regulatory T (Treg) cells, $CD4^{+}$Th2 cells, neutrophils and macrophages [335]. Importantly, fractalkine has been shown to induce HIF-1α protein expression and enhance cell growth in pancreatic cancer via PI3K/Akt and MAPK pathways, thus suggesting a potential mechanism through which fractalkine elicits its pro-tumourigenic functions [194]. Remarkably, cancer cells exhibit a high degree of plasticity, enabling them to adapt and thrive in these harsh conditions. Here the different conditions of the TME were investigated to ascertain if they could alter CX3CR1 surface expression, and to elucidate if fractalkine treatment could alter viability under these

conditions, therefore exploring how the fractalkine:CX3CR1 axis is influenced by the conditions of the TME.

Overall, this chapter uncovers novel data on the biological role of fractalkine in the OAC TME, explores how the physiological conditions influence such effects and delineates the utility of E6130 to reverse any direct detrimental effects of this chemokine in OAC tumours.

3.2 Hypothesis

Fractalkine drives tumourigenic processes in OAC which can be reversed using the CX3CR1 modulator E6130.

Aims:

1. Assess the surface expression of the fractalkine receptor CX3CR1 on OAC cell lines and soluble fractalkine levels in OAC cell line supernatants
2. Elucidate the effects of fractalkine on OAC cell viability and proliferation and the potential of E6130 to reduce such effects.
3. Explore whether the physiological conditions of the tumour microenvironment (acidosis, nutrient deprivation and hypoxia) impact CX3CR1 expression and elucidate the effect of fractalkine on OAC cell lines under such conditions.

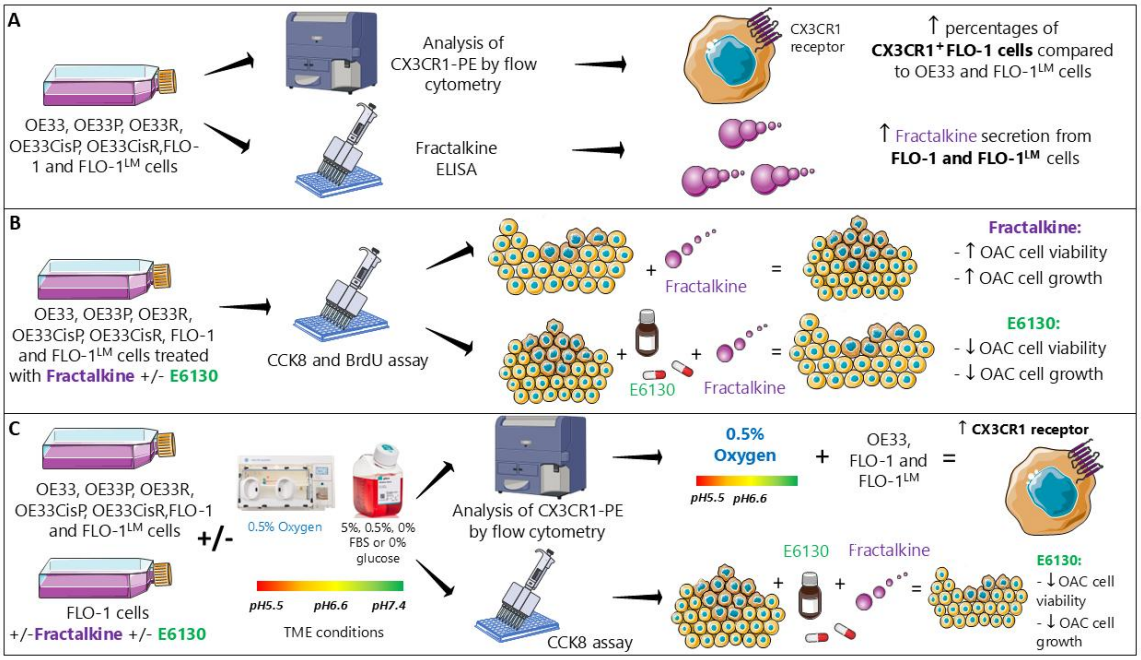

Graphical abstract: **(A)** OE33, OE33P, OE33R, OE33CisP, OE33CisR, FLO-1 and FLO-1^{LM} cells were cultured *in vitro*, CX3CR1 expression was analysed by flow cytometry, at baseline, FLO-1 cells expressed higher (↑)CX3CR1 than OE33 cells and FLO-1^{LM} cells. OAC cell supernatants were assessed for fractalkine by ELISA and FLO-1 and FLO-1^{LM} cells expressed high (↑) levels of fractalkine compared to OE33, OE33P, OE33R, OE33CisP, OE33CisR. **(B)** OAC cell lines were cultured *in vitro*, cell viability was assessed by CCK8 assay and cell proliferation was assessed by BrdU assay. Fractalkine increased (↑) OAC cell viability and proliferation, E6130 decreased (↓) fractalkine-mediated increases in cell viability and cell proliferation. **(C)** OAC cell lines were treated under TME conditions or non-treated, CX3CR1 expression was analysed by flow cytometry and 0.5% Oxygen, moderate and severe acidosis increased (↑) CX3CR1 receptor expression on OE33, FLO-1 and FLO-1^{LM} cells. FLO-1 cell line was treated under TME conditions and cell viability of FLO-1 was assessed by CCK8 assay. E6130 decreased (↓) fractalkine-mediated increases of cell viability under the conditions of the TME. Created with Smart.Servier.com and Biorender.com

Results

3.3 Fractalkine elicits pro-tumourigenic effects on Oesophageal Adenocarcinoma cell lines which can be reversed with the CX3CR1 modulator E6130

To ascertain the pro-tumourigenic effects of fractalkine in OAC, the OE33, FLO-1 and FLO-1^{LM} cell lines were used as *in vitro* tumour models. The OE33 cell line was established from a 73-year-old female patient from the adenocarcinoma of the lower oesophagus. The FLO-1 cell line was derived from a primary distal oesophageal adenocarcinoma in a 68-year-old male patient, with many known mutations. FLO-1^{LM} cell line is a liver metastasis cell line derived from FLO-1 human cells following metastasis in a mouse model, and these lines were selected to investigate if fractalkine has a pro- or anti-tumourigenic effect on primary and metastatic OAC tumours [311]. Moreover, the radioresistant cell line OE33R and its parental cell line OE33P, and the cisplatin resistant cell line OE33CisR and its parental cell line OE33CisP were used as *in vitro* models of radioresistant and chemoresistant OAC cell lines. OE33P, OE33R, OE33CisP and OE33CisR cell lines were generated from the OE33 cell line by our department as previously described[70, 309, 310].

3.3.1 Assessing CX3CR1 expression and fractalkine production in OAC cell lines

3.3.1.1 Differential basal CX3CR1 expression in OAC cell lines

CX3CR1 surface expression by OE33, FLO-1, FLO-1^{LM}, OE33P, OE33R, OE33CisP and OE33CisR cells were analysed by flow cytometry. $CX3CR1^{+}$OE33 cell frequencies were significantly lower than the frequencies of $CX3CR1^{+}$FLO-1 cells; OE33 vs FLO-1 (12.4% vs 21.9%, p=0.036, n=5) and OE33R; OE33 vs OE33R (12.4% vs 22.1%, p=0.040, n=5) **[Figure 3.1A]**.

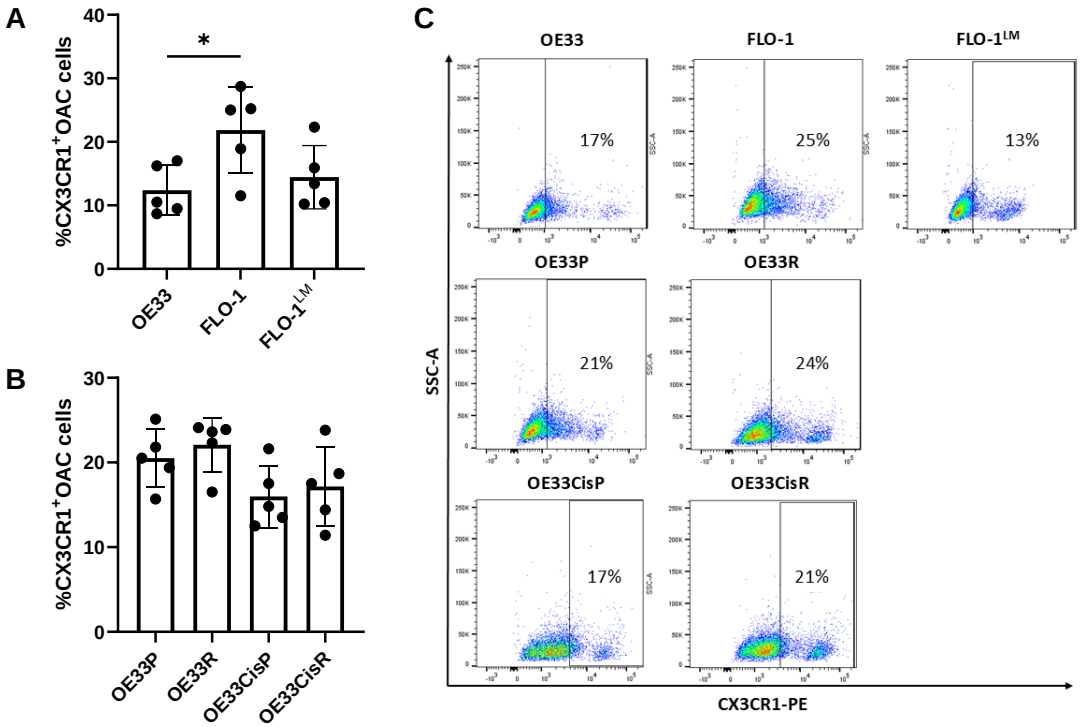

Figure 3.1: Differential surface expression of the fractalkine receptor CX3CR1 in OAC cell lines

(A) Bar charts showing the frequencies of CX3CR1^{+}OE33, FLO-1 and FLO-1^{LM} cells, and **(B)** CX3CR1^{+}OE33P, OE33R, OE33CisP and OE33CisR cells. **(C)** Representative dot plots showing gating of CX3CR1^{+}OE33, FLO-1, FLO-1^{LM}, OE33P, OE33R, OE33CisP and OE33CisR cell populations after gating on viable cells. Experiments were repeated n=5. *p<0.05, ordinary one-way ANOVA with Tukey multiple comparison test. Mean ± SEM.

Flow cytometric analysis of CX3CR1^{+} OAC cell lines unveiled two distinct populations of CX3CR1^{+} cells referred here as CX3CR1^{low} and CX3CR1^{high}. The two distinct populations were investigated to assess if they differ from the total CX3CR1^{+} population.

CX3CR1^{low}FLO-1 cells were detected at significantly higher frequencies than CX3CR1^{low}FLO-1^{LM} cells; FLO-1 vs FLO-1^{LM} (14.6 vs 8.5%, p=0.046, n=5) and CX3CR1^{low}OE33 cells, OE33 vs FLO-1 (8.5% vs 14.6%, p=0.046, n=5) **[Figure 3.2A left]**. There were no significant differences between the frequencies of CX3CR1^{high}OE33, FLO-1 and FLO-1^{LM} expression or the frequencies of CX3CR1^{low}OE33P, OE33R, OE33CisP and OE33CisR. Frequencies of CX3CR1^{high} OE33R were higher than OE33P (CX3CR1^{high}OE33P vs CX3CR1^{high}OE33R; 3.3% vs 7%, n=5) **[Figure 3.2B right].**

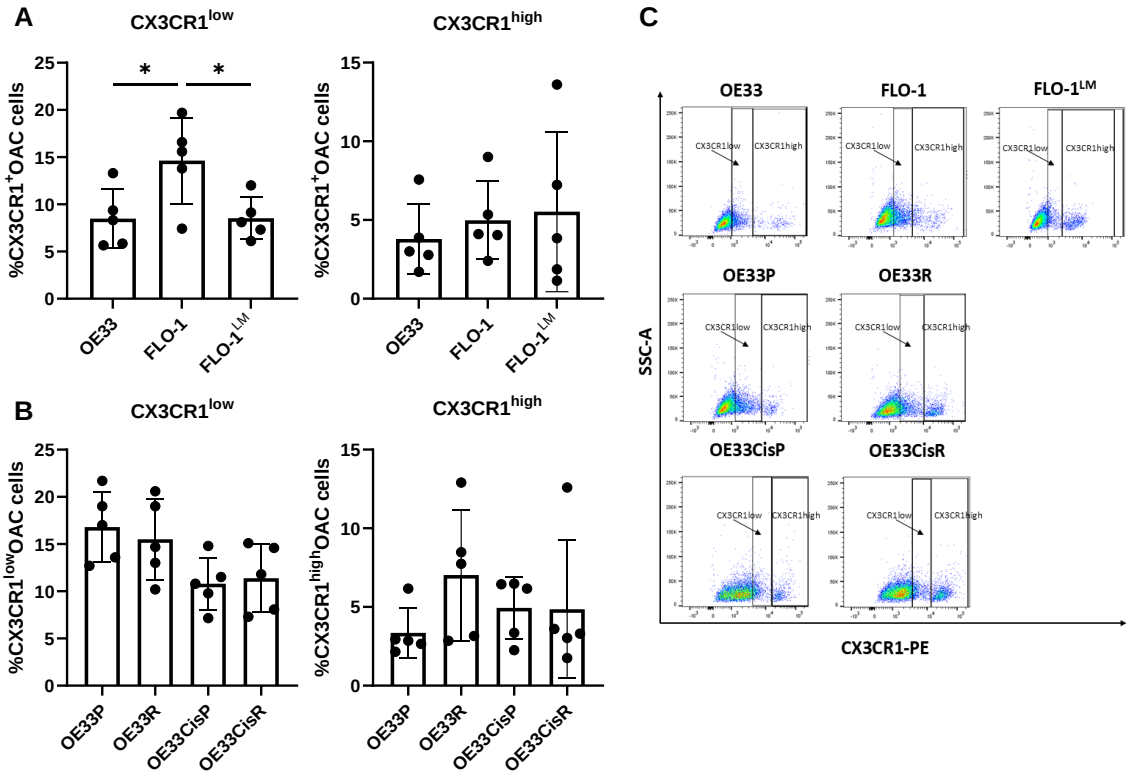

Figure 3.2: Differential abundance of CX3CR1^{low} and CX3CR1^{high} cell populations between OAC cell lines

Bar charts showing the frequencies of **(left)** CX3CR1^{low} and **(right)** CX3CR1^{high} of **(A)** OE33, FLO-1 and FLO-1^{LM} cells and (**B)** OE33P, OE33R, OE33CisP and OE33CisR cells. **(C)** Representative dot plots showing gating of CX3CR1^{low} and CX3CR1^{high}OE33, FLO-1, FLO-1^{LM}, OE33P, OE33R, OE33CisP and OE33CisR after gating on viable cells. Experiments were repeated n=5. *p<0.05, ordinary one-way ANOVA with Tukey multiple comparison test. Mean ± SEM.

3.3.1.2 Fractalkine and E6130 do not affect CX3CR1 receptor expression on FLO-1 cells

Our group have previously demonstrated that fractalkine induces CX3CR1 endocytosis in NK cells and $CD8^+$T cells and here its effects on CX3CR1 surface expression by FLO-1 cells was examined[127, 129]. CX3CR1 expression was assessed by flow cytometry at baseline, and after 24-hour treatment with the vehicle control for fractalkine (0.1% distilled Water), 10 or 100ng of fractalkine, there was no significant differences in % frequencies of FLO-1 cells expressing CX3CR1 expression or in Mean Fluorescence Intensity (MFI) **[Figure 3.3 A,B]**. E6130 is a CX3CR1 modulator and the IC50 of 4.9nM of E6130 has previously shown efficacy to impede NK cell migration towards the chemotactic signals of OAC patient-derived VAT[68, 69]. To assess if E6130 acts through surface expression of the CX3CR1 receptor on FLO-1 cells, its effects on CX3CR1 surface expression on FLO-1 cells was examined and compared to its vehicle control (0.01% DMSO). No significant changes in % frequencies of $CX3CR1^+$ cells or MFI were observed after the cells were treated with 4.9nM of E6130 [**Figure 3.3 C,D]**.

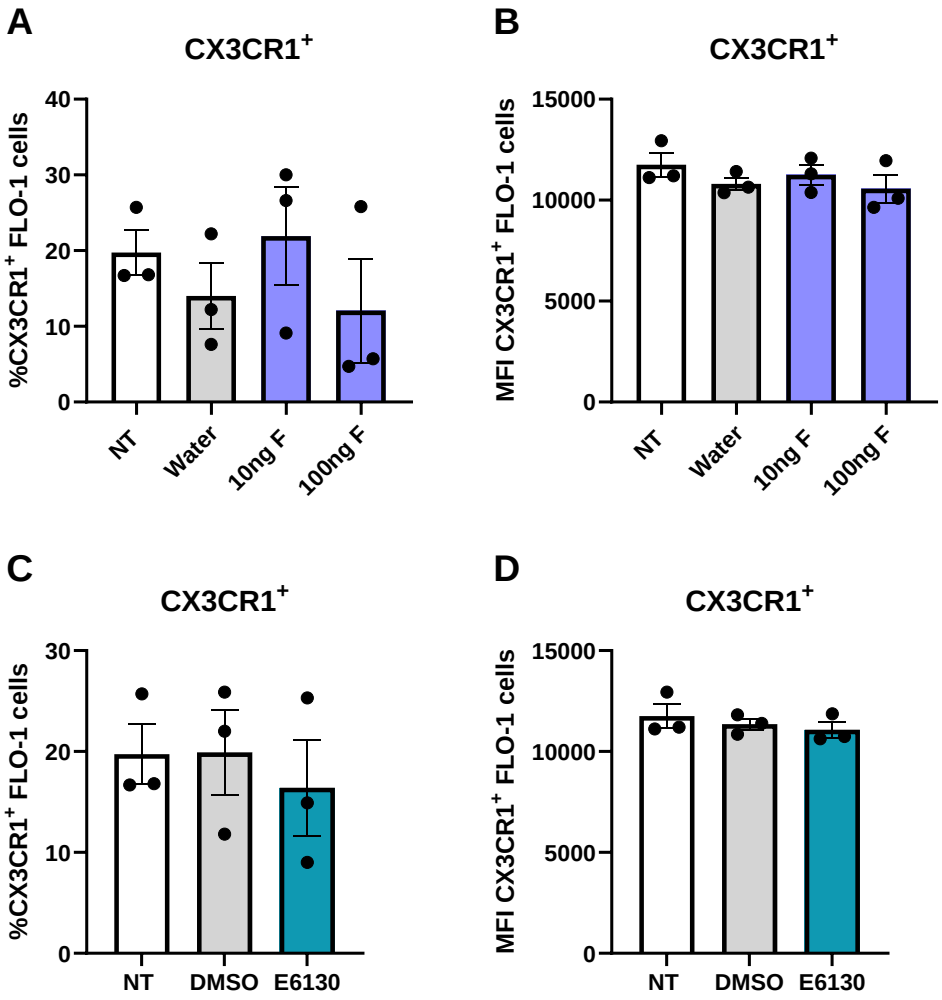

Figure 3.3: Treatment with fractalkine or E6130 does not significantly alter CX3CR1 surface expression on FLO-1 cells

Bar charts showing **(A)** % frequencies or **(B)** MFI of CX3CR1$^+$FLO-1 cells treated for 24 hours with no treatment (NT), treatment with 0.1% water, 10 or 100ng/ml recombinant fractalkine (F). Bar charts showing **(C)** % frequencies or **(D)** MFI of CX3CR1$^+$FLO-1 cells treated for 24 hours with NT, 0.01% DMSO or 4.9nM. Experiments were repeated n=3. Mean ± SEM

3.3.1.3 E6130 did not alter fractalkine production by OE33, FLO-1, FLO-1^{LM}, OE33P, OE33R, OE33CisP and OE33CisR cells

To further delineate the role of the fractalkine:CX3CR1 axis in OAC; fractalkine secretion by OE33, FLO-1, FLO-1^{LM}, OE33P, OE33R, OE33CisP or OE33CisR cells was investigated with and without E6130 treatment.

The OAC cell lines OE33, FLO-1, FLO-1^{LM}, OE33P, OE33R, OE33CisP or OE33CisR were assessed for fractalkine secretion by ELISA. The cells were either previously treated with 4.9nM of E6130 or treated with its vehicle control DMSO (0.01%) for 24 hours, the supernatants were then collected. At baseline (DMSO treated cells), it was observed that FLO-1 and FLO-1^{LM} cells express significantly higher soluble fractalkine secretions compared to OE33 cells; OE33 + DMSO vs FLO-1 + DMSO (0pg/ml vs 21,067.3pg/ml, $p<0.0001$, n=3) ; OE33 + DMSO vs FLO-1^{LM} + DMSO (0% vs 16,710.7pg/ml, p<0001, n=3) **[Figure 3.4A].** Furthermore, even though both cells line secret high levels of fractalkine, FLO-1 cells secreted significantly higher levels of soluble fractalkine compared to FLO-1^{LM}; FLO-1 + DMSO vs FLO-1^{LM} + DMSO (21,067.3pg/ml vs 16,710.7pg/ml, p=0.0005, n=3) **[Figure 3.4A]**. Interestingly, soluble fractalkine was undetectable in OE33CisP and OE33CisR supernatants. A slight difference was observed between the secretion levels of fractalkine of OE33P and OE33R cells when the cells were treated with DMSO; OE33P + DMSO vs OE33R + DMSO (175.2pg/ml vs 49pg/ml, n=3), however it was not significant **[Figure 3.4B].** These levels of fractalkine secretion were much lower than those observed FLO-1 and FLO-1^{LM} cells which highlights the biological differences between the different models of OAC cell lines used. There were no significant differences observed in fractalkine secretions by any cell lines following treatment with E6130 compared to DMSO treated cells, suggesting that E6130 did not alter fractalkine secretions by OAC cells.

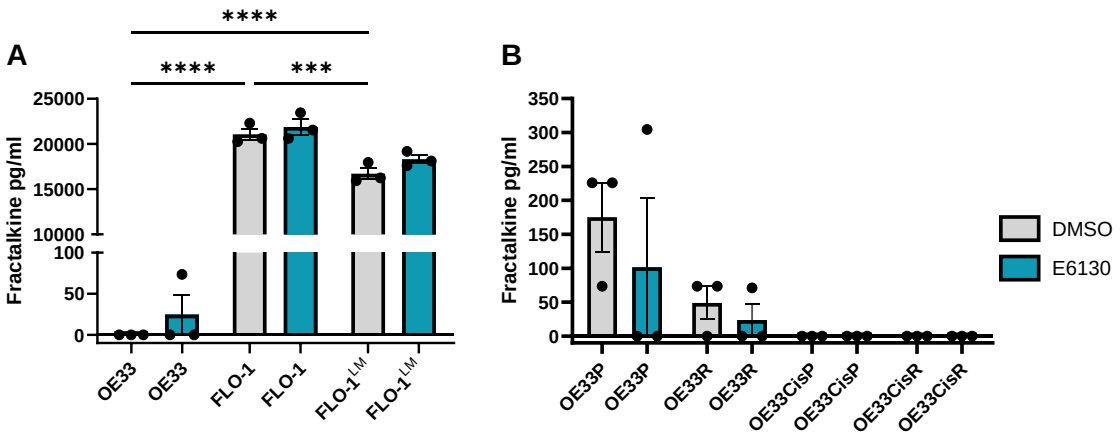

Figure 3.4: FLO-1 and FLO-1^{LM} cells secrete significantly higher levels of fractalkine compared to OE33, and E6130 does not significantly alter these secretions

Bar charts showing fractalkine in pg/ml measured by ELISA in **(A)** OE33, FLO-1 and FLO-1^{LM} cells, **(B)** OE33P, OE33R, OE33CisP and OE33CisR cells when cells were treated for 24 hours with 0.01% DMSO or 4.9nM E6130**.** Experiments were repeated n=3, ***p<0.001, ****<0.0001, by ordinary one-way ANOVA with Tukey multiple comparison test. Mean ± SEM.

3.3.2 Fractalkine increases cell viability in OE33, FLO-1, FLO-1^{LM}, OE33P, OE33R, OE33CisP and OE33CisR and this can be attenuated by E6130

3.3.2.1 Fractalkine increases viability in OE33, FLO-1, FLO-1^{LM}, OE33P, OE33R, OE33CisP and OE33CisR cells

The panel of OAC cells lines were treated with fractalkine at a range of concentrations (0.1 – 200ng/ml) for 24 hours and a CCK-8 assay was performed to assess if their viability was altered. There was a significant increase in OE33 cell viability following 24-hour treatment with 100 and 200ng/ml of fractalkine (FKN), compared to vehicle control (0.1% Water); Water vs 100ng/ml FKN (100.8% vs 119.94, p=0.017, n=5), Water vs 200ng/ml FKN (100.8% vs 118.66%, p=0.033, n=5) **[Fig. 3.5A]**. Similarly, there were significant increases in cell viability for FLO-1 cells treated with 10 and 100ng/ml of fractalkine compared to FLO-1 cells treated with water; Water vs 10ng/ml FKN (101% vs 118%, p=0.028, n=5), Water vs 100ng/ml FKN (101% vs 121.4%, p=0.029, n=5) **[Fig. 3.5B]**. FLO-1^{LM} cells had significantly increased viability following 24-hour treatment with 5ng of fractalkine compared to FLO-1^{LM} cells treated with water, but there were no significant differences with higher concentrations of fractalkine for FLO-1^{LM} cells; Water vs 5ng/ml FKN (95.2% vs 127.6%, p=0.037, n=5) **[Fig. 3.5C]**.

There were significant increases in cell viability for OE33P cells treated with 100 and 200ng/ml of fractalkine compared to OE33P cells treated with the vehicle control of fractalkine, water; Water vs 100ng/ml FKN (98.8% 116.6%, p= 0.016, n=5), Water vs 200ng/ml FKN (98.8% vs 124.2%, p=0.0002, n=5) **[Figure 3.5D].** OE33R cells exhibited significantly increased viability following treatment with 5, 100 and 200ng of fractalkine compared to OE33R cells treated with water; Water vs 5ng/ml FKN (102.4% vs 115.4%, p=0.037, n=5), Water vs 100ng/ml FKN (102.4% vs 115.2%, p=0.043, n=5), Water vs 200ng/ml FKN (102.4% vs 123.8%, p<0.0001; n= 5) **[Figure 3.5E]**.

These data suggest that fractalkine treatment increases cell viability in OE33P and OE33R cells at different concentrations, with OE33R cells being sensitive to doses as low as 5ng of the chemokine. The cell viability of OE33P and OE33R cells treated with 5ng, 100ng and 200ng of recombinant fractalkine were compared, to assess if fractalkine had a significantly differential effect between the cell lines. When cells were treated with 200ng/ml of fractalkine, it elicited slightly but significantly stronger effects in OE33R cell

viability, compared to OE33P cells; OE33P + 200ng/ml FKN vs OE33R + 200ng/ml FKN (115.2% vs 121.5%, p=0.0476, n=5-6) **[Figure 3.5F],** suggesting that radioresistant tumours might be more susceptible to the pro-tumourigenic effects of fractalkine.

To evaluate the effect of fractalkine on OE33CisP and OE33CisR cell viability, cells were treated at a low concentration of fractalkine (10ng/ml) and two high concentrations of fractalkine (100 and 200ng/ml) as these concentrations elicited the most significant increases in cell viability for the previous OAC cell lines evaluated. There was a significant increase in cell viability for OE33CisP cells treated with 10 and 200ng/ml of fractalkine compared to OE33CisP cells treated with water; Water vs 10ng/ml FKN (102.4% vs 119%, p= 0.032, n=5), Water vs 200ng/ml FKN (102.4% vs 114.4%, p=0.017, n=5) **[Figure 3.5G].** OE33CisR cells exhibited significantly increased viability following treatment with 10, 100 and 200ng of fractalkine compared to OE33CisR cells treated with water; Water vs 10ng/ml FKN (101.5% vs 123.3%, p=0.007, n=5), Water vs 100ng/ml FKN (102.4% vs 126.2%, p=0.045, n=5), Water vs 200ng/ml FKN (102.4% vs 119%, p=0.014; n=5) **[Figure 3.5H]**.

The cell viability of OE33CisP and OE33CisR cells treated with 10ng, 100ng and 200ng of recombinant fractalkine was compared, to assess if fractalkine had a significant different effect on both cell lines. There were no significant differences between the two cell lines when their sensitivity to fractalkine was compared suggesting that chemoresistant tumours are equally susceptible to the tumourigenic effects of the chemokine **[Figure 3.5I].**

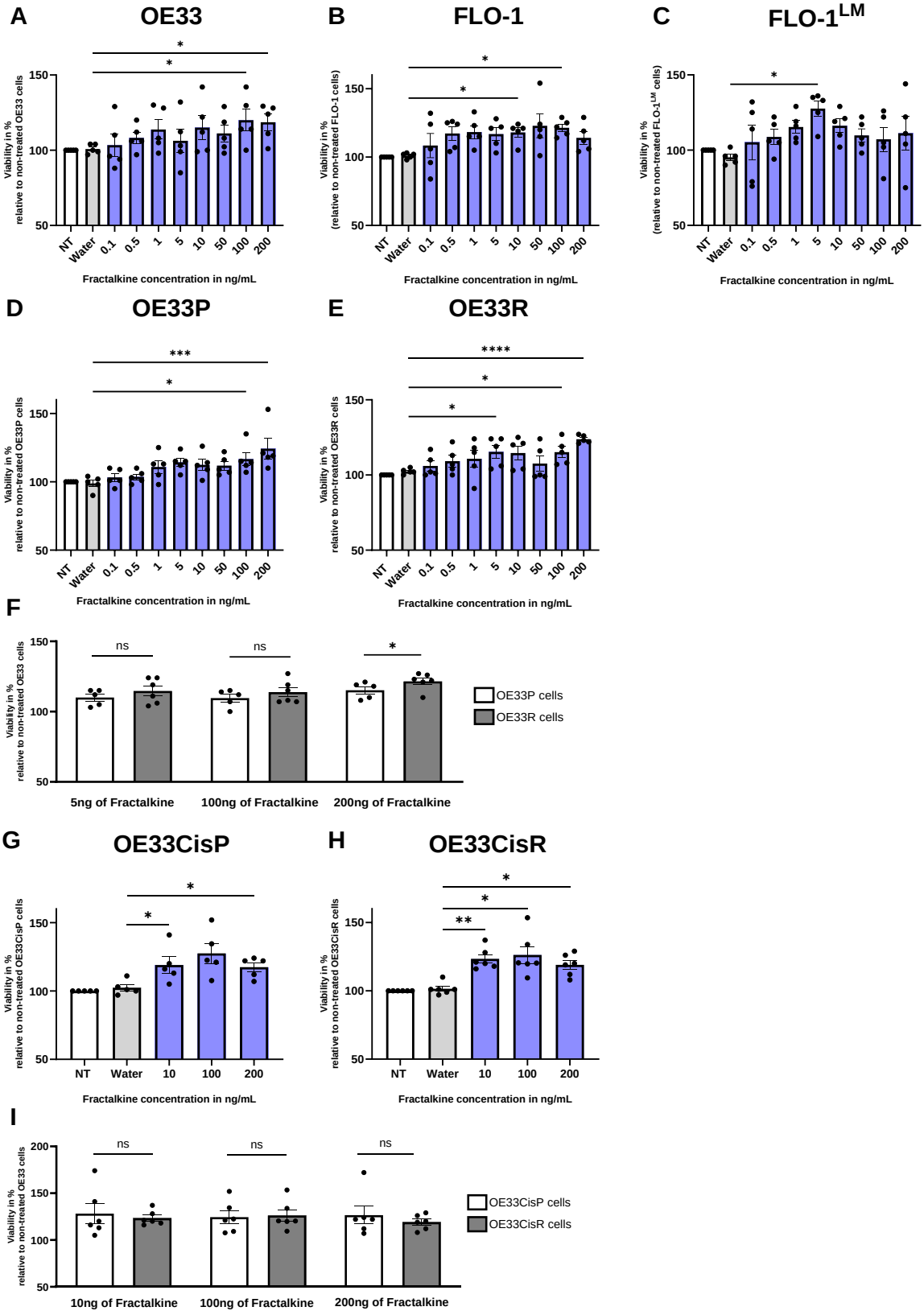

Figure 3.5: **Significantly increased viability following 24-hour treatment with high doses of fractalkine in OE33, FLO-1, OE33P, OE33R, OE33CisP and OE33CisR cell lines and following 24-hour treatment with low doses of fractalkine in FLO-1, FLO-1^{LM}, OE33R, OE33CisP and OE33CisR cell lines**

Bar charts showing % of **(A)** OE33, **(B)** FLO-1, **(C)** FLO-1^{LM}, **(D)** OE33P, **(E)** OE33R, **(G)** OE33CisP and **(I)** OE33CisR cell viability measured by CCK8 assay after no treatment (NT), treatment with 0.1% water (vehicle control for fractalkine) or 0.1, 0.5, 1, 5, 10, 50, 100, 200 ng/ml of recombinant fractalkine for 24 hours. **(F)** Bar chart showing comparison of % viability of OE33P and OE33R cells treated with 5, 100 or 200ng/ml of recombinant fractalkine for 24 hours. **(I)** Bar chart showing comparison of % viability of OE33CisP and OE33CisR cells treated with 10, 100 or 200ng/ml of recombinant fractalkine for 24 hours. Experiments were repeated n=5-6. *p<0.05, **p<0.01, ***p<0.001, ****p<0.0001, by ordinary one-way ANOVA with Tukey multiple comparison test (A, B, C, D, E, G, H) or unpaired t test (F, I). Mean ± SEM.

3.3.2.2 E6130 attenuates fractalkine-induced increases in OE33, FLO-1, FLO-1^{LM}, OE33P, OE33R, OE33CisP and OE33CisR cell viability

Since increased cell viability was observed in the OAC cell lines following 24-hour fractalkine treatment, the CX3CR1 modulator E6130 was next investigated to evaluate if it could reverse or attenuate such effects. The IC50 of 4.9nM of E6130 has previously shown efficacy to impede NK cell migration in studies done by our group[68, 69]. However, we explored multiple doses to evaluate if A) OAC cell lines were sensitive to different concentrations of E6130 and B) if the IC50 value was optimal for impeding the non-chemotactic effects of fractalkine. Importantly, the cell lines were treated slightly different during these experiments because of their differential sensitivity to fractalkine. OE33 cell lines were treated with 100 and 200ng/ml fractalkine, while FLO-1 and FLO-1^{LM} were treated with 10 and 100ng/ml based on their sensitivities to these doses, which were identified in the previous experiments.

To determine the optimal dose at which E6130 could alter OE33 cell viability induced by fractalkine treatment, OE33 cells were pre-treated for 1 hour with a range of increasing concentrations of E6130 and then treated with 200ng/ml of fractalkine (one of the doses of fractalkine in which most profound increase to OE33 cell viability was observed) **[Figure 3.5]**, for 24 hours. Following treatment, cell viability was measured by CCK-8 assay. Pre-treatment with 4.9nM E6130 significantly decreased the effects of 200ng/ml of fractalkine (FKN) on OE33 cells, compared to treatment with vehicle control for E6130 (0.01% DMSO) DMSO + 200ng/ml FKN vs 4.9nM E6130 + 200ng/ml FKN (129.4% vs 100.2%, p=0.0032, n=7) **[Figure 3.6 A].** Other concentrations of E6130 didn't significantly decrease the effects of fractalkine on OE33 cells **[Figure 3.6A].**

Next, the effects of this optimal dose of 4.9nM E6130 on OE33 cells treated with 100 and 200ng/ml of fractalkine was assessed in comparison to OE33 cells treated with the vehicle control of E6130 and 100 and 200ng/ml of fractalkine. These doses of fractalkine were selected because they elicited the most profound effects **[Figure 3.5]**. OE33 cells were either pre-treated for 1 hour with 0.01% DMSO or 4.9nM of E6130 and then treated with high doses of fractalkine (100 and 200ng/ml), for 24 hours. Cell viability was measured by CCK-8 assay. OE33 cells treated with DMSO and 100ng or 200ng of fractalkine had significantly increased cell viability compared to the OE33 cells treated with DMSO alone;

DMSO vs DMSO + 100ng/ml FKN (99% vs 115.5 %, p= 0.03, n=6); DMSO vs DMSO + 200ng/ml FKN (99% vs 117.6%, p=0.017, n=6). E6130 significantly decreased the effects of fractalkine on OE33 cells when cells were treated with 4.9nM E6130 and 100ng/ml of fractalkine; DMSO + 100ng/ml FKN vs E6130 + 100ng/ml FKN (115.5% vs 96.7%, p=0.03, n=6) and when OE33 cells were treated with 4.9nM and 200ng/ml of fractalkine; DMSO + 200ng/ml FKN vs E6130 + 200ng/ml FKN (117.6% v 97.8%, p=0.018, n=6) **[Figure 3.6B].**

E6130's effect was evaluated in the same manner in FLO-1 and FLO-1^{LM} cells using low dose (10ng/ml) and high dose (100ng/ml) of fractalkine, reflective of the doses eliciting the most significant effects in section 3.3.2.1. Cell viability was significantly increased when FLO-1 cells were treated with DMSO and 10ng of fractalkine compared to DMSO alone; DMSO vs DMSO + 10ng/ml FKN (104.5% vs 131%, p= 0.042, n=6) **[Figure 3.6C, left]** and when FLO-1 cells were treated with DMSO and 100ng/ml compared to DMSO alone; DMSO vs DMSO + 100ng/ml FKN (107% vs 145.8%, p= 0.037, n=6) **[Figure 3.5C, right]**. E6130 at 4.9nM, 10nM, 100nM and 1000nM significantly decreased the effects of 10ng fractalkine on FLO-1 cell viability; DMSO + 10ng/ml FKN vs 4.9nM E6130 + 10ng/ml FKN (127.8% vs 100%, p=0.009, n=6), DMSO + 10ng/ml FKN vs 10nM E6130; 127.8% vs 99%, p=0.005, n=6), DMSO + 10ng/ml FKN vs 100nM E6130 (127.8% vs , 98.3%, p=0.005, n=6), DMSO + 10ng/ml FKN vs 1000nM E6130 (127.8% vs 98.2%, p= 0.004, n=6) **[Figure 3.6C, left]**. There was also a significant difference when cells were treated with 100ng of fractalkine and pretreated with 0.1nM, 4.9nM and 10nM E6130; DMSO + 100ng/ml FKN vs 0.1nM E6130 (145.8% vs 102.5 %, p= 0.012, n=6), DMSO + 100ng/ml vs 4.9nM E6130, (145.8% vs 105%, p=0.023, n=6), DMSO + 100ng/ml FKN vs 10nM E6130, (145.8% vs 100.7%, p=0.007, n=6) **[Figure 3.6C, right].** Cell viability was significantly increased when FLO-1^{LM} cells were treated with DMSO and 10ng of fractalkine compared to water alone; Water vs DMSO + 10ng/ml FKN (104.5% vs 131%, p=0.002, n=6) **[Figure 3.6D, left]**. E6130 at 4.9nM significantly decreased the effects of fractalkine on FLO-1^{LM} cells viability treated with 10ng of fractalkine; DMSO + 10ng/ml FKN vs 4.9nM E6130 + 10ng/ml FKN (131% vs 104.3%, p=0.027, n=6) **[Figure 3.6D, left].** However, when FLO-1^{LM} cells were treated with 100ng/ml, there were no significant increases in cell viability with this

concentration of fractalkine, and no significant decreases when the cells were pre-treated with E6130 **[Figure 3.6D, right]**.

The effect of E6130 was evaluated in the same manner in OE33P and OE33R cells using 10, 100 and 200ng/ml of fractalkine, reflective of the doses eliciting significant effects in section 3.3.2.1. OE33P cells exhibited increased viability following 24-hour treatment with fractalkine compared to cells treated with DMSO; DMSO vs DMSO + 10ng/ml FKN (102.6% vs 118%, p=0.035, n=5), DMSO vs DMSO + 100ng/ml FKN (102.6% vs 120.6%, p=0.002, n=5), DMSO vs DMSO + 200ng/ml FKN (102.6% vs 121.8%, p=0.035, n=5) **[Figure 3.6E].** Pre-treatment with 4.9nM E6130 on OE33P cells significantly attenuated fractalkine-induced cell viability with 10, 100 and 200ng/ml of fractalkine compared to cells treated with DMSO and 10, 100 and 200ng/ml of fractalkine; DMSO + 10ng/ml FKN vs E6130 + 10ng/ml FKN (118% vs 97.6%, p=0.015, n=5), DMSO + 100ng/ml FKN vs E6130 + 100ng/ml FKN (120.6% vs 106.6%, p=0.047, n=5), DMSO + 200ng/ml FKN vs E6130 + 200ng/ml FKN (121.8% vs 96.4%, p=0.029, n=5) **[Figure 3.6E]**. OE33R exhibited increased cell viability induced by 10, 100 and 200ng/ml of fractalkine compared to DMSO treated cells; DMSO vs DMSO + 10ng/ml FKN (100.2% vs 110%, p=0.027, n=5), DMSO vs DMSO + 100ng/ml FKN (100.2% vs 112.6%, p=0.009, n=5), DMSO vs DMSO + 200ng/ml FKN (100.2% vs 111.8%, p=0.032, n=5) **[Figure 3.6F]**, This increased cell viability was attenuated by pretreatment with 4.9nM E6130; DMSO + 10ng/ml FKN vs E6130 + 10ng/ml FKN (110% vs 98.8%, p=0.032, n=5), DMSO + 100ng/ml FKN vs E6130 + 100ng/ml FKN (112.6% vs 94.4%, p=0.032, n=5), DMSO + 200ng/ml FKN vs E6130 + 200ng/ml FKN (111.8% vs 92.4%, p=0.041, n=5) **[Figure 3.6F].** The effectiveness of 4.9nM of E6130 to attenuate the fractalkine-mediated alterations was also compared between the OE33P and OE33R cells. Our data revealed no significant differences between the sensitivity of OE33P and OE33R to E6130, suggesting that radioresistant tumours respond to E6130 treatment to a similar extent as their radiosensitive counterparts **[Figure 3.6G].**

The effects of E6130 on OE33CisP and OE33CisR viability following fractalkine treatment were assessed in a similar manner as OE33P and OE33R. OE33P cells exhibited increased viability following 24-hour treatment with fractalkine compared to cells treated with DMSO; DMSO vs DMSO + 10ng/ml FKN, (102.2% vs 122%, p=0.012, n=5), DMSO vs

DMSO + 100ng/ml FKN (102.2% vs 122.1%, p=0.035, n=5), DMSO vs DMSO + 200ng/ml FKN (102.2% vs 120.4%, p=0.035, n=5) **[Figure 3.6H].** Increases in cell viability of OE33CisP induced by 10, 100 and 200 ng/ml of fractalkine were significantly attenuated by pre-treating cells with 4.9nM E6130 compared to cells treated with fractalkine; DMSO + 10ng/ml FKN vs E6130 + 10ng/ml FKN (122% vs 88.8%, p=0.012, n=5), DMSO + 100ng/ml FKN vs E6130 + 100ng/ml FKN (122.1% vs 101.9%, p=0.040, n=5), DMSO + 200ng/ml FKN vs E6130 + 200ng/ml FKN (120.4% vs 87.8 %, p=0.009, n=5) **[Figure 3.6H]**. However, OE33CisR exhibited significantly increased cell viability induced by DMSO and 10 and 200ng/ml of fractalkine only; DMSO vs DMSO + 10ng/ml FKN (103.8% vs 125.5%, p=0.031, n=6), DMSO vs DMSO + 200ng/ml FKN (103.8% vs 124.7%, p=0.032, n=6) **[Figure 3.6I]**. This fractalkine-induced increased viability was attenuated by pretreatment with 4.9nM E6130; DMSO + 10ng/ml FKN vs E6130 + 10ng/ml FKN (125.5% vs 91.7%, p=0.0002, n=6), DMSO + 200ng/ml FKN vs E6130 + 200ng/ml FKN (124.7% vs 91.7%, p=0.0003, n=6) **[Figure 3.6I].** The effectiveness of E6130 pretreatment was compared between the OE33CisP and OE33CisR cells. There were no significant differences found between OE33CisP and OE33CisR, suggesting once more that chemo resistant tumours are as amenable to E6130 treatment as their chemo sensitive counterparts **[Figure 3.6J].**

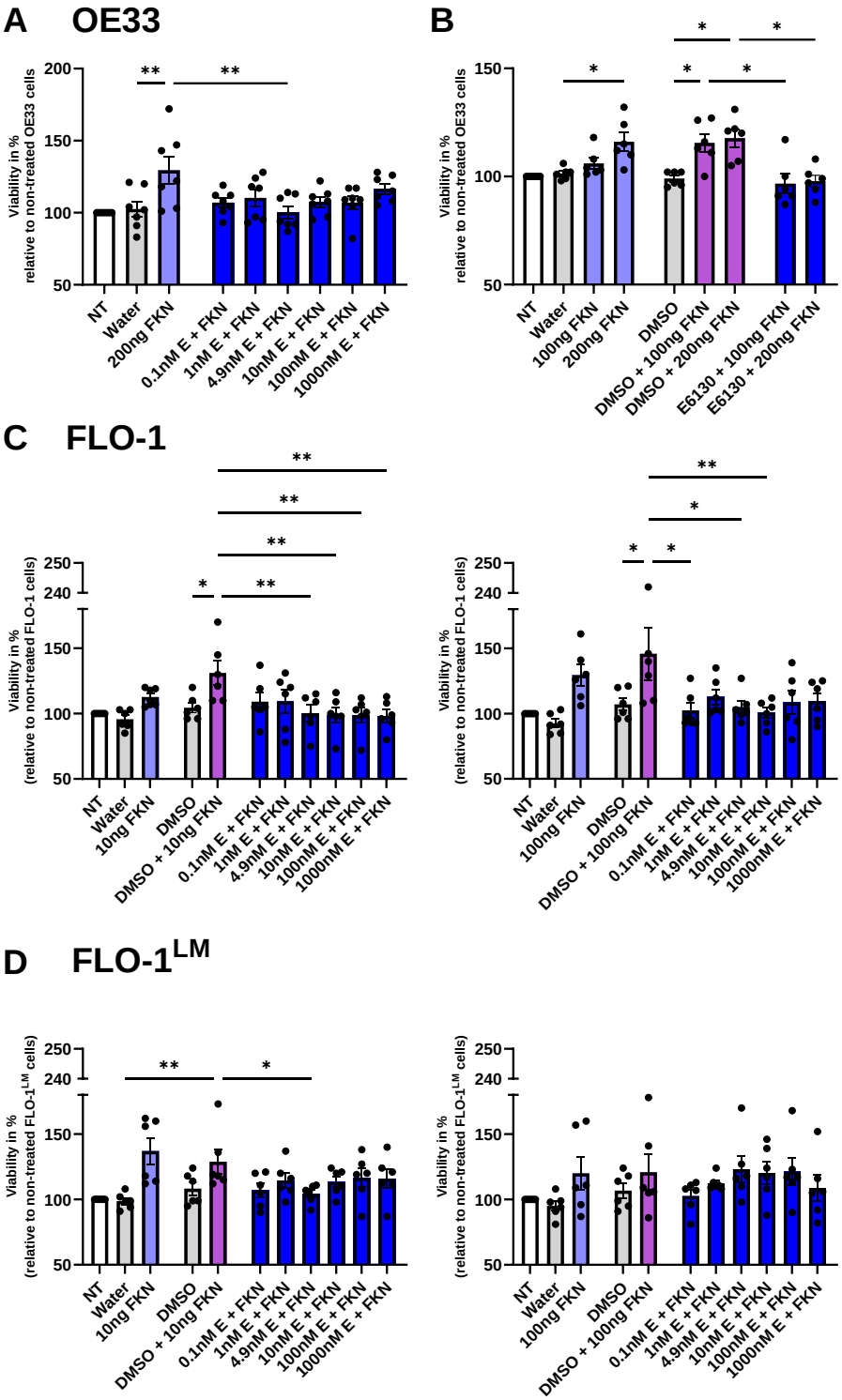
A OE33
B
C FLO-1
D FLO-1LM
Viability in % relative to non-treated OE33 cells
Viability in % (relative to non-treated FLO-1 cells)
Viability in % (relative to non-treated FLO-1LM cells)
NT
Water
200ng FKN
0.1nM E + FKN
1nM E + FKN
4.9nM E + FKN
10nM E + FKN
100nM E + FKN
1000nM E + FKN
100ng FKN
DMSO
DMSO + 100ng FKN
DMSO + 200ng FKN
E6130 + 100ng FKN
E6130 + 200ng FKN
10ng FKN
DMSO + 10ng FKN

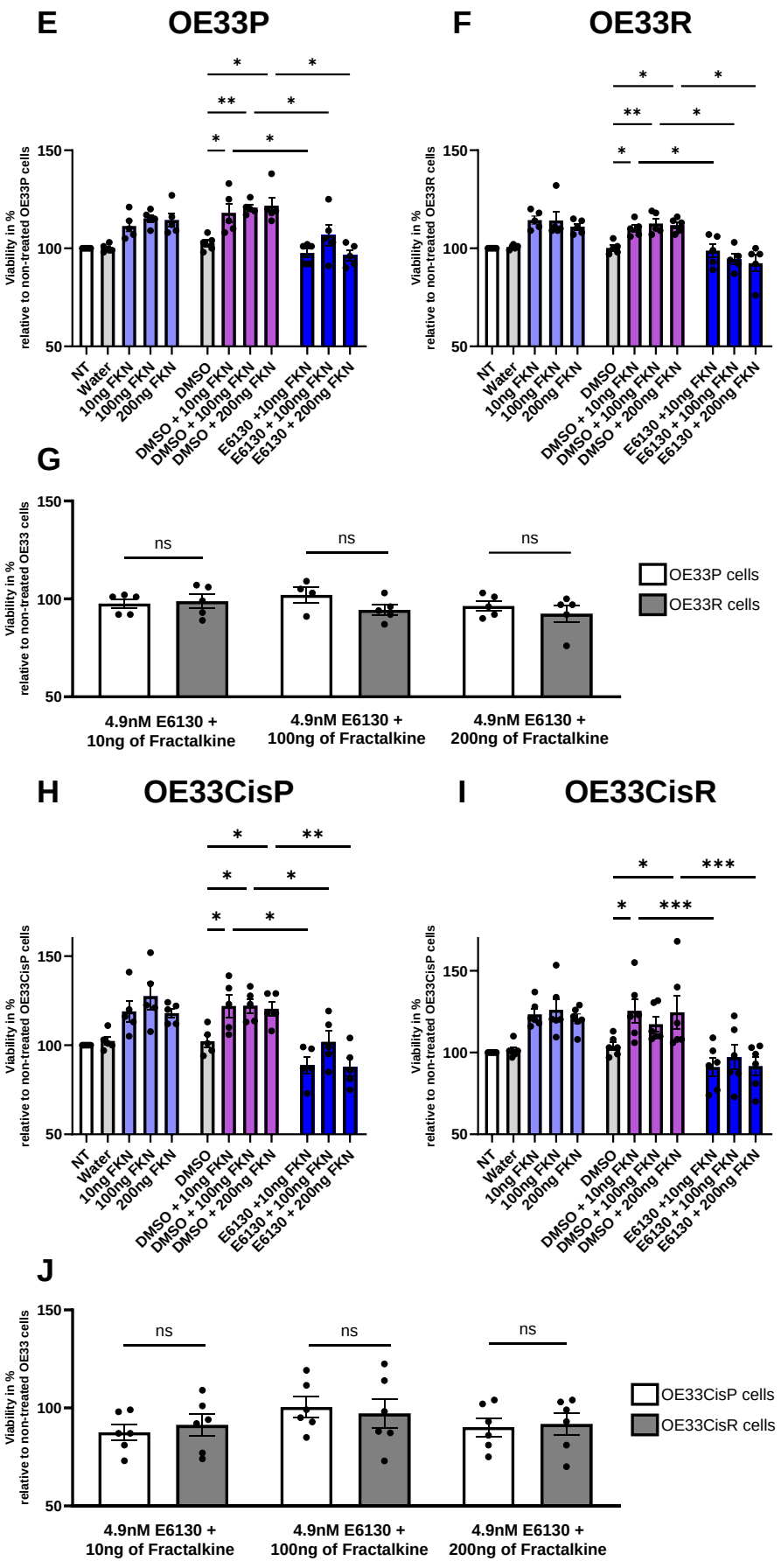
E
OE33P
F
OE33R
Viability in % relative to non-treated OE33P cells
Viability in % relative to non-treated OE33R cells
150
100
50
NT
Water
10ng FKN
100ng FKN
200ng FKN
DMSO
DMSO + 10ng FKN
DMSO + 100ng FKN
DMSO + 200ng FKN
E6130 +10ng FKN
E6130 + 100ng FKN
E6130 + 200ng FKN
G
Viability in % relative to non-treated OE33 cells
ns
OE33P cells
OE33R cells
4.9nM E6130 + 10ng of Fractalkine
4.9nM E6130 + 100ng of Fractalkine
4.9nM E6130 + 200ng of Fractalkine
H
OE33CisP
I
OE33CisR
Viability in % relative to non-treated OE33CisP cells
Viability in % relative to non-treated OE33CisR cells
J
Viability in % relative to non-treated OE33 cells
OE33CisP cells
OE33CisR cells
4.9nM E6130 + 10ng of Fractalkine
4.9nM E6130 + 100ng of Fractalkine
4.9nM E6130 + 200ng of Fractalkine

Figure 3.6: Significantly enhanced OE33, FLO-1, FLO-1^{LM}, OE33P, OE33R, OE33CisP and OE33CisR cell viability following 24-hour fractalkine treatment can be attenuated with E6130.

Bar chart showing % of **(A)** OE33 cell viability following no treatment (NT), treatment with 0.1% water (vehicle control for fractalkine), 200ng/ml recombinant fractalkine (FKN) or 0.1, 1, 4.9, 10, 100 or 1000nM E6130 + 200ng/ml F for 24 hours, experiments were repeated n=7. Bar chart showing % of **(B)** OE33 cell viability following no treatment, treatment with 0.1 % water, 100 or 200ng/ml FKN, 0.01 % DMSO (vehicle control for E6130) +/- 100 or 200ng/ml FKN, E6130 + 100 or 200ng/ml FKN for 24 hours. Experiments were repeated n=6. Bar charts showing % viability of **(C)** FLO-1 cells and **(D)** FLO-1^{LM} cells with no treatment (NT), treated with 0.1% water, 10 or 100ng/ml recombinant fractalkine (FKN), 0.01% DMSO +/- 10 or 100ng/ml recombinant fractalkine (FKN), E6130 + 10 or 100ng/ml recombinant fractalkine (FKN) for 24 hours, n=6. Bar charts showing % of OE33P **(E),** OE33R **(F), (H)** OE33CisP and **(I)** OE33CisR cell viability measured by CCK8 assay following no treatment (NT), treatment with 0.1 % water, 10, 100 or 200ng/ml recombinant fractalkine (FKN), 0.01% DMSO +/- 10, 100 or 200ng/ml recombinant fractalkine (FKN), 4.9nM E6130 + 10, 100 or 200ng/ml recombinant fractalkine (FKN) for 24 hours. Bar charts showing comparison of % viability of **(G)** OE33P and OE33R cells and **(J)** OE33CisP and OE33CisR cells treated with 4.9nM E6130 + 10, 100 or 200ng/ml of recombinant fractalkine (FKN) for 24 hours. *$p<0.05$, **$p<0.01$, ***$p<0.001$ by ordinary one-way ANOVA with Tukey multiple comparison test (A, B, C, D, E, F, H, I) or unpaired t test (G, J). Mean ± SEM.

3.3.3 Fractalkine increases cell proliferation in OE33, FLO-1, FLO-1^{LM}, OE33P and OE33R cells and E6130 attenuates such fractalkine-induced increases in cell proliferation

3.3.3.1 Fractalkine increases cell proliferation in OE33, FLO-1, FLO-1^{LM}, OE33P and OE33R cells

As another measure of fractalkine's pro-tumour effects in OAC, cell proliferation was assessed in the panel of OAC cells lines following treatment with fractalkine at a range of concentrations (0.1 to 200ng/ml) for 24 hours. A BrdU assay was performed to assess if their viability was altered. Proliferation of OE33 cells was significantly increased following 24-hour treatment with 200ng/ml of fractalkine; Water vs 200ng/ml FKN (97.3% vs 112.6%, p=0.031, n=7) **[Figure 3.7A]**. FLO-1 cell proliferation was significantly increased following 24-hour treatment with 10, 100 and 200ng/ml of fractalkine; Water vs 10ng/ml FKN (99.8% vs 109.4%, p=0.015, n=5), Water vs 100ng/ml FKN (99.8% vs 113.4%, p=0.004, n=5), Water vs 200ng/ml FKN (99.8 vs 118%, p=0.017, n=5) **[Figure 3.7B]**. FLO-1^{LM} cell proliferation was significantly increased with 100ng/ml of fractalkine treatment; Water vs 100ng/ml FKN (100.8% vs 109.7 %, p=0.01, n=6) **[Figure 3.7C]**. These data suggest that fractalkine elicits a proliferative effect on both FLO-1 and FLO-1^{LM} cells, with FLO-1 cells displaying sensitivity to lower doses of the chemokine.

Fractalkine's effect on proliferation was also assessed in the parental and radioresistant cell lines OE33P and OE33R. Significantly increased levels of cell proliferation were observed in OE33P cells treated with 10 and 100ng/ml of fractalkine, compared to OE33P cells treated with water; Water vs 100ng/ml FKN (97.4% 111.6%, p= 0.004, n=5), Water vs 100ng/ml FKN (97.4% vs 109.4%, p=0.027, n=5) **[Figure 3.7D].** OE33R cells exhibited significantly increased levels of proliferation following treatment with 10 and 100ng of fractalkine, compared to OE33R cells treated with water; Water vs 10ng/ml FKN (99% vs 111.5%, p=0.022, n=5), Water vs 100ng/ml FKN (99% vs 111%, p=0.033; n=5) **[Figure 3.7E]**. The cell proliferation of OE33P and OE33R cells treated with 10ng, 100ng and 200ng of recombinant fractalkine was compared, to assess if fractalkine-mediated effects differed between the cell lines. There were no significant differences in cell proliferation between the two cell lines when their sensitivity to fractalkine was compared suggesting

that radioresistant tumours are equally susceptible to the tumourigenic effects of the chemokine **[Figure 3.7F].**

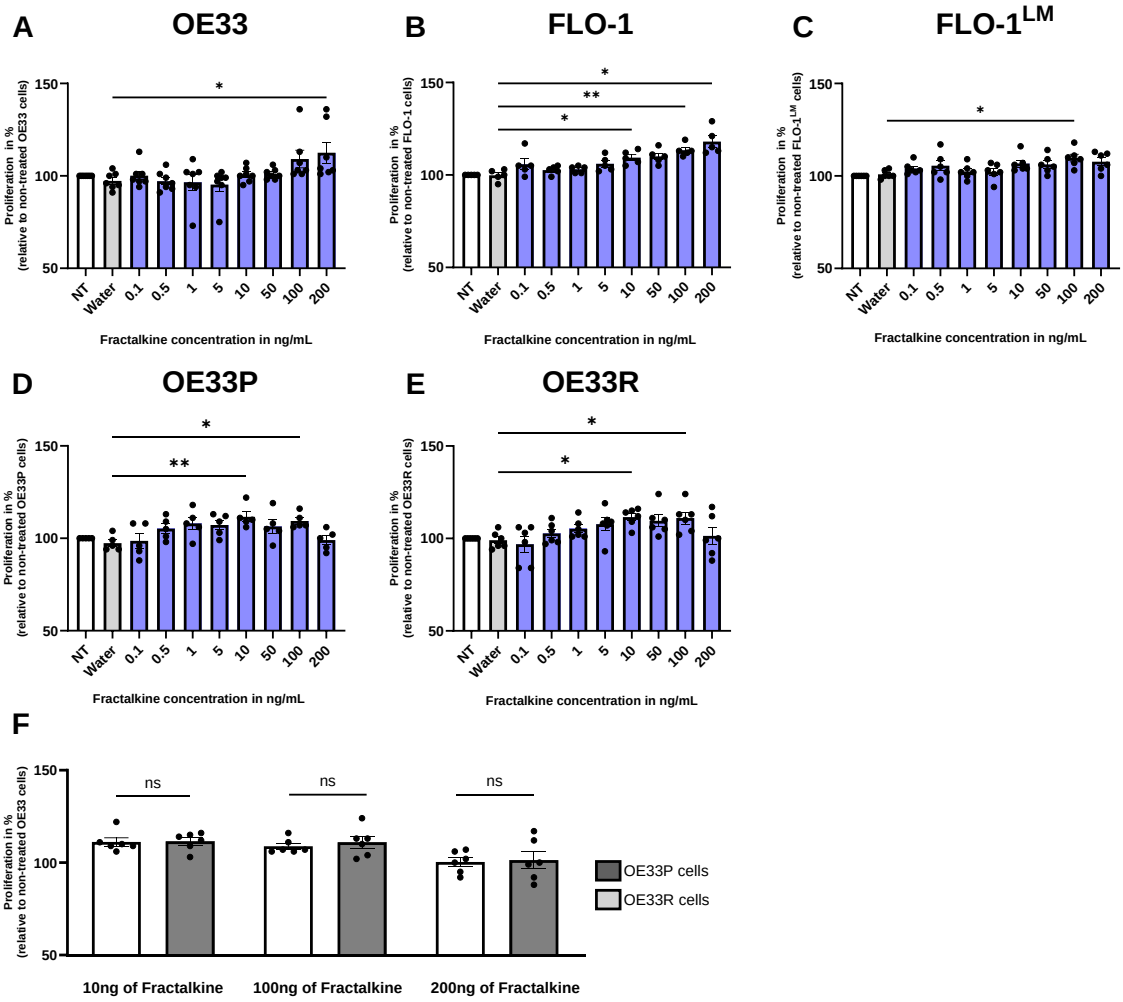

Figure 3.7 : Significantly increased proliferation following 24-hour treatment with high doses of fractalkine in OE33, FLO-1, FLO-1^{LM}, OE33P and OE33R cell lines and following 24-hour treatment with low doses of fractalkine in FLO-1 cell lines.

Bar charts showing % of **(A)** OE33**, (B)** FLO-1, **(C)** FLO-1^{LM}**, (D)** OE33P and **(E)** OE33R cell proliferation measured by BrdU assay following no treatment (NT), treatment with 0.1% water (vehicle control for fractalkine) or 0.1, 0.5, 1, 5, 10, 50, 100, 200 ng/ml of recombinant fractalkine for 24 hours. **(F)** Bar charts showing comparison of % proliferation of OE33P and OE33R cells treated with 10, 100 or 200ng/ml of fractalkine for 24 hours. Experiments were repeated n=5-7. *p<0.05, *p<0.01 by ordinary one-way ANOVA with Tukey multiple comparison test or unpaired t test where appropriate. Mean ± SEM.

3.3.3.2 E6130 attenuates fractalkine-induced increases in OE33, FLO-1, FLO-1^{LM}, OE33P and OE33R cell proliferation

Since increased cell proliferation was observed in OE33 cell lines following 24-hour fractalkine treatment, the CX3CR1 modulator E6130 was next investigated to evaluate if it could reverse or attenuate such effects in OE33, FLO-1, FLO-1^{LM}, OE33P and OE33R cell proliferation. DMSO + 100ng of fractalkine significantly increased cell proliferation of OE33 cells compared to DMSO alone; DMSO vs DMSO + 100ng/ml FKN (100.3% vs 111.8%, p=0.007, n=6). Although none-significant, DMSO + 200ng/ml of fractalkine also increased proliferation of OE33 cells compared to DMSO alone; DMSO vs DMSO + 200ng/ml FKN (100.3% vs 109.5%, p=0.062, n=6) **[Figure 3.8A]**. Significantly decreased OE33 cell proliferation was observed when the cells were treated with 4.9nM E6130 and 100ng and 200ng of fractalkine, compared to DMSO and 100ng and 200ng of fractalkine; DMSO + 100ng/ml FKN vs 4.9nM E6130 + 100ng/ml FKN (111.8% vs 98.5%, p=0.0011, n=6), DMSO + 200ng/ml FKN vs 4.9nM E6130 + 200ng/ml FKN (109.5% vs 96%, p=0.0009, n=6) **[Figure 3.8A].**

Similarly, DMSO + 10ng or 100ng of fractalkine significantly increased cell proliferation of FLO-1 cells compared to DMSO alone, DMSO vs DMSO + 10ng/ml FKN (99.6% vs 108.2%, p=0.006, n=5), DMSO vs DMSO + 100ng/ml FKN (99.6% vs 109.6%, p=0.001, n=5) **[Figure 3.8B]**. Pre-treatment with 4.9nM E6130 significantly attenuated the proliferative effects of 10ng/ml but not 100ng/ml of fractalkine on FLO-1 cells; DMSO + 10ng/ml FKN vs 4.9nM E6130 + 10ng/ml FKN (108.2% vs 97.6%, p=0.0004, n=5) **[Figure 3.8B]**. Fractalkine did not induce proliferation of FLO-1^{LM} cells when pre-treated with DMSO and E6130 did not decrease proliferation of FLO-1^{LM} cells **[Figure 3.8C]**. Since the pre-metastatic cell lines OE33 and FLO-1 responded to fractalkine following pre-treatment with DMSO and since E6130 could attenuate such fractalkine-induced effects, these data indicate that different OAC cell lines may elicit different responses to pharmacological agents and illustrates the need to use several cell line models in such studies.

OE33P cells exhibited significant increases in cell proliferation when treated with DMSO and 10 and 100ng/ml of fractalkine compared to OE33P cells treated with DMSO alone; DMSO vs DMSO + 10ng/ml FKN (98.4% vs 109.6%, p=0.002), DMSO vs DMSO +

100ng/ml FKN (98.4% vs 108%, p=0.018, n=6) **[Figure 3.8D]**. This increased proliferation was attenuated by pre-treating cells with 4.9nM of E6130; DMSO + 10ng/ml FKN vs E6130 + 10ng/ml FKN (109.6% vs 99%, p=0.006, n=6), DMSO + 100ng/ml FKN vs E6130 + 100ng/ml FKN (108% vs 97.7%, p=0.008, n=6) **[Figure 3.8D].** Similarly, OE33R cells exhibited significant increases in proliferation when treated with DMSO and 10 and 100ng/ml of fractalkine for 24-hours, compared to DMSO alone; DMSO vs DMSO + 10ng/ml FKN (97% vs 113%, p=0.007, n=6), DMSO vs DMSO + 100ng/ml FKN (97% vs 108.9%, p=0.022, n=6) **[Figure 3.8E].** This increased proliferation was attenuated by pre-treating cells with 4.9nM of E6130; DMSO + 10ng/ml FKN vs E6130 + 10ng/ml FKN, (113% vs 100.3%, p=0.002, n=6), DMSO + 100ng/ml FKN vs E6130 + 100ng/ml FKN (108.9% vs 97.9%, p=0.043, n=6) **[Figure 3.8E]**. The effectiveness of 4.9nM of E6130 to attenuate the alterations following treatment with 10ng, 100ng and 200ng of recombinant fractalkine was also compared between the OE33P and OE33R cells. There were no significant differences in cell proliferation between the two cell lines when treated with E6130 and both concentrations of fractalkine, suggesting that radioresistant tumours are equally susceptible to the anti-tumourigenic effects of E6130 **[Figure 3.8F].**

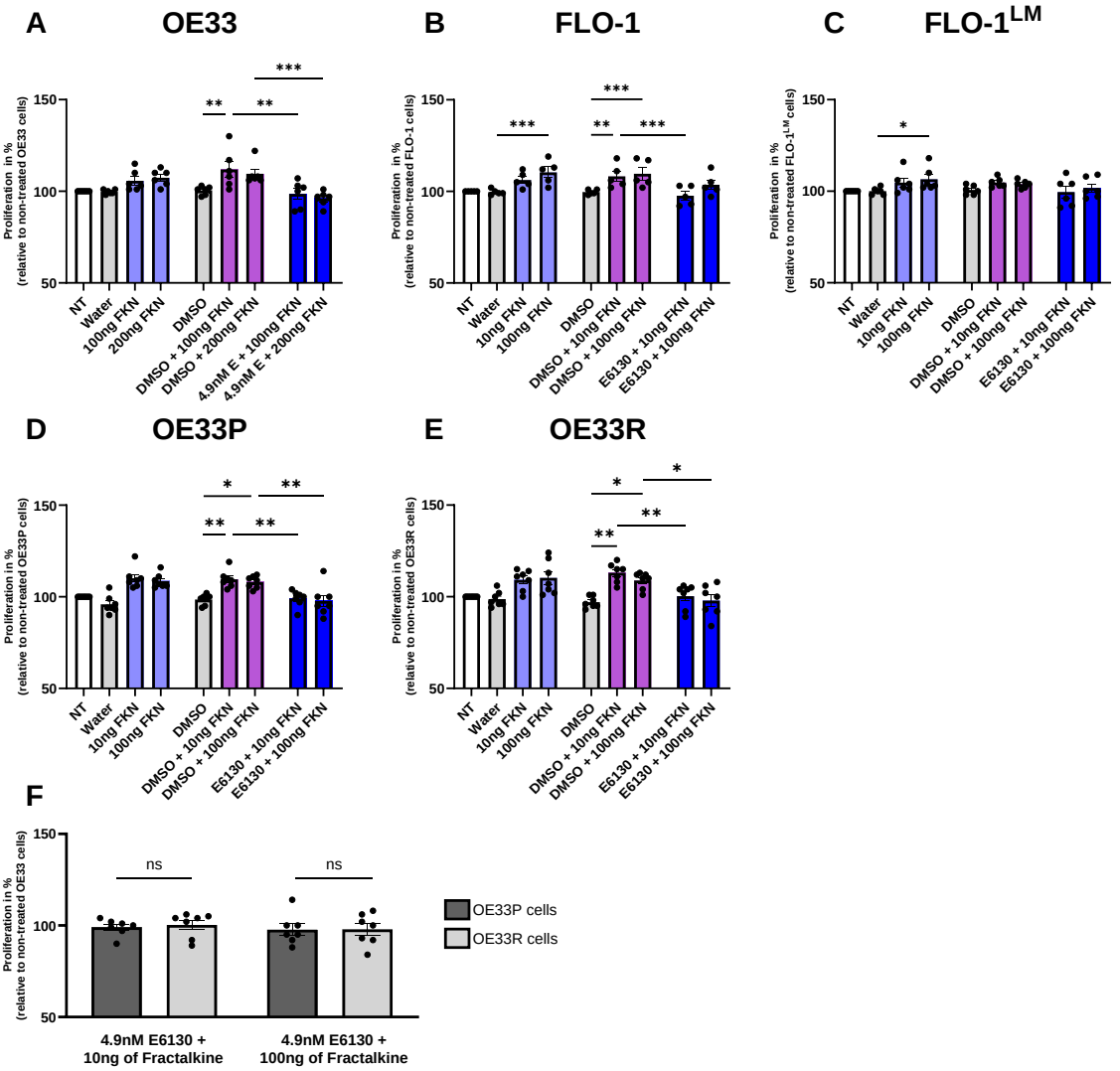

Figure 3.8: Fractalkine-mediated enhancement of OE33, FLO-1, OE33P and OE33R cell proliferation can be attenuated with E6130.

Bar charts showing % of **(A)** OE33, **(B)** FLO-1, **(C)** FLO-1^{LM}, **(D)** OE33P and **(E)** OE33R cells with no treatment (NT), treatment with 0.1 % water, 10 100 or 200ng/ml recombinant fractalkine (FKN), 0.01% DMSO +/- 10, 100 or 200ng/ml FKN, 4.9nM E6130 + 10, 100 or 200ng/ml FKN for 24 hours. **(F)** Bar chart showing comparison of % proliferation of OE33P and OE33R cells treated with 4.9nM E6130 + 10 or 100ng/ml of F for 24 hours. Experiments were repeated n=5-7. *p<0.05, **p<0.01, ***p<0.001, by ordinary one-way ANOVA **with Tukey multiple comparison test (A, B, C, D, E) or unpaired t test (F)**. Mean ± SEM

3.3.4 Assessing the effects of the tumour microenvironment on CX3CR1 expression on OAC cells.

3.3.4.1 Acidosis and 0.5% hypoxia significantly alters CX3CR1 expression on OE33, FLO-1 and FLO-1^{LM} cells.

It is well established that the TME elicits profound effects on tumour growth and anti-cancer drug efficacy. Here, we examined how acidosis, nutrient deprivation and hypoxia affect CX3CR1 surface expression on OE33, FLO-1 and FLO-1^{LM} cells thus shedding light on how these physiological conditions might affect the efficacy of E6130 in vivo. OE33, FLO-1 and FLO-1^{LM} cells were treated with media containing different doses of FBS (5%, 0.5% and 0% FBS) or media with no glucose to simulate nutrient deprivation in the TME, media with different pHs (pH 6.6 and 5.5) to simulate acidosis, or the cells were put under hypoxic conditions at 0.5% oxygen levels for 24 hours. OAC cells were analysed as total CX3CR1^{+} CX3CR1^{low} and CX3CR1^{high} cell populations, as previously shown in the gating strategy in **[Figure 3.1]** and **[Figure 3.2].**

Under hypoxic conditions for 24 hours, significantly higher frequencies of CX3CR1^{+}OE33 cells were observed; NT vs 0.5% hypoxia (12.4% vs 28.3%, p=0.024, n=4-5) **[Figure 3.9A top]** and significantly higher frequencies of CX3CR1^{low}OE33 cells NT vs 0.5% hypoxia (8.5% vs 21.3%, p=0.007, n=4-5) **[Figure 3.9A middle].** FLO-1 cells under hypoxic conditions exhibited non-significant increases in CX3CR1^{+} cells; NT vs 0.5% hypoxia (21.9% vs 40.7%, p=0.090, n=4-5) **[Figure 3.9B top]**. FLO-1^{LM} cells expressed CX3CR1 at significantly higher frequencies under hypoxic conditions compared to non-treated cells; NT vs 0.5% hypoxia (14.4% vs 43%, p=0.017, n=4-5) **[Figure 3.9C top].** Hypoxic conditions seem to drive a CX3CR1^{high} phenotype in FLO-1^{LM} cells as their expression was significantly higher than non-treated ones; NT vs 0.5% hypoxia (5.5% vs 18%, p=0.0001, n=4-5) **[Figure 3.9C bottom].**

Under the conditions of acidosis, the abundance of CX3CR1^{high} OE33 cells were significantly increased when treated with media with a pH of 5.5 compared to non-treated cells; NT vs pH5.5, (3.4% vs 10.1%, p=0.026, n=5) **[Figure 3.9A bottom].** This suggests that acidosis favours a CX3CR1^{high} phenotype in OE33 cells. Lower acidic conditions also elicited effects on FLO-1 cells, with significantly increased frequencies of CX3CR1^{+} FLO-1 cells compared to non-treated cells; NT vs pH6.6 (21.9% vs 45.2%,

p=0.034, n=5) **[Figure 3.9B top]**. When separated into CX3CR1^{low} and CX3CR1^{high}, frequencies of CX3CR1^{high} FLO-1 cells were notably increased when treated with acidic conditions at a pH of 6.6; NT vs pH6.6 (5% vs 16.2%, p=0.070, n=5) which suggests that this population is favoured under acidic conditions of the TME **[Figure 3.9B bottom]**. Interestingly, acidic conditions at pH5.5 substantially increased frequencies of CX3CR1^{low}FLO-1^{LM} cells compared to NT cells; NT vs pH5.5 (8.5% vs 27.7%, p=0.057, n=5) **[Figure 3.9C middle].**

Overall, expression of the receptor CX3CR1 on the three different cell lines was higher following culture under the conditions of acidosis and hypoxia, suggesting that E6130 would elicit more profound effects under these physiological conditions in the OAC TME.

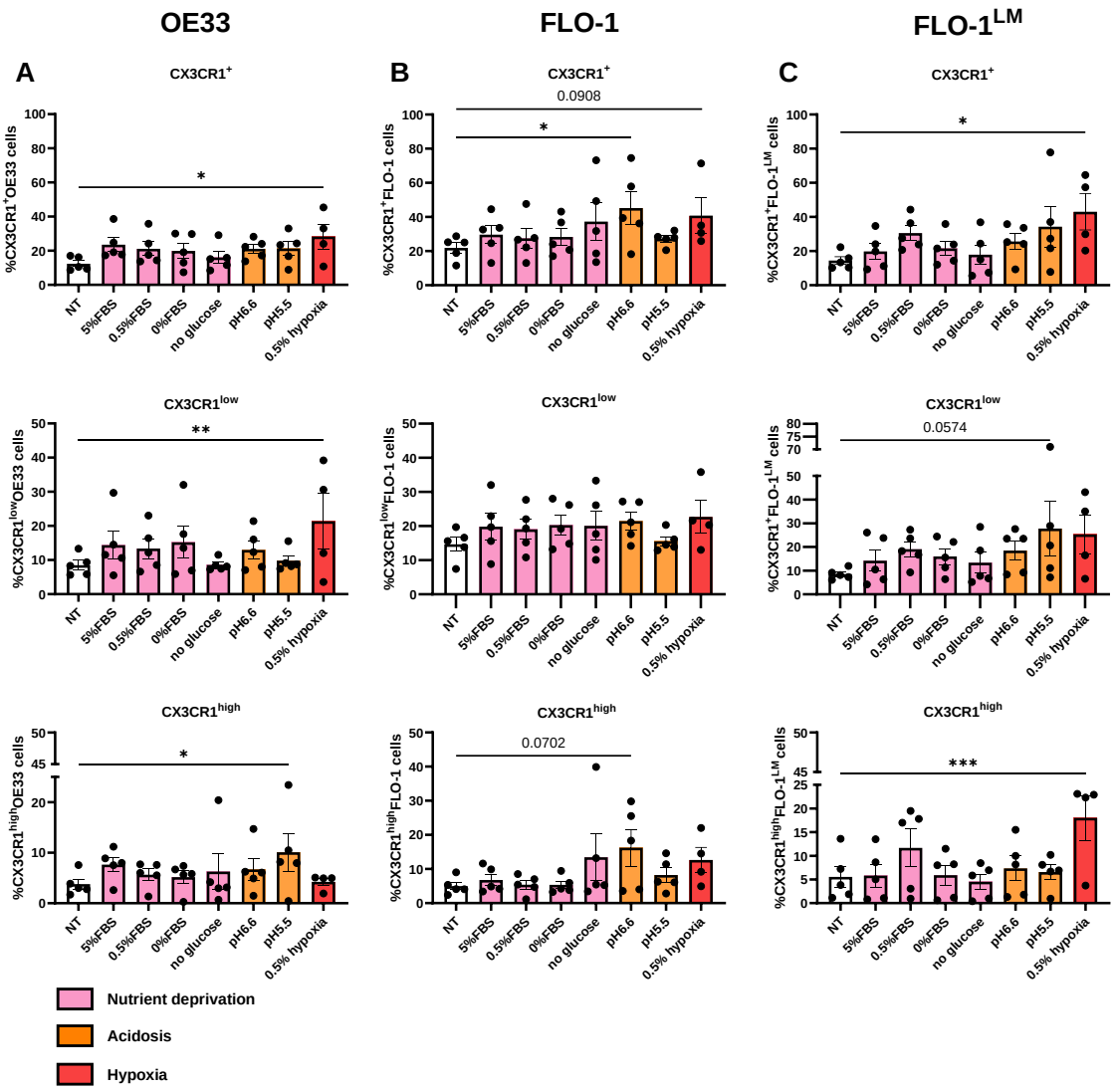

Figure 3.9: Acidosis and 0.5% hypoxia significantly increase the abundance of CX3CR1^{+} OE33, FLO-1 and FLO-1^{LM} cells.

Bar charts of % frequencies CX3CR1^{+}(top), CX3CR1^{low} (middle) and CX3CR1^{high} (bottom) OE33 **(A)** FLO-1 **(B)** and FLO-1^{LM} **(C)** cells treated with 5%, 0.5%, 0% FBS, pH 6.6 and pH 5.5 media, no-glucose media and under severe hypoxia (0.5% oxygen), n=4-5, *p<0.05, **p<0.01, ***p<0.001 by ordinary one-way ANOVA with Tukey multiple comparison test. Mean ± SEM.

3.3.4.2 Conditions of the TME do not significantly alter CX3CR1 expression on radioresistant or cisplatin resistant cell lines.

Using the same methodology as in section 3.4.4.1, CX3CR1 expression on OE33P, OE33R, OE33CisP and OE33CisR cells was screened under the physiological conditions of acidosis, nutrient deprivation and hypoxia.

Similarly to what was observed with OE33 cells, culturing the OE33P cells with media at pH5.5 significantly increased frequencies of $CX3CR1^{+}$OE33P cells compared to non-treated cells; NT vs pH5.5 (20.5% vs 34.9%, p=0.047, n=5) and similar results were seen in the $CX3CR1^{high}$ population where higher frequencies of $CX3CR1^{high}$OE33P cells were observed under acidic conditions; NT vs pH5.5, (3.7% vs 10.7%, p=0.017, n=5) **[Figure 3.10A]**. This could suggest that the $CX3CR1^{high}$ population of OE33P cells is more responsive to acidic conditions. However, no significant changes were observed in OE33R cells under the different conditions of the TME, suggesting that they have a different sensitivity to their microenvironment compared to OE33P and is perhaps an indicator of their robustness **[Figure 3.10B].**

When OE33CisP and OE33CisR cells were treated with the same conditions, no significant changes in frequencies of $CX3CR1^{+}$, $CX3CR1^{low}$ and $CX3CR1^{high}$ cells were observed **[Figure 3.10 C, D].**

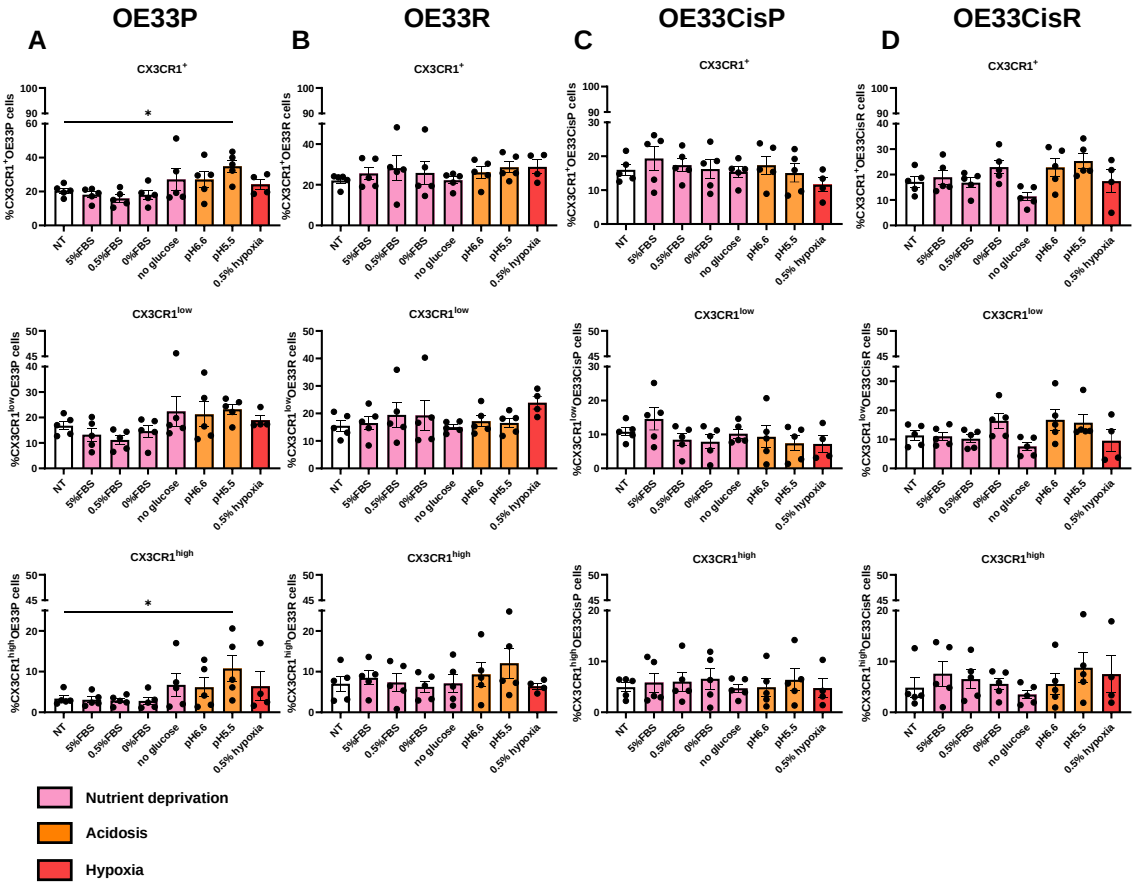

Figure 3.10: Acidosis significantly increases frequencies of CX3CR1^{+}OE33P cells but not OE33R, OE33CisP or OE33CisR cells.

Bar charts of % frequencies CX3CR1^{+}(top), CX3CR1^{low} (middle) and CX3CR1^{high} (bottom) OE33P **(A)** and OE33R **(B)** OE33CisP **(C)** and OE33CisR **(D)** cells treated with 5%, 0.5%, 0% FBS, pH 6.6 and pH 5.5 media, no-glucose media and under severe hypoxia (0.5% oxygen), n=4-5, *p<0.05, by ordinary one-way ANOVA with Tukey multiple comparison test. Mean ± SEM.

These results confirm that OE33, FLO-1, FLO-1^{LM}, OE33P, OE33R, OE33CisP and OE33CisR respond to TME conditions in a distinct manner, with greatest increases in CX3CR1 expression observed in OE33, FLO-1 and FLO-1^{LM} cells. CX3CR1 receptor on treatment resistant cell lines was not affected by the physiological conditions of the TME.

3.3.4.3 E6130 maintains its ability to reverse fractalkine's pro-tumourigenic effects under the conditions of the TME

In the previous sections, the cell line FLO-1, was shown to be sensitive to fractalkine's pro-tumourigenic effects, even at low doses and was shown to secrete the chemokine in significantly high concentrations. Furthermore, under acidosis (pH 6.6), CX3CR1 expression was significantly increased by FLO-1 cells suggesting an even higher susceptibility to fractalkine under the conditions of the TME. Given these collective findings, the effects of fractalkine and the efficacy of E6130 were assessed in FLO-1 cells under the conditions of the TME.

FLO-1 cells were first seeded overnight, and after 16 hours their media was changed to media either containing no FBS or a media with a pH of 6.6 for 24 hours. Alternatively, they were cultured in a hypoxic chamber at 0.5% oxygen levels for 24 hours. Following this, the cells were maintained in these conditions and treated with 10ng or 100ng/ml of fractalkine or its vehicle control 0.1% water for another 24 hours. Cell viability was assessed following the final 48 hours overall treatment. Under serum deprivation (0% FBS), cell viability was significantly increased when FLO-1 cells were treated with 10ng of fractalkine (FKN) compared to its vehicle control, water; Water vs 10ng/ml FKN (103.2% vs 115.7%, p=0.018, n=7) **[Figure 3.11A].** Similarly, when cells were exposed to a pH of 6.6 and under severe hypoxia, FLO-1 had significantly increased cell viability when treated with 100ng of recombinant fractalkine for 24 hours compared to water; Water vs 100ng/ml FKN (100.6% vs 141.2%, p=0.029, n=7) **[Figure 3.11B]**; Water vs 100ng/ml FKN (99.9% vs 108.8%, p=0.009, n=6) **[Figure 3.11C]**.

The effect of E6130 was also assessed to investigate if E6130 could reduce fractalkine-induced increases in cell viability in FLO-1 cells under these conditions. Following 24-hour treatment under the different TME conditions described above, FLO-1 cells were maintained in these conditions and either pre-treated for 1 hour with 0.01% DMSO or 4.9nM of E6130 and then treated with the same doses of fractalkine for another 24 hours.

Cell viability was then assessed using a CCK8 assay. Under serum deprivation, FLO-1 cells treated with DMSO and 10ng and 100ng of fractalkine had significantly increased cell viability compared to the FLO-1 cells treated with DMSO alone; DMSO vs DMSO + 10ng/ml FKN (102.3% vs 115.4 %, p= 0.018, n=7); DMSO vs DMSO + 100ng/ml FKN (102.3% vs 118.2%, p=0.01, n=7) **[Figure 3.11A].** E6130 significantly decreased the effects of fractalkine on FLO-1 cells when cells were treated with 4.9nM E6130 and 10ng/ml of fractalkine; DMSO + 10ng/ml FKN vs E6130 + 10ng/ml FKN (115.4% vs 95.4%, p=0.031, n=7) **[Figure 3.11A]** and when FLO-1 cells were treated with 4.9nM and 100ng/ml of fractalkine; DMSO + 100ng/ml FKN vs E6130 + 100ng/ml FKN (118.2% vs 96.9%, p=0.0009, n=7) **[Figure 3.11A].** In the same manner, under acidic conditions, FLO-1 cells treated with DMSO and 10ng and 100ng of fractalkine exhibited significantly increased cell viability compared to the FLO-1 cells treated with DMSO alone; DMSO vs DMSO + 10ng/ml FKN (98% vs 141.5 %, p= 0.044, n=7); DMSO vs DMSO + 100ng/ml FKN (98% vs 138.2%, p=0.025, n=7) **[Figure 3.11B].** E6130 significantly decreased the effects of fractalkine on FLO-1 cells when cells were treated with 4.9nM E6130 and 10ng/ml of fractalkine; DMSO + 10ng/ml FKN vs E6130 + 10ng/ml FKN (141.5% vs 78.9%, p=0.044, n=7) **[Figure 3.11B]** and when FLO-1 cells were treated with 4.9nM E6130 and 100ng/ml of fractalkine; DMSO + 100ng/ml FKN vs E6130 + 100ng/ml FKN (138.2% v 83.9%, p=0.022, n=7) **[Figure 3.11B].** Under hypoxic conditions, FLO-1 cells treated with DMSO and 100ng of fractalkine exhibited increased cell viability compared to the FLO-1 cells treated with DMSO alone, however it was not significant; DMSO vs DMSO + 100ng/ml FKN (98.7% vs 111.9%, p=0.07, n=6) **[Figure 3.11C].** E6130 however significantly decreased the effects of fractalkine on FLO-1 cells when cells were treated with 4.9nM E6130 and 10ng/ml of fractalkine; DMSO + 10ng/ml FKN vs E6130 + 10ng/ml FKN (109.9% vs 91.7%, p=0.024, n=6) **[Figure 3.11C]** and when FLO-1 cells were treated with 4.9nM and 100ng/ml of fractalkine; DMSO + 100ng/ml FKN vs E6130 + 100ng/ml FKN (111.9% v 95.5%, p=0.025, n=6) **[Figure 3.11C].**

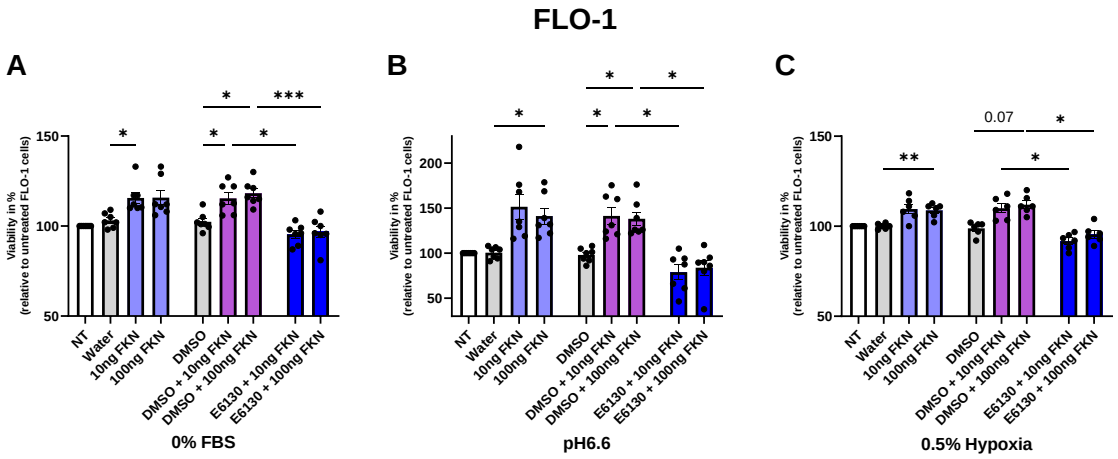

Figure 3.11: Fractalkine-mediated increases in FLO-1 cell viability can be attenuated with E6130 under conditions of nutrient deprivation, acidosis and hypoxia

Bar charts showing % of FLO-1 cells treated for 24 hours with media at **(A)** 0.5% FBS **(B)** pH 6.6 or **(C)** under 0.5% hypoxia followed by 24-hour treatment with 0.1 % water, 10 or 100ng/ml recombinant fractalkine (FKN), 0.01% DMSO +/- 10 or 100ng/ml recombinant fractalkine, 4.9nM E6130 + 10 or 100ng/ml recombinant fractalkine (FKN), or no treatment (NT). Experiments were repeated n=6-7. *p<0.05, **p<0.01, ***p<0.001, by ordinary one-way ANOVA with Tukey multiple comparison test. Mean ± SEM

Next, fractalkine and E6130's biological effects on FLO-1 cell viability under the three different conditions of the TME were compared to normal conditions (complete DMEM, cDMEM) to ascertain whether E6130 retained efficacy. Under acidic conditions of pH6.6, cell viability was significantly increased when FLO-1 cells were treated with 10ng of fractalkine compared to cells under normal conditions (cDMEM); cDMEM vs pH6.6 (112.3% vs 137.3%, p= 0.047, n=7) **[Figure 3.12A].** Similarly, FLO-1 cells treated with 100ng of fractalkine had a significantly higher cell viability compared to cells under normal conditions; cDMEM vs pH6.6 (108.9% vs 141.2%, p=0.019, n=7) **[Figure 3.12B].** When FLO-1 cells were treated with E6130 and 10ng or 100ng of fractalkine, there were notable differences however non-significant between cells under normal conditions and acidic conditions; 10ng FKN: cDMEM vs pH 6.6 (99.1% vs 79%, n=6-7); 100ng FKN: cDMEM vs pH6.6 (96.9% vs 83.9%, n=6-7). There was also a noticeable decrease between cells under hypoxic conditions compared to cDMEM when cells were treated with E6130 and 10ng of fractalkine; cDMEM vs 0.5 % Hypoxia (99.1% vs 91.7%, p=0.087, n=6-7) **[Figure 3.12C]**. These data show that fractalkine's effects on FLO-1 cell viability are significantly more pronounced under the conditions of acidosis while the efficacy of E6130 is retained under the physiological conditions of the TME.

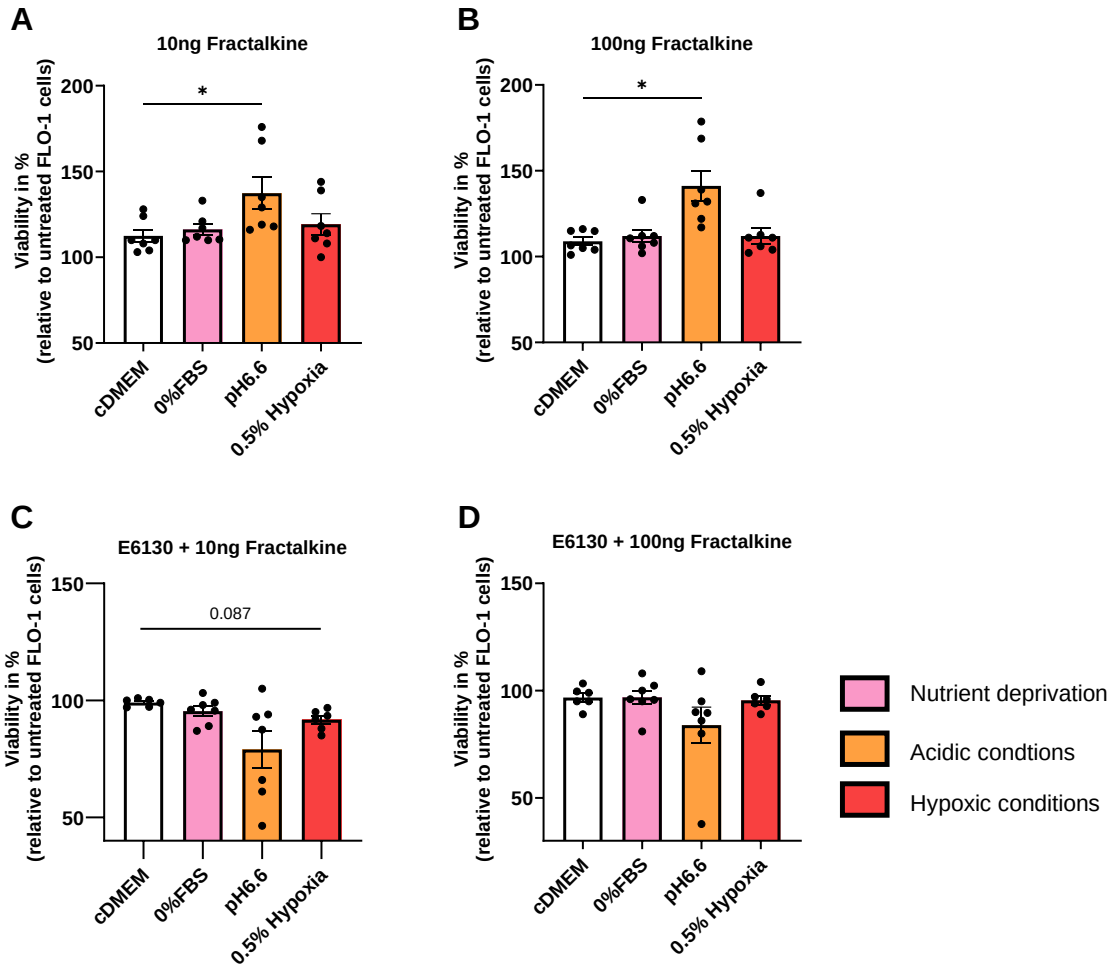

Figure 3.12: Fractalkine-mediated effects on FLO-1 cell viability are significantly enhanced under acidic conditions.

Bar charts showing comparison of % viability under normal conditions (cDMEM), nutrient deprivation (0% FBS), acidic conditions (pH 6.6) and hypoxic conditions (0.5% Hypoxia) for 24 hours of FLO-1 cells treated with **(A)** 10ng/ml recombinant fractalkine, **(B)** 100ng/ml recombinant fractalkine, **(C)** 4.9nM E6130 + 10ng/ml of recombinant fractalkine or **(D)** 4.9nM E6130 + 100ng/ml of recombinant fractalkine for another 24 hours. Experiments were repeated n=6-7. *$p<0.05$, by ordinary one-way ANOVA with Tukey multiple comparison test. Mean ± SEM.

3.4 Discussion

It is well established that chemokines play a crucial role in guiding both innate and adaptive immune cells towards solid tumours thus influencing the immune contexture of the TME [132-135, 153, 224-226]. In addition, the hijacking of the chemokine system by metastatic tumour cells is widely reported placing chemokine-targeted therapies as a desirable therapeutic concept [135, 153, 154, 162, 189, 209, 216, 328, 336-341]. Our group's published work shows that CX3CR1 modulation with E6130 can reduce NK cell migration towards the chemotactic cues of OAC patient-derived omentum and redirect NK cells towards the soluble cues of OAC tumour [69, 127, 342]. These compelling data reveal how E6130 can potentially augment anti-tumour immunity in OAC, but it is not yet fully understood how this will directly affect cancer cell growth, survival and spread. This chapter examined the direct effects of fractalkine and E6130 on OAC tumour cell viability and proliferation and investigated whether such effects were more/less pronounced under the conditions of the TME and in the treatment resistant setting.

This study demonstrates for the first time that fractalkine elicits a pro-tumourigenic response in oesophageal cancer cells. Data presented here show a consistent and significant but small increase in the cell viability and proliferation of OE33, FLO-1 and FLO-1^{LM} cells, when cells are grown in the presence of fractalkine. This is in line with previous research on gastric, pancreatic and lung cancer which demonstrated similar effects on cancer cell proliferation and survival [189, 194, 195]. Indeed, when CX3CR1-overexpressing gastric cell lines MKN-28, SGC-7901 and MKN-45 were treated with 200ng/ml of fractalkine in optimal culture conditions, there was a significant increase in cell proliferation and viability [189]. These results were associated with fractalkine:CX3CR1 activation of Akt kinase. Furthermore, phosphorylated (p)-Akt (Ser-473) kinase has been shown to play a role in controlling apoptosis and proliferation in many different types of cells [189]. As the hypothesis for this project is that targeting the fractalkine receptor could be beneficial for the treatment of OAC, showing that fractalkine also elicits pro-tumourigenic effects further supports this hypothesis and emphasises the dual benefit of E6130 in OAC patients. Interestingly, OE33, FLO-1 and FLO-1^{LM} cells exhibited differential susceptibilities to fractalkine exposure. As FLO-1 cell populations express significantly higher frequencies of $CX3CR1^{+}$ cells compared to OE33 cells, it was

expected that fractalkine would elicit a greater effect on these cells. Indeed, FLO-1 cells exhibited increased cell viability and proliferation at lower doses of fractalkine (10ng) as well as at those higher doses to which OE33 cells responded (100 and 200ng of recombinant fractalkine). As the data generated for this project showed that fractalkine had a direct role in promoting cell viability and proliferation in OAC cells, the effects of a CX3CR1 modulator, E6130, in combination with fractalkine in OAC cells were next evaluated. E6130 pre-treatment attenuated the effects of high doses of fractalkine on OE33 and FLO-1 cell viability. As mentioned before, research in our group highlighted the potential of E6130 to redirect NK cells away from VAT and towards tumour in OAC and here the data support its utility via its direct attenuation of fractalkine's pro-tumourigenic effects [69, 127]. Interestingly, FLO-1^{LM} cells showed mixed results in this study: the cells exhibited significantly increased cell viability and proliferation at only 5ng/ml and 100ng/ml of recombinant fractalkine, respectively. If the cells respond to lower concentrations of fractalkine but not to higher concentrations, this could be due to receptor saturation on FLO-1^{LM} cells, as they express the CX3CR1 receptor at lower levels than their parental line FLO-1. Similarly, research on pancreatic cancer cell migration revealed that CXCL12 stimulates cell movement in a biphasic manner. Optimal stimulation occurred at a concentration of 10 nmol/L, while concentrations of 100 nmol/L or higher did not enhance migration [337, 343, 344]. Moreover, when FLO-1^{LM} cells were pretreated with E6130, the results were inconclusive, as it significantly attenuated FLO-1^{LM} cell viability when the cells were treated with 10ng/ml of recombinant fractalkine, but it did not attenuate cell viability for the higher concentration of fractalkine used nor did it attenuate fractalkine-induced increases in proliferation for both concentrations used. Differences between the FLO-1 and FLO-1^{LM} cell lines could also be due to the tissue microenvironments they were derived from. As FLO-1^{LM} cell line was derived from a liver metastasis, this could provide valuable insight for E6130 treatment: indeed, treating the FLO-1 cell line with E6130 has a stronger effect on reducing cell viability and proliferation indicating its higher level of potency at the primary tumour site.

The panel of OAC cell lines studied here exhibit differential expression of the fractalkine receptor CX3CR1, with significantly higher percentage frequencies of CX3CR1-expressing FLO-1 compared to OE33 cells. Upon flow cytometric analysis, $CX3CR1^{+}$ cells could be

divided further into two distinct populations: CX3CR1^{low} and CX3CR1^{high}. Such expression patterns have been shown to identify distinct phenotypes and homeostatic properties on memory T cells by Gerlach, C *et al.* [345]. The cell lines FLO-1 and FLO-1^{LM} secreted considerably higher levels of soluble fractalkine compared to all other OAC cell lines. Changes in CX3CR1 receptor expression on cancer cells when fractalkine binds to its receptor has not been reported, but it was demonstrated that soluble fractalkine binding to CX3CR1 induced an increase of fractalkine secretion in an autocrine manner in aortic smooth muscle cells [194, 346]. Together with CX3CR1^{+} cells being most abundant among FLO-1 cells, this placed FLO-1 as the most suitable model for studying the Fractalkine:CX3CR1 axis in OAC and this cell line was carried forward for further interrogation in Chapter 4. These data further confirm the variations in fractalkine signalling between OAC cell lines and highlight the importance of examining differences in targetable pathways when considering the most suitable cell line model. E6130 did not seem to alter the receptor expression or fractalkine secretion on the OAC cell lines and could perhaps elicit its effects by alteration through allosteric confirmation, like Repertaxin, a small molecule inhibitor of CXCR1 which functions via a non-competitive allosteric binding and prevents signalling, or by biased signalling, such as AMD11070, a CXCR4 antagonist [347, 348]. The effects of E6130 on CX3CR1 and FLO-1 cells were further investigated in chapter 4.

The vast majority of OAC cancer patients often encounter a significant challenge during their treatment journey, where they develop resistance to standard-of-care therapies due to genetic changes or acquisition of specific mechanisms in the tumour cells. Consequently, finding effective treatment options for cancer patients with treatment-resistant tumours becomes a critical area of research and a significant clinical challenge in improving overall patient outcomes [42, 43, 349]. Fractalkine has been considered as a potential player in chemotherapy resistance in pancreatic cancer, due to its mediation of apoptosis resistance via the activation of the AKT/NF-kB/p65 signalling cascade [194]. Here, the effects of fractalkine and E6130 were examined in the treatment-resistant setting using radioresistant cell line OE33R and its parental cell line OE33P, and the cisplatin-resistant cell line OE33CisR and its parental cell line OE33CisP [70, 309, 310]. All 4 cell lines exhibited significantly enhanced viability following fractalkine treatment with

slight but significantly higher effects observed in the OE33R cell line when treated with 200ng of fractalkine compared to OE33P cells, which is in line with their higher CX3CR1 expression. Even though OE33P and OE33CisP are parental cell lines, they have been mock-treated as often as their treatment-resistant counterparts and therefore have much older passages than OE33 cells, which could explain why they are sensitive to lower doses of fractalkine compared to OE33 cells [70, 309, 310]. E6130 pre-treatment reduced fractalkine-induced increases in cell viability and proliferation in all 4 cell lines when they were treated with low (10ng) and high (100 and 200ng) doses of fractalkine. These results demonstrate that the treatment-resistant cell lines respond almost identically to their parental counterpart, which shows promise in using E6130 in OAC patients who do not have a durable response to first-line chemoradiotherapy.

E6130 could retain the ability to attenuate the effects induced by fractalkine in conditions that simulate nutrient deprivation, acidosis and hypoxia. Hypoxia has been shown to impact the fractalkine:CX3CR1 axis in pancreatic, prostate and ovarian cancer, as the CX3CR1 gene has response elements that can bind to HIF-1α, which upregulates CX3CR1 expression [216, 218, 222]. Moreover, in prostate cancer, hypoxia results in increased NF-κB activation which in turn increases CX3CR1 expression [222]. ADAM10 and TACE/ADAM17 have also been shown to be upregulated in a hypoxic setting, which can lead to enhanced cleaving of soluble fractalkine [350-353]. Here, these data show that fractalkine had a more profound impact on FLO-1 cells when cultured in moderate acidic conditions (pH6.6) as there was a significant increase in cell viability compared to optimal conditions (cDMEM). This is not surprising as the previous data presented showed that $CX3CR1^{+}$FLO-1 cell frequencies were significantly higher when cultured in moderate acidic conditions compared to normal conditions. This is line with previous research in our group that showed that acidosis could increase the expression of immune checkpoints on T cells, which could contribute to disease progression in OAC [106]. Additionally, OE33 and $FLO\text{-}1^{LM}$ cells had a particularly higher percentage of cells expressing CX3CR1 in severe acidic conditions at pH5.5 and hypoxia. As hypoxia and acidosis are common features of OAC, CX3CR1 receptor increase on cancer cells could enable a survival benefit to these cells in the presence of fractalkine. On the contrary, treatment-resistant cell lines do not respond the same way to the harsh

microenvironment as they could have already acquired other survival advantages needed to resist treatments.

The findings presented here highlight the pivotal role of the fractalkine-CX3CR1 axis in OAC cells, particularly in promoting cell viability and proliferation and these effects can be attenuated by the CX3CR1 modulator E6130. Importantly, radioresistant and cisplatin resistant OAC cells exhibit similar responses to their parental counterparts, with fractalkine enhancing their viability and proliferation, effects which are also mitigated by E6130. These results suggest that treatment resistance did not impair the functional relevance of the fractalkine-CX3CR1 axis, and this pathway remains a viable therapeutic target in resistant disease states. FLO-1 and FLO-1^{LM} cell lines which have metastatic potential exhibit significantly higher levels of fractalkine expression compared to OE33, OE33P, OE33R, OE33CisP, and OE33CisR. This suggests a potential mechanism by which these cells enhance their invasive and migratory capabilities. Moreover, the TME influences CX3CR1 expression in primary and metastatic OAC cells and E6130 retains its effect in reducing fractalkine-increased cell viability under the conditions of acidosis, nutrient deprivation and hypoxia. Together, these findings emphasize the multifaceted role of the fractalkine-CX3CR1 axis in OAC progression and resistance and provide a strong rationale for further exploration of CX3CR1-targeted therapies.

3.5 Highlights

- Significantly higher percentages of $CX3CR1^{+}$cells among FLO-1 cells compared to OE33 and FLO-1^{LM} cells, while FLO-1 and FLO-1^{LM} secrete fractalkine abundantly compared to OE33, OE33P, OE33R, OE33CisP and OE33CisR.
- Fractalkine increases cell viability and proliferation in OE33, FLO-1 and FLO-1^{LM} cell lines and this can be attenuated by E6130.
- Radioresistant OAC cells (OE33R) and cisplatin resistant cells (OE33CisR) respond similarly to their parental cell lines, whereby fractalkine increases cell viability and proliferation and these effects can be attenuated by E6130.
- Higher frequencies of $CX3CR1^{+}$OE33, FLO-1 and FLO-1^{LM} cells are observed following culture under conditions of acidosis and severe hypoxia (0.5% oxygen).
- E6130 retains its utility to attenuate fractalkine-induced increases in FLO-1 cell viability under the physiological conditions of the TME.

Chapter 4 – Examining the fractalkine:CX3CR1 axis in the oesophageal adenocarcinoma FLO-1 cell line and investigating its role in metastatic processes and stemness

4.1 Introduction

Patients presenting with metastatic oesophageal adenocarcinoma (OAC) face dismal survival rates of less than 6% [5, 7]. The most common organs of metastasis include the liver, lymph nodes, omentum, lung, bones and brain with the liver being involved in as many as 60% of metastatic cases [354, 355]. This chapter will explore the pro-metastatic effects of fractalkine in the OAC cell line FLO-1, which has previously been shown to spontaneously metastasise to the liver of mice and thus provides a more fitting cell line model to study metastasis [311].

Cancer cells transition to metastasis by enhancing their ability to migrate, invade surrounding tissues, and resisting apoptosis, and this is characterised by phenotype changes, in a process known as epithelial-mesenchymal transition (EMT). Fractalkine has previously been reported as a driver of tumour development by promoting metastasis and invasion in gastric, prostate, lung, and kidney primary cancers [173, 189, 192, 193, 195, 356]. In prostate cancer cell lines, fractalkine enhanced EMT and promoted metastasis via the TACE/TGF-α/EGFR pathway [192, 193]. Similarly, in lung cancer patient samples, higher levels of fractalkine expression were associated with higher tumour stage and lymph node metastasis, while fractalkine knockdown in lung cancer cell lines reduced activation of JNK and MMP-2/MMP-9, while also decreasing cell migration and invasion [200]. Upregulation of the transcription factor SLUG has been linked to OAC progression, promoting the expression of mesenchymal markers such as the intermediate filament protein vimentin, and subsequently reducing E-cadherin expression [357, 358]. Reduced E-cadherin expression allows cancer cells to detach, migrate, and establish new tumours in different organs or tissues [359]. Here, we examined the effects of fractalkine on SLUG, E-cadherin and vimentin expression in FLO-1 cells. Cancer stem cells (CSC) have been shown to play a key role in promoting metastatic malignancies, with stemness markers such as CD44, CD133 and ALDH1 correlating with poorer disease outcomes in gastroesophageal cancer patients [360]. As $CX3CR1^{high}$ breast and prostate cancer cells exhibit enhanced metastatic transcriptomic profiles in murine models [361] and bone marrow cell-derived fractalkine has been implicated in $CX3CR1^{+}$ stem-like prostate cancer cell metastasis to the bone marrow, in this chapter, fractalkine was hypothesised to have a pro-metastatic role in OAC by influencing CSC migration [362]. Moreover,

fractalkine has been shown to influence cellular metabolism and to increase iron transporter transferrin 1 receptor CD71 in macrophages [363]. Considering this, EMT markers, CSC markers and metabolic markers were examined here in $CX3CR1^-$ and $CX3CR1^+$ FLO-1 cells. In addition, the effects of fractalkine treatment on FLO-1 cell invasion and migration were interrogated to elucidate whether the chemokine plays a role in OAC metastasis.

Cancer cells manipulate apoptosis mechanisms to persist and proliferate, and this can be done by accelerating cell cycle progression [364]. In OAC, overexpression of oncogenes such as cyclin D1 and cyclin E1 disrupts normal cell cycle regulation, further promoting proliferation [98]. These adaptations collectively contribute to the aggressive nature of OAC and other tumours [365]. Interestingly, fractalkine-induced increases in prostate and pancreatic cancer cell proliferation were reportedly mediated by cell cycle changes by upregulating G1/S phase [194, 223]. Given this together with fractalkine's proliferative effects on OAC cell lines, its effects on FLO-1 cell cycle will be assessed here.

This chapter focussed on investigating the effects of fractalkine in metastasis and stemness, using FLO-1 cells as the most suitable *in vitro* model from our previously screened cell line panel. Here, fractalkine:CX3CR1 signalling was interrogated for its role in FLO-1 cell cycle and invasive/migratory capacity. The $CX3CR1^+$FLO-1 cell population was examined for its survival advantage compared to its $CX3CR1^-$ counterpart and these cells were assessed for their stemness, metabolic profile and EMT phenotype. Overall, this chapter further delineates the pro-tumourigenic role of fractalkine and uncovers key mechanisms by which this chemokine can influence OAC tumour progression.

4.2 Hypothesis

Fractalkine drives metastatic processes in OAC and the CX3CR1 modulator E6130 can limit such detrimental effects.

Aims:

1. Investigate the effects of fractalkine and E6130 on FLO-1 cell cycle distribution
2. Elucidate the effects of fractalkine and E6130 on FLO-1 cell invasion and epithelial-mesenchymal transition

3. Assess CX3CR1 surface expression patterns on FLO-1 cells and its association with viability
4. Investigate if CX3CR1 expression on FLO-1 cells relates to stemness and metastatic potential

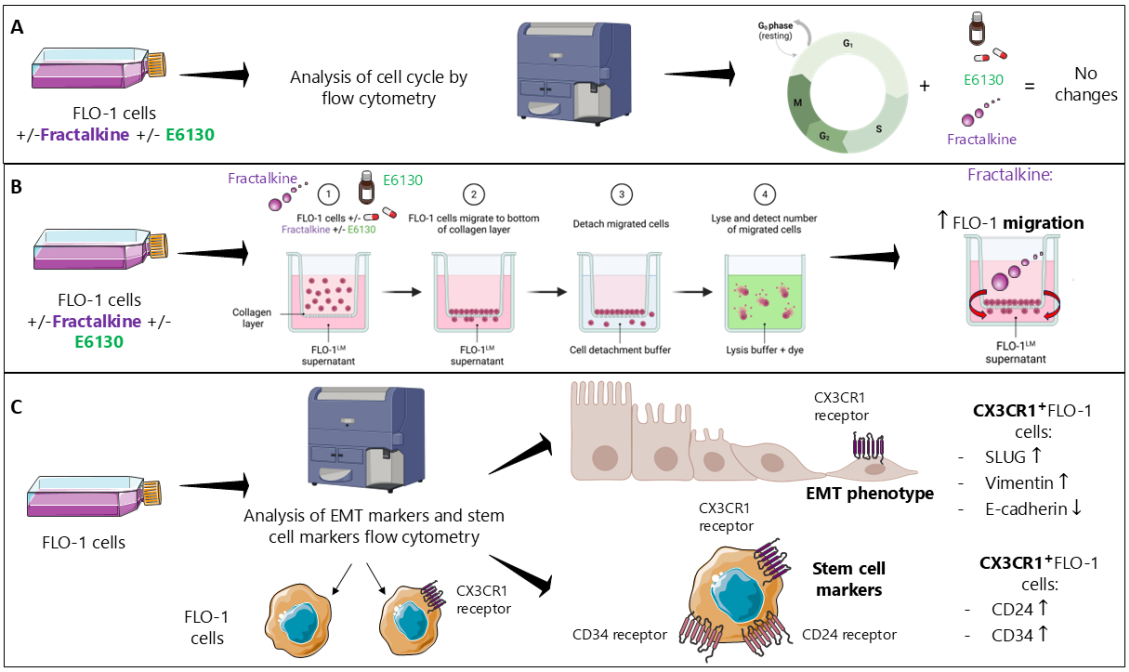

Graphical abstract: (A) FLO-1 cells were cultured *in vitro* with fractalkine and/or E6130, cell cycle distribution was analysed by flow cytometry. Fractalkine and E6130 did not alter cell cycle distribution. **(B)** FLO-1 cells were cultured *in vitro* with fractalkine and/or E6130 to assess their cell invasion and migration towards FLO-1^{LM} supernatant using an invasion assay. Fractalkine increased (↑) FLO-1 cell migration towards FLO-1^{LM} supernatant. **(C)** FLO-1 cells were cultured *in vitro,* EMT and stem cell markers were analysed by flow cytometry on $CX3CR1^{+}$ and $CX3CR1^{-}$ cells. $CX3CR1^{+}$ FLO-1 cells have a more pronounced EMT phenotype (higher (↑) SLUG and Vimentin expression, lower (↓) E-cadherin expression). $CX3CR1^{+}$FLO-1 cells are associated with markers with stem-like properties (higher (↑) expression of CD24 and CD34). Created with Smart.Servier.com and Biorender.com

Results

4.3 Examining the fractalkine:CX3CR1 axis in the oesophageal adenocarcinoma FLO-1 cell line and investigating its role in metastatic processes and stemness

In chapter 3, the cell line FLO-1, which has metastatic potential [311], was shown to be sensitive to fractalkine's pro-tumourigenic effects, even at low doses and was shown to secrete the chemokine in significantly high concentrations. Furthermore, under acidosis CX3CR1 expression was significantly increased by FLO-1 cells suggesting an even higher susceptibility to fractalkine under the conditions of the TME. Given these collective findings, the experiments in this chapter were conducted on FLO-1 cells only.

4.3.1 Treatment with fractalkine and E6130 did not alter FLO-1 cell cycle distribution

To further delineate how fractalkine elicits its effects on FLO-1 cell viability and proliferation, its effects on cell cycle phase distribution were examined. FLO-1 cells were treated with 0.1% water, 10ng or 100 ng of fractalkine (FKN) and/or pretreated with 4.9nM of E6130 or 0.01% DMSO or left non-treated for 24 hours. Cell cycle was analysed by flow cytometry using PI staining to analyse G0/G1, S and G1/M phases on the cell. Treatment with 10ng of 100 ng of fractalkine did not change cell cycle distribution in FLO-1 cells, nor did treatment with E6130 +/- fractalkine **[Figure 4.1]**. These data suggest that neither fractalkine or E6130 alter cell cycle distribution in FLO-1 cells and perhaps use different mechanisms to alter cell cycle viability and proliferation.

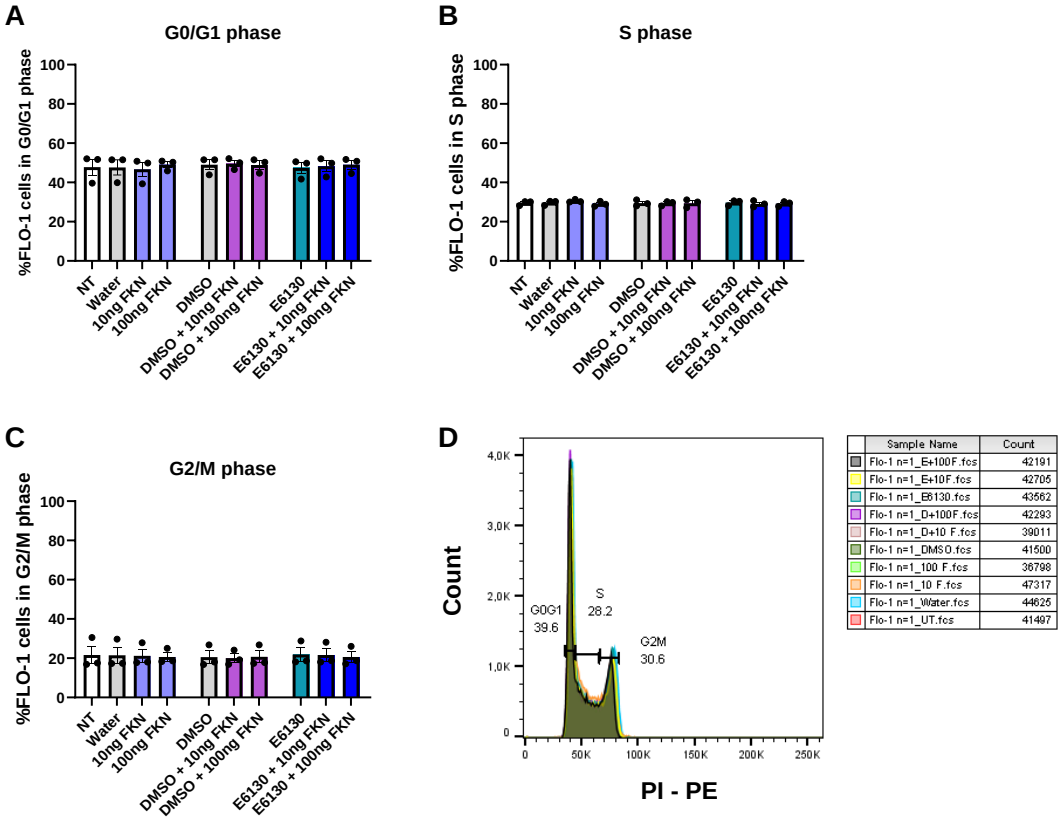

Figure 4.1: 24-hour treatment with fractalkine or E6130 did not alter cell cycle distribution of FLO-1 cells.

Bar charts showing cell cycle distribution of **(A)** G0/G1 phase, **(B)** S phase and **(C)** G2/M phase following 24-hour treatment with 0.1 % water, 10 or 100ng/ml recombinant fractalkine (F), 0.01% DMSO +/- 10 or 100ng/ml recombinant fractalkine (FKN), 4.9nM E6130 + 10 or 100ng/ml recombinant fractalkine (FKN) or no treatment. **(D)** Representative histogram showing gating of G0/G1 phase, S phase and G2/M phase on FLO-1 cells. Experiments were repeated n=3. Mean ± SEM

4.3.2 Fractalkine increases migration of FLO-1 cells and CX3CR1 expression in FLO-1 cells is associated with a more pronounced EMT phenotype

4.3.2.1 Fractalkine increases migration of FLO-1 cells towards FLO-1^{LM} supernatants

To assess if fractalkine elicited effects on OAC cell invasive and migratory capabilities, an extracellular matrix invasion and migration assay (recapitulating basement membrane matrix of proteins of tumours) was used. Serum-free media (DMEM) was considered a negative control (-ve) and DMEM supplemented with 20% FBS was considered as a positive control (+ve). There was higher FLO-1 cell migration towards the positive control compared to the negative control, which demonstrates the functionality of this assay; -ve vs +ve (1.7% vs 4%, p=0.077, n=5) **[Figure 4.2]**. Following 24-hour incubation, non-treated FLO-1 cells did not significantly migrate towards 100ng of recombinant fractalkine (FKN) compared to the negative control (RPMI media), and treatment with 4.9nM E6130 did not alter FLO-1 cell migration towards 100ng of fractalkine **[Figure 4.2A]**. FLO-1^{LM} cell supernatants were used here to crudely recapitulate the soluble cues of the metastatic liver microenvironment. Interestingly, treatment of FLO-1 cells with fractalkine increased their migration towards FLO-1^{LM} cell supernatants **[Figure 4.2B, C]**. Indeed, FLO-1 cells had significantly enhanced migration towards FLO-1^{LM} supernatant when the cells were pre-treated with 100ng of recombinant fractalkine compared to cells left non-treated; NT vs 100ng FKN (2.2% vs 3.8%, p=0.015, n=5) and had enhanced migration compared to cells treated with the vehicle control for fractalkine, water; Water vs 100ng FKN (2.2% vs 3.8%, p=0.062, n=5) **[Figure 4.2B]**. When the cells were pretreated with E6130, there was reduced migration of FLO-1 cells compared to cells treated with the vehicle control for E6130, 0.01% DMSO; DMSO vs E6130 (2.5% vs 1.4%, p=0.358, n=5), however this was not significant. Moreover, there was reduced migration of FLO-1 cells towards FLO-1^{LM} supernatant when cells were pre-treated with E6130 and treated with fractalkine compared to cells treated with DMSO and fractalkine; DMSO + 100ng FKN vs E6130 + 100ng FKN (4% vs 2.9%, p=0.745, n=5), however this was not significant. There was a significant difference in migration of FLO-1 towards FLO-1^{LM} supernatant when E6130 pre-treatment only was compared to E6130 and treated with fractalkine; E6130 vs E6130 + 100ng FKN (1.4% vs 2.9%, n=0.022, n=5) **[Figure 4.2C]**. These data suggest that exposure to fractalkine primes OAC tumour cells for migration

towards soluble factors in the metastatic microenvironment of the liver and that this can override E6130's potential to reduce such migration.

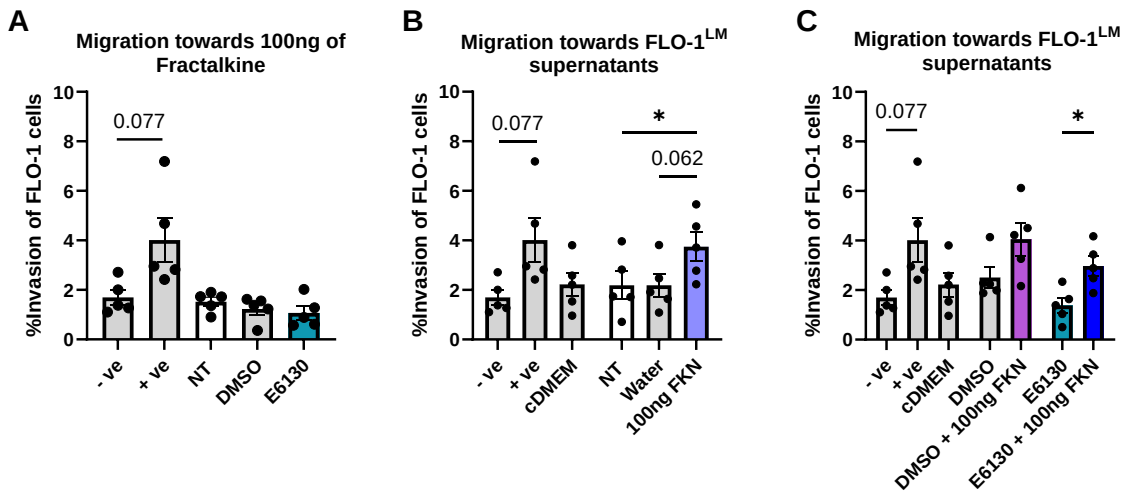

Figure 4.2: Fractalkine treatment of FLO-1 cells increases their migration towards FLO-1^{LM} supernatants

Bar charts showing % invasion of FLO-1 cells towards DMEM media only (negative control, -ve), DMEM supplemented with 20% FBS (positive control, +ve) **(A)** 100ng of recombinant fractalkine (FKN) **(B)** and **(C)** FLO-1^{LM} supernatants (n=3) following no treatment (NT), treatment with 0.1% water, 100ng of recombinant fractalkine (FKN), 0.01% DMSO +/- 100ng of fractalkine (FKN) and 4.9nM E6130 +/- 100ng of fractalkine (FKN) for 24 hours. Experiments were repeated n=5. *p<0.05, by ordinary one-way ANOVA with Tukey multiple comparison test. Mean ± SEM.

4.3.2.2 CX3CR1^{+} FLO-1 cells express significantly higher expression of SLUG and vimentin, and significantly lower expression of E-cadherin compared to CX3CR1^{-} cells.

To investigate whether CX3CR1 expression correlates with the metastatic properties of OAC tumour cells, the basal expression of a few markers associated with EMT-like properties such as SLUG, vimentin, E-cadherin were assessed by flow cytometry in CX3CR1^{+} and CX3CR1^{-} FLO-1 cells. SLUG and vimentin were assessed by MFI as their percentage expression was close to 100% **[Figure 4.3D]**. SLUG and vimentin expression were significantly higher in CX3CR1^{+}FLO-1 cells compared to CX3CR1^{-} FLO-1 cells; SLUG: CX3CR1^{-} vs CX3CR1^{+} (MFI: 2152.25 vs 2972, p=0.007, n=4), Vimentin: CX3CR1^{-} vs CX3CR1^{+} (MFI:7621 vs 12346.8, p=0.019, n=4) **[Figure 4.3 A,B]**. Moreover, E-cadherin was significantly decreased in CX3CR1^{+}FLO-1 cells compared to CX3CR1^{-} FLO-1 cells; E-cadherin: CX3CR1^{-} vs CX3CR1^{+} (16.5% vs 4.6%, p=0.006, n=4) **[Figure 4.3C]**. For the purposes of this experiment only, FLO-1 cells could not be stained with CX3CR1-PE as PE was already used for SLUG staining. CX3CR1^{+}FLO-1 cells were stained with CX3CR1-BV421 instead; however, no differences were observed with CX3CR1^{low} and CX3CR1^{high} FLO-1 cells when stained with this antibody, and therefore only markers on CX3CR1^{+} and CX3CR1^{-} FLO-1 cells were assessed **[Figure 4.3D]**.

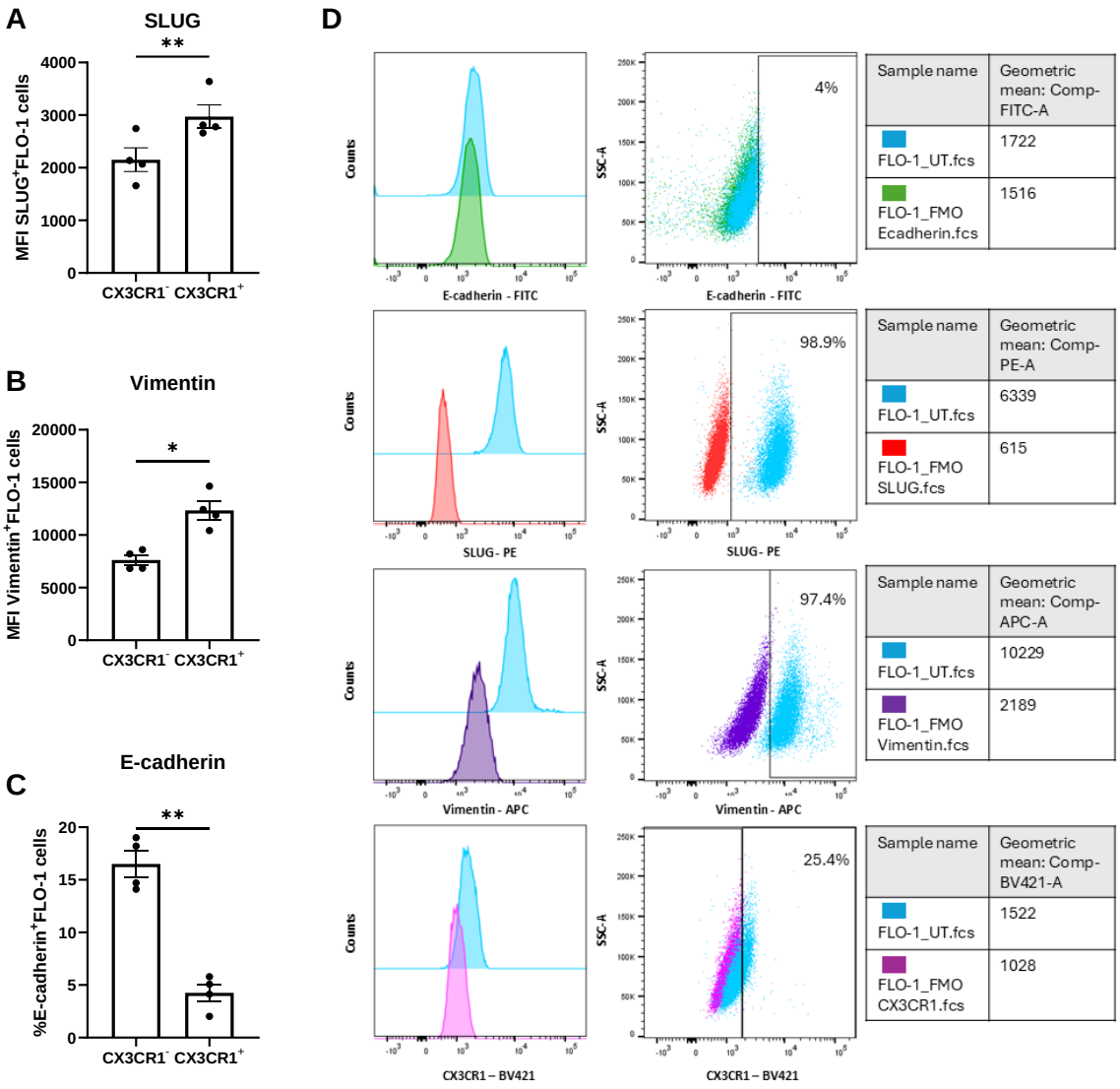

Figure 4.3: CX3CR1⁺FLO-1 cells express significantly higher levels of SLUG and vimentin, and express significantly lower levels of E-cadherin compared to CX3CR1⁻ FLO-1 cells

Bar charts showing basal MFI of **(A)** SLUG and **(B)** Vimentin or basal % expression of **(C)** E-cadherin in CX3CR1⁻ and CX3CR1⁺FLO-1 cells. **(D)** Representative histograms (left) and dot plots (right) showing gating of SLUG**,** Vimentin, E-cadherin and CX3CR1⁺FLO-1 cell population compared to FMO control after gating on viable cells. Experiments were repeated n=4. *p<0.05, **p<0.01, by parametric paired t-test. Mean ± SEM

To investigate if fractalkine and/or E6130 influenced SLUG, vimentin and E-cadherin expression on $CX3CR1^{+}$ and $CX3CR1^{-}$ FLO-1 cells, FLO-1 cells were treated with 0.1% water, 10ng or 100 ng of fractalkine (FKN) and/or pretreated with 4.9nM of E6130 or 0.01% DMSO or left non-treated for 24-hour treatment and expression of SLUG, vimentin and E-cadherin was analysed by flow cytometry on total FLO-1 cells, on $CX3CR1^{+}$ and $CX3CR1^{-}$ FLO-1 cells. No significant differences were observed in SLUG or vimentin expression **[Figure 4.4 A,B,C,D,E,F]**. E-cadherin was significantly decreased when treated with 10 and 100ng of FKN compared to non-treated (NT) $CX3CR1^{-}$ FLO-1 cells; $CX3CR1^{-}$: NT vs 10ng FKN (16.5% vs 6.7%, p=0.009, n=4); NT vs 100ng FKN (16.5% vs 8.4%, p=0.026, n=4) **[Figure 4.4H]**. However, there were no significant differences between fractalkine- and water-treated $CX3CR1^{-}$ FLO-1 cells, therefore questioning the significance of the previous results **[Figure 4.4H]**. Thus, treatment with fractalkine and/or E6130 had no significant effects on SLUG, vimentin and E-cadherin expression on $CX3CR1^{+}$ and $CX3CR1^{-}$ FLO-1 cells.

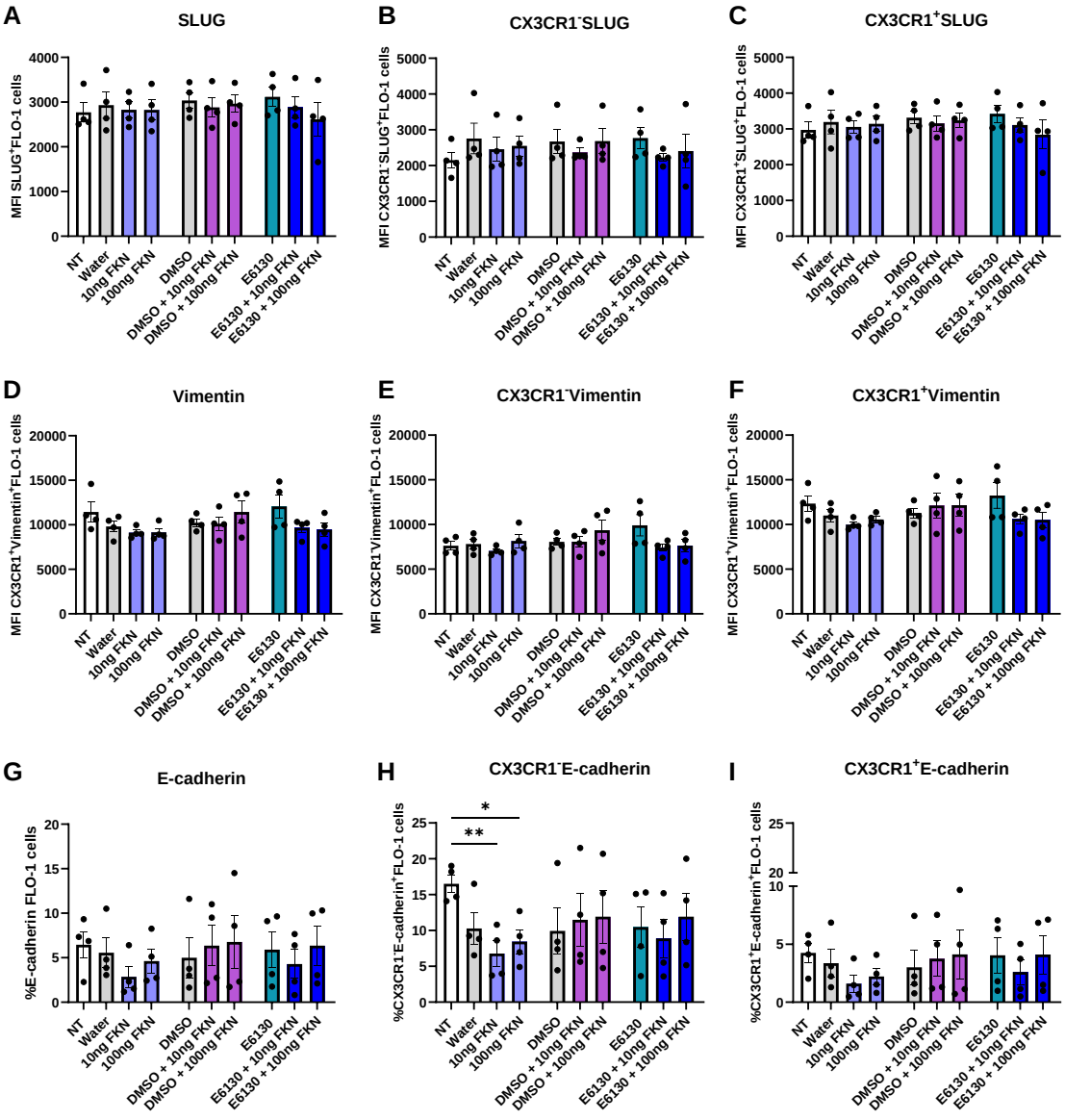

Figure 4.4: 24-hour treatment with fractalkine or E6130 did not significantly alter expression of SLUG, vimentin or E-cadherin of CX3CR1$^+$ or CX3CR1$^-$ FLO-1 cells.

Bar charts showing MFI **(A,B,C,D,E,F)** or % expression **(G,H,I)** of **(A,B,C)** SLUG, **(D,E,F)** vimentin and **(G,H,I)** E-cadherin following 24-hour treatment with 0.1 % water, 10 or 100ng/ml recombinant fractalkine (FKN), 0.01% DMSO +/- 10 or 100ng/ml recombinant fractalkine, 4.9nM E6130 + 10 or 100ng/ml recombinant fractalkine (FKN) or no treatment on **(A,D,G)** total FLO-1 population **(B,E,H)** CX3CR1$^-$ FLO-1 cells and **(C,F,I)** CX3CR1$^+$ FLO-1 cells. Experiments were repeated n=4. *p<0.05, **p<0.01, by ordinary one-way ANOVA with Tukey multiple comparison test. Mean ± SEM

4.3.3 CX3CR1$^-$ FLO-1 cells express CX3CR1 4 days after cell sorting

4.3.3.1 CX3CR1-PE antibody staining on CX3CR1$^+$FLO-1 cells is no longer detected after 72 hours sub-culture

As fractalkine increased FLO-1 cell viability, proliferation, and migration, the characteristics of CX3CR1$^+$FLO-1 cells and how they differ from CX3CR1$^-$FLO-1 cells were further evaluated to comprehend if the CX3CR1 receptor on OAC cells present a survival advantage. Given that CX3CR1$^-$ FLO-1 cells reduce E-cadherin in response to fractalkine raised the question of whether CX3CR1 surface expression is transient and therefore, not the best way to phenotype populations. Cell sorting was used to investigate the different populations and their survival. FLO-1 cells were separated into CX3CR1$^+$ and CX3CR1$^-$ populations by flow cytometry cell sorting, then cultured further to observe viability and CX3CR1 expression, following no treatment or treatment with fractalkine. Firstly, optimisation was required to assess the duration that the FLO-1 cells would remain stained with CX3CR1-PE antibody, i.e. if FLO-1 cells were sorted using the CX3CR1-PE antibody, then could this staining be used to reliably detect CX3CR1$^+$ and CX3CR1$^-$ FLO-1 cells and following subsequent sub-culture and treatment with fractalkine. Cells sub-cultured following CX3CR1-PE staining had almost no traces of antibody staining after 72 hours; 72hrs (1.34%), showing that CX3CR1-PE antibody staining is not retained following 72 hours and cells would need to be re-stained following sorting, culture and treatments **[Figure 4.6A]**. Additionally, two detachment methods were assessed for their efficacy to lift cells without cleaving CX3CR1 i.e. trypsin and cell scraping. We commonly use trypsin to detach cells for sub-culture, however it has been shown that it can cleave cell surface proteins and impact cell functions [366-368]. Therefore, CX3CR1 expression was assessed after they were lifted with trypsin (0hr trypsin) or by cell scraping (0hr scraped), and cells that were scraped had higher but non-significantly increased CX3CR1 expression compared to cells lifted with trypsin; 0hr trypsin vs 0hr scraped (17.8% vs 30.4%, n=3) **[Figure 4.6A]**.

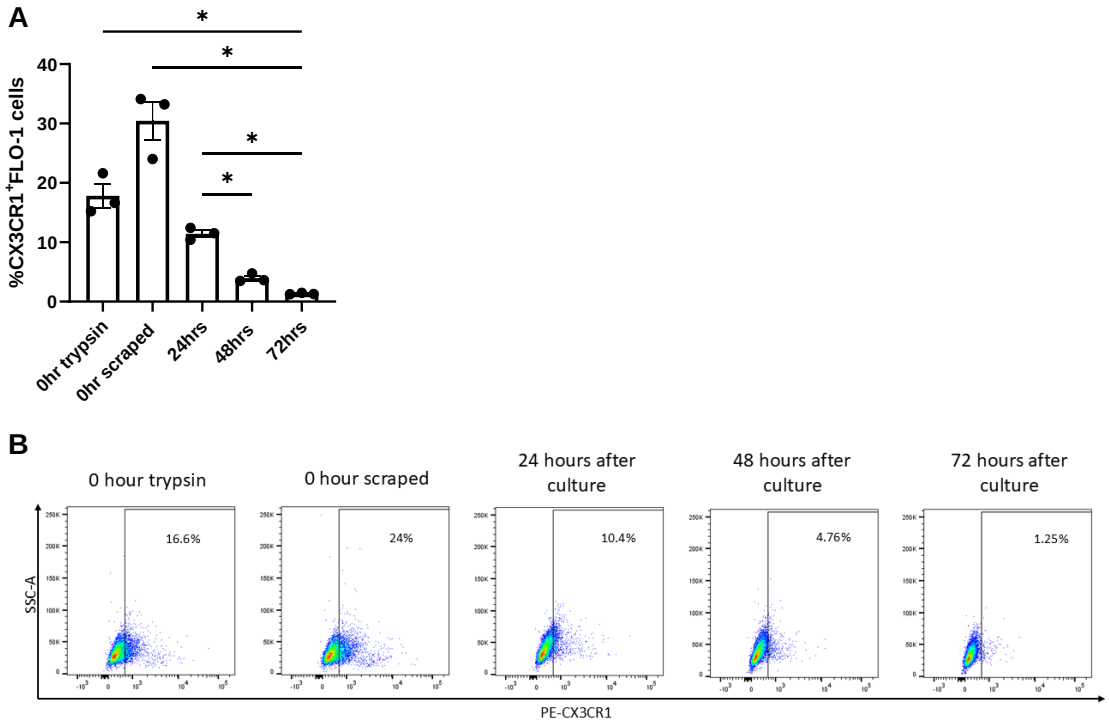

Figure 4.5: CX3CR1 surface expression on FLO-1 cells is no longer detected 72 hours after staining with PE antibody

(A) Bar chart showing % expression of CX3CR1^{+}FLO-1 cells at 0 hour (hr) using trypsin to detach cells or by scraping cells and 24 hours (hrs), 48hrs or 72hrs after CX3CR1-PE antibody stain and subsequent cell culturing. **(B)** Representative dot plots showing gating of CX3CR1^{+}FLO-1 cell population after gating on viable cells. Experiments were repeated n=3. *p=0.05, ordinary one-way ANOVA with Tukey multiple comparison test. Mean ± SEM

4.3.3.2 CX3CR1^{-}FLO-1 cells express CX3CR1 on their surface 4 days after cell sorting

Following the optimisation described above, FLO-1 cells were lifted by gentle cell scraping, stained with CX3CR1-PE antibody and sorted into CX3CR1^{-} and CX3CR1^{+} populations. They were subsequently counted and sub-cultured. As cell sorting produces stress and some cell death, the cells were left for 4 days to recover and reach confluency. The unstained/unsorted FLO-1 cells used for cell sorting were also subsequently sub-cultured to act as a control of the mixed CX3CR1 population. The CX3CR1^{-} population was assessed 4-, 5- and 6-days following cell sorting **[Figure 4.6D]**. Surprisingly, the CX3CR1^{-} sorted cells exhibited higher CX3CR1 expression compared to the unsorted control cells after 4 days; Ctrl vs Day 4 (14.1% vs 22.2%, n=1-3). Interestingly, CX3CR1 expression then significantly decreased on the CX3CR1^{-} sorted cells 6 days after sorting; Day 4 vs Day 6 (22.2% vs 10%, p=0.019, n=3) **[Figure 4.6A]**. When CX3CR1^{-} cells were separated into low and high CX3CR1 cells, frequencies of CX3CR1^{low} cells were significantly higher at Day 4 than at Day 6; Day 4 vs Day 6 (21.4% vs 8.37%, p=0.014, n=3) and frequencies of CX3CR1^{high} were significantly higher at Day 5 than at Day 6 on FLO-1 cells; Day 5 vs Day 6 (2.2% vs 1.6%, p=0.026, n=3) **[Figure 4.6 B,C]**. These data suggest that CX3CR1 surface expression on FLO-1 cells is transient and that perhaps, mixed populations are somehow advantageous.

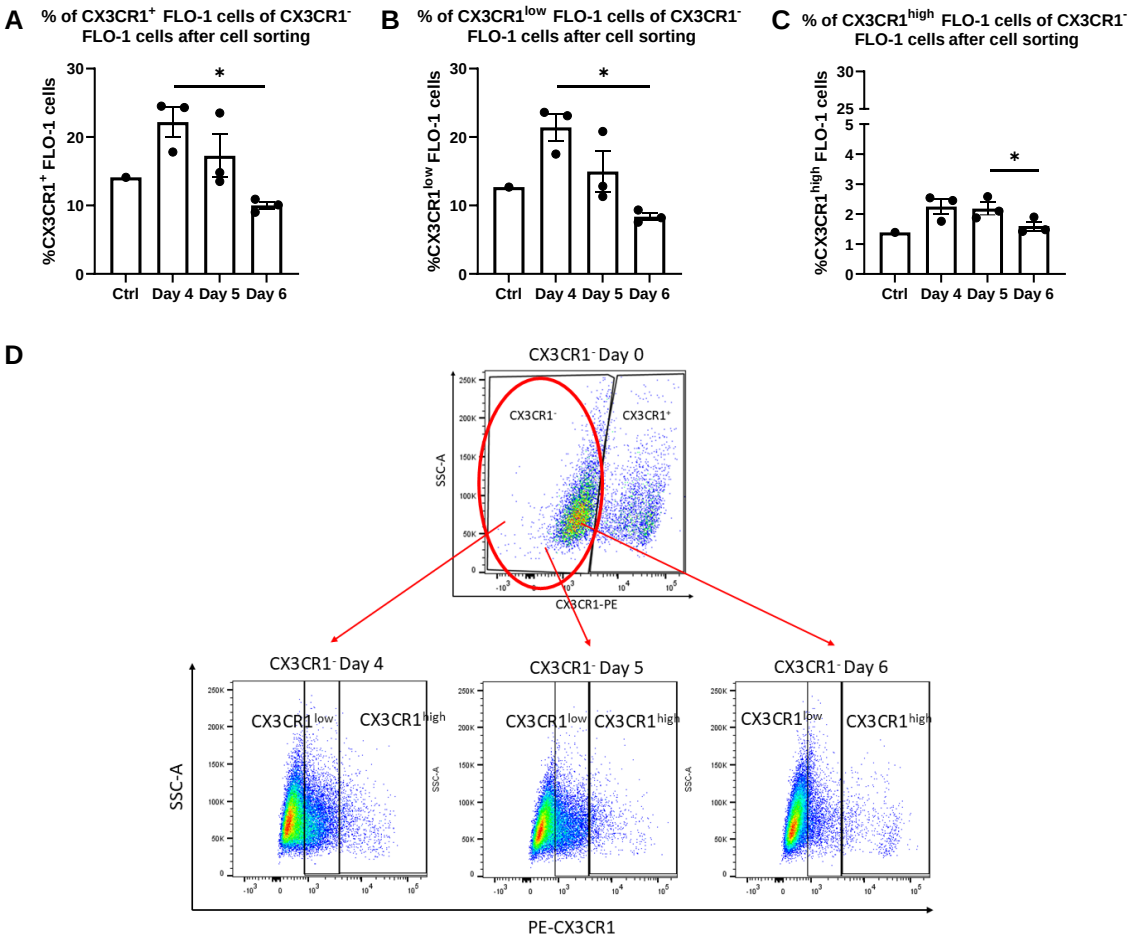

Figure 4.6: Sorted CX3CR1^{-}FLO-1 cells express CX3CR1 on their surface 4 days after cell sorting

Bar charts showing % expression of **(A)** CX3CR1^{+} **(B)** CX3CR1^{low} and **(C)** CX3CR1^{high} FLO-1 cells at Day 4, Day 5 and Day 6 after cell sorting into CX3CR1^{-}FLO-1 cells. Unstained/unsorted cells used for cell sorting and subsequently sub-cultured were used as a control (Ctrl) for mixed CX3CR1 population **(D)** Representative dot plots showing gating of CX3CR1^{+}, CX3CR1^{low} and CX3CR1^{high}FLO-1 cell population at Day 4, Day 5 and Day 6 after cell sorting of cells into CX3CR1^{-} and CX3CR1^{+}FLO-1 cells (Day 0) after gating on viable cells. Experiments were repeated n=3. *p<0.05, ordinary one-way ANOVA with Tukey multiple comparison test. Mean ± SEM

4.3.3.3 Fractalkine did not significantly enhance cell viability or alter CX3CR1 surface expression of FLO-1 cells, following sorting into CX3CR1^{+} and CX3CR1^{-} populations

At Day 4 after cell sorting into CX3CR1^{+} and CX3CR1^{-} populations, FLO-1 cells were treated with 100ng of recombinant of fractalkine or its vehicle control (0.1% water). After 24-hour treatment, CX3CR1 expression was assessed on both populations. There were no significant differences observed as both populations had mixed CX3CR1^{+} and CX3CR1^{-} FLO-1 cells and seem to return to a heterogenous population. However, it must be noted that sorted CX3CR1^{+} FLO-1 cells exhibited higher CX3CR1 expression than sorted CX3CR1^{-} cells; (17.3% vs 30.9%, n=3) **[Figure 4.7A]**.

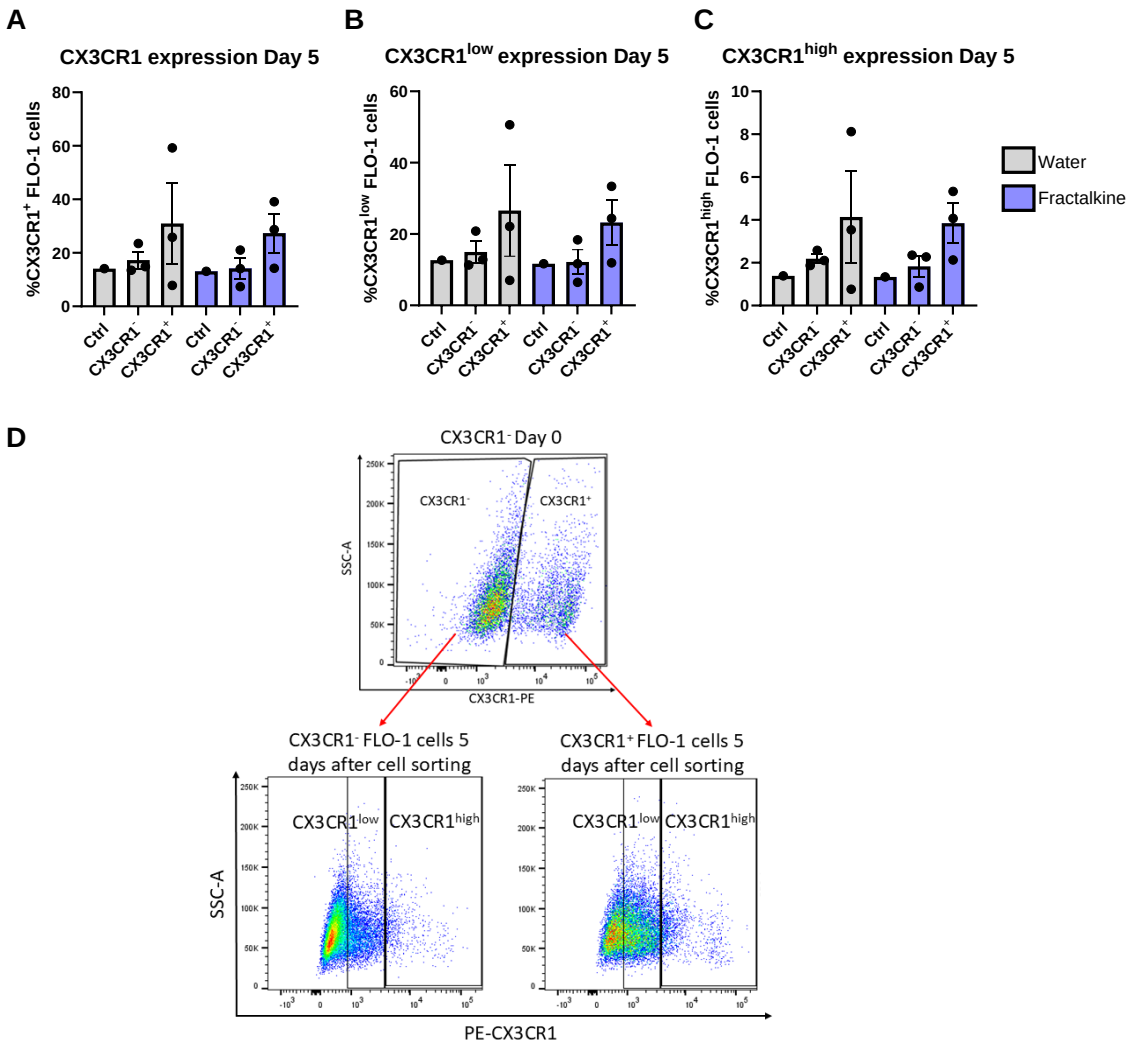

Figure 4.7: Sorted CX3CR1^{+} and CX3CR1^{-} cells revert to their original heterogenous populations and fractalkine doesn't alter CX3CR1 surface expression in these populations.

Bar charts showing % expression of CX3CR1^{+}FLO-1 cells of **(A)** CX3CR1^{+} **(B)** CX3CR1^{low} and **(C)** CX3CR1^{high} cells at Day 5 after cell sorting and following 24-hour treatment with 0.1% water or 100ng of recombinant fractalkine. Unstained cells used for cell sorting and subsequently sub-cultured were used as a control (Ctrl) for mixed CX3CR1 population **(D)** Representative dot plots showing gating of CX3CR1^{+}, CX3CR1^{low} and CX3CR1^{high}FLO-1 cell population on day 5 after cell sorting (day 0) after gating on viable cells. Experiments were repeated n=3. Mean ± SEM

4.3.3.3 Cell sorting significantly decreases FLO-1 cell viability and fractalkine does not significantly alter viability following sorting

Following 24-hour fractalkine treatment described above, FLO-1 cell viability was assessed using a CCK8 assay. Fractalkine did not significantly alter cell viability in sorted $CX3CR1^{+}$ and $CX3CR1^{-}$ cell populations, however sorted $CX3CR1^{+}$ cells had overall higher cell viability compared to sorted $CX3CR1^{-}$ cells; $CX3CR1^{-}$(water) vs $CX3CR1^{-}$(fractalkine) vs $CX3CR1^{+}$(water) vs $CX3CR1^{+}$(fractalkine) (35.5% vs 42.7% vs 47.5% vs 49.3%, n=3) **[Figure 4.8A]**. The sorted cells had significantly lower cell viability compared to the control (mixed CX3CR1 population, none-sorted); Ctrl vs $CX3CR1^{-}$(water) (100% vs 35.5%, p=0.006, n=3); Ctrl vs $CX3CR1^{-}$(fractalkine) (100% vs 42.7%, p=0.008, n=3); Ctrl vs $CX3CR1^{+}$(water) (100% vs 47.5%, p=0.001, n=3); Ctrl vs $CX3CR1^{+}$(fractalkine) (100% vs 49.3%, p=0.003, n=3), which could imply that cell sorting is a stressful event on cells and cell growth is impaired or slower following this process **[Figure 4.8A]**. Moreover, the results above demonstrate that CX3CR1 surface expression is transient on FLO-1 cells and is not the optimal approach to isolate $CX3CR1^{-}$ and $CX3CR1^{+}$ FLO-1 cells **[Figure 4.8]**.

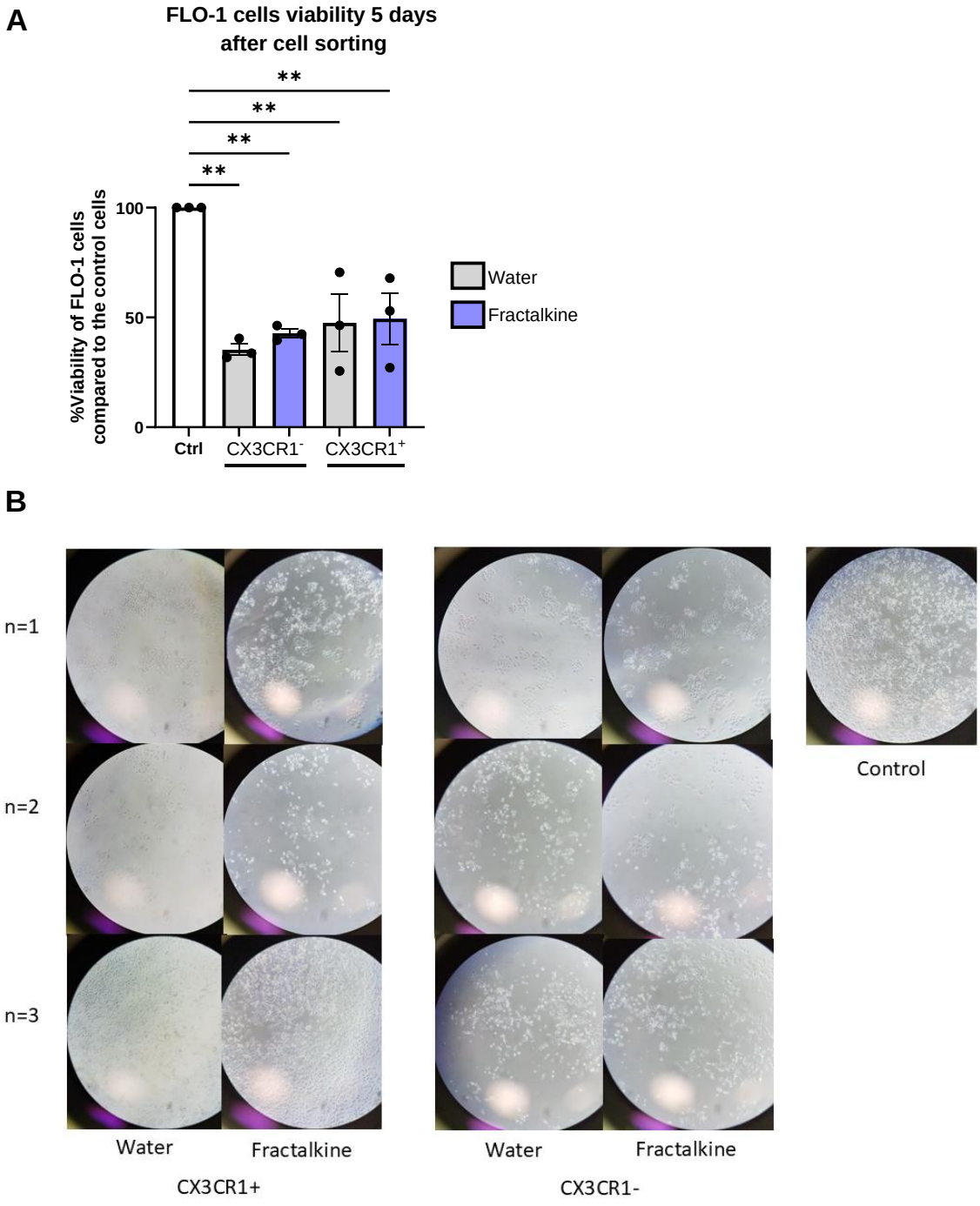

Figure 4.8: Cell sorting significantly decreases FLO-1 cell viability and fractalkine does not significantly alter viability following sorting

(A) Bar charts showing % of CX3CR1^{+} and CX3CR1^{-} FLO-1 cells treated for 24 hours with 0.1 % water or 100ng/ml recombinant fractalkine 5 days after cell sorting. Unstained/unsorted cells used for cell sorting and subsequently sub-cultured were used as a control (Ctrl) for mixed CX3CR1 population. **(B)** Photographs of CX3CR1^{+} and CX3CR1^{-} FLO-1 cells at Day 5 through 20X magnification light microscope (Inverso TC100, Scientific Laboratory supplies). Experiments were repeated n=3. *p<0.05, **p<0.01, by ordinary one-way ANOVA with Tukey multiple comparison test. Mean ± SEM

4.3.4 CX3CR1^{+}FLO-1 cells express higher levels of markers associated with stem-like properties compared to CX3CR1^{-}FLO-1 cells

As the previous experiments demonstrated that sorted CX3CR1^{-} FLO-1 cells express CX3CR1 on their cell surface after 4 days and that sorted cells have lower baseline viability and no responsiveness to the proliferative effects of fractalkine, it was hypothesised that CX3CR1 expression might confer a survival advantage to OAC cancer cells. To further investigate differences in CX3CR1^{+} and CX3CR1^{-} FLO-1 cells, the basal expression of a few markers associated with stem-like properties (CD24, CD34 and CD44) [369, 370] and metabolic properties (CD71 and CD98) were assessed as a measure of stemness/persistence and increased metabolic rate [371, 372]. Frequencies of CD24^{+}CX3CR1^{-}FLO-1 cells were observed to be substantially lower than CD24^{+}CX3CR1^{+}FLO-1 cells; CD24: CX3CR1^{-} vs CX3CR1^{+}(21.7% vs 45%, p=0.0881, n=3) **[Figure 4.9A.i]** while there were significantly lower frequencies of CD24^{+}CX3CR1^{-}FLO-1 cells compared to CD24^{+}CX3CR1^{high}FLO-1 cells; CD24: CX3CR1^{-} vs CX3CR1^{high} (21.7% vs 61.1%, p=0.047, n=3) **[Figure 4.9A.ii]**. Moreover, there were significantly lower frequencies of CD34^{+}CX3CR1^{-}FLO-1 cells compared to CD34^{+}CX3CR1^{+}FLO-1 cells; CD34: CX3CR1^{-} vs CX3CR1^{+}(13.4% vs 82.4%%, p= 0.017, n=3) **[Figure 4.9B.i].** In addition, there were substantially lower frequencies of CD34^{+} cells among CX3CR1^{-}FLO-1 cells compared to CX3CR1^{high}FLO-1 cells; CD34: CX3CR1^{-} vs CX3CR1^{high} (13.4% vs 84.5, p=0.0722, n=3) **[Figure 4.9B.ii]**. There were no significant differences observed between the frequencies of CX3CR1^{+}FLO-1 cells and CX3CR1^{-}FLO-1 expressing CD44, CD71 and CD98 **[Figure 4.9C, D, E]**.

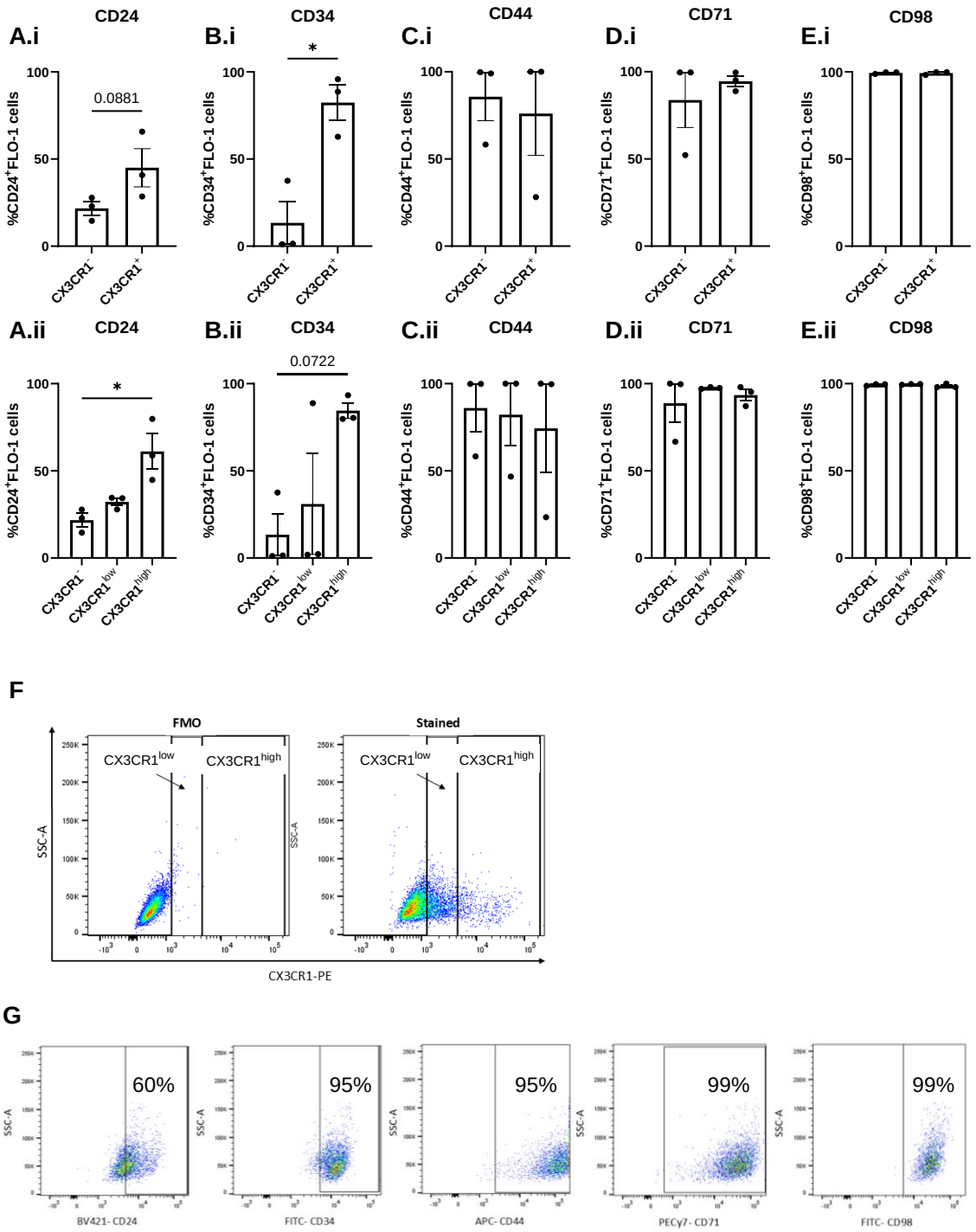

Figure 4.9: CX3CR1^{+} and CX3CR1^{high} FLO-1 cells express significantly higher levels of cancer stemness markers CD34 and CD24, respectively compared to CX3CR1^{-} FLO-1 cells

Bar charts showing basal % expression of **(A)** CD24 **(B)** CD34 **(C)** CD44 **(D)** CD71 and **(E)** CD98 in **(i)** CX3CR1^{-} and CX3CR1^{+}FLO-1 cells and in **(ii)** CX3CR1^{-}, CX3CR1^{low} and CX3CR1^{high} FLO-1 cells. **(F)** Representative dot plots showing gating of CX3CR1^{-}, CX3CR1^{low} and CX3CR1^{high}FLO-1 cell population stained with PE-CX3CR1 compared to FMO control after gating on viable cells. **(F, G)** Representative dot plot showing gating of CX3CR1^{-}, CX3CR1^{+}, CX3CR1^{low} and CX3CR1^{high} FLO-1 cells **(F)** and CD24^{+}, CD34^{+},

$CD44^+$, $CD71^+$ and $CD98^+$ FLO-1 cells within these populations **(G).** Experiments were repeated n=3. *$p<0.05$, parametric paired t-test. Mean ± SEM

4.4 Discussion

Patients who do not respond to standard-of-care treatment, which is approximately 70% of all OAC patients, are likely to develop recurrence and metastasis to distal sites, severely worsening quality of life for these patients [45, 373]. Primary OAC tumours are inclined to metastasise to sites such as the liver and the omentum [354, 355]. Therefore, there is an urgent need to better understand metastatic development in OAC and to develop novel approaches to therapeutically target metastasis. Chapter 3 demonstrated that the fractalkine-CX3CR1 axis may have an important role in OAC tumour progression, as it was shown to promote cell viability and proliferation in the 7 different cell lines assessed. Fractalkine has been explored in the context of metastasis in other malignancies, and it has been shown that overexpression of CX3CR1 leads to increased gastric cancer cell survival, proliferation and metastasis [189]. Therefore, we investigated whether fractalkine could alter other tumourigenic processes in OAC, such as cell cycle of cancer cells, invasion and migration, EMT, and cancer stemness. Moreover, as E6130 showed promising results in chapter 3 by attenuating fractalkine-induced pro-tumourigenic effects, its effects on cell cycle, invasion, migration, and EMT were assessed in the FLO-1 cell line.

Fractalkine has been shown to increase proliferation, viability and migration by altering cell cycle phases in different cancers, mainly in the G1/S phase [194, 223]. Data shown here show that treatment with fractalkine or E6130 did not alter any of the cell cycle phases in FLO-1 cells. Therefore, fractalkine most likely elicits its enhancement of cell viability and proliferation in OAC cell lines via a different mechanism. One potential mechanism could be via activation of signalling pathways such as PIK3/AKT or NF-κB [194, 203].

As mentioned previously, fractalkine has been shown to promote cancer cell invasion, migration and EMT marker expression in other malignancies [192-194, 208]. For instance, a study in a colorectal cancer mouse model demonstrated that cancer cells that metastasised to the liver produced abundant levels of fractalkine, while CX3CR1-deficient mice had reduced liver metastasis and lower macrophage accumulation in metastasised lesions [209]. Furthermore, targeting fractalkine to reduce cancer cell metastasis has already been explored beyond OAC and it has been reported that inhibition of fractalkine

can reduce pancreatic cancer cell viability and motility [203]. The results shown here are in accordance with these studies. Indeed, FLO-1 cells treated with 100ng of fractalkine migrated towards fractalkine-rich FLO-1^{LM} supernatant at significantly higher levels than non-treated cells. This may indicate that high fractalkine levels in the primary TME promote the invasiveness of OAC tumours. However, E6130 was not able to significantly reduce such fractalkine-induced increases in the invasion of FLO-1 cells, which shows that E6130 alone cannot attenuate the migration of fractalkine-primed FLO-1 cells towards the soluble cues of FLO-1^{LM} cells. FLO-1^{LM} cells, which are derived from the spontaneous metastasis of FLO-1 cells to the liver of a mouse, most likely produce other chemokines that attract FLO-1 cells and therefore, modulation of more than one chemokine pathways might be more preferential to target this migration [311]. Unpublished data from our group has demonstrated that the CXCR4 antagonist AMD3100 decreased OE33 cell invasion towards lymph node conditioned media generated from OAC patient samples. Additionally, 24-hour co-culture of OE33 cells with liver conditioned media generated from OAC patient samples significantly increased CXCR4 expression on these cells. These data suggest that targeting CX3CR1 and CXCR4 could prove beneficial to reduce OAC cell metastasis.

EMT plays a crucial role in the progression of OAC by enhancing tumour cell invasion, metastasis, and resistance to therapy. This process involves the loss of epithelial characteristics, such as E-cadherin expression, and the acquisition of mesenchymal traits, including increased n-cadherin, vimentin, and SNAIL/SLUG transcription factors, which enable cancer cells to become more migratory and invasive [38, 193, 217, 218, 357, 358, 374]. Baseline expression of SLUG and vimentin were significantly higher in $CX3CR1^{+}$ FLO-1 cells compared to $CX3CR1^{-}$ FLO-1 cells and the opposite was seen in expression of E-cadherin, further demonstrating that $CX3CR1^{+}$ FLO-1 cells present a more metastatic profile than $CX3CR1^{-}$ FLO-1 cells. However, results shown here demonstrate that fractalkine did not directly alter SLUG, vimentin or E-cadherin EMT markers by FLO-1 cells. This contrasts with previous research on prostate, pancreatic and breast cancer cells where fractalkine has been demonstrated to promote SLUG and downregulate E-cadherin expression [193, 217, 375]. However, in ovarian cancer cells, fractalkine was shown to increase metastasis through expression of SNAIL, Twist, N-cadherin, and P-

cadherin in under hypoxic conditions [218]. Therefore, fractalkine may induce EMT markers other than SLUG, vimentin and E-cadherin in OAC, and future experiments are needed to evaluate this under hypoxic and/or acidic conditions as the results from chapter 3 show increased effects of fractalkine on cell viability under these physiological conditions. E6130 did not reduce markers of EMT, which contrasts with preliminary data from our group which showed that CX3CR1 antagonism with AZD8797 in OE33 cells reduces expression of EMT markers such as SLUG and vimentin (unpublished results). This highlights possible differences between the mechanism of action of AZD8797 (a CX3CR1 antagonist) and E6130 (a CX3CR1 modulator), and also highlights possible differences between the biology of the two OAC cell lines. Given the contrast between the EMT phenotype of $CX3CR1^+$ FLO-1 cells and the observation that fractalkine does not induce such changes, an investigation of eotaxin-3's effects on these EMT markers might also reveal how CX3CR1 signalling impacts EMT.

CX3CR1 upregulation and higher expression in different cancers has mostly been associated with poorer disease prognosis, however its role in OAC has not yet been elucidated [189, 202]. The pilot data generated here demonstrated that FLO-1 cells revert to their mixed population 4 days after cell sorting into $CX3CR1^-$ and $CX3CR1^+$ cells. These data could indicate that heterogenous populations of $CX3CR1^-$ and $CX3CR1^+$ cells may provide a survival advantage to FLO-1 cells. Interestingly, fractalkine treatment did not alter viability in either sorted $CX3CR1^-$ or $CX3CR1^+$ FLO-1 cells. In fact, both the sorted fractions of FLO-1 cells had significantly lower viability compared to unsorted FLO-1 cells, suggesting that the survival of the cells was significantly compromised by the process. Moreover, the sorted $CX3CR1^+$ fraction of FLO-1 cells yielded low numbers, thus CX3CR1 expression and CCK8 could only be evaluated at one time point (day 5). More thorough studies perhaps using gene knock-out of CX3CR1 on FLO-1 cells are needed to more accurately confirm how the $CX3CR1^+$ and $CX3CR1^-$ cell populations interact and differ in viability and growth. However, a return to a mixed population suggests a survival advantage. This is in line with results in other cancers, where for instance in epithelial ovarian cancer, it was found that higher expression of CX3CR1 was associated with an overall unfavourable survival for these patients, and in murine models of colorectal cancer, $CX3CR1^+$ cancer cells exhibit a survival advantage through the fractalkine-

CX3CR1 axis, which facilitated tumour cell migration, generation of a pro-metastatic niche, and attraction of inhibitory myeloid cells, contributing to immune evasion and resistance to therapies like anti-PD-1 [219, 376].

Given these data and given that cell sorting compromised the viability of FLO-1 cells, the CSC and metabolic features of CX3CR1$^-$ and CX3CR1$^+$ FLO-1 cells were evaluated by flow cytometric analysis of unsorted mixed populations. CD24 and CD34 expression were significantly higher on CX3CR1$^+$ compared to CX3CR1$^-$ FLO-1 cells. The overexpression of the CSC marker CD24 has a reported association with worse patient prognosis in breast, prostate, colorectal, gastric, ovarian cancer, non-small cell lung carcinomas and OSCC [377-384]. Moreover, studies on gastric cell lines have associated CD24 expression with increased cancer cell growth, invasion and migration and have shown that downregulation of the CSC markers results in improved chemosensitivity, increased apoptosis and inhibition of cell proliferation [385, 386]. It has been reported that CD24 is expressed on chemo-resistant OE33 and OE19 cells and that these cells resisted apoptosis and formed spheres, which is a typical feature of CSCs [387]. Similarly, CD34 has been shown to correlate with poor prognosis in OAC and therefore could be used as a potential prognostic biomarker [388]. Moreover, a study found that CD34 expression increased in peritumoral adipose tissue during OAC development in rats and that adipose-derived stem cells treated with peritumoral conditioned medium showed increased CD34 expression, particularly in samples from chemo-resistant patients [389]. Therefore, these data show that CX3CR1$^+$ FLO-1 cells, by expressing higher CD24 and CD34 expression, have stem-like properties which supports the hypothesis that CX3CR1 promotes cancer cell survival in OAC.

In conclusion, experiments conducted in this chapter sought to further elucidate the role of fractalkine in OAC tumour progression, as chapter 3 highlighted the role of the fractalkine-CX3CR1 axis in promoting OAC cell viability and proliferation. Here, fractalkine treatment increased invasion and migration of FLO-1 cells towards FLO-1^{LM} supernatants supporting a pro-metastatic role. However, this was not inhibited by pre-treatment with E6130, strongly indicating that there are multiple chemotactic cues in the FLO-1^{LM} supernatants, which were used to simulate the metastatic niche of the liver in OAC. In addition, CX3CR1$^+$FLO-1 cells contain higher proportions of cells with stem-like

and metastatic phenotype compared to CX3CR1^{-}FLO-1 cells. Finally, pilot data separating these two populations show that CX3CR1^{-}FLO-1 cells might benefit from contact with CX3CR1^{+}FLO-1 cells and vice versa, suggesting that CX3CR1 expression on FLO-1 cells provides a survival advantage. Together, these findings demonstrate the complicated role of the fractalkine-CX3CR1 axis in OAC metastasis and further *in vivo* experiments are warranted to confirm if targeting this axis could prevent/limit metastasis in OAC.

4.5 Highlights

- Fractalkine increases FLO-1 cell invasion and migration towards FLO-1^{LM} supernatants.
- CX3CR1 expression in FLO-1 cells is associated with a more pronounced EMT phenotype.
- CX3CR1 expression in FLO-1 cells express higher levels of markers associated with stemness.

Chapter 5 – Exploring the biological effects of E6130 on tumour cells and intratumoural and circulating NK cells in OAC patients

5.1 Introduction

Oesophageal adenocarcinoma (OAC) is an exemplary model of obesity-associated and inflammation-driven cancer [23, 390]. Visceral adipose tissue (VAT), which is the intra-abdominal fat, is found to be one of the main initiators of chronic and systemic inflammation [31]. Our group has reported that the obese condition in OAC patients contributes to tumour cell proliferation, migration, and metastatic phenotype [37, 38]. Furthermore, our group has shown that visceral obesity is characterised by immune dysfunction in OAC and that the largest depot of VAT in humans known as the omentum, is the source of many driving factors in this dysregulation [33, 39-41, 126, 128, 129]. In the setting of obesity, fractalkine facilitates the recruitment of immune cells, particularly monocytes and macrophages into adipose tissue, where they contribute to chronic low-grade inflammation, as fractalkine:CX3CR1 interaction modifies monocyte adhesion to adipocytes and correlates with obesity [206].

In OAC patients with obesity, our group have shown that NK cell infiltration of tumours negatively correlates with visceral obesity [127]. Our data show that this is at least partially due to the erroneous fractalkine-mediated recruitment of NK cells to the visceral adipose tissue [68, 69, 127]. Furthermore, exposure to the VAT microenvironment impedes the migration of NK cells towards tumour and this can be alleviated by CX3CR1 antagonism [69]. Interestingly, our group also reported that fractalkine mediates the conversion of NK cells from $CX3CR1^{+}CD27^{-}$ to $CX3CR1^{-}CD27^{+}$ and increases their IFN-γ and TNF-α production [127]. Collectively, these data strongly suggest that exposure to fractalkine and/or OAC patient-derived VAT alters NK cell phenotype and function. Our group have also shown that E6130 can redirect NK cells away from soluble factors in OAC-patient derived adipose conditioned media (ACM) and towards tumour conditioned media (TCM) in a novel *ex vivo* model highlighting the therapeutic potential of this CX3CR1 modulator to boost NK cell infiltrations of OAC tumours in patients with the condition of obesity [68, 69]. However, little is known about the possible non-chemotactic effects of E6130 on NK cells [185]. In this chapter, E6130's ability to attenuate fractalkine-induced increases in OAC cell viability and proliferation was validated in OAC patient tumour samples together with its effects on cytotoxicity and cytokine release. Fractalkine levels in tumour tissue, normal adjacent oesophageal and gastric tissues,

adipose tissue, liver tissue and serum of OAC patients were evaluated to compare fractalkine levels in the circulation, the TME and extratumoural tissues of interest. Lastly, E6130's effect on NK cell phenotype in blood and tumour was assessed to ascertain if it elicited any undesirable non-chemotactic effects on NK cells. Therefore, this chapter aims to elucidate the non-chemotactic effects of E6130, to further understand the potential of this chemokine therapy in OAC, and ascertain any off-target effects. A mixed cohort of samples from oesophageal, gastric and oesophageal-gastric junctional adenocarcinomas patients were separated into oesophageal adenocarcinoma (OAC) and gastric adenocarcinoma (GAC) cohorts and used in these studies due to proximal tumour location.

5.2 Hypothesis

The CX3CR1 modulator E6130 elicits anti-tumour effects in OAC patient samples.

Aims:

1. Investigate if E6130 alters LDH release and tumour cell viability in OAC patient tumour samples
2. Evaluate fractalkine as a biomarker of tumour stage and treatment response in OAC serum and patient tissues
3. Assess if E6130 alters NK cell activation, inhibition and cytotoxic markers in healthy donor blood and OAC patient blood
4. Assess if E6130 alters NK cell activation, inhibition and cytotoxic markers in intratumoural NK cells from OAC patients

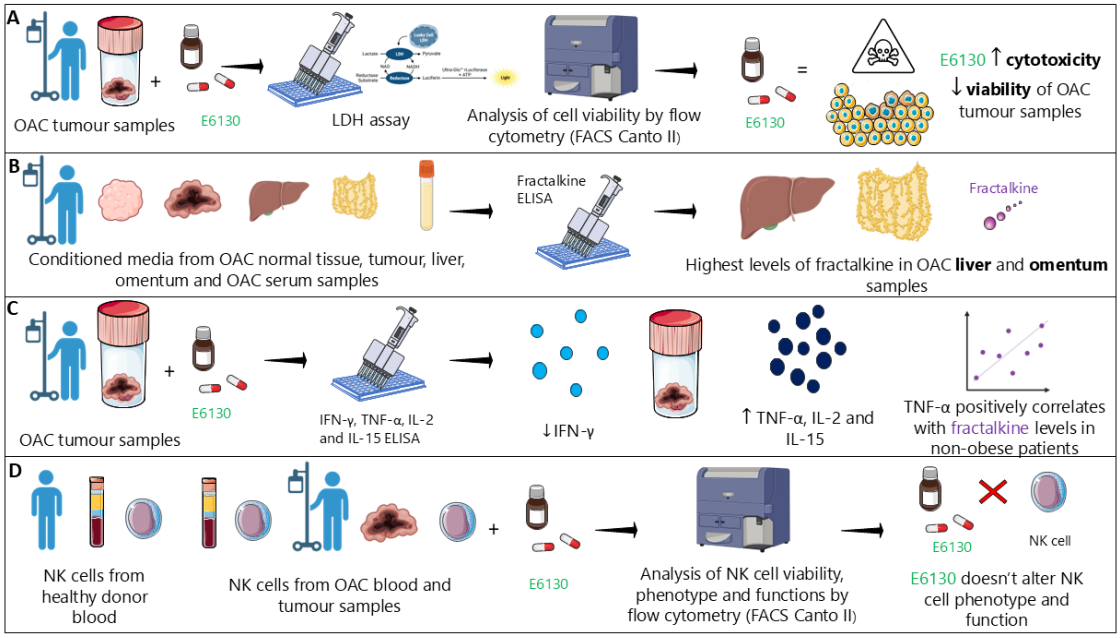

Graphical abstract: (A) OAC tumour patient samples were treated with E6130. Cytotoxicity was assessed with an LDH assay and cell viability by flow cytometry. E6130 increased (↑) cytotoxicity and reduced (↓) cell viability in OAC tumour samples. **(B)** Conditioned media from OAC normal tissue, tumour, liver and omental patient samples and OAC serum patient samples were assessed for fractalkine levels by ELISA, with highest fractalkine levels found in the liver and omentum conditioned media of OAC patients. **(C)** OAC patient tumour samples were treated with E6130 and IFN-γ, TNF-α, IL-2 and IL-15 levels were assessed by ELISA. E6130 reduced (↓) IFN-γ levels and increased (↑) TNF-α, IL-2 and IL-15 levels. TNF-α levels positively correlated with fractalkine levels in OAC tumour patient samples without obesity. **(D)** NK cells from healthy donor blood, OAC patient blood and OAC patient tumour samples were treated with E6130 and analysed for cell viability, phenotype and function by flow cytometry. E6130 treatment did not alter viability, phenotype or function of NK cells. Created with Smart.Servier.com and Biorender.com

Results

5.3 Exploring the biological effects of E6130 on tumour cells and intratumoural and circulating NK cells in OAC patients

5.3.1 E6130 significantly decreased viability and increased cytotoxicity in OAC and GAC patient tumour samples

5.3.1.1 E6130 significantly decreased viability and increased cytotoxicity in OAC and GAC patient tumour samples

As E6130 reduced fractalkine-induced viability and proliferation in chapter 3, E6130-induced cytotoxicity was evaluated in OAC and GAC patient tumour conditioned media (TCM) and normal adjacent tissue samples (normal oesophageal conditioned media, NOCM and normal gastric conditioned media, NGCM) using a lactate dehydrogenase (LDH) assay following 24-hour treatment with E6130 or DMSO. The LDH assay was performed using TCM from these samples. Following 24-hour treatment with E6130, OAC and GAC patient tumour samples exhibited significantly higher percentages of cytotoxicity compared to non-treated (NT) or DMSO treated; NT vs E6130 (24.44% vs 30.87%, p=0.0024, n=10); DMSO vs E6130 (24.48% vs 30.87%, p=0.022, n=10) **[Figure 5.1A left]**. There were no differences in cytotoxicity levels in normal oesophageal and normal gastric samples when they were treated with E6130 **[Figure 5.1A middle and right]**. Matched normal oesophageal and tumour LDH release were compared by subtracting %LDH release with DMSO treatment from %LDH release with E6130 treatment, and TCM had significantly higher % LDH release compared to its matched NOCM; NOCM vs TCM (0.3139% vs 10%, p=0.0286, n=4) and similarly TCM had significantly higher %LDH release compared to its matched NGCM; NGCM vs TCM (-4.255% vs 10%, p=0.0286, n=4) **[Figure 5.1B]**.

Tumour regression grade (TRG) is an established means of stratifying patients based on treatment response [391, 392]. A TRG between 1-2 usually indicates none to rare residual cancer cells following treatments (good responders), whereas TRG 3-5 indicates residual cancer cells to almost all cancer cells remaining after treatment [391, 392]. TRG 3 to 5 can indicate that patients are resistant to treatments (weak to poor responders). The TRG of OAC samples that had neoadjuvant treatment was compared, and LDH release is lower

in samples with TRG from 3-5 compared to TRG 1-2; NT: TRG 1-2 vs TRG 3-5 (27.6% vs 10%, n=3), DMSO: TRG 1-2 vs TRG 3-5 (26.2% vs 7.4%, n=3); E6130: TRG 1-2 vs TRG 3-5 (35.1% vs 17.7%, n=3), however no statistical significances were observed, perhaps , due to small patient numbers available when stratifying patients by TRG **[Figure 5.1C, left]**. Body Mass Index (BMI) of OAC patients was also compared, a BMI of under 24.9kg/m^2 was considered for patients without obesity and a BMI over 25kg/m^2 was considered for patients who are overweight or with obesity. There were no significant differences observed when tumour samples were stratified by BMI **[Figure 5.1C, right]**.

To further confirm the effects of E6130 on tumour cell viability, viability using a live/dead stain was analysed by flow cytometry after samples from patient tumours were treated for 24 hours with E6130 and were compared to DMSO treated samples. Tumour cell population was gated on $CD31^-CD45^-$ cells from total cell population. E6130 slightly but significantly decreased live tumour cells and $CX3CR1^+$live tumour cells; live tumour cells: DMSO vs E6130 (88% vs 83.6%, p=0.037, n=10); $CX3CR1^+$live tumour cells: DMSO vs E6130 (55.2% vs 53.1%, p=0.018, n=10) **[Figure 5.1D]**.

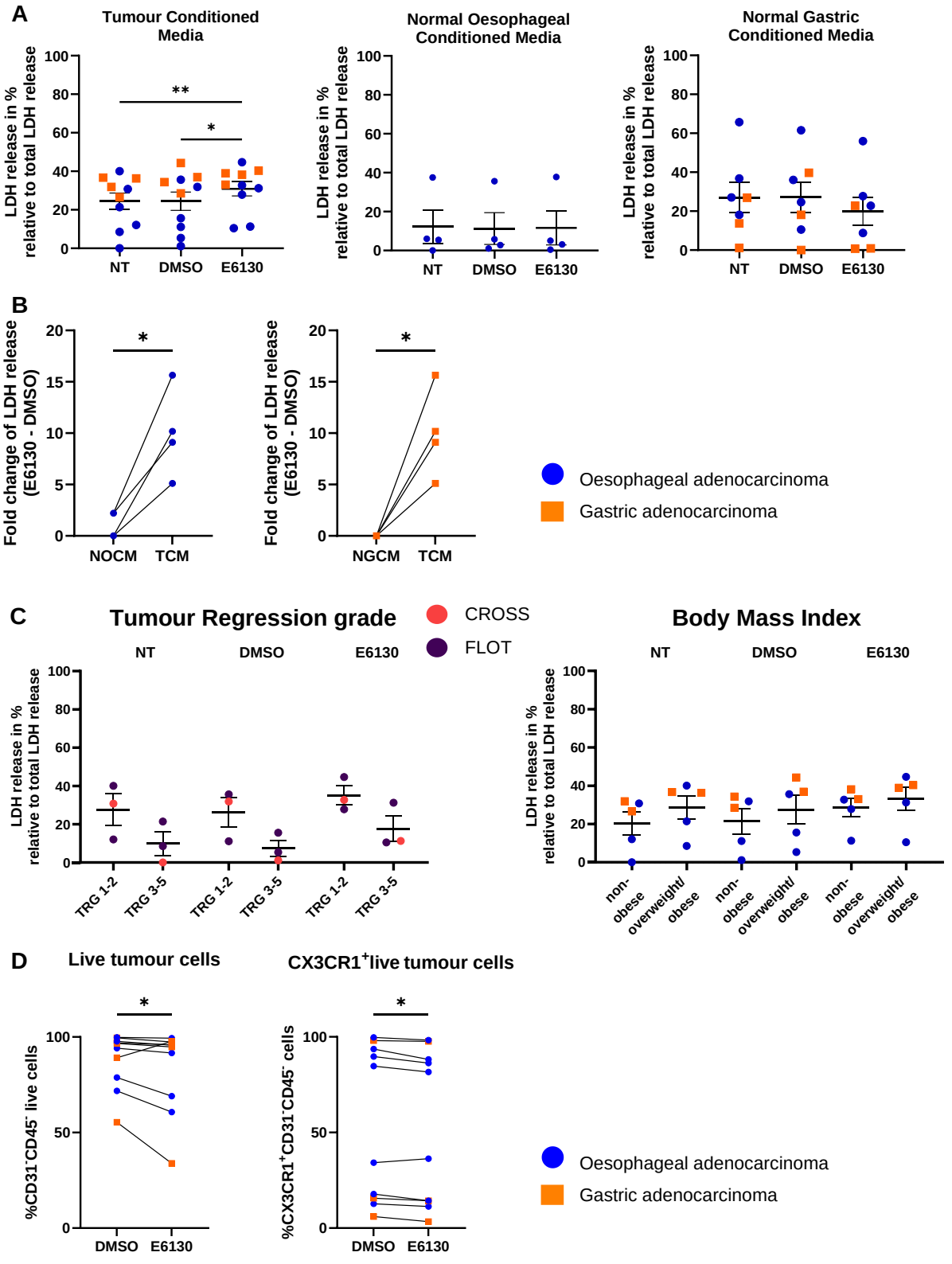

Figure 5.1: Significantly reduced viability and significantly increased cytotoxicity in OAC and GAC patient tumour following 24-hour treatment with E6130.

(A) Dot plots showing LDH release in % following 24-hour treatment with 0.01% DMSO, E6130 or no treatment (NT) in OAC and GAC tissue (n=10), normal adjacent oesophageal tissue (n=4) and normal adjacent gastric tissue (n=6). **(B)** Dot plots showing LDH release

in % (%E6130 - %DMSO) of matched normal oesophageal conditioned media (NOCM) compared to tumour conditioned media (TCM) and matched normal gastric conditioned media (NGCM) compared to TCM (n=4). **(C)** Dot plot showing LDH release in % following 24-hour treatment with 0.01% DMSO, E6130 or no treatment (NT) in oesophageal tumour tissue by tumour regression grade and neoadjuvant treatment (CROSS n=2, pink; FLOT n=4, purple) (left) and Body Mass Index (BMI) (non-obese n=5, overweight/obese n=5). **(D)** Dot plots showing the frequencies of **(left)** live and **(right)** $CX3CR1^{+}$ live tumour cells from OAC and GAC patients following 24-hour treatment with 0.01% DMSO and 4.9nM E6130. *p<0.05, **p<0.01, by Friedmann test (A), Wilcoxon t-test (C, D) or Mann-Whitney test (B) where appropriate. Mean ± SEM.

5.3.1.2 E6130 significantly increased the frequencies of CX3CR1^{+}FasL^{+} tumour cells in OAC and GAC patient-derived tumour

Death receptor ligands TRAIL and FasL were assessed following treatment for 24 hours with E6130 on OAC and GAC patient tumours and were compared to DMSO treated samples. TRAIL receptor expression was not altered by E6130 treatment, however higher frequencies of CX3CR1^{+}FasL^{+} tumour cells were observed on E6130 treated samples compared to DMSO treated samples; DMSO vs E6130 (15.2% vs 21.6%, p=0.012, n=10) **[Figure 2B, right]**.

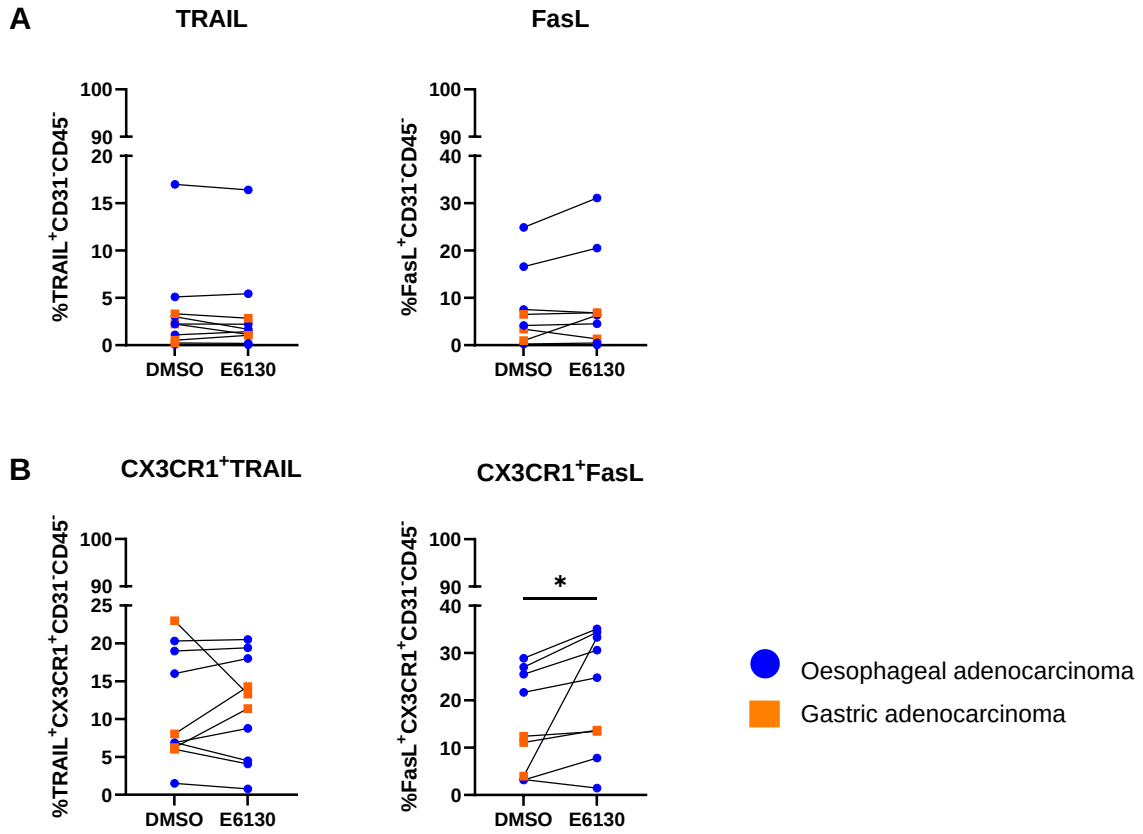

Figure 5.2: 24-hour treatment with E6130 significantly increased frequencies of CX3CR1$^+$FasL$^+$ tumour cells in OAC patient-derived tumours

Dot plots showing the frequencies of **(A)** TRAIL$^+$ and FasL$^+$ and **(B)** CX3CR1$^+$ TRAIL$^+$ and CX3CR1$^+$ FasL$^+$ tumour cells from OAC and GAC patients following 24-hour treatment with 0.01% DMSO and 4.9nM E6130. Experiments were repeated n=10. *p<0.05, by Wilcoxon t-test. Mean± SEM.

The data presented here demonstrated that 24-hour treatment with E6130 reduces viability and increases cytotoxicity of OAC and GAC tumour samples. Moreover, E6130 did not seem to affect normal adjacent oesophageal and gastric tissue as E6130 did not alter cytotoxicity in these samples.

5.3.2 Investigating the levels of fractalkine in OAC and GAC patient tumour and serum samples

5.3.2.1 Significantly higher levels of fractalkine in adipose conditioned media (ACM) and liver conditioned media (LCM) compared to TCM, NOCM and serum

Our group have previously reported high levels of fractalkine in the omentum compared with the tumour and serum of OAC patient [127, 129]. Here, the levels of fractalkine were measured by ELISA in TCM, NOCM, NGCM, adipose conditioned media (ACM), liver conditioned media (LCM) and serum of OAC and GAC patients to confirm previous observations and compare all groups in this cohort to LCM, NOCM and NGCM where we have previously not reported the levels of fractalkine. NOCM, TCM and serum have significantly lower expression of fractalkine compared to ACM and LCM; NOCM vs ACM (1477pg/ml vs 40207pg/ml, p=0.018, n=7); TCM vs ACM (1223pg/ml vs 40207pg/ml, p=0.0001, n=7-20); serum vs ACM (1392pg/ml vs 40207pg/ml, p=0.041, n=7-10); and LCM; NOCM vs LCM (1477pg/ml vs 38803pg/ml, p=0.012,n=7-9); TCM vs LCM (1223pg/ml vs 38803pg/ml, p=0.0001, n=9-20); serum vs LCM (1392pg/ml vs 38803pg/ml, p=0.027, n=9-10); **[Figure 5.3]**.

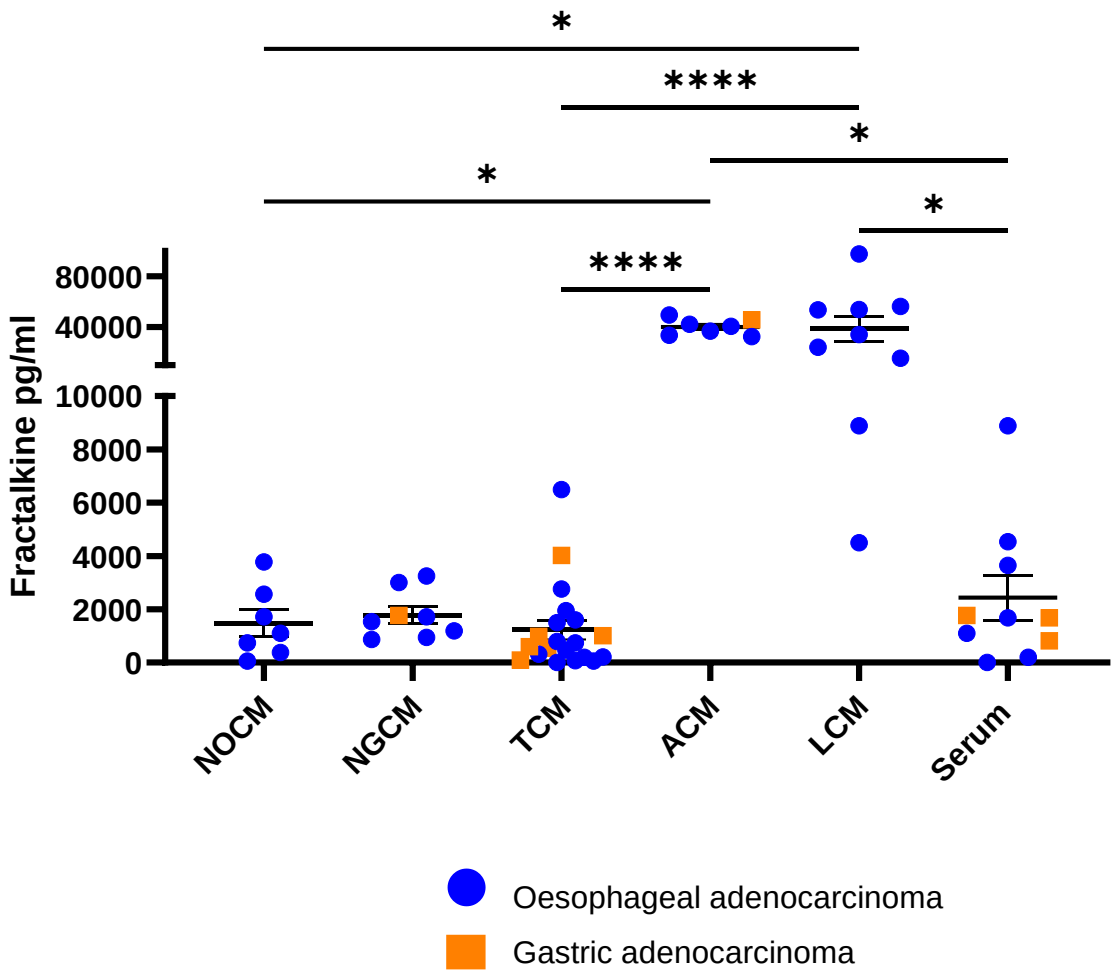

Figure 5.3: ACM and LCM had significantly higher levels of soluble fractalkine compared to NOCM, TCM and serum samples from OAC and GAC patients

Dot plot showing levels of soluble fractalkine in normal oesophageal conditioned media (NOCM) (n=7), normal gastric conditioned media (NGCM) (n=8), tumour conditioned media (TCM) (n=20), adipose conditioned media (ACM) (n=7), liver conditioned media (LCM) (n=9) and serum (n=10) of OAC and GAC patients, in pg/ml. *p<0.05, ***p<0.001, ****p<0.0001, by Kruskal Wallis with post-hoc Dunn's test. Mean± SEM.

5.3.2.2 TCM levels of fractalkine in OAC and GAC patients without obesity are significantly higher compared to patients who are overweight or with obesity.

Following analysis fractalkine concentrations in these samples, the matched tissue samples were correlated to identify any associations between them. There were no significant correlations in fractalkine levels between the different OAC and GAC patient compartments **[Figure 5.4]**. In addition, TCM OAC and GAC patients were stratified by their type of neoadjuvant treatment or if they did not receive any treatment prior to the sample being taken (naïve), their tumour regression grade, positivity of their nodal status and Body Mass Index (BMI). The TCM of OAC and GAC patients without obesity had significantly higher levels of fractalkine compared to patients who were overweight or with obesity; BMI: non-obese vs overweight/obese (1939pg/ml vs 507.1pg/ml, p=0.035, n=20) **[Figure 5.5, BMI]**. TCM of OAC and GAC patients treated with the CROSS (paclitaxel, carboplatin, radiotherapy) and FLOT (5-fluorouracil, leucovorin, oxaliplatin and docetaxel) regimen have substantially higher fractalkine levels compared to naïve treatment, but due to the small amount of patients who were treatment naive (n=2) compared to CROSS (n=5) and FLOT (n=13), it was not significant; naïve vs CROSS vs FLOT (332pg/ml vs 1004pg/ml vs 1444pg/ml) **[Figure 5.5]**. There was no significant difference in fractalkine levels in the TCM of OAC and GAC patients when stratified by tumour regression grade or nodal status. Furthermore, NOCM, NGCM, ACM, LCM and serum from OAC and GAC patients were stratified by their type of neoadjuvant treatment or if they did not receive any treatment prior to the sample being taken (naïve), their tumour regression grade, positivity of their nodal status and BMI. There were no significant differences observed between these and they were summarised in **[Table 5.1, 2, 3, 4].**

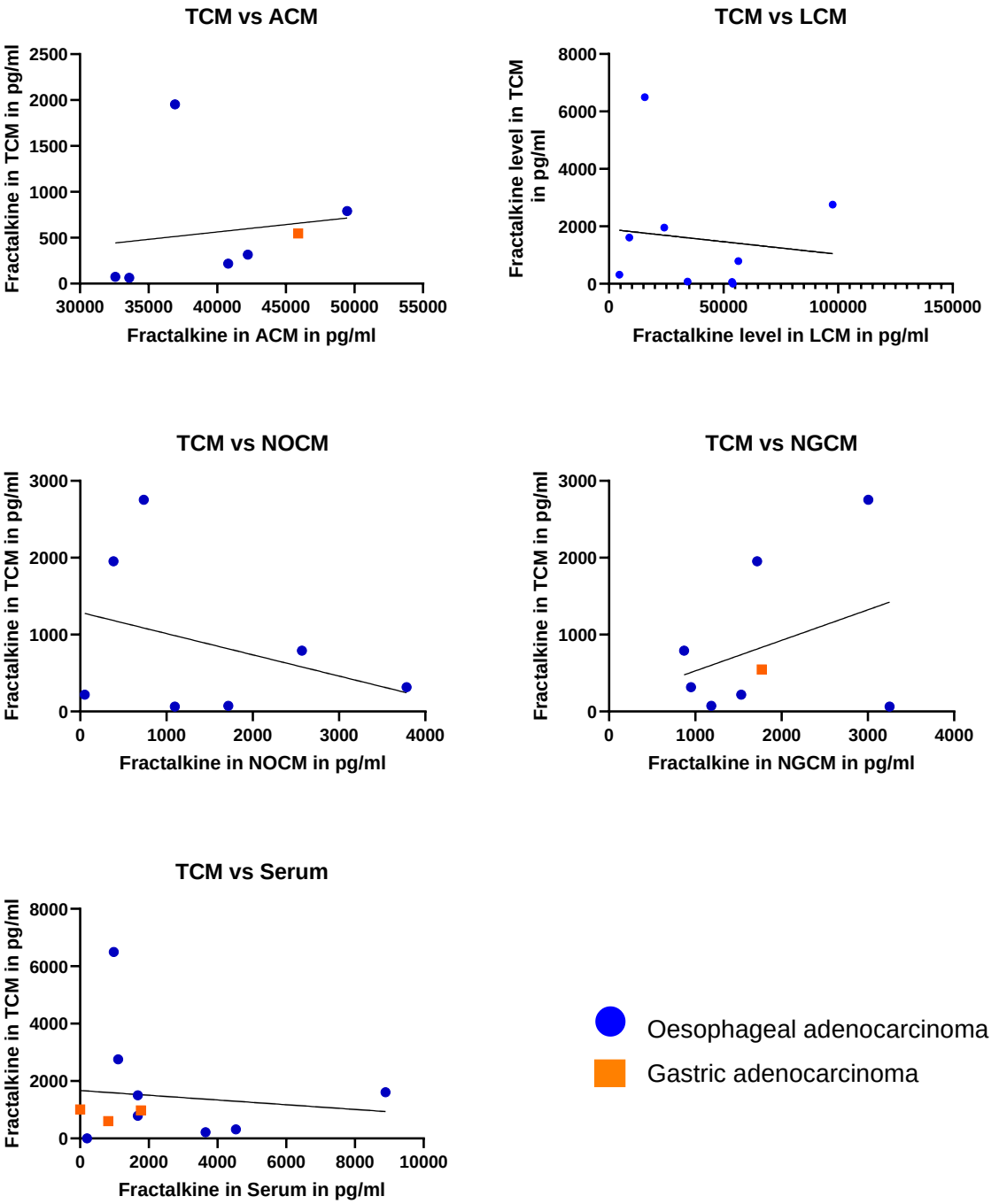

Figure 5.4: No correlations between levels of fractalkine in TCM compared to ACM, LCM, NOCM, NGCM and serum of OAC and GAC patients

Line graphs showing correlations of levels of soluble fractalkine between tumour conditioned media (TCM) and adipose conditioned media (ACM) (n=7), liver conditioned media (LCM) (n=9), normal oesophageal conditioned media (NOCM) (n=7), normal gastric conditioned media (NGCM) (n=8) and serum (n=10) of oesophageal adenocarcinoma (OAC) and gastric adenocarcinoma (GAC) patients, in pg/ml, by Spearman Correlation.

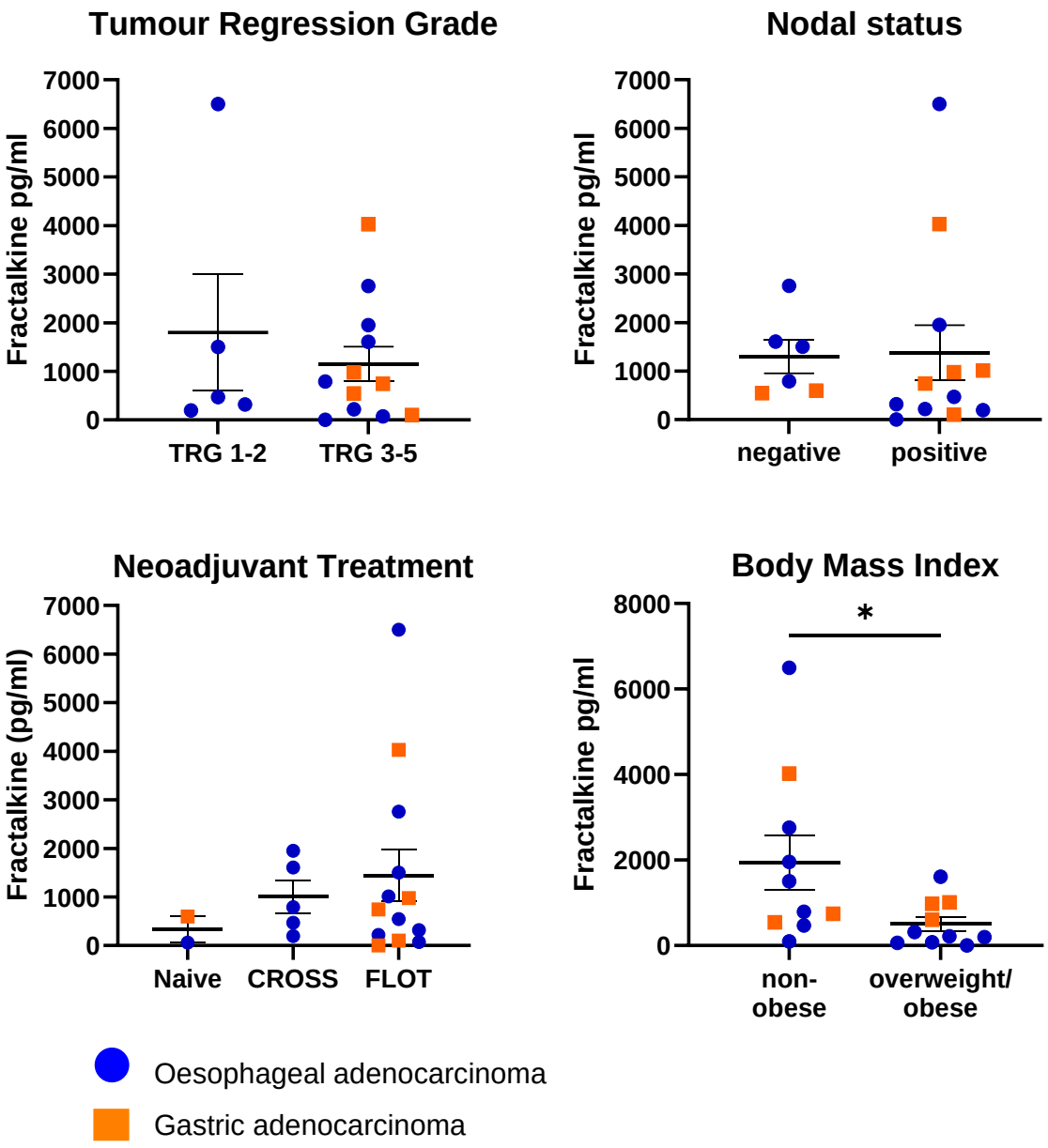

Figure 5.5: Significantly higher levels of intratumoural soluble fractalkine in OAC and GAC patients without obesity compared to patients with overweight or obesity

Dot plots showing levels of fractalkine in TCM by tumour regression grade (TRG 1-2 n=5, TRG 3-5 n= 13), nodal status (negative n= 6, positive n=12), neoadjuvant treatment (naïve n=2, CROSS n=5, FLOT n=13) and Body Mass Index (BMI) (non-obese n=10, overweight/obese n=10), by Mann-Whitney t-test, *p<0.05. Mean± SEM.

Table 5.1: Mean fractalkine levels per tumour regression grade

Source	TRG 1-2 (pg/ml)	TRG 3-5 (pg/ml)
NOCM	3783 (n=1)	1092 (n=5)
NGCM	951 (n=1)	1680 (n=6)
LCM	39666 (n=5)	32404 (n=3)
ACM	42225 (n=1)	41128 (n=5)
Serum	2274 (n=4)	3607 (n=4)

Table 5.2: Mean fractalkine levels per nodal status

Source	Negative nodal status (pg/ml)	Positive nodal status (pg/ml)
NOCM	1653 (n=2)	1746 (n=4)
NGCM	1882 (n=3)	951 (n=5)
LCM	54321 (n=3)	31043 (n=6)
ACM	47676 (n=2)	37220 (n=5)
Serum	1345 (n=4)	2015 (n=5)

Table 5.3: Mean fractalkine levels per neoadjuvant treatment regimen

Source	Naïve (pg/ml)	CROSS (pg/ml)	FLOT (pg/ml)
NOCM	1096 (n=1)	385 (n=2)	52 (n=4)
NGCM	3252 (n=1)	1294 (n=2)	1689 (n=5)
LCM	53680 (n=1)	29834 (n=3)	41208 (n=5)
ACM	33584 (n=1)	43193 (n=2)	40370 (n=4)
Serum	N/A	5288 (n=2)	1850 (n=7)

Table 5.4: Mean fractalkine levels per Body Mass Index

Source	Non-obese (pg/ml)	Overweight/obese (pg/ml)
NOCM	1477 (n=2)	2199 (n=5)
NGCM	1294 (n=2)	1738 (n=5)
LCM	33080 (n=3)	31079 (n=5)
ACM	43193 (n=2)	39013 (n=5)
Serum	1727 (n=2)	2827 (n=7)

5.3.3 E6130 significantly increased TNF-α, IL-2 and IL-15 but decreased IFN-γ production in OAC and GAC tumour samples

5.3.3.1 E6130 increased TNF-α, IL-2 and IL-15 secretion by OAC and GAC patient tumour

To determine if treatment with E6130 alters cytokine expression intratumourally, tumour samples were treated with 4.9nM E6130 or its vehicle control 0.01% DMSO for 24-hours. The tumour conditioned media (TCM) was collected, and cytokine levels were determined by ELISA. E6130 significantly decreased IFN-γ compared to DMSO treated TCM; IFN-γ: DMSO vs E6130 (36.9 pg/ml vs 17.2 pg/ml, p=0.031; n=7). However, E6130 significantly increased TNF-α, IL-2 and IL-15 levels compared to DMSO treated samples; TNF-α : DMSO vs E6130 (119.4pg/ml vs 238.4%, p=0.031, n=8); IL-2: DMSO vs E6130 (0.1775 pg/ml vs 15.65 pg/ml; p=0.032, n=8); IL-15: DMSO vs E6130 (21.66 pg/ml vs 33.01 pg/ml; p=0.039, n=9) **[Figure 5.6]**.

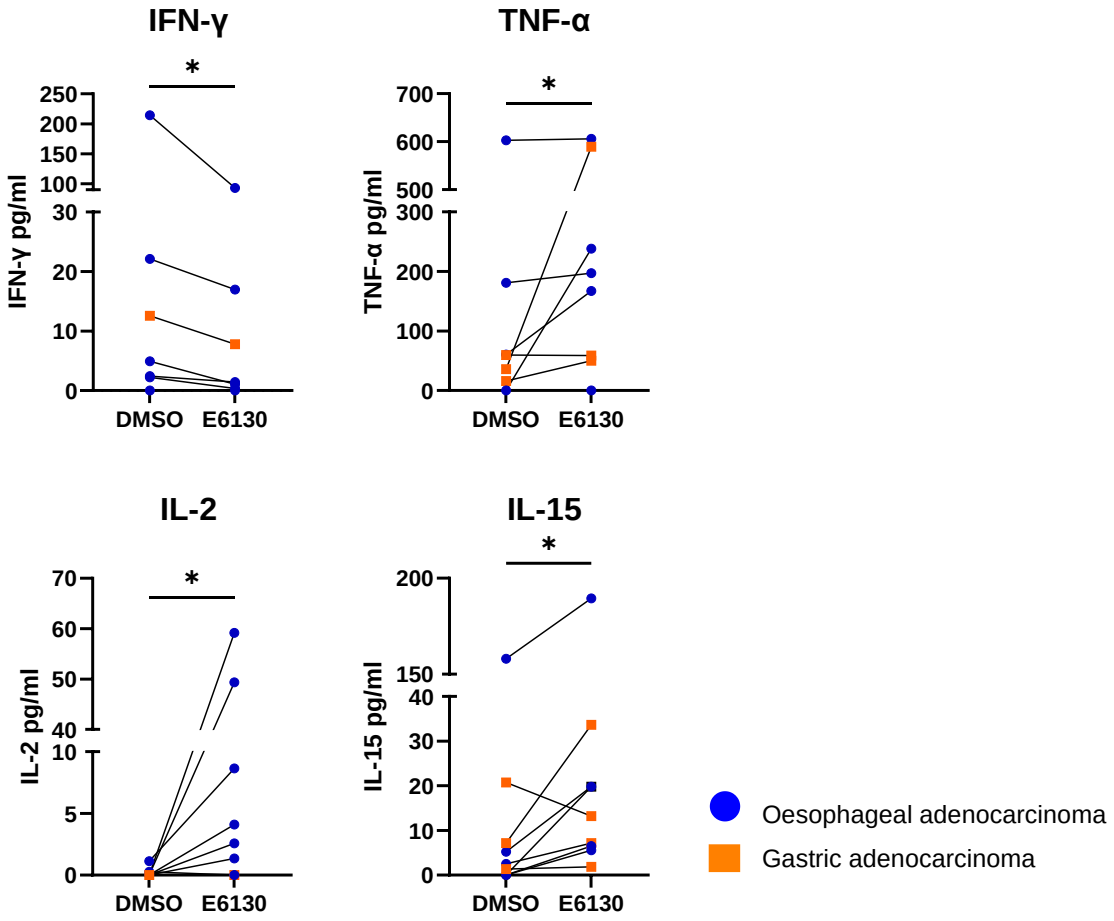

Figure 5.6: E6130 decreased IFN-γ and increases TNFα, IL-15 and IL-2 release in OAC and GAC tumour tissue.

Dot plot showing IFN-γ, TNFα, IL-2 and IL-15 in pg/ml measured by ELISA of OAC and GAC tumour tissue following 24-hour treatment with 0.01% DMSO or 4.9nM of E6130. A total of n=7-9 samples were measured. *p<0.05, by Wilcoxon test. Mean± SEM.

5.3.3.2 Fractalkine levels correlate with TNF-α levels in OAC and GAC patient tumour samples

Baseline levels of fractalkine in TCM were compared to baseline levels of IFN-γ, TNF-α, IL-2 and IL-15 of matched tumour OAC and GAC patient samples. Fractalkine levels significantly positively correlated with TNF-α levels of OAC and GAC patient samples; p=0.0037, r=0.5855 **[Figure 5.7B]**. The levels of IFN-γ, IL-2 and IL-15 did not significantly correlate with fractalkine levels of matched tumour patient samples **[Figure 5.7A, B, D]**. Baseline %LDH release and %LDH release after treatment with E6130 (%LDH release after DMSO treatment was subtracted from %LDH release after E6130 treatment to assess LDH release) were also plotted against their matched baseline fractalkine levels, however there were no significant correlations between them **[Figure 5.7E, F]**.

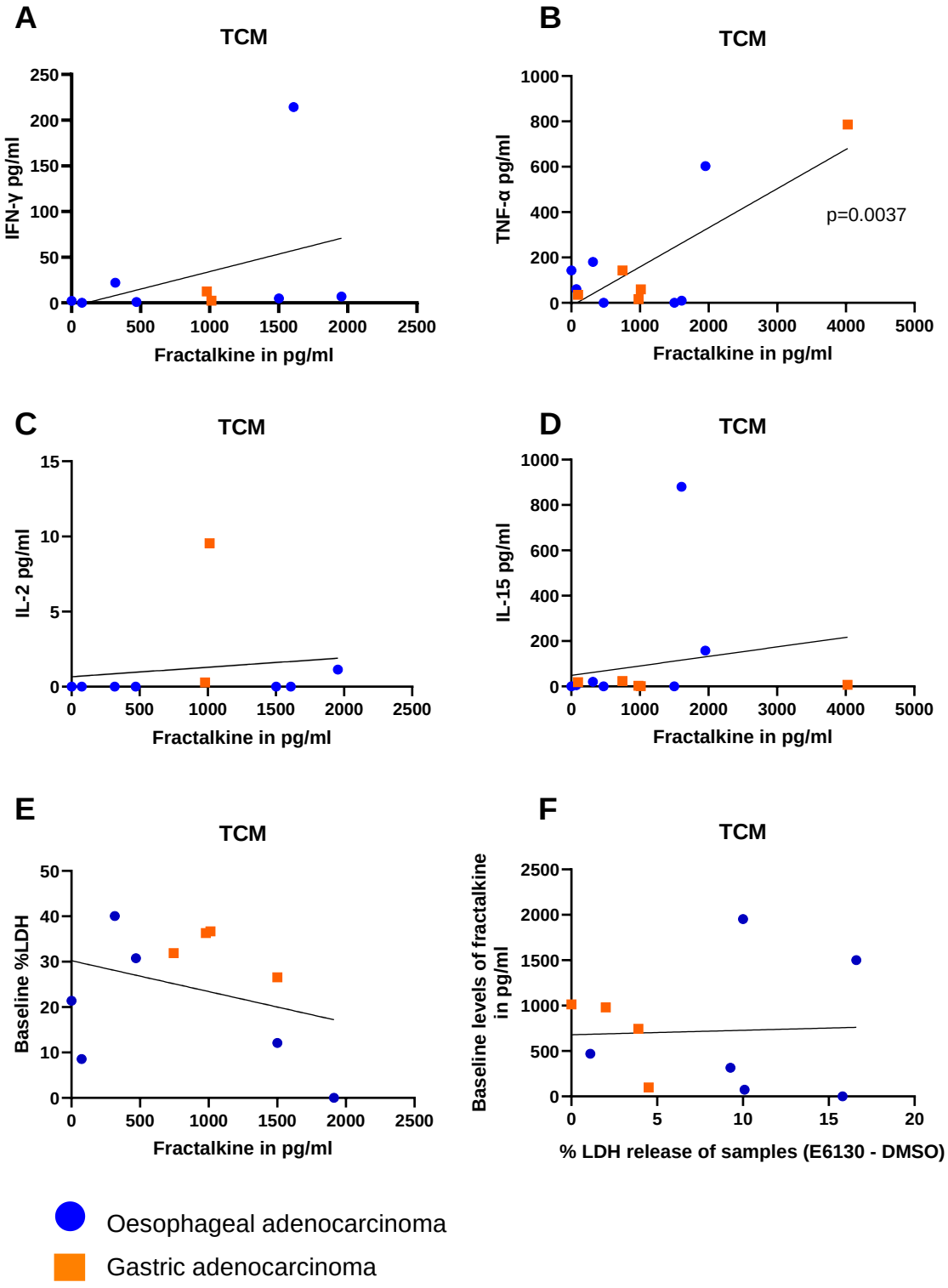

Figure 5.7: Significant positive correlation between TNF-α and fractalkine levels in matched OAC and GAC patient tumour samples

Line graphs showing correlations of levels of soluble fractalkine and **(A)** IFN-γ (n=9), **(B)** TNF-α (n=12), **(C)** IL-2 (n=9), **(D)** IL-15 (n=10), **(E)** baseline %LDH release (n=10) and **(F)** %LDH release of E6130 – DMSO treated sample (n=10) in the TCM of OAC and GAC patients, in pg/ml, by Spearman Correlation.

5.3.3.3 Baseline fractalkine levels correlate with baseline TNF-α levels in OAC and GAC patient tumour samples without obesity, but do not correlate with patients who are overweight or with obesity

As the previous data demonstrated that the TCM of OAC and GAC patients without obesity is significantly higher compared to the patients who are overweight or with obesity, the correlation between baseline levels of fractalkine in TCM compared to baseline levels of TNF-α of matched tumour OAC and GAC patient samples was further stratified by BMI. Fractalkine levels significantly positively correlated with TNF-α levels of OAC and GAC patient samples without obesity; p=0.0218, r=0.7692 **[Figure 5.8 left]**. However, fractalkine levels did not correlate with TNF-α levels of OAC and GAC patient samples who are overweight or with obesity **[Figure 5.8 right].** This data highlighted significant differences in the TME of patients without obesity compared to patients who are overweight or with obesity.

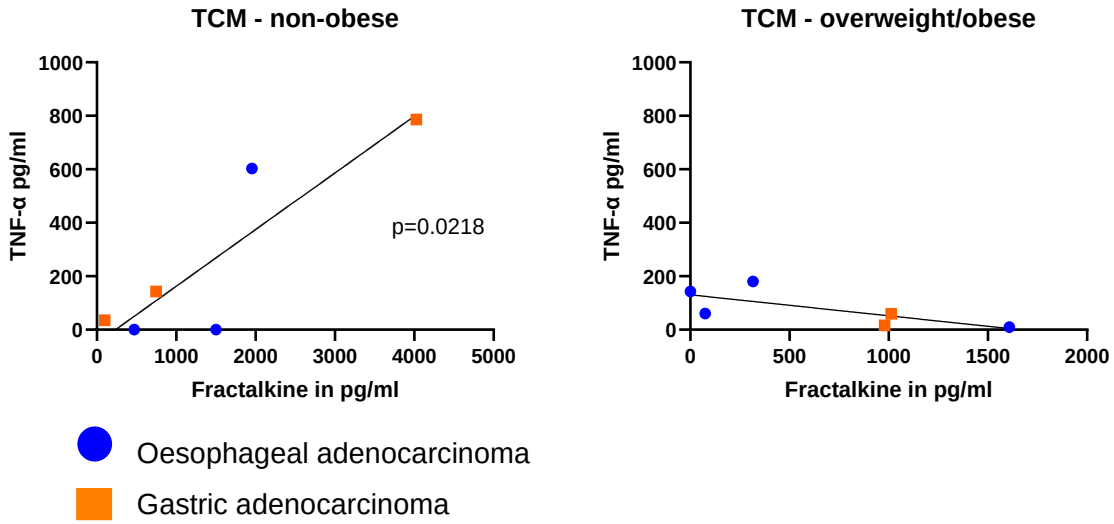

Figure 5.8: Significant positive correlation between TNF-α levels and fractalkine levels in matched OAC and GAC patient tumour samples without obesity, but not with patients with overweight or obesity

Line graphs showing correlations of levels of soluble fractalkine and TNF-α in OAC and GAC patients without obesity (**left**, n=6) and in OAC and GAC patients who are overweight or with obesity (**right**, n=6), in pg/ml, by Spearman Correlation.

Therefore, these results show that there are higher levels of fractalkine in ACM and LCM compared to TCM, NOCM and serum of OAC and GAC patients, however these do not correlate between them. Fractalkine levels do not differ by tumour regression grade, nodal status or neoadjuvant treatment however they do differ in BMI. TNF-α has been shown to induce expression of fractalkine [393, 394], which is confirmed here as there is a positive correlation between levels of fractalkine and TNF-α levels in matched OAC and GAC TCM, and more specifically in patients without obesity.

5.3.4 E6130 did not significantly alter the phenotype of NK cells from healthy donors or OAC and GAC patients

5.3.4.1 E6130 did not alter CX3CR1 expression on NK cells

Our research group has also shown the non-chemotactic effects of fractalkine on peripheral blood derived NK cell phenotype and function [127]. Given this, it was pertinent to also explore E6130's effects on NK cell phenotype and function. Before investigating this in OAC patient derived NK cells, NK cells derived from healthy donor blood were first examined.

Peripheral blood mononuclear cells (PBMCs) from healthy donors were either not treated, treated with fractalkine or its vehicle control water, or pretreated with E6130 or its vehicle control DMSO an hour prior to fractalkine treatment. NK cell population was determined by gating on $CD56^{+}CD3^{-}$ lymphocytes. Frequencies of $CX3CR1^{+}$NK cells treated for 24 hours with 100ng of recombinant fractalkine (FKN) were significantly lower compared to cells treated for 24 hours with its vehicle control, water; water vs FKN (62.6% vs 20%, p=0.009, n=4) **[Figure 5.9A]**, in line with our previous findings [127]. NK cells pre-treated with E6130 did not change CX3CR1 receptor expression, and pre-treatment with E6130 did not reverse fractalkine's endocytosis of CX3CR1 receptor on NK cells; E6130 vs E6130 + FKN (63.2% vs 21.6%, p=0.04, n=4) **[Figure 5.9A]**.

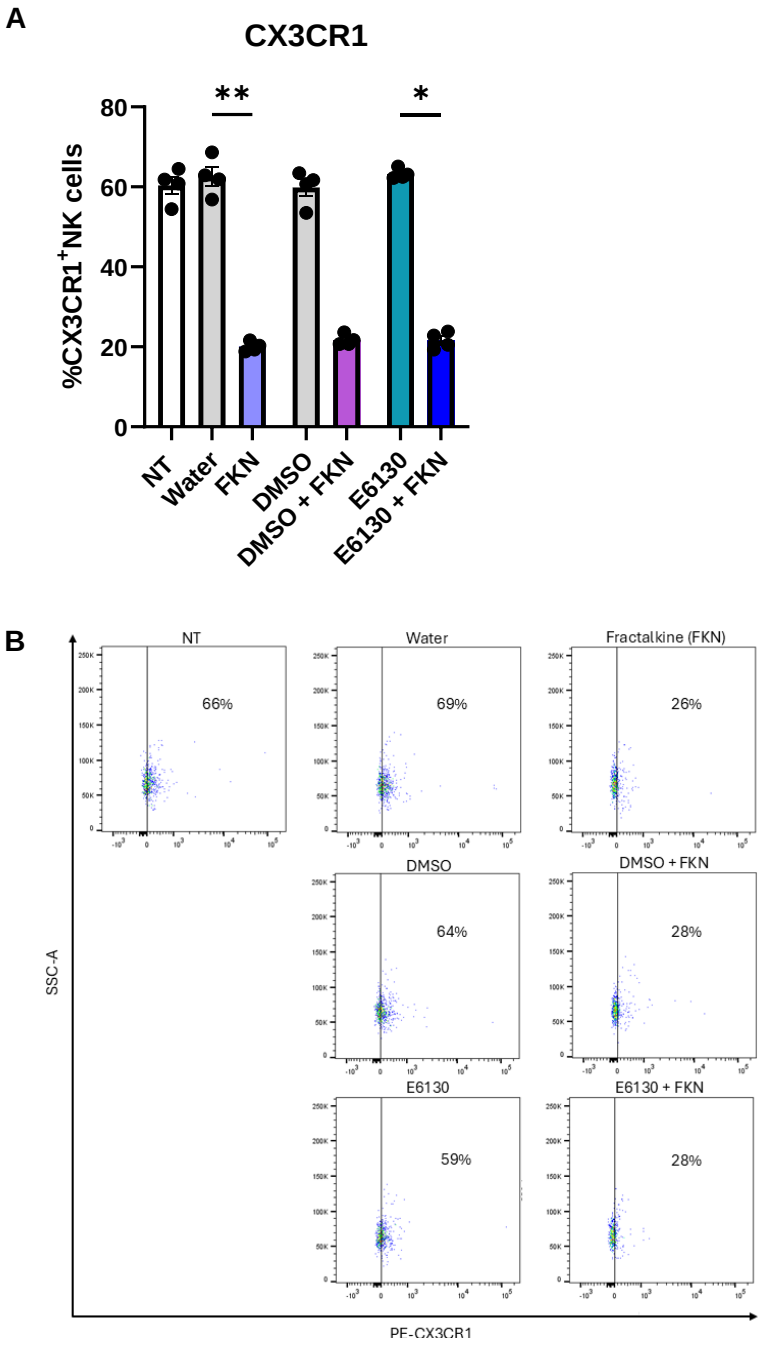

Figure 5.9: E6130 did not alter CX3CR1 surface expression by healthy donor blood-derived NK cells

(A) Bar chart showing the frequencies of CX3CR1^{+}NK cells following no treatment (NT) or following 24-hour treatment with 0.1% water, 100ng/ml of recombinant fractalkine (FKN), 0.01% DMSO +/- 100ng of fractalkine and 4.9nM E6130+/- 100ng of fractalkine. **(B)** Representative dot plots showing gating of CX3CR1^{+}NK cell previously gated on total lymphocytes, viable cells and CD56^{+}CD3^{-} cells following no treatment (NT) or following 24-hour treatment with 0.1% water, 100ng/ml of recombinant fractalkine (FKN), 0.01% DMSO +/- 100ng of fractalkine and 4.9nM E6130+/- 100ng of fractalkine. Experiments were repeated n=4. *p<0.05, **p<0.01, by Friedman test with post-hoc Dunn's test. Mean± SEM.

5.3.4.2 E6130 did not significantly alter activation and cytotoxic marker surface expression by healthy donor blood-derived NK cells

Next, the activation marker NKp30, maturation marker CD27, death receptors TRAIL and FasL, degranulation marker CD107a and cytokines IFN-γ, TNF-α and IL-10 expression were evaluated following 24-hour treatment with E6130 and with or without fractalkine on NK cells from healthy donors. These markers were chosen based on our previous findings that fractalkine increases CD27, IFN-γ, TNF-α and FasL expression by NK cells. Fractalkine and E6130 did not significantly alter NKp30, TRAIL, FasL, CD107a, or IL-10 expression on total NK or CX3CR1^{+}NK cells. Fractalkine notably increased frequencies of CX3CR1^{+}CD27^{+} NK cells; Water vs FKN (9.2% vs 15.3%, n=3) **[Figure 5.10B.ii]** and CX3CR1^{+}IFN-γ^{+}NK cells; Water vs FKN (19.1% vs 27.3%, p=0.0571, n=3) **[Figure 5.311B.ii]** and significantly increased frequencies of CX3CR1^{+}TNF-α^{+}NK cells; Water vs FKN (27.5% vs 36.5%, p=0.034, n=3) **[Figure 5.11C.ii]**. However, E6130 did not significantly alter these fractalkine-induced increased frequencies **[Figure 5.10 and 5.11]**.

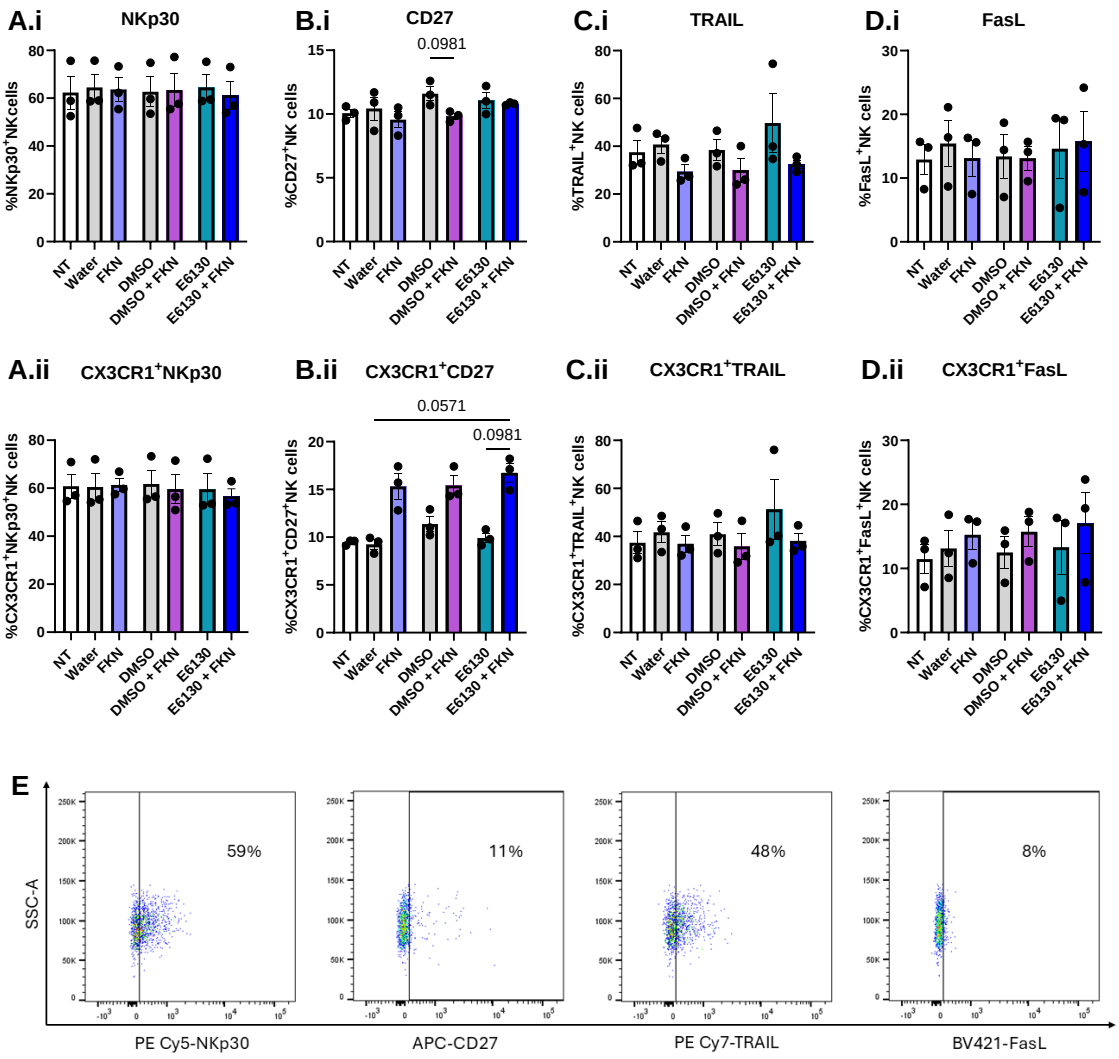

Figure 5.10: E6130 did not significantly alter the surface expression of activation, maturation or cytotoxic markers by healthy donor blood-derived NK cells

Bar charts showing the frequencies of **(A)** NKp30$^+$ **(B)** CD27$^+$ **(C)** TRAIL$^+$ and **(D)** FasL$^+$ **(i)** NK cells and **(ii)** CX3CR1$^+$NK cells following no treatment (NT) or following 24-hour treatment with 0.1% water, 100ng/ml of recombinant fractalkine (FKN), 0.01% DMSO +/- 100ng of fractalkine and 4.9nM E6130+/- 100ng of fractalkine. **(E)** Representative dot plots showing gating of NKp30, CD27, TRAIL and FasL$^+$NK cell previously gated on total lymphocytes, viable cells and CD56$^+$CD3$^-$ cells following no treatment. Experiments were repeated n=3. *p<0.05, by Friedman test with post-hoc Dunn's test. Mean± SEM.

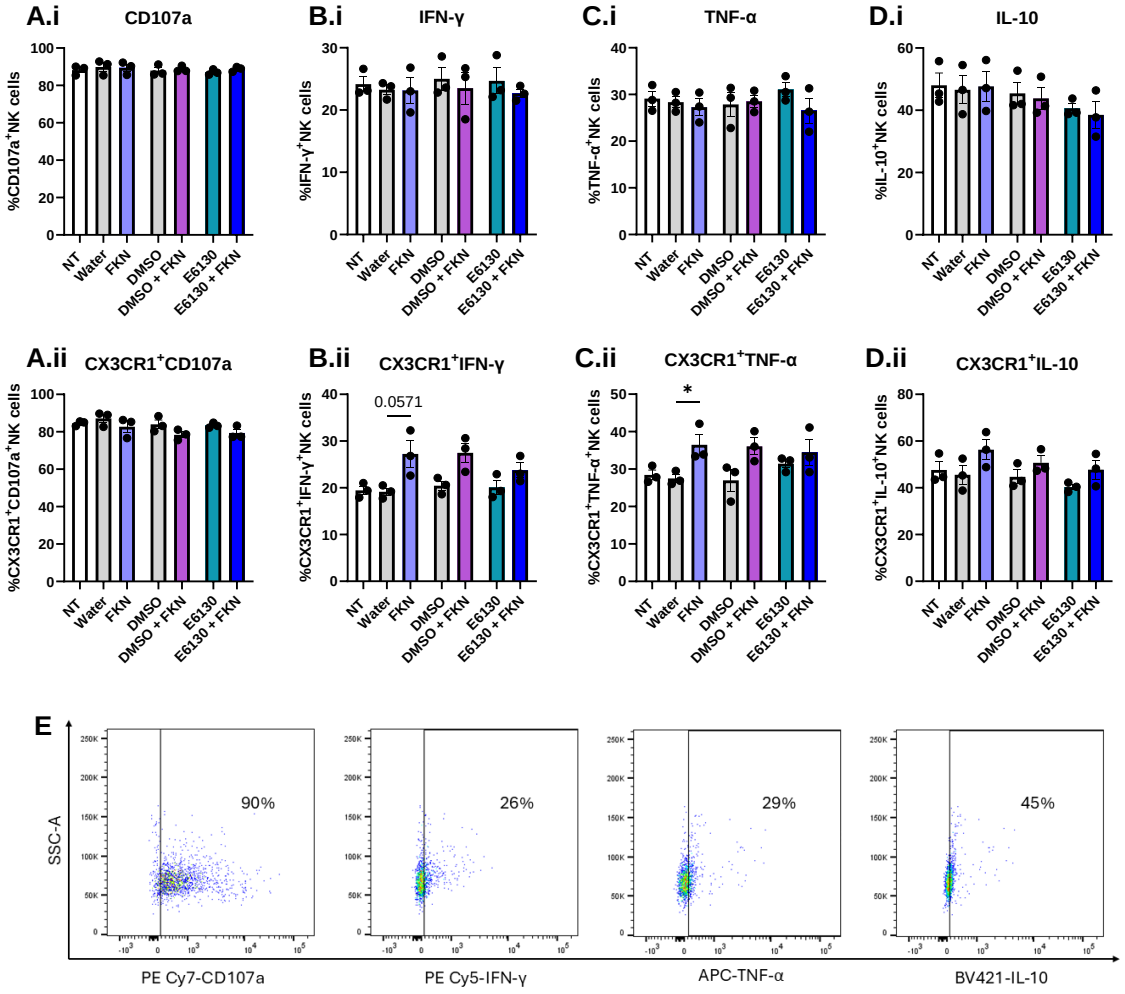

Figure 5.11: E6130 did not significantly alter degranulation or cytokine production by healthy donor blood-derived NK cells

Bar charts showing the frequencies of **(A)** CD107a$^+$ **(B)** IFN-γ$^+$ **(C)** TNF-α$^+$ and **(D)** IL-10$^+$ **(i)** NK cells and **(ii)** CX3CR1$^+$NK cells following no treatment (NT) or following 24-hour treatment with 0.1% water, 100ng/ml of recombinant fractalkine (FKN), 0.01% DMSO +/- 100ng of fractalkine and 4.9nM E6130+/- 100ng of fractalkine. **(E)** Representative dot plots showing gating of CD107a, IFN-γ, TNF-α and IL-10 $^+$NK cell previously gated on total lymphocytes, viable cells and CD56$^+$CD3$^-$ cells following no treatment. Experiments were repeated n=3. *p<0.05, by Friedman test with post-hoc Dunn's test. Mean± SEM.

5.3.4.3 E6130-treated TCM derived from non-obese OAC and GAC patients significantly increases NKp46 and CX3CR1$^-$NKG2D surface expression by healthy donor blood-derived NK cells

The soluble microenvironment of the tumour tissue has diverse effects on lymphocyte phenotype and function [60, 68, 71, 110, 395]. Our group has previously shown that tumour conditioned media (TCM) from OAC patients with obesity significantly decreases activation markers NKp30, NKp46 and NKG2D, degranulation marker CD107a, and TCM from patients who are obese significantly increases TRAIL, IFN-γ, TNF-α, and IL-10 expression [68]. To continue investigating the effects of E6130 on NK cells in the tumour microenvironment, healthy donor-derived PBMCs were cultured in OAC and GAC patient-derived tumour tissue conditioned media (TCM) for 24 hours from patients with or without obesity. The TCM was generated from OAC tumour tissue previously treated with 4.9nM of E6130 or its vehicle control 0.01% DMSO for 24 hours. As a control, PBMCs were cultured in cRPMI with 20% of the well volume with M199 for 24 hours (M199), to ensure effects seen were not due to the decreasing levels of FBS in the media. The activation markers NKG2D, NKp30, NKp46, inhibition markers NKG2A, TIGIT, PD-1, the degranulation marker CD107a, the cytotoxic markers TRAIL and FasL, and the expression of the cytokines IFN-γ, TNF-α, and IL-10 were evaluated. It is important to note that the previous data from our group used Visceral Fat Area (VFA) to distinguish between OAC patients with or without obesity, however for this study VFA could not be obtained and Body Mass Index (BMI) was instead used to separate the samples into patients without obesity and patients with obesity [68].

5.3.4.3.1 E6130-treated TCM derived from OAC and GAC patients without obesity significantly increases NKp46 and CX3CR1$^-$NKG2D surface expression by healthy donor blood-derived NK cells

There was a significant difference in the frequencies of CX3CR1$^-$NK cells cultured in TCM + DMSO from patients with obesity compared to CX3CR1$^+$NK cells; TCM + DMSO (obese): CX3CR1$^-$NK cells vs CX3CR1$^+$NK cells (34.8% vs 65.2%, p= , n=3) and similarly the frequencies of CX3CR1$^-$NK cells cultured in TCM + E6130 from patients with obesity were lower than CX3CR1$^+$NK cells; TCM + E6130 (obese): CX3CR1$^-$NK cells vs CX3CR1$^+$NK cells (34.7% vs 62.3%, p=0.0585, n=3) **[Figure 5.12A.ii]**. The frequencies of NKG2D$^+$NK

cells were higher when cultured with TCM from patients with obesity compared to TCM from patients without obesity, however there were no differences between DMSO and E6130 treated TCM; NKG2D: TCM+E6130 (non-obese) vs TCM+E6130 (obese) (17.1% vs 32.2%, p=0.0774, n=3) and similarly in frequencies of $CX3CR1^{-}NKG2D^{+}$NK cells cultured in TCM + DMSO from patients with obesity compared to $CX3CR1^{+}$NK cells $CX3CR1^{-}NKG2D^{+}$NK cells; TCM+E6130 (non-obese) vs TCM+E6130 (obese); (15.4% vs 36.3%, p=0.043, n=3) **[Figure 5.12B.i and ii]**. There was a significant difference in the frequencies of $NKp46^{+}$NK cells cultured in TCM + DMSO compared to cells treated with TCM + E6130 from patients without obesity; NKp46: TCM+DMSO (non-obese) vs TCM+E6130 (non-obese) (60.1% vs 87.2%, p=0.035, n=3) and similarly in frequencies of $CX3CR1^{+}NKp46^{+}$NK cells; TCM+DMSO vs TCM+E6130; (53% vs 88.5%, p=0.006, n=3) **[Figure 5.12D.i and ii]**.

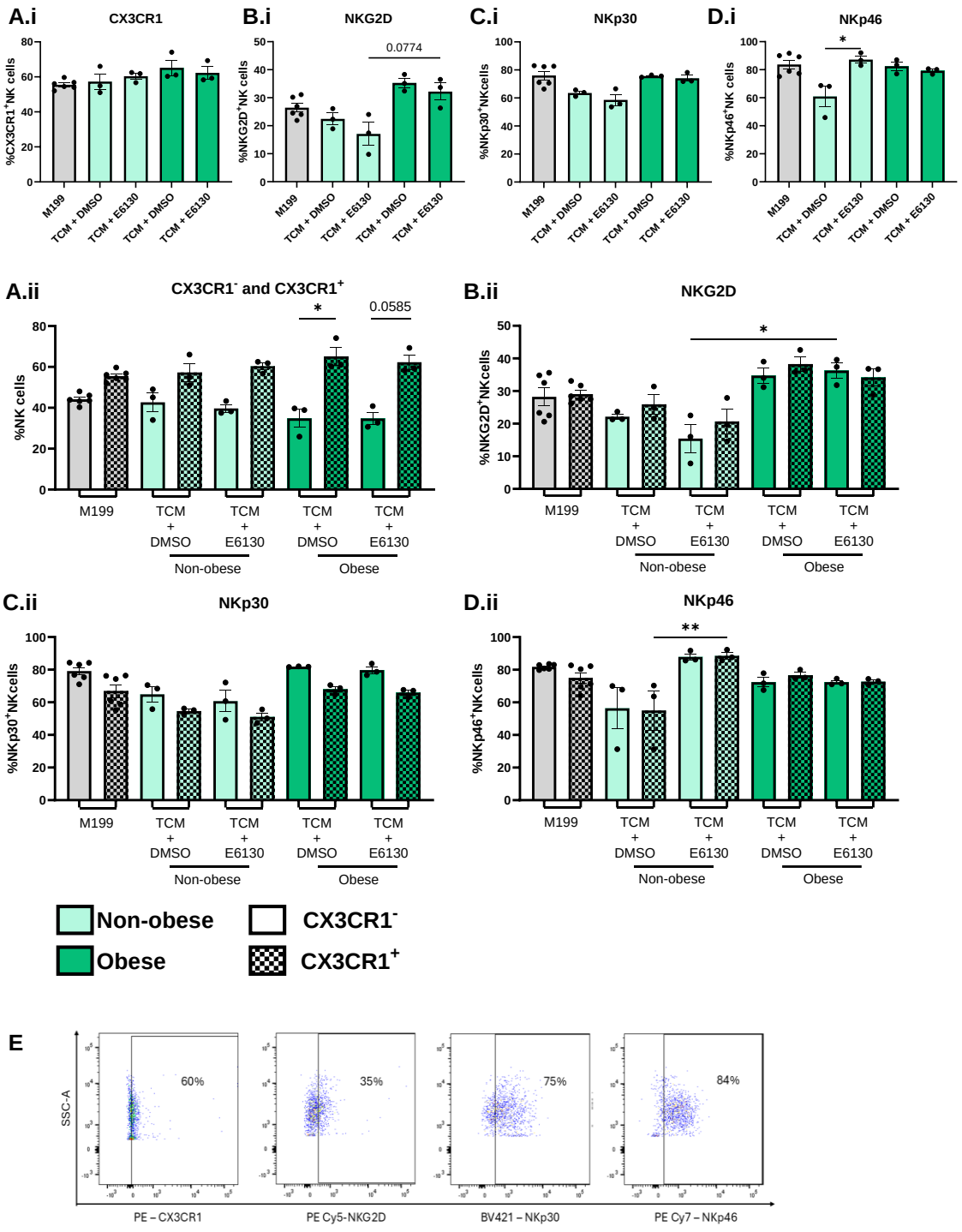

Figure 5.12: TCM treated with E6130 significantly increased frequencies of NKp46$^+$NK cells and CX3CR1$^+$ NKp46$^+$NK cells compared to TCM treated with DMSO.

Bar charts showing the frequencies of **(A)** CX3CR1$^+$, **(B)** NKG2D$^+$, **(C)** NKp30$^+$ and **(D)** NKp46$^+$ **(i)** NK cells or **(ii)** CX3CR1$^-$ (no pattern) or CX3CR1$^+$ (checkered pattern) NK cells cultured in 20% M199 media (grey, n=6) or 20% OAC and GAC patient-derived TCM + DMSO (0.01%) or 20% OAC patient-derived TCM + E6130 (4.9nM) from non-obese (light green) or obese (dark green) OAC and GAC patients. **(E)** Representative dot plots showing gating of NKG2D, NKp30 and NKp46$^+$NK cell previously gated on total

lymphocytes, viable cells and $CD56^{+}CD3^{-}$ cells following no treatment. Experiments were repeated n=3-6. *p<0.05, **p<0.01 by Kruskal Wallis with post-hoc Dunn's test. Mean± SEM.

5.3.4.3.2 No significant differences in inhibition markers expression on healthy NK cells when cultured in TCM treated with E6130 from OAC and GAC patients with or without obesity

The frequencies of $CX3CR1^{-}NKG2A^{+}$NK cells cultured in 20%M199 were higher compared to $CX3CR1^{+}NKG2A^{+}$NK cells; M199: $CX3CR1^{-}NKG2A^{+}$NK cells vs $CX3CR1^{+}NKG2A^{+}$NK cells (75.8% vs 60.7%, p=0.0700, n=6) **[Figure 5.13A.ii]**. The frequencies of $CX3CR1^{+}TIGIT^{+}$NK cells cultured in TCM + E6130 from patients without obesity were lower compared to $CX3CR1^{+}TIGIT^{+}$NK cells; $CX3CR1^{+}TIGIT^{+}$NK cells + TCM + E6130: non obese vs obese (10.9% vs 36.7%, p=0.0843, n=3) **[Figure 5.13B.ii]**. Overall, there were no significant differences in the frequencies of NKG2A, TIGIT and PD-1 expression on NK cells.

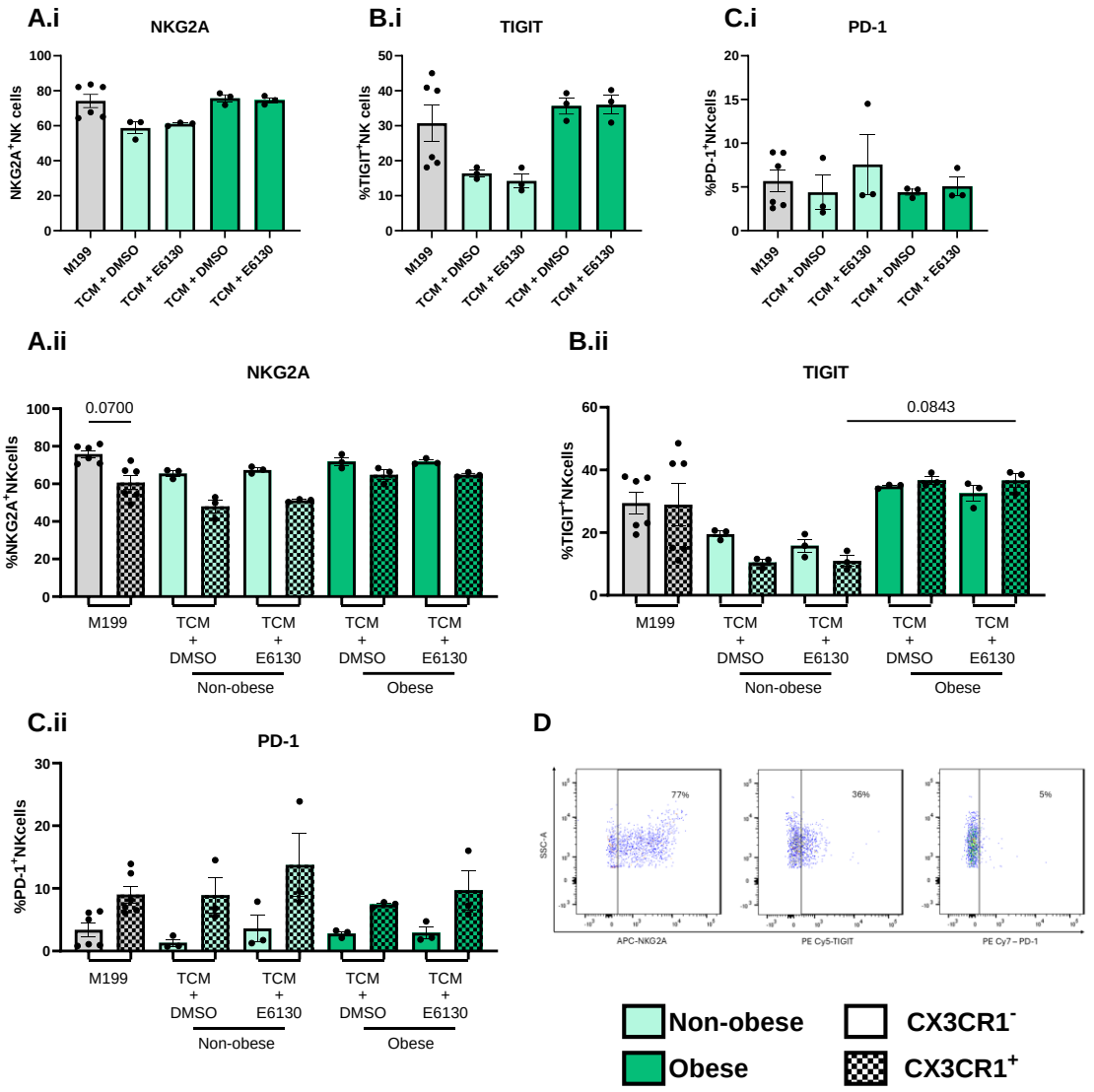

Figure 5.13 : OAC and GAC patient-derived TCM cultured in E6130 did not significantly alter inhibitory receptor surface expression on healthy donor blood-derived NK cells

Bar charts showing the frequencies of **(A)** NKG2A$^+$, **(B)** TIGIT$^+$ and **(C)** PD-1$^+$ **(i)** NK cells or **(ii)** CX3CR1$^-$ (no pattern) or CX3CR1$^+$ (checkered pattern) NK cells cultured in 20% M199 media (grey, n=6) or 20% OAC patient-derived TCM + DMSO (0.01%) or 20% OAC patient-derived TCM + E6130 (4.9nM) from non-obese (light green) or obese (dark green) OAC patients. **(D)** Representative dot plots showing gating of NKG2A$^+$, TIGIT$^+$ and PD-1$^+$NK cell previously gated on total lymphocytes, viable cells and CD56$^+$CD3$^-$ cells following no treatment. Experiments were repeated n=3-6. *p<0.05, by Kruskal Wallis with post-hoc Dunn's test. Mean± SEM.

5.3.4.3.3 DMSO-treated TCM derived from OAC and GAC patients with obesity significantly decreases CX3CR1^{+}TRAIL^{+}NK cells but E6130-treated TCM does not

Frequencies of CX3CR1^{+}TRAIL^{+}NK cells were significantly lower when cells were cultured in TCM derived from patients with obesity compared to M199; CX3CR1^{+}TRAIL: M199 vs TCM + DMSO (obese); 38.7% vs 15.7%, p=0.025, n=3-6) and TCM treated with E6130 increased frequencies of CX3CR1^{+}TRAIL^{+}NK; CX3CR1^{+}TRAIL: TCM + E6130 (obese); (24.7%) **[Figure 5.14A.ii]**. Frequencies of CX3CR1^{-}FasL^{+}NK cells were significantly lower when cells were cultured in TCM + E6130 from patients without obesity compared to NK cells cultured in TCM + E6130 from patients with obesity; CX3CR1^{-}FasL^{+}NK cells + TCM + E6130: non-obese vs obese (2.4% vs 44.4%, p=0.021, n=3) **[Figure 5.14B.ii]**. Frequencies of CX3CR1^{-}CD107a^{+}NK cells were significantly higher when cells were cultured in TCM + DMSO from patients without obesity compared to NK cells cultured in TCM + E6130; CX3CR1^{-}CD107a^{+}NK cells + TCM (non-obese): DMSO vs E6130 (79.5% vs 3.1%, p=0.004, n=3) **[Figure 5.14C.ii]** and frequencies of CX3CR1^{-}CD107a^{+}NK cells were significantly higher when cells were cultured in TCM + DMSO from patients without obesity compared to NK cells cultured in TCM + DMSO from patients with obesity; CX3CR1^{-}CD107a^{+}NK cells + TCM + DMSO: non-obese vs obese (79.5% vs 43.3%, p=0.027, n=3) **[Figure 5.14C.ii].**

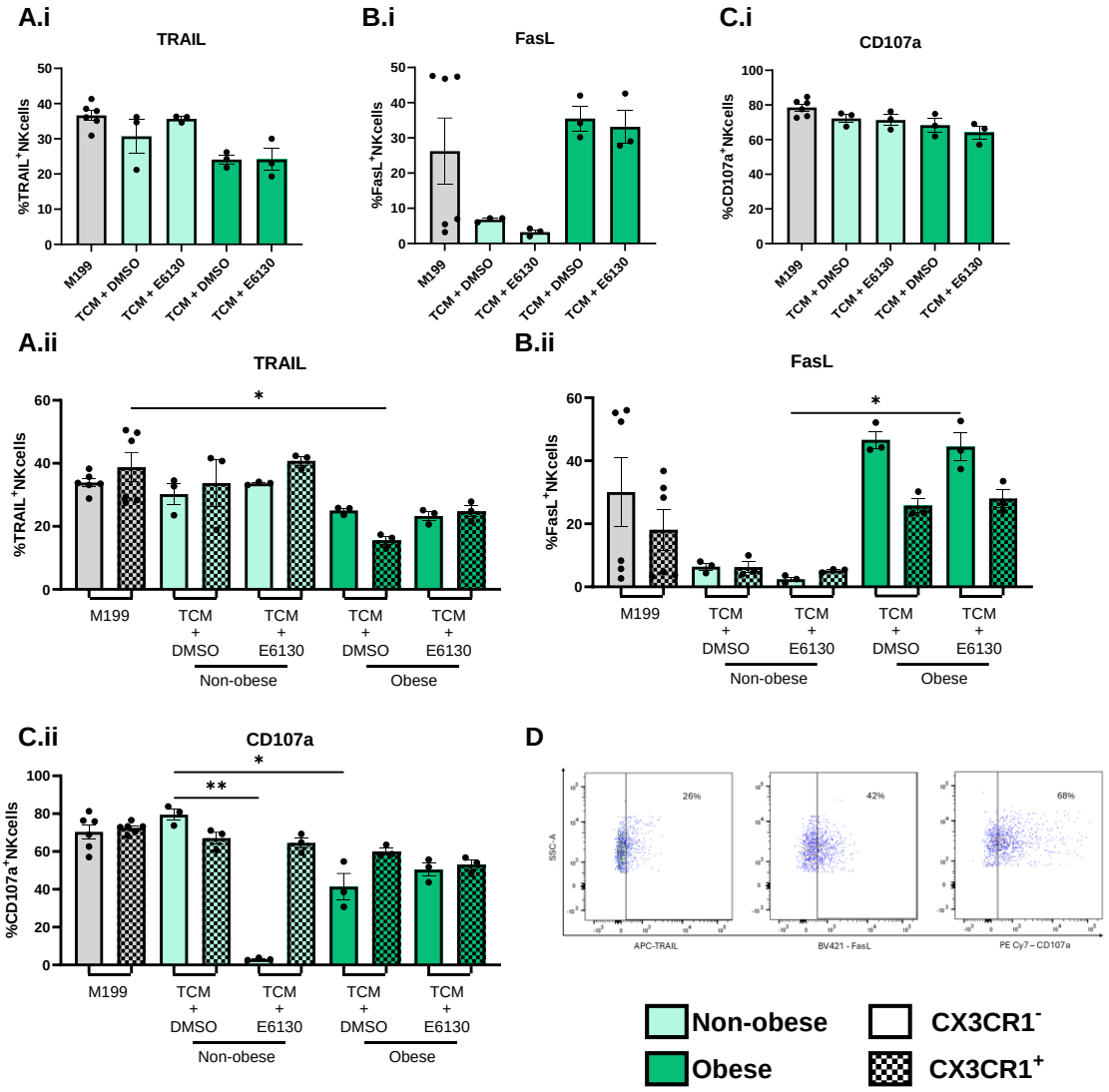

Figure 5.14: Significantly lower frequencies of CX3CR1$^+$TRAIL$^+$NK cells following culture in TCM derived from OAC and GAC patients with obesity

Bar charts showing the frequencies of **(A)** TRAIL$^+$, **(B)** FasL$^+$ and **(C)** CD107a$^+$ **(i)** NK cells or **(ii)** CX3CR1$^-$ (no pattern) or CX3CR1$^+$ (checkered pattern) NK cells cultured in 20% M199 media (grey, n=6) or 20% OAC and GAC patient-derived TCM + DMSO (0.01%) or 20% OAC patient-derived TCM + E6130 (4.9nM) from non-obese (light green) or obese (dark green) OAC and GAC patients. **(D)** Representative dot plots showing gating of TRAIL$^+$, FasL$^+$ and CD107a$^+$ NK cell previously gated on total lymphocytes, viable cells and CD56$^+$CD3$^-$ cells following no treatment. Experiments were repeated n=3-6. *p<0.05, **p<0.01 by Kruskal Wallis with post-hoc Dunn's test. Mean± SEM.

5.3.4.3.4 DMSO-treated TCM derived from OAC and GAC patients with obesity significantly decreases CX3CR1^{+}TRAIL^{+}NK cells but E6130-treated TCM does not

TCM from patients without obesity significantly increased frequencies of TNF-α producing NK cells compared to M199; TNF-α: M199 vs TCM + DMSO (non-obese) (15.6% vs 22.2%, p=0.037, n=3-6) and frequencies of TNF-α producing NK cells cultured in TCM from patients without obesity were noticeably lower compared to non-obese TCM; TNF-α: TCM + DMSO (non-obese) vs TCM + DMSO (obese) (22.2% vs 15.9%, p=0.0697, n=3) **[Figure 5.15B.i]**. Frequencies of CX3CR1^{-}IL-10^{+}NK cells cultured in TCM + E6130 from patients without obesity were lower than when cultured in TCM + E6130 from patients with obesity; CX3CR1^{-}IL-10^{+}NK cells + TCM + E6130: non-obese vs obese (46.5% vs 85.1%, p=0.0794, n=3) **[Figure 5.15C.ii].**

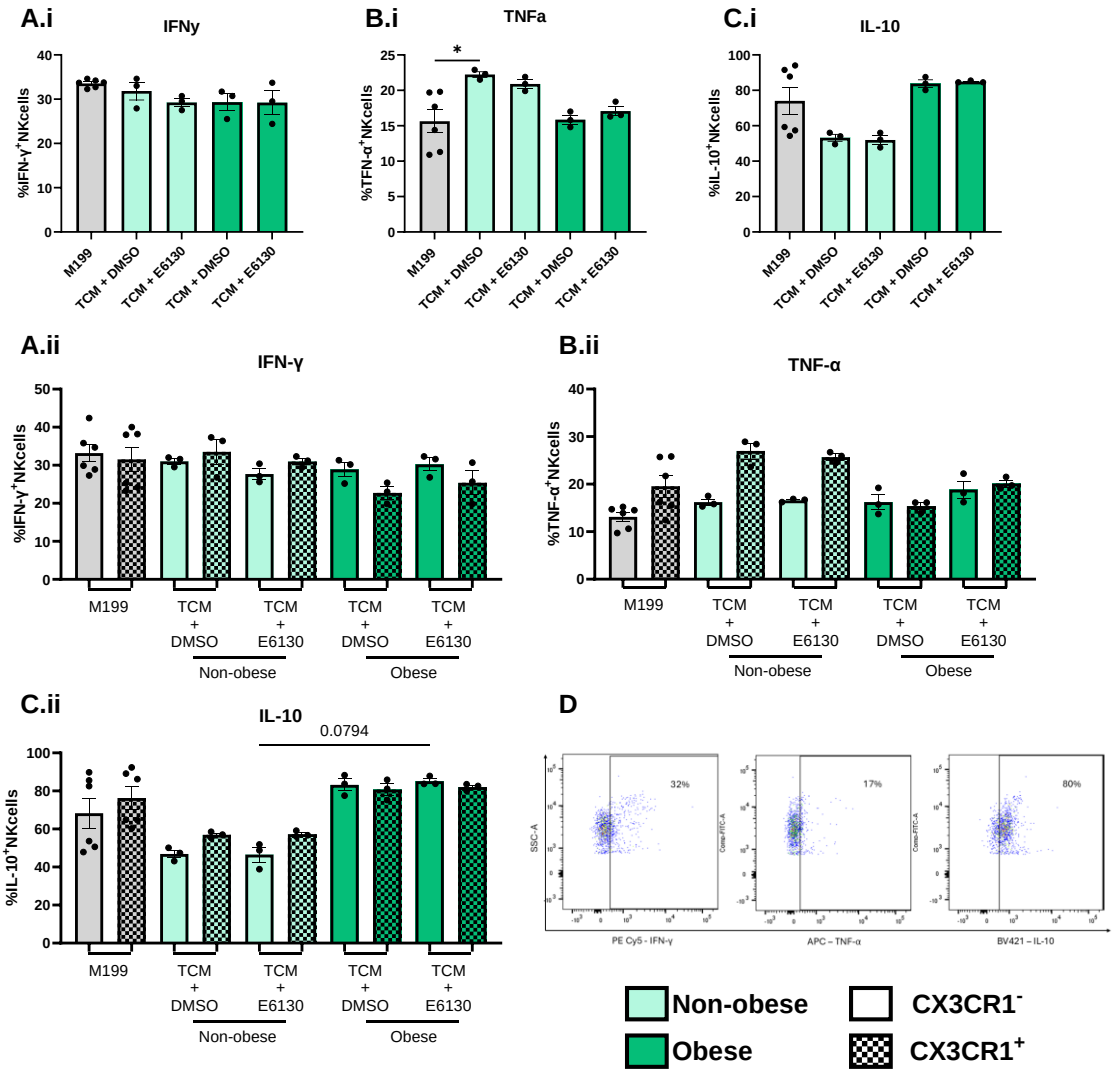

Figure 5.15: TCM from OAC and GAC patients without obesity significantly increases the frequencies of TNF-α$^+$ producing NK cells

Bar charts showing the frequencies of **(A)** IFN-γ$^+$, **(B)** TNF-α$^+$ and **(C)** IL-10$^+$ **(i)** NK cells or **(ii)** CX3CR1$^-$ (no pattern) or CX3CR1$^+$ (checkered pattern) NK cells cultured in 20% M199 media (grey, n=6) or 20% OAC and GAC patient-derived TCM + DMSO (0.01%) or 20% OAC and GAC patient-derived TCM + E6130 (4.9nM) from non-obese (light green) or obese (dark green) OAC and GAC patients. **(D)** Representative dot plots showing gating of IFN-γ$^+$, TNF-α$^+$ and IL-10$^+$ NK cell previously gated on total lymphocytes, viable cells and CD56$^+$CD3$^-$ cells following no treatment. Experiments were repeated n=3-6. *p<0.05, by Kruskal Wallis with post-hoc Dunn's test. Mean± SEM

5.3.3.4 E6130 did not significantly alter the phenotype of NK cells from OAC and GAC patients

The effects of E6130 were next evaluated using NK cells derived from the blood of a small cohort of OAC and GAC patients. PBMCs from OAC and GAC patient donors were either not treated, treated with E6130 or its vehicle control DMSO for 24 hours. The activation markers NKG2D, NKp30, NKp46, inhibition markers NKG2A, TIGIT, PD-1, the cytotoxic markers TRAIL and FasL were evaluated. Similarly to NK cells from healthy donors, E6130 had no significant effects on either NK cells or $CX3CR1^{+}$NK cells from OAC and GAC patients. **[Figure 5.16 and 5.17]**. Frequencies of $PD\text{-}1^{+}$NK cells and $CX3CR1^{+}PD\text{-}1^{+}$NK cells treated with E6130 were slightly lower compared to NK cells treated with DMSO; PD-1: DMSO vs E6130 (11% vs 8.6%, n=4), $CX3CR1^{+}$PD-1 (8.4% vs 7.4%, n=4) **[Figure 5.16 and 5.17].**

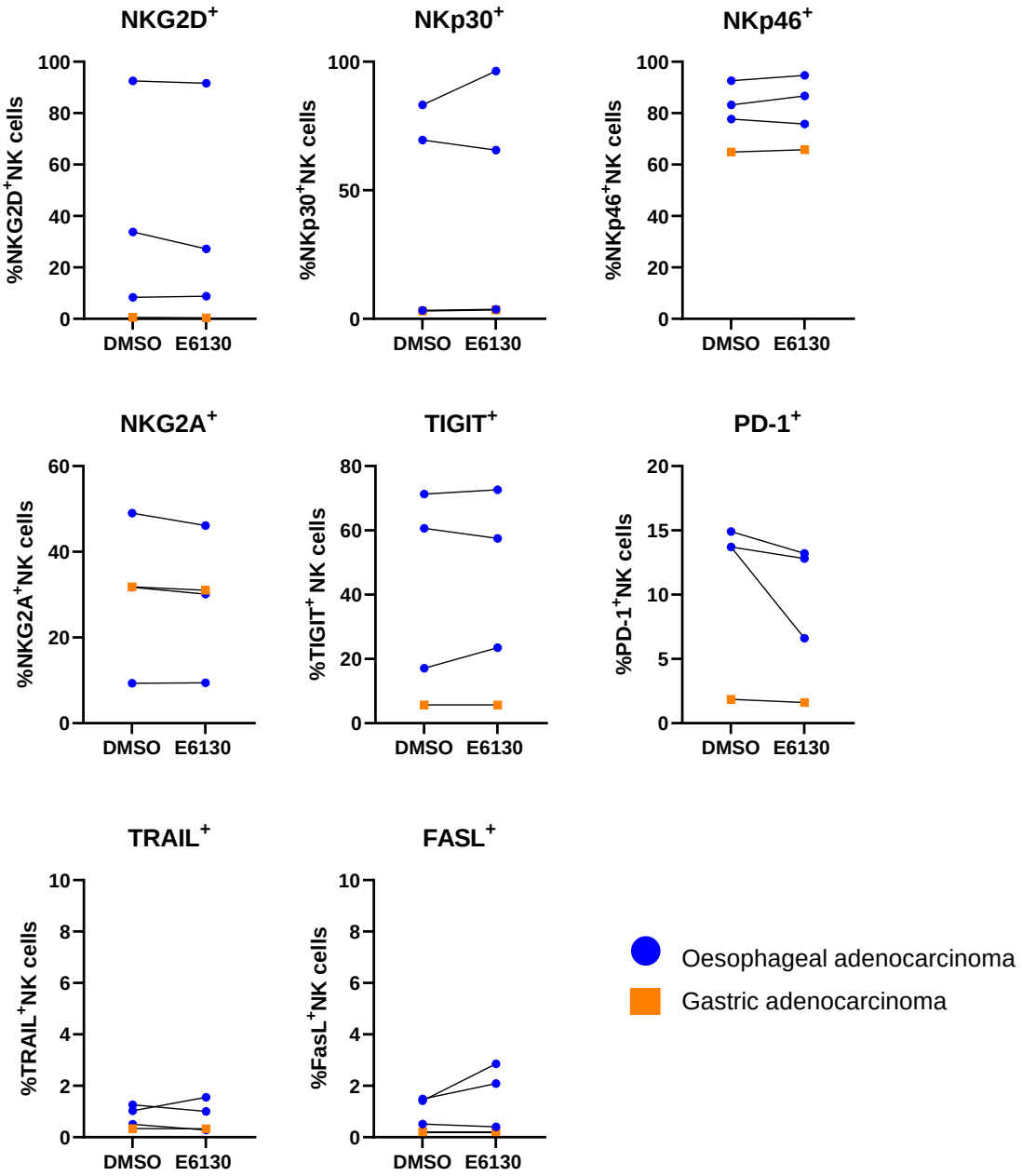

Figure 5.16: E6130 did not significantly alter the phenotype of OAC and GAC patient blood-derived NK cells

Dot plots showing the frequencies of NKG2D$^+$, NKp30$^+$, NKp46$^+$, NKG2A$^+$, TIGIT$^+$, PD-1$^+$, TRAIL$^+$ and FasL$^+$ NK cells from OAC and GAC patients following 24-hour treatment with 0.01% DMSO and 4.9nM E6130. Experiments were repeated n=4. Mean± SEM.

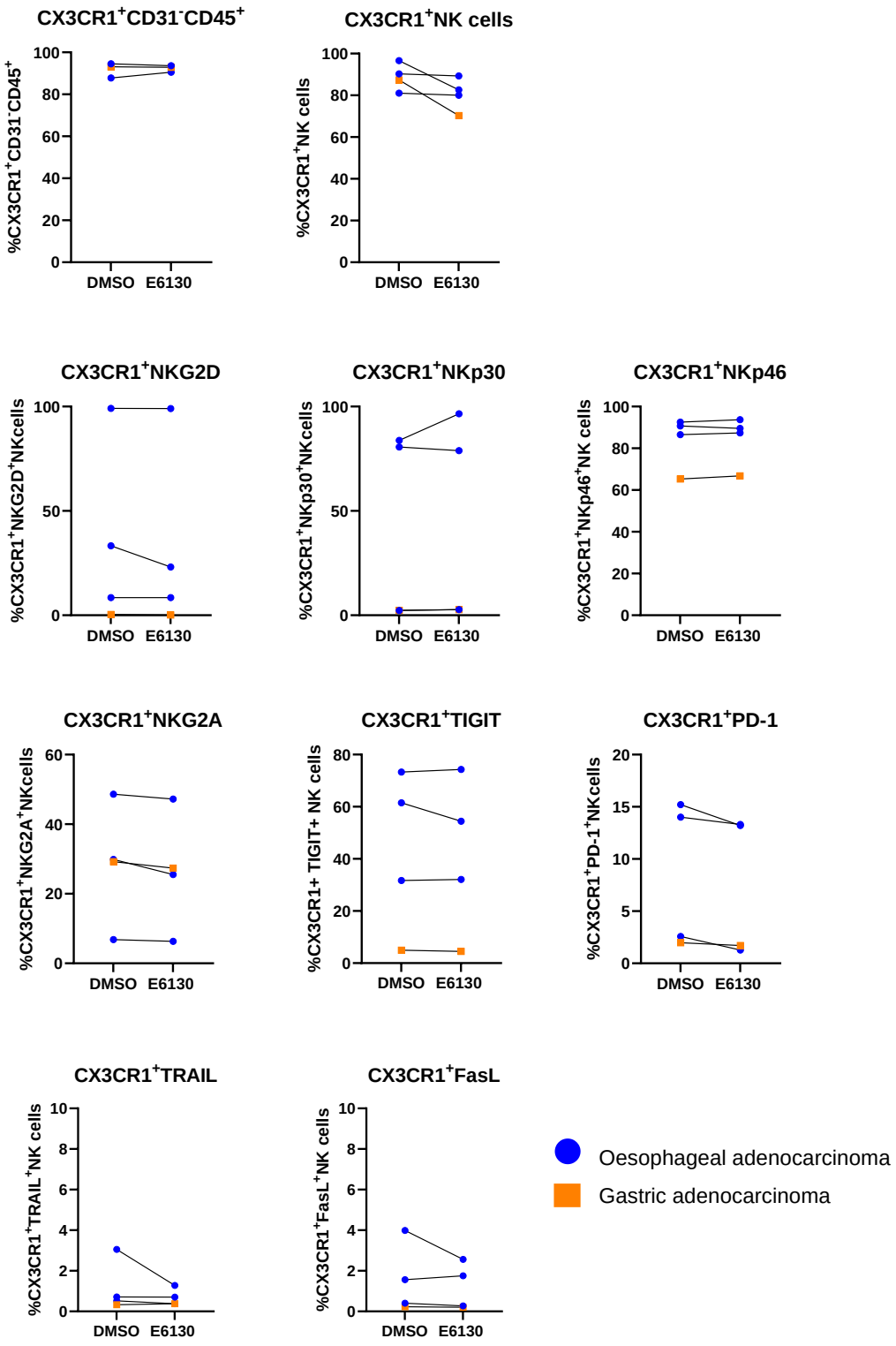

Figure 5.17: E6130 did not significantly alter the phenotype of intratumoural CX3CR1$^+$NK cell from OAC and GAC patients

Dot plots showing the frequencies of NKG2D$^+$, NKp30$^+$, NKp46$^+$, NKG2A$^+$, TIGIT$^+$, PD-1$^+$, TRAIL$^+$ and FasL$^+$ of CX3CR1$^+$NK cells from OAC and GAC patients following 24-hour treatment with 0.01% DMSO and 4.9nM E6130. Experiments were repeated n=4. Mean± SEM.

5.3.3.4 E6130 significantly decreased frequencies of CX3CR1^{+} intratumoural leukocytes and NK cells from OAC and GAC patients

NK cells were isolated from OAC and GAC patients to examine whether 24-hour E6130 treatment on tumour samples altered NK cell functions intratumourally. Leukocyte population was gated by CD31^{-}CD45^{+} cells from total cells. E6130 did not alter NKp30, TRAIL, FasL or PD-1 expression on NK cells from tumour patient samples **[Figure 5.18A and B]**. However, frequencies of CX3CR1 expressing leukocytes and NK cells were slightly but significantly decreased with E6130 treatment compared to DMSO treatment; CX3CR1^{+}leukocytes % expression: DMSO vs E6130 (38% vs 32.2%, p=0.009, n=11); CX3CR1^{+}leukocytes MFI: DMSO vs E6130 (678 vs 435, p=0.001, n=11); CX3CR1^{+}NK cells MFI: DMSO vs E6130 (1971 vs 1129, p=0.0.24, n=11) **[Figure 5.18C]**. Therefore, E6130 seems to only influence CX3CR1 expression on immune cells, but not their functional marker expression.

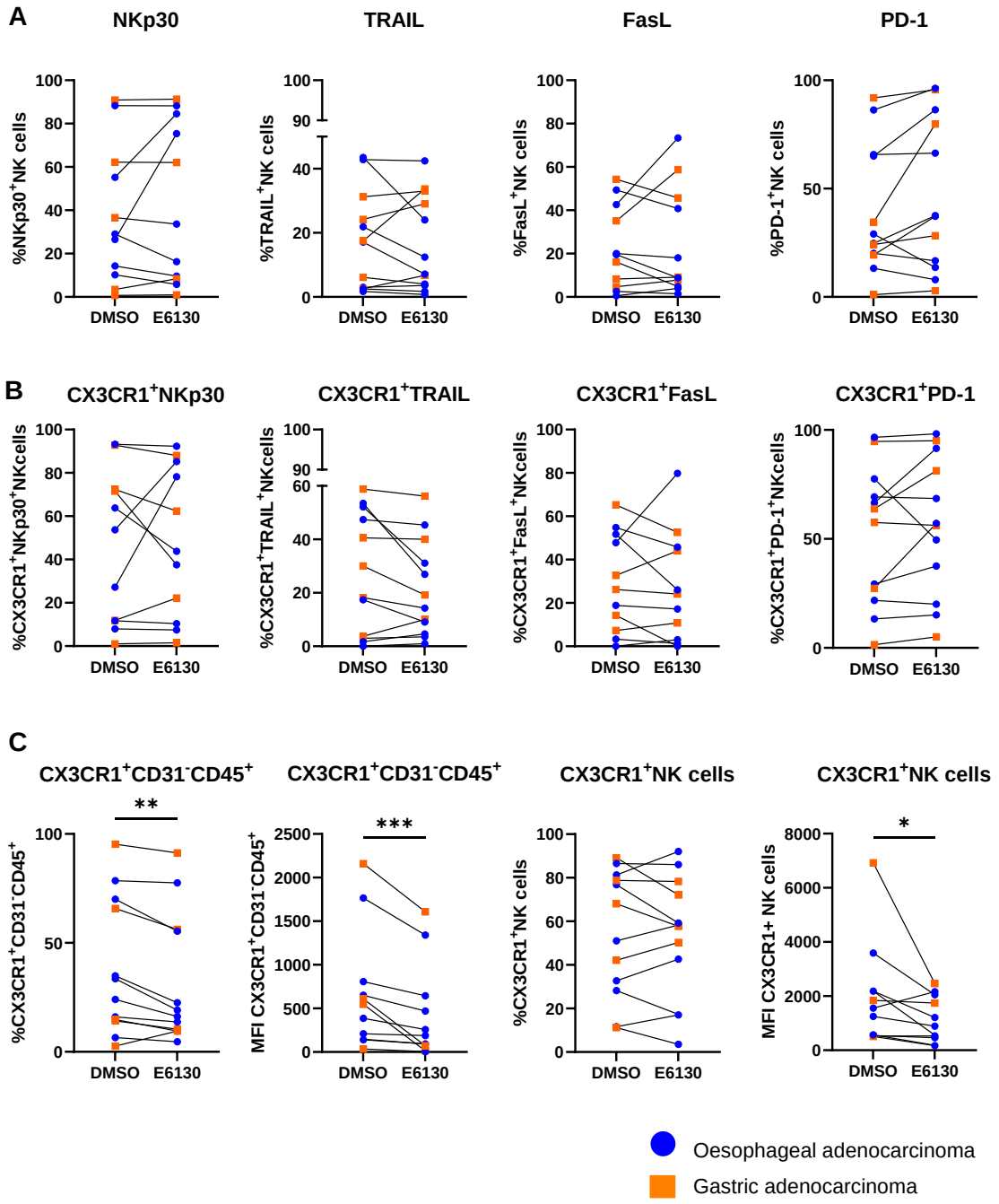

Figure 5.18: 24-hour treatment with E6130 significantly decreases % frequencies of intratumoural CX3CR1$^+$CD31$^-$CD45$^+$ leukocytes and reduces MFI of CX3CR1 expression by intratumoural NK cells from OAC patients

Dot plots showing the frequencies of NKp30$^+$, TRAIL$^+$, PD-1$^+$ and FasL$^+$ of **(A)** NK cells and **(B)** CX3CR1$^+$NK cells and **(C)** frequencies of CX3CR1$^+$CD31$^-$CD45$^+$ and NK cells from OAC and GAC patients following 24-hour treatment with 0.01% DMSO and 4.9nM E6130. Experiments were repeated n=11. **p<0.01, ***p<0.001, by Wilcoxon t-test. Mean± SEM.

5.4 Discussion

Chemokines play a crucial role in guiding immune cells to the tumour site and offer desirable immunotherapeutic targets to remodel the immune profile of tumours and promote tumour eradication [36, 133, 134, 224-226]. However, despite a plethora of clinical trials, chemokine-targeted therapies have not had the success of other cancer immunotherapies. We have previously reported that the soluble chemotactic cues of extratumoural tissues such as the omentum and the liver in OAC patients can recruit anti-tumour NK and T cells [68, 69, 110, 127-129, 395]. Furthermore, NK cell viability, phenotype and function is profoundly altered following exposure to the soluble cues of these tissues. Importantly, our group has demonstrated that the erroneous NK cell migration to the soluble cues of the omentum can be redirected to the soluble cues of OAC tumour using CX3CR1 modulator E6130 [68]. E6130 is a highly selective and orally available modulator of the fractalkine receptor CX3CR1 which has shown efficacy in a mouse model of intestinal bowel disease (IBD) [185]. Therefore, as we propose that therapeutically targeting the fractalkine:CX3CR1 pathway with E6130 would be a viable treatment approach for OAC patients by enhancing intratumoural infiltration of NK cells, its non-chemotactic effects must also be interrogated. This chapter aimed to investigate if E6130 alters NK cells beyond its effects on their chemotaxis and to further evaluate its potential as an anti-cancer agent in the setting of OAC.

Patient-derived tumour tissue explants crucially help to capture the multicellular and heterogeneous nature of the solid TME and allow researchers to study the true complexity of tumour biology. *Ex vivo* studies using such samples are invaluable for bridging the gap between *in vitro* studies and *in vivo* studies in the development of more personalized and effective cancer therapies [349]. Here, tumour explants were used to further test the anti-cancer efficacy of E6130. The effects of E6130 on tumour cell viability and cytotoxicity were first investigated in this chapter. LDH release by OAC patient tumour tissue explants were measured following treatment with E6130. Measuring LDH release to assay cancer cell cytotoxicity following drug treatment is a widely used and reliable technique [396]. These results demonstrated strong tumouricidal activity induced by E6130 in *ex vivo* tumour compared to non-treated and vehicle treated tissue. Moreover, flow cytometry results showed reduced viability of live cells and $CX3CR1^{+}$ live

cells following 24-hour treatment with E6130. Furthermore, normal adjacent oesophageal and gastric tissue were not affected by E6130 treatment. This further confirms our hypothesis that E6130 could become a strong candidate for a future therapy as it demonstrates direct and specific anti-tumour properties against OAC cells and did not appear to elicit toxic effects on adjacent non-malignant tissue. Several chemokine therapies have been trialled in cancer with mixed outcomes due to factors such as low receptor coverage, poor receptor selectivity and the redundancy of the chemokine system [162]. Plerixafor, a CXCR4 antagonist, has been approved to mobilise haematopoietic stem cells for autologous transplantation in multiple myeloma (NCT04552743) and since then, this antagonist and another CXCR4 antagonist, BL-8040, are being repurposed in clinical trials in ovarian, gastric and pancreatic cancer (NCT02179970, NCT03281369)[226]. However, targeting specific chemokines is not straightforward as they might have both a pro- and anti-tumourigenic role, for example inhibition of CCL2 was shown as a promising approach in mouse models of breast cancer as it reduced metastasis by restraining monocytes to the bone marrow, however, interrupting the inhibition of the chemokine reversed this effect as it released those monocytes in abundance and led to increased metastasis [232]. Targeting fractalkine with E6130 has however a key advantage compared to other chemokine receptors because it only has one receptor and E6130 is more selective than previously tested antagonists, such as AZD8797 which had cross-selectivity for other chemokine receptors. Importantly, even though Eotaxin-3 (CCL26) was shown to bind CX3CR1, our group has found that Eotaxin-3 is present at very low levels in the omentum, which suggests that fractalkine is the main CX3CR1 ligand driver of NK cell migration [129].

To further delineate the direct anti-cancer effects of E6130 on OAC patient tumour beyond viability/cytotoxicity, death receptor ligand expression was assessed following E6130 treatment *ex vivo*. Expression of the death receptor Fas ligand (FasL) was significantly higher in CX3CR1^{+}tumour cells following E6130 treatment. Consequences of overexpression of FasL on tumour cells has contradictory reports in the literature, as studies have found including in OAC, that many tumours exploit FasL expression as an immune evasion strategy by inducing apoptosis in infiltrating Fas-sensitive immune cells, particularly cytotoxic T lymphocytes (CTLs) and NK cells, thereby suppressing anti-

tumour immunity [397, 398]. Some studies have even focused on anti-FasL therapies to overcome the pro-tumourigenic effects [397]. However, others have shown that this is context dependent: increased FasL expression can promote Fas-mediated apoptosis in Fas-sensitive tumour cells, enhancing tumour clearance [399]. Since increased FasL surface expression in OAC patient tumour is paralleled by increased cell death following E6130 treatment, it is likely that this is a means through which E6130 enhances apoptosis.

Our group and others have previously reported on the important role of fractalkine in adipose tissue inflammation, and we have confirmed higher levels of fractalkine in the omentum of OAC patients compared to tumour and serum [127, 129]. Here, in a separate cohort, these results were confirmed as the levels of fractalkine in the adipose (n=7) and liver (n=9) tissues of OAC patients were significantly higher compared to tumour (n=20), normal oesophageal adjacent tissue (n=7-8), and serum (n=10). In chapter 4, results showed the possible pro-metastatic role of fractalkine, as fractalkine enabled FLO-1 cell migration towards the chemotactic cues for the liver metastasis derived cell line FLO-1^{LM}. As the liver is the most common site of metastasis in OAC, and our previous studies have already shown that T and NK cells are pulled to liver, fractalkine could be an important mediator of immune cell migration and cancer cell metastasis to the liver in OAC [39, 126, 128, 354, 355]. High fractalkine levels have been reported in other cancers to be linked with poorer survival outcomes, increased cell survival and growth in gastric, ovarian and pancreatic cancer [189, 202, 219]. However, the results presented here on this cohort of patients demonstrate that there are no apparent correlations between tumour regression grade or nodal status and fractalkine levels of tumour samples from OAC patients. Interestingly, OAC and GAC patients without obesity had significantly higher levels of intratumoural fractalkine compared to patients with obesity. One study in gastric cancer has demonstrated that higher fractalkine expression in tumour samples correlated with higher NK cells and $CD8^{+}$T cell infiltration, while also correlating with better prognosis [43]. Here, the data suggest that in the tumour of OAC patients without obesity, higher expression of fractalkine could be a pro-inflammatory response to recruit immune cells to the tumour site, however due to much higher levels in the omentum and liver, two major sites of chronic-inflammation, higher expression at the tumour site in OAC patients without obesity would still not counteract immune cell migration towards

the fractalkine-rich omentum and liver. Importantly, E6130 held utility regardless of obesity status. The results show no apparent correlations between matched levels of fractalkine in the different tissues and serum tested. It must be noted that the samples comprise a cohort of OAC, GAC and OGJ patients of different tumour stages TRGs, and receiving different treatment regimens, with very few samples from patients who haven't received neoadjuvant treatment or at TRG 1-2. Therefore, more statistical power would be required to deduce conclusions on fractalkine's potential as a prognostic biomarker in OAC **[Table 2.3]**. Our research has previously shown that there are no significant differences in fractalkine levels in serum [129]. Although the results suggest here a key role in fractalkine's involvement in OAC immune cell migration and metastasis, more data and a larger cohort is needed to confirm whether it has any prognostic value.

Cytokine levels were evaluated following treatment with E6130 in OAC tumour samples, and interestingly, E6130 significantly decreased IFN-γ levels in TCM, which suggests that E6130 may influence cytokine production in the TME. This is in line with our group's previous results where we found that NK cell production of IFN-γ is significantly increased by fractalkine treatment [127]. Decreasing IFN-γ levels at the tumour site could reduce pro-inflammatory effects and contribute to regulating cytokine production in the TME. However, TNF-α, IL-2 and IL-15 were significantly increased with E6130 treatment. Increased TNF-α in the TME is likely to promote apoptosis through binding to its receptors TNFR1 and TNFR2, thus identifying a second mechanism through which E6130 might induce OAC tumour cell death [400]. However, it must be noted that TNF-α can also induce fractalkine expression and vice versa, suggesting that this increase might later lead to further fractalkine production [127, 393, 394]. Indeed, our data show that baseline TNF-α expression positively correlated with fractalkine levels in OAC tumour levels, and more specifically OAC patients without obesity, further highlighting immune dysregulation in OAC patients who are overweight or obese. As IL-2 and IL-15 are important cytokines for NK cell proliferation and activation, E6130-mediated increases in their levels could boost activation of NK cells at the tumour site and help to alleviate some of the previously reported suppression of NK cells within the obese OAC TME [281, 283, 290, 401]. Induction of TNF-α, IL-2 and IL-15 cytokines in the TME could overall have an immunostimulatory role, as our group has shown that OAC tumours are depleted in

NK cells particularly in OAC patients with obesity [127]. E6130 could therefore help to redirect NK cell migration away from VAT and towards the oesophageal tumour site as we have previously shown but in addition, it could also sustain and activate such infiltrates via elevated IL-2 and IL-15. It must also be noted that IL-2 also supports regulatory T cell (Tregs) persistence, which could be an undesirable effect in this context [281, 283]. Thus, further multiplex ELISAs which were beyond the scope of this study are needed to confirm E6130 impact on the inflammatory profile of OAC tumours.

E6130 did not alter activating or inhibitory receptor expression or cytokine production in NK cells derived from healthy donor blood or OAC patient blood. Furthermore, it could not prevent fractalkine-induced endocytosis of $CX3CR1^{+}$, nor did it reduce receptor expression when NK cells were treated with E6130 alone, suggesting that E6130 doesn't block fractalkine:CX3CR1 binding. The latter does not align with *Wakita et al*'s findings, where they found that E6130 reduced surface expression of CX3CR1 on NK cells after pre-treating NK cells with for E6130 for 30 min, however here the cells were treated for 24 hours [185]. Therefore, further studies are needed to evaluate the effects of E6130 on CX3CR1 expression on NK cells at different time points. Our group have previously found that the effects of fractalkine are dependent on the CX3CR1 expression levels, with high expressing $CD8^{+}$ T cells and NK cells being more susceptible to its effects compared to low expressing $CD4^{+}$ T cells [127, 129]. We propose that the same may be true for E6130. However, in OAC patient tumour samples, E6130 slightly but significantly lowered $CX3CR1^{+}$ expression on leukocytes and NK cells. This demonstrates varying results, and this could suggest that E6130-induced reduction in CX3CR1 expression is context dependent. Our previous studies have already shown how intratumoural NK cells have impaired activating markers, thus intratumoural NK cell phenotype is vastly different and these cells might exhibit a different susceptibility to E6130 [68].

Our research has previously demonstrated increased CD27, IFN-γ or TNF-α expression by NK cells when exposed to the soluble cues of the omentum and hypothesise that this could be due to exposure to the high levels of fractalkine in this compartment [127]. Here, E6130 did not alter fractalkine-induced elevations in CD27, IFN-γ or TNF-α expression from healthy donor NK cells, demonstrating that E6130 did not seem to counteract fractalkine-elicited effects on NK cell functions beyond migration[68].

Interestingly, treatment with E6130 could potentially enable NKp46 receptor recovery in the OAC TME as TCM treated with E6130 significantly increased NKp46 expression compared to non-treated TCM. Our group has previously shown that it is expressed at lower levels in the omentum, liver and tumour of OAC patients compared to the circulation; thus, increasing NKp46 could enable activation of cytotoxic effector functions and boost NK cell activation within the TME [39, 68]. However, our group has previously shown that OAC TCM from patients with obesity reduces NKp46 expression on healthy NK cells, and not TCM from patients without obesity [68]. As patients in this study were stratified as patients with or without obesity using Body Mass Index (BMI), due to unavailable Visceral Fat Area (VFA) data, this could explain differential results, compared to previous work from our group. Furthermore, our data also revealed that decreased TNF-α production and TRAIL expression by NK cells following TCM exposure could be partially recovered by E6130, although these results were non-significant. Overall, our data suggest that while E6130 can redirect NK cells from the chemotactic cues of the omentum towards the soluble cues of the TME, it did not significantly alter NK cell phenotype, function and cytotoxicity.

The results of this chapter aimed to further investigate the anti-tumour potential of E6130 in OAC tumour cells and its non-chemotactic effects on NK cells. As our group has already established how E6130 could affect NK cell migration away from the chemotactic cues of the omentum and redirect them towards the oesophageal tumour, data here confirm that E6130 did not alter NK cell phenotype, function or cytotoxicity in healthy donors or in NK cells from OAC patients [68]. However, E6130 presents an added anti-cancer role by directly reducing viability, inducing cytotoxicity and increasing cytokine production in tumour samples from OAC patients. Therefore, this reinforces our hypothesis that E6130 can halt tumour progression in OAC in 2 ways; 1) boosting NK cell migration to the tumour site (based on previous data [68, 69]) and 2) via direct tumouricidal activity (based on data presented in chapter 3, 4 and 5).

5.5 Highlights

- E6130 significantly decreases viability and increases cytotoxicity in OAC patient tumour samples.

- Highest levels of fractalkine detected in the VAT and liver tissue compartments of OAC patients.
- Fractalkine levels positively correlate with TNF-α levels in OAC tumour patient samples without obesity
- E6130 significantly increases TNF-α, IL-2 and IL-15 but decreases IFN-γ secretion in OAC tumour samples.
- TCM from OAC patients without obesity treated with E6130 significantly increased NKp46 expression on NK cell compared to treatment with non-treated TCM

Chapter 6 - Exploring the applicability of the NK cell therapy KHYG-1 in OAC

6.1 Introduction

Natural killer (NK) cells are a crucial component of anti-tumour immunity [239, 240, 242, 243]. However, the solid tumour microenvironment (TME) often impedes their anti-cancer activity, inducing NK cell dysfunction, and facilitating immune evasion and progression of tumour growth [241, 242]. Furthermore, the infiltration of NK cells into solid tumours has been associated with improved prognosis [243, 402-405]. We previously reported that soluble factors released by tumours from OAC patients with obesity significantly decrease NK cell cytotoxic functions but increase cytokine production [11]. Moreover, our group showed that NK cell abundance in OAC patient tumours negatively correlates with visceral obesity, due in part to their erroneous migration towards the visceral adipose tissue (VAT) [11, 12]. Therefore, our group has identified two significant challenges for effective NK cell-mediated immunity in OAC patients with the condition of obesity i.e. effectively infiltrating tumour and successfully eliciting their functions within the TME.

In the last ten years, chimeric antigen receptor (CAR) therapies have come to the fore for their potential to transform patient outcomes in poor prognosis cancer, with NK cells now being explored in this space [246-250]. They offer an adept alternative to T cells as they do not require antigen recognition to kill tumour cells, are not major histocompatibility restricted (MHC) and have potential to become an off-the-shelf option. In addition, they also are proven to secrete less cytokines associated with cytokine release syndrome such as IL-1β, IL-2, and IL-6 [239, 245, 406, 407]. However, immune cell therapies for solid tumours still face major obstacles to effectively home towards the tumour in sufficient numbers and to function under the harsh conditions of the immunosuppressive TME [241]. Moreover, our previous data suggest that such challenges would be exacerbated in cancer patients with obesity, and this must be considered when developing cell-based immunotherapies for obesity-associated cancer [68, 69, 127].

NK cells can be sourced from the peripheral blood, cord blood, clonal NK cell lines, or induced pluripotent stem cells. A key advantage of NK cell lines is their immediate availability and potential for genetic modification. This allows therapeutic augmentation of cancer cell recognition and destruction by NK cell therapies in the immunosuppressive

solid TME through increased expression of chimeric antigen receptors (CARs), chemokine receptors or specific tumour-targeting receptors [241, 242, 245, 251]. NK-92 cells are an NK cell line derived from the peripheral blood of a patient with rapidly progressive non-Hodgkin's lymphoma and have been the most studied in clinical trials for various cancer types, including colorectal, pancreatic, breast and gastric cancer, due to their robust anti-tumour activity and safety profile [242, 252, 254]. KHYG-1 cells are derived from a patient with aggressive NK cell leukaemia and are also being explored as they have been shown to have increased cytotoxicity compared to NK-92 cells [255, 256]. KHYG-1 cells exhibit high expression of key activating receptors, such as NKp44, and NKG2D, which contribute to their potent cytotoxic response [255, 256]. Based on their higher cytotoxicity, previously demonstrated safety profile and their reported ability to discriminate between malignant and non-malignant cells, the KHYG-1 cell line was selected for this study to evaluate its potential as a NK cell therapy for OAC and to test whether it is susceptible to the same challenges as blood-derived NK cells under the conditions of obesity [255, 266, 289, 408].

Due to their role in guiding immune cells to the tumour TME [36, 133, 134, 224], chemokines are an important immunotherapeutic tool to remodel the immune profile of tumours and promote tumour eradication [225, 226]. Genetic engineering of NK cells to express specific chemokine receptors has emerged as a promising strategy to overcome the poor infiltration of NK cells into the TME and enhance their tumour-homing capacity [330, 409]. Moreover, transfection of chemokine receptor mRNA in human NK cells has been shown to not impact their viability, function, or phenotype, but rather to improve migration and killing abilities [293-295]. *Ex vivo* upregulation of CXCR3 expression on NK cells improved their migration towards the tumour site in xenograft models of melanoma, which was shown to also increase CXCL10/IP-10 expression in the TME, resulting in overall enhanced NK cell infiltration to the tumour site and reduced tumour burden [296]. Recently, NK-92 and primary NK cells from peripheral blood were genetically engineered to overexpress CCR4 and CCR2B receptors and were shown to retain their NK cell functions while migrating towards their chemokine ligands CCL22 and CCL2, showing how engineering chemokine receptors on NK cells can improve NK cell therapies for solid tumours [298]. Here, the KHYG-1 cell therapy's migratory patterns

were assessed, as well as their chemokine receptor profile to ascertain whether KHYG-1 cell therapy is predisposed to the erroneous migration towards OAC patient-derived VAT as previously observed in blood-derived NK cells [68, 69, 127]. In addition, the potential of chemokine receptor modulation and/or antagonism to counteract any such migration of KHYG-1 cells towards VAT was also assessed. In light of our reports of immune suppression of blood-derived NK cells within the VAT and tumour derived from OAC patients with obesity, the effects of these microenvironments on KHYG-1 phenotype and function were also assessed. Overall, this chapter will provide novel insights on KHYG-1 cell therapy applicability in OAC and uncover potential challenges the tumoural and extratumoural tissues might present for such a treatment.

6.2 Hypothesis

NK cell therapy KHYG-1 holds potential for OAC but may be susceptible to the chemotactic cues of OAC omentum and immunosuppressive mechanisms of the OAC TME.

Aims:

1. Compare phenotypical and functional markers of KHYG-1 cells to healthy donor blood-derived NK cells
2. Assess migration of KHYG-1 cells towards visceral adipose and tumour conditioned media from OAC patients
3. Investigate the effects of the soluble visceral adipose tissue and tumour microenvironment of OAC patients with or without obesity on KHYG-1 cell phenotype and function
4. Evaluate if E6130 or AMG487 can block KHYG-1 cell migration to the adipose tissue conditioned media of OAC patients and whether the supplementation of IP-10 to the tumour conditioned media can increase KHYG-1 cell migration towards chemotactic cues of OAC tumour

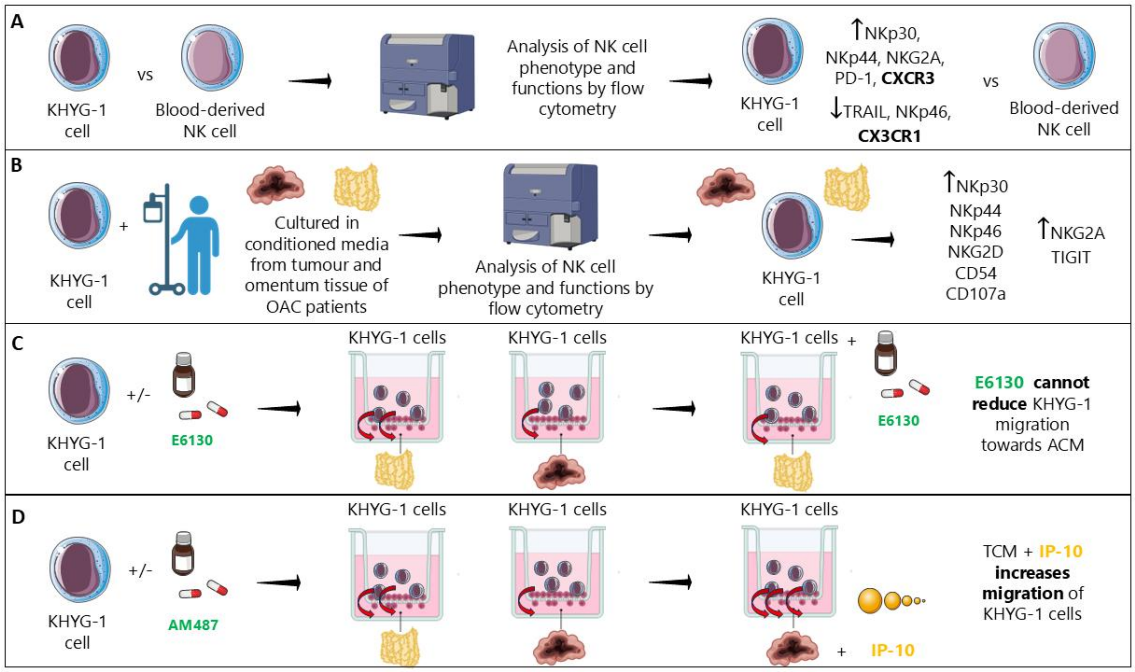

Graphical abstract: (A) Blood-derived NK cells and KHYG-1 cells were compared by analysing phenotypical and functional functions by flow cytometry. KHYG-1 cells express higher (↑) NKp30, NKp44, NKG2A, PD-1 and CXCR3 but lower (↓) TRAIL, NKp46 and CX3CR1 compared to blood-derived NK cells. **(B)** KHYG-1 cells cultured in conditioned media from tumour and omentum tissue of OAC patients were analysed by phenotypical and functional functions by flow cytometry. KHYG-1 cells express high (↑) levels of NKp30, NKp44, NKp46, NKG2D, CD54 and CD107a but also high (↑) levels NKG2A and TIGIT when co-cultured conditioned media from tumour and omentum tissue of OAC patients. **(C)** KHYG-1 cells migrate towards conditioned media from tumour and omentum tissue of OAC patients and E6130 cannot reduce KHYG-1 migration towards conditioned media from omentum tissue of OAC patients. **(D)** KHYG-1 cells migrate towards conditioned media from tumour and omentum tissue of OAC patients and IP-10 added to conditioned media from tumour tissue of OAC patients increases KHYG-1 migration. Created with Smart.Servier.com and Biorender.com

Results

6.3 Exploring the applicability of the NK cell therapy KHYG-1 in OAC

6.3.1 KHYG-1 cells are phenotypically and functionally different to healthy donor blood-derived NK cells

6.3.1.1 KHYG-1 cells are predominantly CD56^{bright}

KHYG-1 cells are a well-established natural killer (NK) cell therapy that were isolated from the peripheral blood of a patient with an aggressive leukaemia and some studies have found that they are more cytotoxic than the NK-92 cell therapy, which is already in clinical trials [410]. Therefore, as we hypothesised that cell line-derived NK cell therapies may have potential as a therapy for OAC patients, KHYG-1 cell phenotype and function was compared to healthy donor blood-derived NK cells. Firstly, their CD56 expression was assessed, and KHYG-1 cells are mostly CD56^{bright} rather than CD56^{dim}, compared to PBMC derived NK cells (NK-PBMC); CD56^{dim}: NK-PBMC vs KHYG-1 (96% vs 15.8%, n=3); CD56^{bright}: NK-PBMC vs KHYG-1 (6% vs 82.4%, n=3) **[Figure 6.1]**.

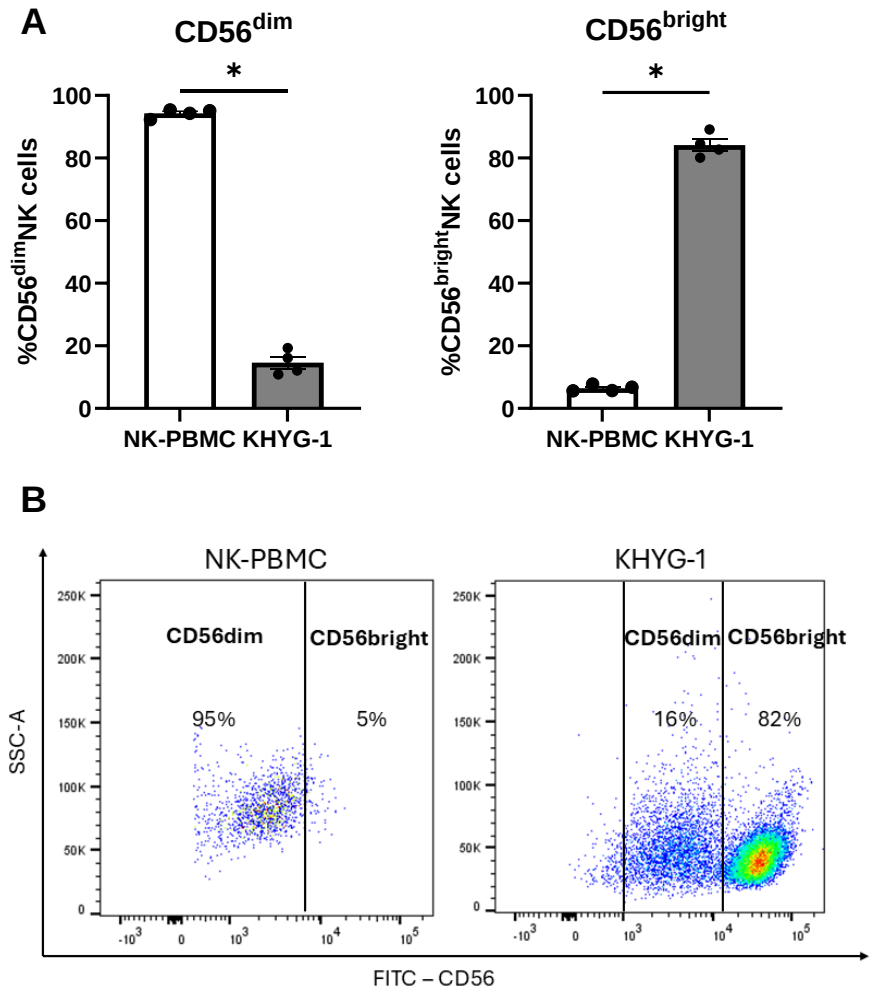

Figure 6.1: KHYG-1 cells are predominantly CD56^{bright}

(A) Bar charts showing % cell frequency of CD56^{dim} and CD56^{bright} NK cells derived from healthy donor-derived PBMC (NK-PBMC) and KHYG-1 cells (n=4) **(B)** Representative dot plots showing gating of CD56^{dim} and CD56^{bright} NK cells previously gated on viable cells. *p<0.05, by Mann-Whitney test. Mean± SEM.

6.3.1.2 KHYG-1 cells differ significantly from healthy donor blood-derived NK cells in their activation marker and death receptor ligand expression

Next, basal levels of activation and maturation marker surface expression was evaluated on KHYG-1 and healthy donor blood-derived NK cells without prior cytokine activation; including NKG2D, a master regulator of NK cells; NKp30, expressed on all mature and activated NK cells; NKp46, part of the natural cytotoxicity receptor (NCR) family and expressed by all NK cells independently of their activation status and CD27, a maturation marker [61]. Death receptor ligand TRAIL and FasL surface expression were also assessed.

NKG2D, NKp30 and FasL were expressed at similar frequencies on both types of NK cells. However, significantly lower frequencies were observed of $NKp46^{+}$ and lower frequencies were observed of $CD27^{+}$KHYG-1 cells compared to NK-PBMC; NKp46: NK-PBMC vs KHYG-1 (83.2% vs 1.2%, p=0.029, n=4), CD27: NK-PBMC vs KHYG-1 (10.1% vs 0%, n=3). Moreover, KHYG-1 cells did not express high levels of death receptor ligand TRAIL compared to NK-PBMC: TRAIL: NK-PBMC vs KHYG-1 (55.3% vs 0.28%, p=0.029, n=4) **[Figure 6.2]**.

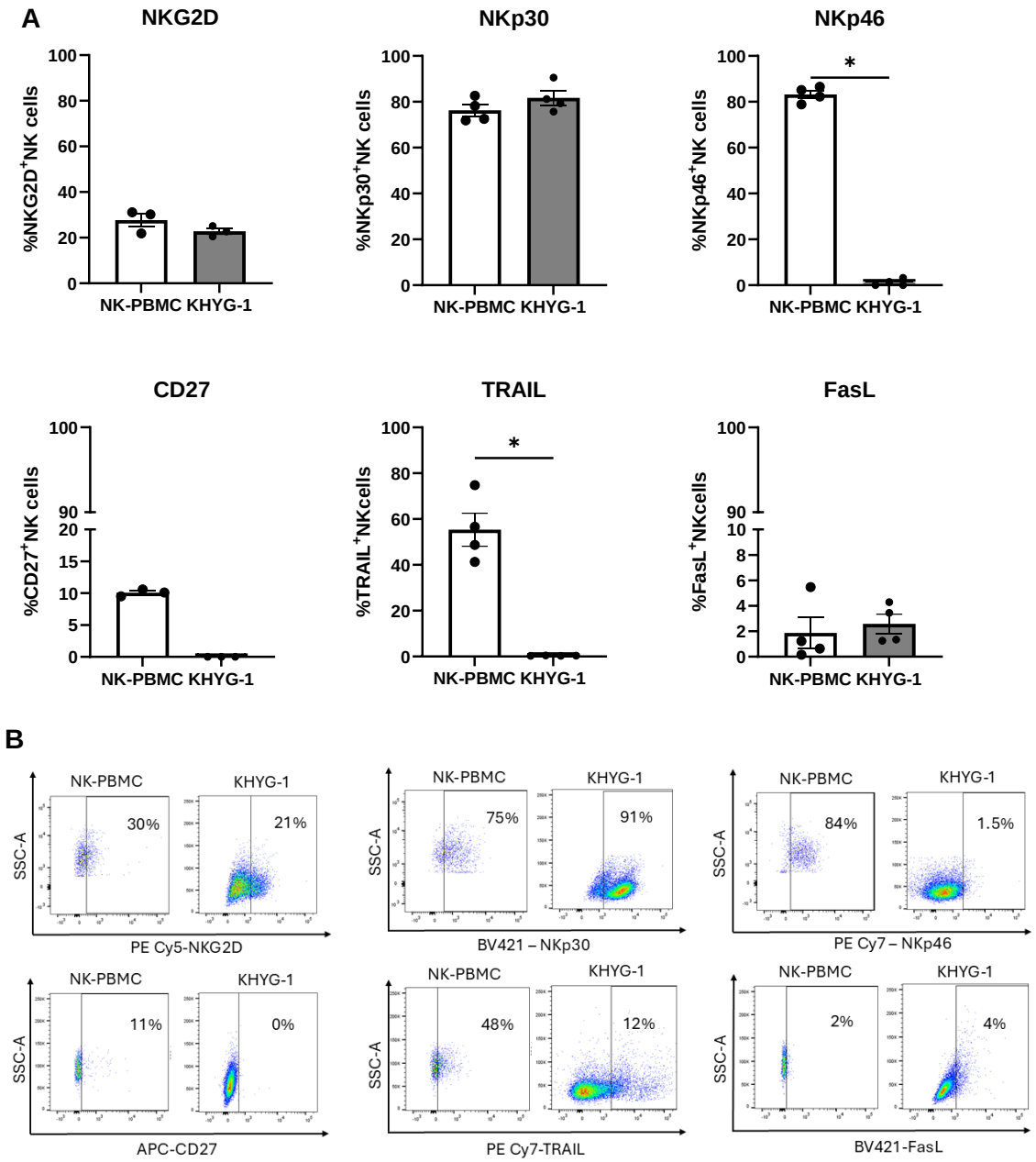

Figure 6.2: Healthy donor blood-derived NK cells express significantly higher NKp46, CD27 and TRAIL, compared to KHYG-1 cells

(A) Bar charts showing % cell frequency of NKG2D$^+$, NKp30$^+$, NKp46$^+$, CD27$^+$, TRAIL$^+$ and FasL$^+$ NK cells derived from PBMC (NK-PBMC) and KHYG-1 cells (n=3-4). **(B)** Representative dot plots showing gating of NKG2D$^+$, NKp30$^+$, NKp46$^+$, CD27$^+$, TRAIL$^+$ and FasL$^+$ NK-PBMC vs KHYG-1 previously gated on viable cells. *p<0.05, by Mann-Whitney test. Mean± SEM.

6.3.1.3 KHYG-1 cells differ significantly from healthy donor blood-derived NK cells in their inhibitory receptor and immune checkpoint expression

The inhibitory member of the NKG2 family, NKG2A and the immune checkpoints PD-1 and TIGIT were next compared on the two different types of NK cells basally. Significantly higher frequencies of $NKG2A^+$ and $PD\text{-}1^+$KHYG-1 cells were observed compared to NK-PBMC basally; NKG2A: NK-PBMC vs KHYG-1 (42.2% vs 83.6%, p=0.029, n=4), PD-1: NK-PBMC vs KHYG-1 (3% vs 14.3%, n=4). There were no significant differences observed in TIGIT frequencies between NK-PBMC and KHYG-1 cells **[Figure 6.3]**.

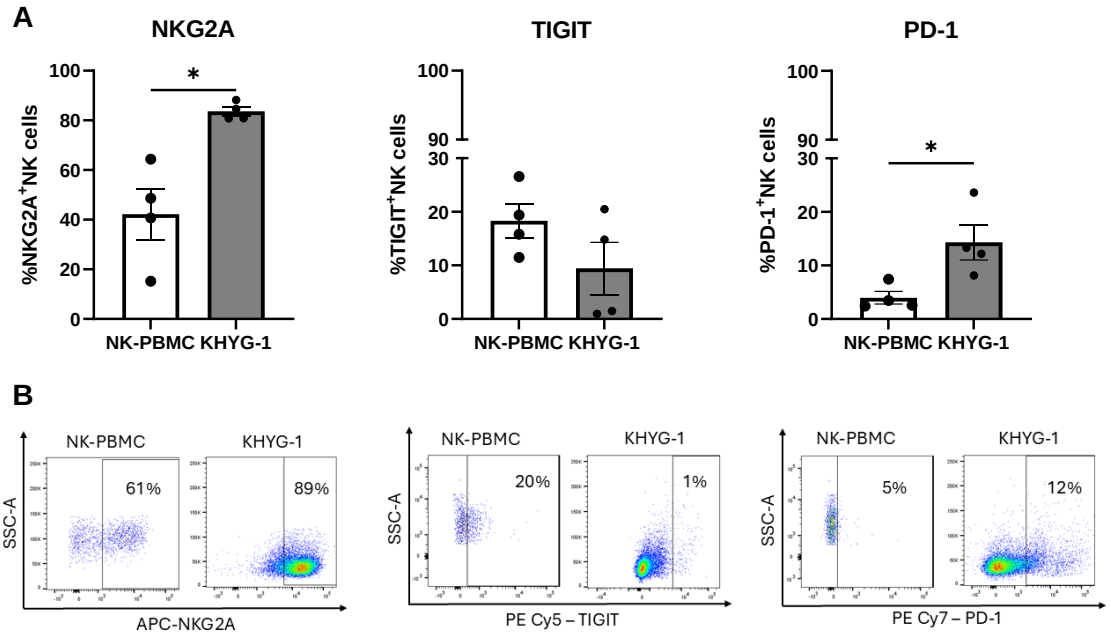

Figure 6.3: Basal NKG2A and PD-1 expression is significantly higher on KHYG-1 cells compared to healthy donor blood-derived NK cells

(A) Bar charts showing % cell frequency of NKG2A$^+$, TIGIT$^+$ and PD-1$^+$ NK cells derived from PBMC (NK-PBMC) and KHYG-1 cells (n=4). **(B)** Representative dot plots showing gating of NKG2A$^+$, TIGIT$^+$ and PD-1$^+$NK-PBMC vs KHYG-1 previously gated on viable cells. *p<0.05, by Mann-Whitney test. Mean± SEM.

6.3.1.4 KHYG-1 cells express significantly less CX3CR1 compared to blood-derived NK cells

Chemokine receptors CX3CR1, CCR2 and CCR6 were also evaluated on the surface expression of the two NK cell type at basal levels. As our group has shown that the soluble adipose tissue of OAC patients is abundant in fractalkine, MCP-1 (CCL2) and MIP-3α (CCL20) [128], the expression of the receptors for these chemokine ligands (CX3CR1, CCR2 and CCR6, respectively) were evaluated on KHYG-1 cells to assess if they could potentially be attracted to these chemotactic cues. Since fractalkine has been identified as a key driver of blood-derived NK cell migration to the visceral adipose tissue, CX3CR1 surface expression by KHYG-1 cells was of particular interest here [68, 69, 127]. Significantly lower frequencies of $CX3CR1^{+}$KHYG-1 cells were observed compared to NK-PBMC basally; CX3CR1: NK-PBMC vs KHYG-1 (67.2% vs 15.7%, p=0.029, n=4). CCR2 was not expressed on KHYG-1 cells **[Figure 6.4]**.

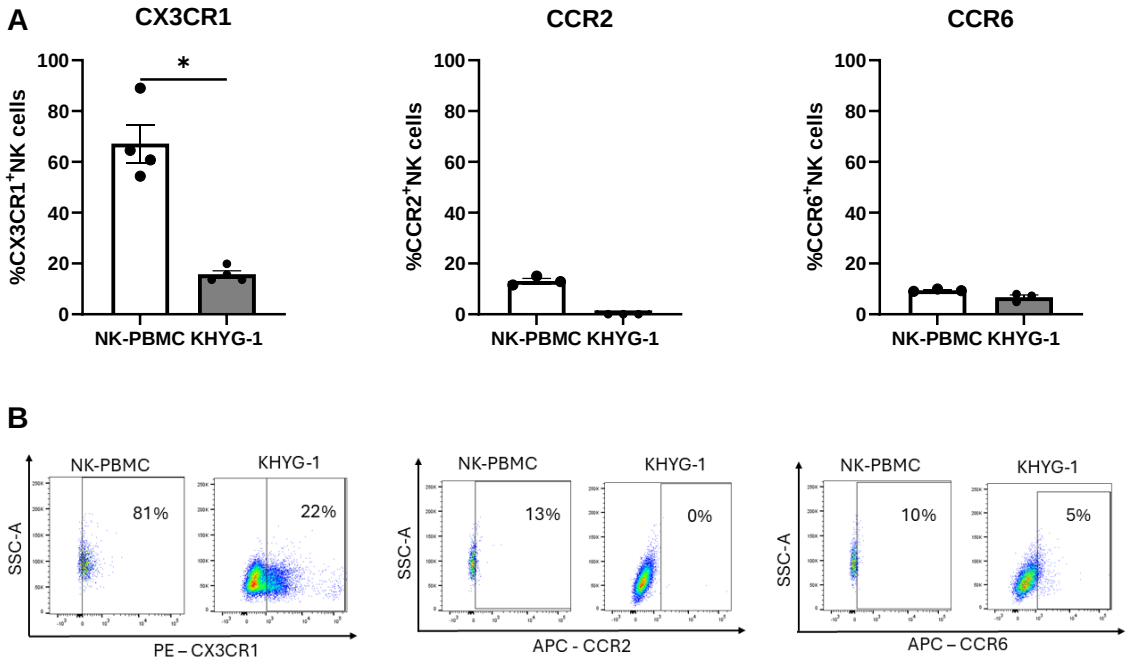

Figure 6.4: KHYG-1 cells express significantly less CX3CR1 compared to blood-derived NK cells basally

(A) Bar charts showing % cell frequency of CX3CR1$^+$, CCR2$^+$ and CCR6$^+$ NK cells derived from PBMC (NK-PBMC) and KHYG-1 cells (n=4). **(B)** Representative dot plots showing gating of CX3CR1$^+$, CCR2$^+$ and CCR6$^+$ NK-PBMC vs KHYG-1 previously gated on viable cells. *p<0.05, by Mann-Whitney test. Mean± SEM.

6.3.1.5 KHYG-1 cells actively migrated towards the soluble chemotactic cues of OAC patient-derived adipose tissue and tumour tissue

Our group has previously shown that blood-derived NK cells migrated towards the soluble chemotactic cues of the adipose tissue conditioned media (ACM) of OAC patients, at the expense of effective migration towards those of tumour conditioned media [68, 69, 127]. The previous results demonstrated that KHYG-1 cells express significantly less CX3CR1 on their cell surface compared to blood-derived NK cells. Here, KHYG-1 cell migration towards ACM and towards tumour tissue conditioned media (TCM) from OAC patients was evaluated to assess if KHYG-1 cells migrate towards OAC patient-derived ACM at significantly higher levels than OAC patient-derived TCM, as we have shown for blood-derived NK cells [68, 69, 127]. Serum-free M199 was considered a negative control and M199 supplement with 20% FBS (FBS) was considered as a positive control. There was a significantly higher KHYG-1 cell migration towards the positive control (FBS) compared to the negative control (M199), which demonstrates the functionality of this assay; M199 vs FBS (Fold change: 1 vs 8.2, p=0.021, n=9). Similarly to previous results from our group with blood-derived NK cells, there was a significantly higher KHYG-1 cell migration towards ACM compared to the negative control; M199 vs ACM (Fold change: 1 vs 9.2, p= 0.003, n=9). Moreover, there was a significantly higher KHYG-1 cell migration towards TCM compared to the negative control; M199 vs TCM (Fold change: 1 vs 3.4, p= 0.003, n=9). There was a significantly higher KHYG-1 cell migration towards ACM compared to TCM; ACM vs TCM (Fold change: 9.2 vs 3.4, p= 0.004, n=9) **[Figure 6.5]**.

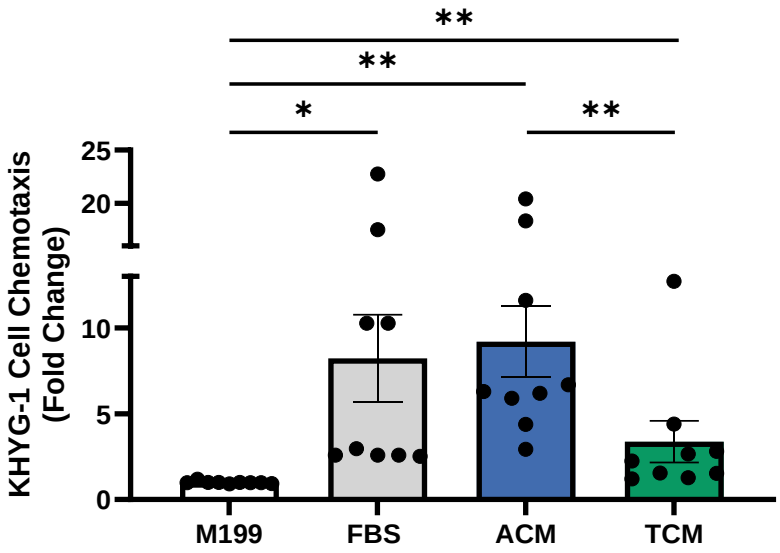

Figure 6.5: KHYG-1 cells actively migrate towards the soluble chemotactic cues of OAC patient-derived adipose tissue and tumour tissue, with significantly higher levels of migration towards the VAT

Bar chart showing the paired fold change chemotaxis relative to M199 of KHYG-1 cells towards (FBS) or adipose conditioned media (ACM), or tissue conditioned media (TCM). *p<0.05, **p<0.01, ***p<0.001, by one sample t-test (M199 vs FBS, ACM or TCM) or Mann-Whitney test (ACM vs TCM) where appropriate. Mean± SEM.

Therefore, these results show that KHYG-1 cell activation, inhibition and chemokine markers differ significantly from NK-PBMC. Interestingly, these data strongly indicate active migration of KHYG-1 cells towards the soluble chemotactic cues of the VAT and tumour compartments of OAC patients, with significantly higher levels of migration towards the VAT.

6.3.2 Investigating the effects of the soluble visceral adipose tissue of OAC patients with or without obesity on KHYG-1 cell phenotype and function

Our group has previously shown that the soluble microenvironment of the OAC patient-derived visceral adipose tissue can alter NK cells significantly by reducing expression of NKp30, but by also increasing expression of TRAIL and FasL [342]. Moreover, our group has also shown that the soluble microenvironment of ACM from OAC patients without obesity can increase frequencies of IL-10, IFN-γ and TNF-α producing NK cells [342]. To elucidate how KHYG-1 cells would function under this microenvironment and if they responded differently than NK cells from healthy donor PBMCs to OAC ACM, KHYG-1 cells were cultured in 20% ACM diluted in complete RPMI (cRPMI, 10% FBS) for 24 hours. The ACM samples were generated from OAC patients with or without obesity to evaluate the impact of obesity on immunomodulation and the media used to generate ACM. As controls, KHYG-1 cells were cultured in their usual culture media cRPMI to assess baseline levels (non-treated, NT) or cultured with 20% M199 diluted in cRPMI for 24 hours as a control for the ACM.

6.3.2.1 Culture in ACM derived from OAC patients did not significantly alter activation and maturation marker surface expression by KHYG-1 cells

There were no significant differences in the surface expression of NKp30, NKp46 and NKG2D on KHYG-1 cells when they were cultured in 20% M199 or in ACM. Activation marker NKp44 was also evaluated as it has been reported to be highly expressed on KHYG-1 cells, and the results here indicate that culture in ACM did not alter NKp44 expression [255]. Adhesion molecule CD54 (ICAM-1) involved in NK cell activation and function was also assessed here and there were no differences in expression after ACM treatment. Another marker of NK cell activation CD69 was assessed and culture in ACM did not significantly increase its expression on KHYG-1 cells. Lastly, the expression of CD16, a marker of NK cell activation of cytotoxic functions, was slightly increased on

KHYG-1 cells following culture in ACM from patients with obesity compared to NT KHYG-1 cells; CD16: NT vs ACM (obese) (0.68% vs 2.18%; p=0.0607, n=6) **[Figure 6.6A]**.

6.3.2.2 Culture in ACM derived from OAC patients with obesity significantly increased the frequencies of TRAIL $^{+}$ and FasL^{+} KHYG-1 cells

TRAIL^{+} and FasL^{+}KHYG-1 cell frequencies were significantly increased following culture in ACM from patients with obesity compared to non-treated KHYG-1 cells and to KHYG-1 cells treated with 20% M199; TRAIL: NT vs ACM (obese) (3.9% vs 55.4%, p=0.042, n=6); M199 vs ACM (obese) (3.7% vs 55.4%, p= 0.009, n=6); FasL: NT vs ACM (obese) (3% vs 39.4%, p=0.019, n=6); M199 vs ACM (obese) (2.3% vs 39.4%, p= 0.01, n=6). The degranulation marker CD107a was also assessed here, however there were no significant differences following culture in ACM. **[Figure 6.6A]**.

6.3.2.3 Serum reduction significantly decreased TNF-α and IL-10 production by KHYG-1 cells

Frequencies of IFN-γ, TNF-α and IL-10 producing KHYG-1 cells were assessed following culture in ACM. Culture in 20% M199 significantly decreased frequencies of TNF-α and IL-10 producing KHYG-1 cells compared to NT cells; TNF-α: NT vs M199 (12.3% vs 2.4%, p=0.033, n=6); IL-10: NT vs M199 (MFI: 4087 vs 1118, p=0.037, n=6). However, culture in ACM from patients without obesity increased frequencies of TNF-α and IL-10 producing KHYG-1 cells compared to cells treated with M199; TNF-α: M199 vs ACM (non-obese) (2.4% vs 7.6%, p=0.037, n=6); IL-10: M199 vs ACM (non-obese) (MFI: 1118 vs 4211, p=0.026, n=6). Therefore, serum reduction significantly decreases TNF-α and IL-10 producing KHYG-1 cells, but KHYG-1 cells treated with non-obese ACM do not and therefore overcame the effects of serum reductions. There were no significant differences observed in IFN-γ producing KHYG-1 cells **[Figure 6.6C]**.

6.3.2.4 Culture in ACM from OAC patients with or without obesity increased frequencies of inhibitory markers NKG2A and TIGIT on KHYG-1 cells

Inhibitory marker NKG2A, and immune checkpoint receptors TIGIT and PD-1 surface expression by KHYG-1 cells was assessed following 24-hour culture in ACM from OAC patients with or without obesity. Significantly higher frequencies of NKG2A^{+}KHYG-1 cells were observed following culture in ACM from OAC patients without obesity compared

to NT; NKG2A: NT vs ACM (non-obese) (98.1% vs 99.7%, p=0.023, n=6). Culture in ACM from OAC patients with obesity increased the frequencies of TIGIT^{+}KHYG-1 cells compared to cells treated with M199; TIGIT: M199 vs ACM (obese) (10% vs 48.6%, p=0.0607, n=6). No significant differences were observed on the expression of PD-1 on KHYG-1 cells **[Figure 6.6D]**.

6.3.2.5 Culture in ACM from OAC patients with obesity increased CCR5 surface expression on KHYG-1 cells

Chemokine receptors CCR3, CCR5, CCR6 and CX3CR1 expression were assessed following culture in ACM. As our group has shown that remodelling of OAC TCM by supplementation with RANTES (CCL5) and MIP-1α (CCL3) can boost blood-derived NK cell migration towards TCM, and that blood-derived NK cells from both non-cancer and OAC patients express the receptors for these chemokine ligands (CCR3 and CCR5) [68], the expression of these receptors was evaluated on KHYG-1 cells. This would indicate if KHYG-1 cell migration towards OAC tumour could also be augmented following chemokine profile remodelling of the tumour. Culture in ACM from OAC patients with or without obesity did not alter surface expression of CCR6, CCR3 and CX3CR1 on KHYG-1 cells. However, significantly increased frequencies of CCR5^{+}KHYG-1 cells were observed following culture in ACM from patients with obesity compared to M199 treatment; CCR5: M199 vs ACM (obese) (14.1% vs 45.5%, p=0.048, n=6) **[Figure 6.6E].**

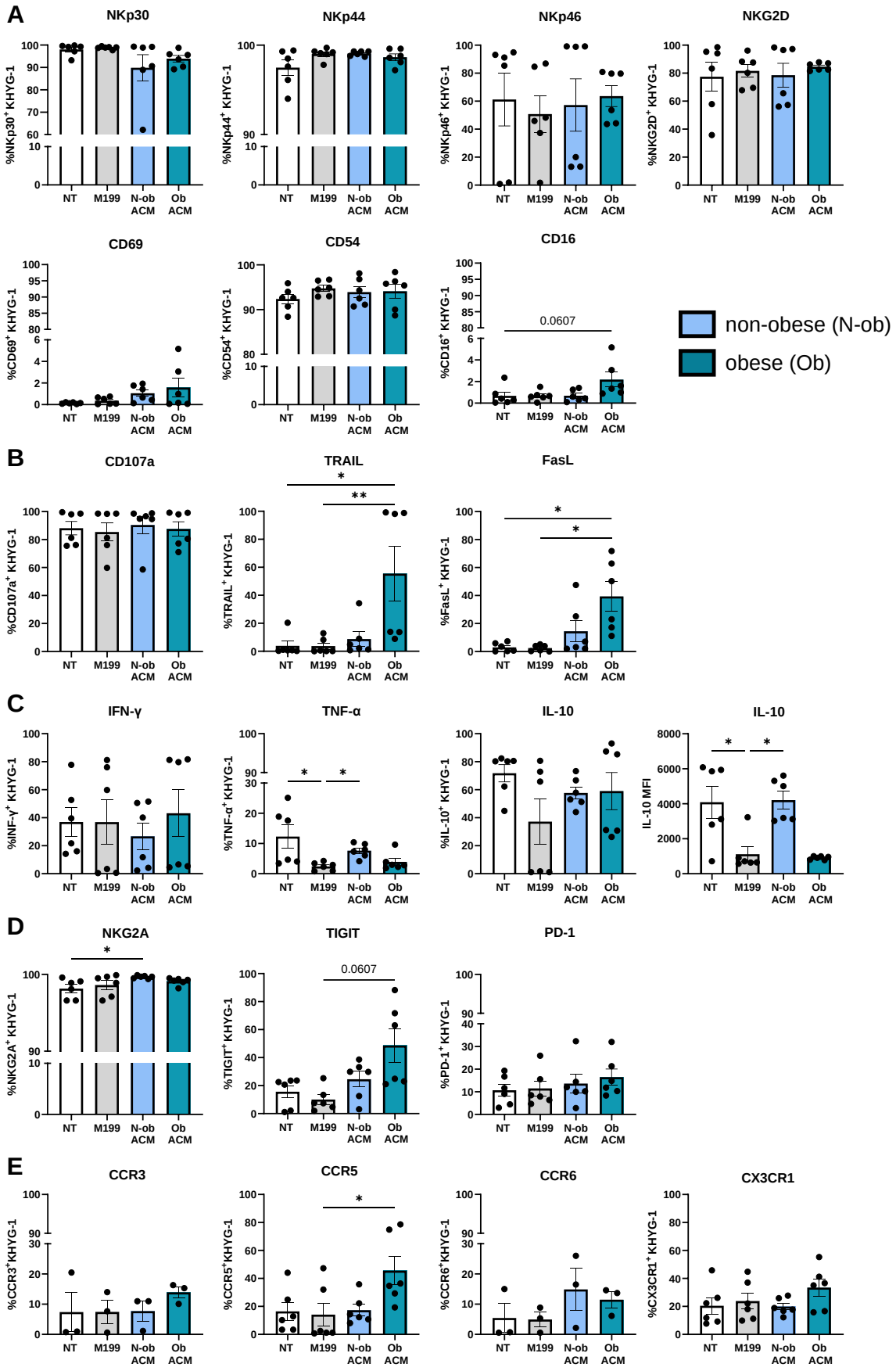
A
NKp30
NKp44
NKp46
NKG2D
%NKp30+ KHYG-1
%NKp44+ KHYG-1
%NKp46+ KHYG-1
%NKG2D+ KHYG-1
CD69
CD54
CD16
%CD69+ KHYG-1
%CD54+ KHYG-1
%CD16+ KHYG-1
0.0607
non-obese (N-ob)
obese (Ob)
B
CD107a
TRAIL
FasL
%CD107a+ KHYG-1
%TRAIL+ KHYG-1
%FasL+ KHYG-1
C
IFN-γ
TNF-α
IL-10
IL-10
%INF-γ+ KHYG-1
%TNF-α+ KHYG-1
%IL-10+ KHYG-1
IL-10 MFI
D
NKG2A
TIGIT
PD-1
%NKG2A+ KHYG-1
%TIGIT+ KHYG-1
%PD-1+ KHYG-1
E
CCR3
CCR5
CCR6
CX3CR1
%CCR3+ KHYG-1
%CCR5+ KHYG-1
%CCR6+ KHYG-1
%CX3CR1+ KHYG-1
NT
M199
N-ob ACM
Ob ACM

F

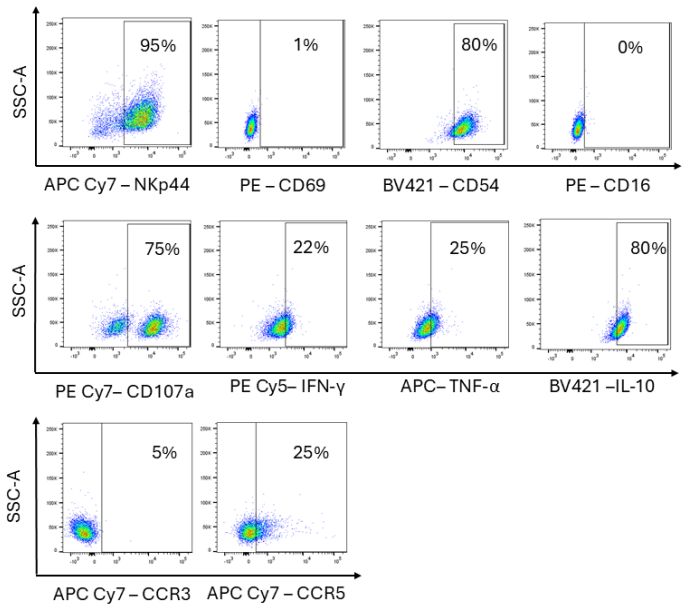

Figure 6.6: Activation markers on KHYG-1 cells were not significantly altered following treatment with OAC adipose tissue conditioned media

Bar charts showing % cell frequency of **(A)** activation markers NKp30$^+$, NKp44$^+$, NKp46$^+$, NKG2D$^+$, CD69$^+$, CD54$^+$ and CD16$^+$, **(B)** degranulation marker CD107a$^+$, and death receptors TRAIL$^+$ and FasL$^+$, **(C)** cytokines IFN-γ $^+$, TNF-α$^+$ and IL-10$^+$, **(D)** inhibition marker NKG2A$^+$ and immune checkpoint inhibitor TIGIT$^+$ and PD-1$^+$, and **(E)** chemokine receptors CCR3$^+$, CCR5$^+$, CCR6$^+$, and CX3CR1$^+$KHYG-1 cells cultured in cRPMI alone (non-treated, NT, white), or cultured in 20% M199 media (grey) or 20% OAC patient-derived ACM (non-obese: light blue, obese: dark blue). Experiments were repeated n=3-6. **(F)** Representative dot plots showing gating of NKp44$^+$, CD69$^+$, CD54$^+$, CD107a$^+$, CD16$^+$, IFN-γ $^+$, TNF-α$^+$, IL-10$^+$, CCR3$^+$ and CCR5$^+$KHYG-1 cells previously gated on viable cells. *p<0.05, **p<0.01, by Kruskal-Wallis with post-hoc Dunn's test. Mean± SEM.

6.3.3 Investigating the effects of the soluble tumour tissue microenvironment of OAC patients with or without obesity on KHYG-1 cell phenotype and function

Our group has reported that TCM from OAC patients with obesity decreased death receptor ligand TRAIL and degranulation marker CD107a expression on blood-derived NK cells. Moreover, TCM from patients with obesity decreased activation markers NKp30 and NKp46 expression, and increased frequencies of IFN-γ, TNF-α and IL-10 producing NK cells [68, 342]. Here, the effects of the soluble TME of OAC patients with or without obesity on KHYG-1 cell phenotype and function by treating KHYG-1 cells was assessed via 24-hour culture in 20% TCM diluted in cRPMI. The same controls of cRPMI (NT) and 20% M199 in cRPMI (M199) were used as above.

6.3.3.1 Culture in TCM from OAC patients did not significantly alter the activation phenotype of KHYG-1 cells

The surface expression of CD54 or other activation markers NKp30, NKp44, NKp46, NKG2D and CD69 on KHYG-1 cells were not significantly altered following culture in TCM from OAC patients with obesity. Frequencies of $CD16^{+}$KHYG-1 cells following culture in TCM from patients without obesity were very slightly but significantly decreased compared to culture in M199; CD16: M199 vs TCM (non-obese) (0.68% vs 0.03%, p=0.033, n=6), but frequencies of $CD16^{+}$KHYG-1 cells were very slightly but significantly higher following culture in TCM from patients with obesity compared to TCM from patients without obesity; CD16: TCM (non-obese) vs TCM (obese) (0.03% vs 0.59%, p=0.033, n=6) **[Figure 6.7A]**.

6.3.3.2 Culture in TCM from OAC patients significantly altered KHYG-1 cell cytotoxicity and degranulation marker expression

Significantly lower frequencies of $FasL^{+}$KHYG-1 cells were observed after culture in 20% M199 compared to NT cells; FasL: NT vs M199 (MFI: 1650.7 vs 543.7, p=0.022, n=6) and compared to culture in TCM from patients without obesity; FasL: M199 vs TCM (non-obese) (MFI: 543.7 vs 1670.2, p=0.042, n=6). Interestingly, KHYG-1 cells cultured in TCM from patients with obesity had a closer FasL MFI to cells treated with M199 compared to cells cultured in TCM from patients without obesity (360.7). Therefore, serum reduction significantly decreased frequencies of $FasL^{+}$KHYG-1 cells, but treatment with TCM from patients without obesity did not reduce frequencies of $FasL^{+}$KHYG-1 cells. Culture in TCM

from patients with obesity significantly increased frequencies of CD107a^{+}KHYG-1 cells compared to NT cells; CD107a: NT vs TCM (obese) (67.1% vs 98.8%, p=0.003, n=6). TRAIL expression was not significantly altered following culture in TCM **[Figure 6.7B]**.

6.3.3.3 Significantly altered frequencies of TNF-α and IL-10 producing KHYG-1 cells following serum reduction.

Culture in M199 significantly decreased frequencies of TNF-α producing KHYG-1 cells compared to NT cells; TNF-α: NT vs M199 (12.3% vs 2.43%, p=0.048, n=6) and culture in TCM from patients without obesity significantly decreased frequencies of TNF-α producing KHYG-1 cells compared to NT cells; TNF-α: NT vs TCM (non-obese) (12.3% vs 2.2%, p=0.008, n=6). Therefore, decreased frequencies of TNF-α producing KHYG-1 cells are due to lower presence of serum in the media. Culture in M199 decreased frequencies of IL-10 producing KHYG-1 cells compared to NT cells; IL-10: NT vs M199 (MFI: 4087.2 vs 1118, p=0.05, n=6) and culture in TCM from patients without obesity significantly increased frequencies of IL-10 producing KHYG-1 cells compared to M199 cells; IL-10: M199 vs TCM (non-obese) (MFI: 1118 vs 3947.8, p=0.048, n=6). Therefore, lower presence of serum in the media does not impact IL-10 producing KHYG-1 cells when cultured in TCM from patients without obesity, but it did decrease IL-10 producing KHYG-1 cells when cultured in TCM from patients with obesity. No significant changes were observed in IFN-γ producing KHYG-1 cells **[Figure 6.7C]**.

6.3.3.4 TCM from OAC patients without obesity decreased frequencies of PD-1^{+} KHYG-1 cells

Significantly decreased frequencies of PD-1^{+}KHYG-1 cells were observed when cells were cultured in TCM from patients without obesity compared to M199, and a noticeable decrease compared to non-treated cells; PD-1: M199 vs TCM (non-obese) (11.5% vs 3.8%, p=0.042, n=6); NT vs TCM (non-obese) (10.6% vs 3.8%, p=0.06, n=6). There were no significant differences on NKG2A or TIGIT expression on KHYG-1 cells when cultured in TCM **[Figure 6.7D]**.

6.3.3.5 TCM from patients with obesity significantly increased frequencies of CX3CR1^{+} KHYG-1 cells compared to TCM from patients without obesity

There was a significant increase in frequencies of CX3CR1^{+}KHYG-1 cells cultured in TCM from patients with obesity compared to cells cultured in TCM from patients without obesity; CX3CR1: TCM (non-obese) vs TCM (obese) (13.8% vs 35.3%, p=0.033, n=6). There were no significant differences in expression of CCR3, CCR5 or CCR6 when KHYG-1 cells were cultured in TCM **[Figure 6.7E]**.

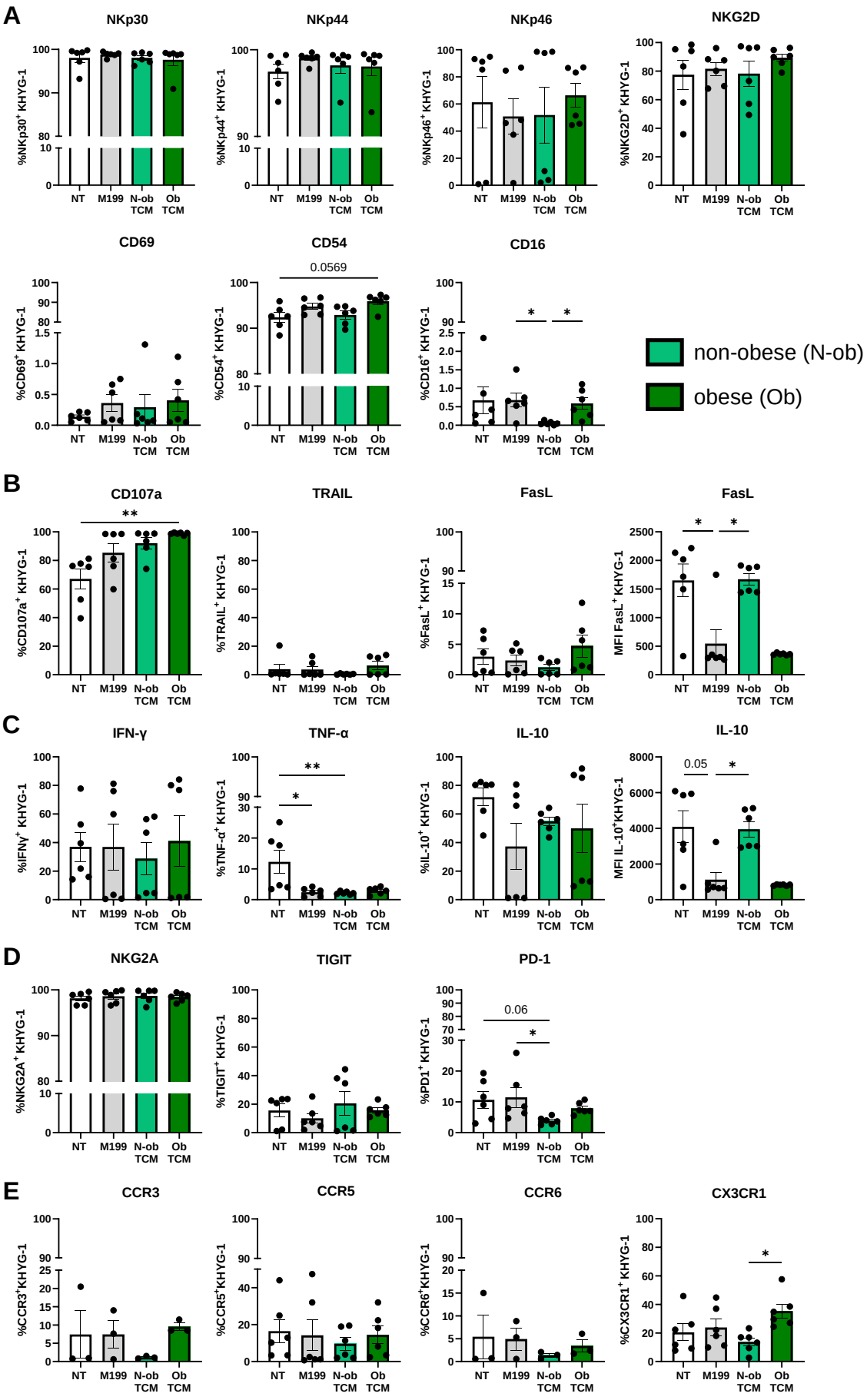
A
NKp30
NKp44
NKp46
NKG2D
CD69
CD54
CD16
0.0569
*
*
non-obese (N-ob)
obese (Ob)
B
CD107a
**
TRAIL
FasL
FasL
*
*
C
IFN-γ
TNF-α
**
*
IL-10
IL-10
0.05
*
D
NKG2A
TIGIT
PD-1
0.06
*
E
CCR3
CCR5
CCR6
CX3CR1
*
NT
M199
N-ob TCM
Ob TCM

Figure 6.7: Activation markers on KHYG-1 cells were not significantly altered following treatment with OAC patient-derived tumour tissue conditioned media

Bar charts showing % cell frequency of **(A)** activation markers NKp30^{+}, NKp44^{+}, NKp46^{+}, NKG2D^{+}, CD69^{+}, CD54^{+} and CD16^{+}, **(B)** degranulation marker CD107a^{+}, and death receptors TRAIL^{+} and FasL^{+}, **(C)** cytokines IFN-γ $^{+}$, TNF-α^{+} and IL-10^{+}, **(D)** inhibition marker NKG2A^{+} and immune checkpoint inhibitor TIGIT^{+} and PD-1^{+}, and **(E)** chemokine receptors CCR3^{+}, CCR5^{+}, CCR6^{+}, and CX3CR1^{+}KHYG-1 cells cultured in cRPMI alone (non-treated, NT, white), or cultured in 20% M199 media (grey) or 20% OAC patient-derived TCM (non-obese: light green, obese: dark green). Experiments were repeated n=3-6. *p<0.05, **p<0.01, by Kruskal-Wallis with post-hoc Dunn's test. Mean± SEM.

6.3.4 Spiking the chemokine profile of OAC tumours with IP-10 enhanced KHYG-1 cell recruitment

6.3.4.1 E6130 did not rescue KHYG-1 cell migration towards the soluble chemotactic cues of OAC patient-derived visceral adipose tissue

Our group has shown that NK cell migration towards the soluble chemotactic cues of the visceral adipose tissue can be overcome when NK cells are treated with the CX3CR1 modulator E6130 or CX3CR1 antagonist AZD8797 [68, 69, 127]. KHYG-1 cell migration towards the ACM generated from OAC patients was next evaluated with and without pretreatment with 4.9nM E6130. First, KHYG-1 cell migration towards a positive and negative control were assessed and different cytokine combinations were evaluated to test if it could boost migration of KHYG-1 cells. KHYG-1 cell media is already supplemented with IL-2, but an additional 2-hour and 24-hour boost +/- IL-15 were tested here. Serum-free M199 was considered a negative control and M199 supplement with 20% FBS (FBS) was considered as a positive control. KHYG-1 cells migration was significantly higher towards the positive control when KHYG-1 cells had an additional 24-hour IL-2 boost; M199 vs FBS+IL-2 (24hrs) (Fold change: 1 vs 15.4, p=0.033, n=1-3) **[Figure 6.8A]**.

KHYG-1 cell migration towards ACM with or without a 24-hour IL-2 boost was next investigated. There was a significantly higher KHYG-1 cell migration towards the positive control (20% FBS) compared to the negative control (M199 only), which demonstrates the functionality of this assay; M199 vs FBS (Fold change: 1 vs 15.2, p=0.031, n=3-4). In line with our previous data, there was a significantly higher KHYG-1 cell migration towards ACM compared to the negative control; M199 vs ACM (Fold change: 1 vs 4.8, p= 0.036, n=3-5). Treatment with 4.9nM E6130 prior to chemotaxis assay did not significantly reduce KHYG-1 cell migration towards ACM; ACM vs ACM+E6130 (Fold change: 4.8 vs 4.4, n=5) **[Figure 6.8B left].** The same experiment was repeated with KHYG-1 cells boosted with a 24-hour IL-2 treatment. Again, there was a significantly higher KHYG-1 cell migration towards the positive control compared to the negative control; M199 vs FBS (Fold change: 1 vs 23.4, p=0.031, n=3). Again, there was a significantly higher KHYG-1 cell migration towards ACM compared to the negative control; M199 vs ACM (Fold change: 1 vs 4, p=0.036, n=3-5). Treatment with E6130 prior to chemotaxis assay did not

significantly reduce KHYG-1 cell migration towards ACM; ACM vs ACM+E6130 (Fold change: 4 vs 4.7, n=5) **[Figure 6.8B right]**. Therefore, E6130 is not an effective means to reduce KHYG-1 cell therapy towards the chemotactic cues of OAC patient-derived VAT.

Next, the migration of KHYG-1 cells towards the chemotactic cues of OAC TCM were evaluated the same way as previously described. Again, there was a significantly higher KHYG-1 cell migration towards the positive control compared to the negative control which demonstrates the functionality of this assay; M199 vs FBS (Fold change: 1 vs 16.8, p=0.048, n=3). KHYG-1 cell migration towards TCM was higher compared to the negative control; M199 vs TCM (Fold change: 1 vs 2.3, n=3) **[Figure 6.8C left].** When the same experiment was repeated with KHYG-1 cells boosted with a 24-hour IL-2 treatment, it did not significantly increase KHYG-1 cell migration towards TCM; M199 vs TCM (Fold change: 1 vs 2.6, n=3) **[Figure 6.8C right].**

Therefore, KHYG-1 cells were able to migrate towards the soluble chemotactic cues of OAC adipose tissue, but E6130 did not prevent this migration. Moreover, treating KHYG-1 cells with an IL-2 boost cannot enhance migration of KHYG-1 cell towards the soluble chemotactic cues of OAC tumour

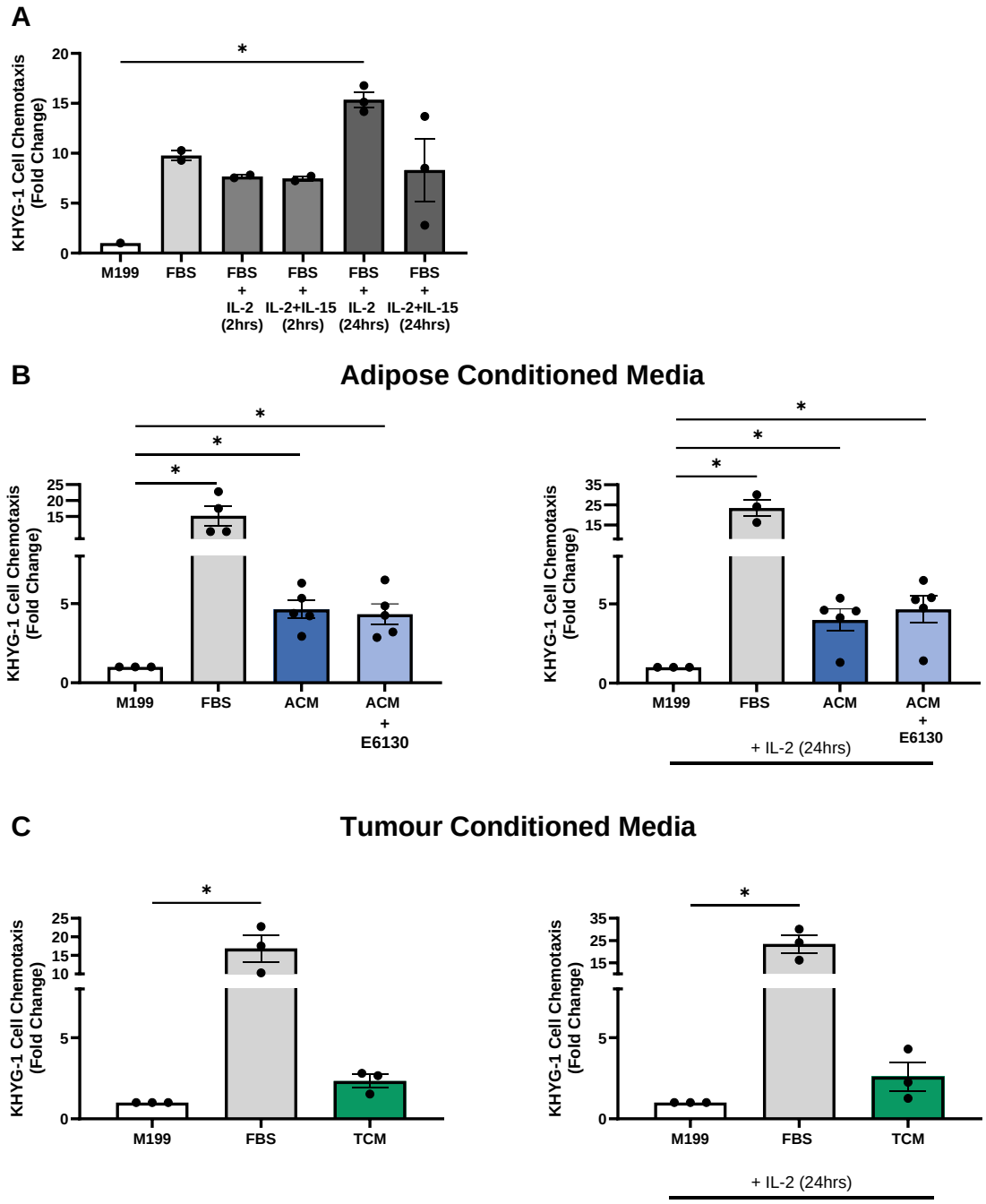

Figure 6.8: E6130 did not significantly reduce KHYG-1 cell migration towards OAC patient-derived ACM

(A) Bar chart showing the paired fold change chemotaxis relative to M199 of KHYG-1 cells towards M199 + 20% FBS (FBS) of non-treated KHYG-1 cells (n=2), with 2hr IL-2 treatment (n=2), or 2hr IL-2+IL-15 treatment (n=2), or 24hr IL-2 treatment (n=3), or 24hr IL-2+IL-15 treatment (n=3). **(B, left)** Bar charts showing the paired fold change chemotaxis relative to M199 of KHYG-1 cells towards (FBS) (n=4) or adipose conditioned media (ACM, n=5), or KHYG-1 pretreated with 4.9nM E6130 (n=5), and **(B, right)** with 24-hour IL-2 boost. **(C, left)** Bar charts showing the paired fold change chemotaxis relative to M199 of NK cells towards FBS (n=3) or tumour conditioned media (TCM, n=5), and **(C, right)** with 24-hour IL-2 boost. *p<0.05, by one sample t test (M199 vs FBS, ACM or TCM) or Mann-Whitney test (ACM vs ACM + E6130) where appropriate. Mean± SEM.

6.3.4.2 KHYG-1 cells express high levels of CXCR3 and spiking the chemokine profile of OAC tumours with IP-10 enhances KHYG-1 cell recruitment

6.3.4.2.1 KHYG-1 cells express much higher levels of CXCR3 compared to blood-derived NK cells

Data from the sections above showed that KHYG-1 cells express lower CX3CR1 but still actively migrated towards ACM. Since E6130 didn't block this migration, other chemokine pathways could be guiding such migration. Results from the baseline screening of chemokine receptor expression in section 6.3.1.4 and 6.3.2.5 in previous sections showed that KHYG-1 cells did not express high levels of CCR2, CCR3, CCR5 or CCR6. Since our group has previously shown that IP-10 (CXCL10) is abundant in the ACM of OAC patients, here the surface expression of the IP-10 receptor, CXCR3, was assessed on KHYG-1 cells [128]. Interestingly, CXCR3 was expressed at a much higher frequency on KHYG-1 cells compared to NK-PBMC; CXCR3: NK-PBMC vs KHYG-1 (2.8% vs 79.9%, n=4) **[Figure 6.9A]**.

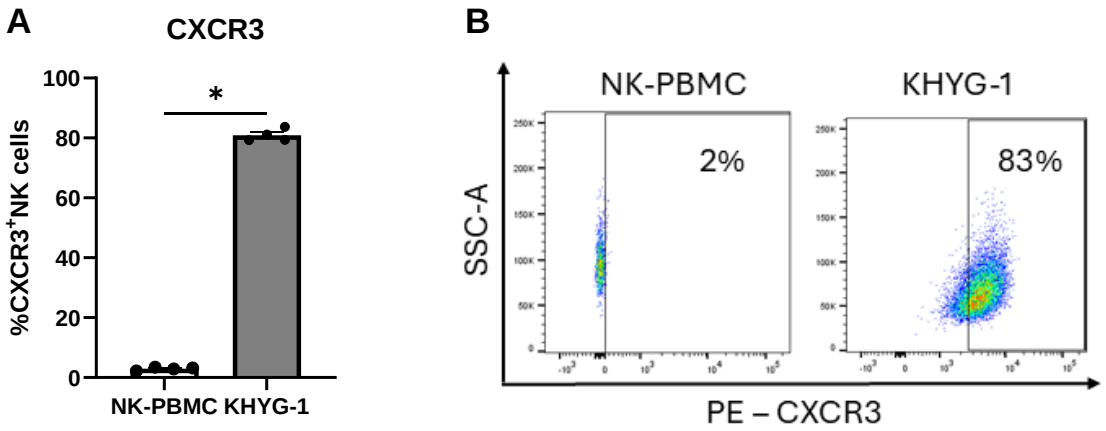

Figure 6.9: KHYG-1 cells express much higher frequencies of CXCR3 compared to blood-derived NK cells

(A) Bar charts showing % cell frequency of $CXCR3^{+}$NK cells derived from PBMC (NK-PBMC) and KHYG-1 cells (n=4). **(B)** Representative dot plots showing gating of $CXCR3^{+}$ NK-PBMC vs KHYG-1 previously gating on viable cells. *$p<0.05$, by Mann-Whitney test Mean± SEM.

6.3.4.2.2 Spiking OAC patient-derived TCM with the chemokine IP-10 (CXCL10) increased KHYG-1 cell migration

To test the hypothesis that KHYG-1 cells might be pulled towards ACM via the CXCR3-IP-10 axis, the migration of KHYG-1 cells towards ACM was investigated with and without pretreatment with 8.2nM of CXCR3 antagonist AMG487. KHYG-1 cell migration was significantly higher towards the positive control (20% FBS) compared to the negative control (M199 only); M199 vs FBS (Fold change: 1 vs 2.8, p=0.006, n=4). KHYG-1 cell migration was significantly higher towards the ACM compared to the negative control; M199 vs ACM (Fold change: 1 vs 10.7, p=0.014, n=4). However, pretreatment with AMG487 did not significantly reduce KHYG-1 cell migration towards ACM as the migration; ACM vs ACM + AMG487 (Fold change: 10.7 vs 9.1, n=4) **[Figure 6.10A]**.

Since supplementation of OAC patient-derived TCM with RANTES and MIP-1α was shown to increase NK cell migration towards TCM, supplementation with IP-10 was assessed to evaluate if it would confer the same for KHYG-1 cells [68]. This was achieved by adding 10ng/ml of IP-10 to the OAC patient-derived TCM. KHYG-1 cell migration was significantly increased towards the positive control compared to the negative control; M199 vs FBS (Fold change: 1 vs 2.8, p=0.006, n=4). KHYG-1 cell migration was significantly increased towards the TCM treated with IP-10 compared to the negative control; M199 vs TCM + IP-10 (Fold change: 1 vs 3.7, p=0.005, n=4), but KHYG-1 cell migration was not significantly increased towards non-treated TCM. Therefore, spiking TCM with IP-10 conferred higher levels of KHYG-1 cell migration **[Figure 6.10B]**.

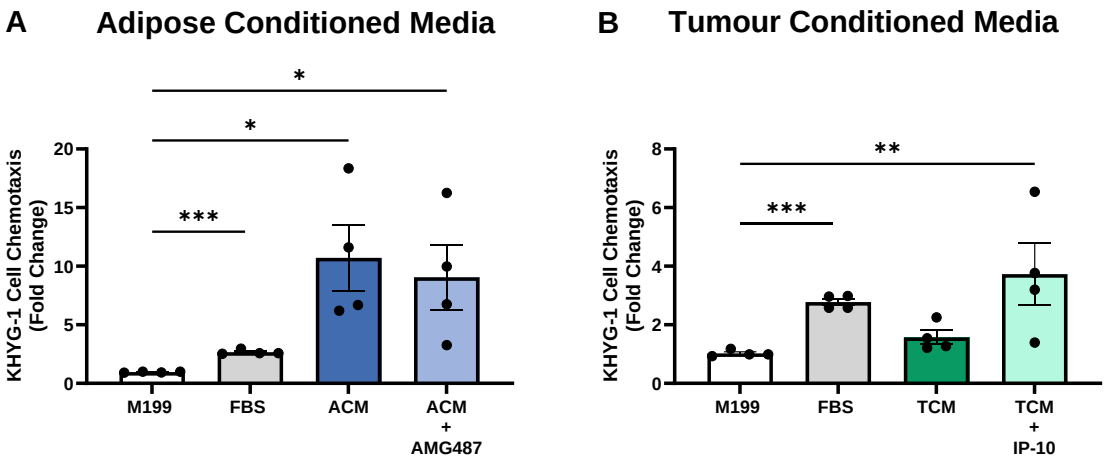

Figure 6.10: Spiking the soluble OAC TME with IP-10 significantly increases KHYG-1 cell migration

(A) Bar chart showing the paired fold change chemotaxis relative to M199 of KHYG-1 cells towards (FBS) (n=4) or adipose conditioned media (ACM, n=4), or KHYG-1 pretreated with 8.2nM AMG487 (n=4). **(B)** Bar chart showing the paired fold change chemotaxis relative to M199 of NK cells towards FBS (n=4) or tumour conditioned media (TCM, n=4) or TCM treated with 10ng/ml of IP-10 (n=4), *p<0.05, **p<0.01, ***p<0.001, by one sample t test (M199 vs FBS, ACM or TCM) or by Mann Whitney test (ACM vs ACM + AMG487, TCM vs TCM + IP-10) where appropriate. Mean± SEM.

6.4 Discussion

The aim of this chapter was to evaluate a cell line-derived NK cell therapy for the treatment of OAC. The KHYG-1 cell line was selected based on its highly cytotoxic activity and amenability to genetic engineering [255, 267]. Here, phenotypical and functional markers of KHYG-1 cells were compared to blood-derived NK cells first to assess if and how they differ. It is well established that $CD56^{dim}$ NK cells elicit higher cytotoxic activity, and express higher levels of the activation receptor CD16 whereas $CD56^{bright}$ NK cells can produce abundant levels of cytokines following monocyte activation, express lower levels of CD16 and have lower cytotoxic functions [411, 412]. The results here confirm that KHYG-1 cells are mostly $CD56^{bright}$ cells and express low CD16 levels basally, which contradicts their reported highly cytotoxic profile as per the reported description of $CD56^{dim}$ NK cells. The data presented here demonstrates that KHYG-1 cells express high NKp30 and NKp44, and upon cytokine activation, they can express high levels of NKG2D and NKp46, which is in line with previous reports on KHYG-1 cell receptor expression [255, 413]. Moreover, the data here show that KHYG-1 cells inherently express higher levels of inhibitory marker NKG2A and immune checkpoint receptor PD-1 compared to blood-derived NK cells. Activated NK cells usually express NKG2A and PD-1, however, overexpression of NKG2A and PD-1 can be associated with chronic effector cell exhaustion, blocking proliferation and cytotoxic functions. Therefore, in the cancer settings, where the ligands for NKG2A and PD-1, HLA-E and PD-L1 and PD-L2, are often elevated on tumour cells, this could potentially lead to inadequate anti-tumour activity [272, 414-417]. KHYG-1 cells have previously been engineered to increase their cytotoxic activity by several means. For example, through the overexpression of epidermal growth factor receptor variant III, CAR-KHYG-1 (EvCAR-KHYG-) cells were primed to more effectively kill EGFRvIII-expressing glioblastoma cells [418]. Therefore, KHYG-1 cells can easily be genetically engineered or modified to augment their killing potential and the data presented here reveal that knock-out of inhibitory receptors might be an additional strategy to achieve this.

Immune cell phenotype and function can be severely altered by the soluble visceral adipose and tumour tissue microenvironment of OAC patients, subsequently influencing the anti-tumour immune response [39, 60, 68, 69, 71, 110, 124, 126, 127, 129, 130]. Our

group has previously demonstrated that blood-derived NK cells from healthy donors exhibited lower expression of activating NK cell receptors (NKRs) NKp30 and NKp46 when cultured in TCM derived from OAC patients with obesity, and lower expression of NKp30 when cultured in OAC patient-derived ACM [68, 69]. Abundant levels of soluble B7-H6, a ligand for NKp30, has been reported in the tumour soluble microenvironment of OAC patients with obesity and we hypothesise that this increased ligand shedding leads to the reduced expression of its receptor NKp30 on NK cells in OAC patients, which is a common immune evasion strategy in cancer [68]. Interestingly, our data show that KHYG-1 cell activating NKRs NKp30, NKp44, NKp46 and NKG2D were not significantly altered by culture in OAC patient-derived ACM or TCM and were expressed at high levels, showing robustness of this cell therapy in the harsh omental and tumour soluble microenvironments. To investigate further the effects of omental and tumour soluble microenvironments on NK cell cytotoxic functions, surface expression of death receptor ligands TRAIL and FasL were assessed, as well as degranulation marker CD107a and activation marker of cytotoxic effector functions CD16 on KHYG-1 cells. Similarly to blood-derived NK cells, the soluble microenvironment of OAC omentum from patients with obesity increased KHYG-1 cell expression of TRAIL and FasL relative to controls, highlighting how ACM from patients with obesity impacts cytotoxic responses of NK cells [342]. CD107a was overall expressed at high levels by KHYG-1 cells and had significantly increased expression when treated with TCM from patients with obesity compared to non-treated cells, demonstrating the cytotoxic potential and perhaps resilience of KHYG-1 cells. However, TRAIL and FasL expression were relatively low in responses to the soluble tumour microenvironment, suggesting that the harsh TME could impact death receptor ligands. KHYG-1 cells have however been shown to be highly cytotoxic in NK cell killing assays against K562 target cells and leukaemia cell lines EM2, EM3 and HL60 [255]. Furthermore, KHYG-1 cells modified with TRAIL variant targeting DR5 (TRAILv-KHYG-1) have shown potential in reducing the viability of ovarian cell line OVCAR-3, and NK-92 cells were engineered with the extracellular domain of TRAIL, resulting in high expression of TRAIL and colorectal cancer cell death, therefore NK cell cytotoxicity can be enhanced against TRAIL sensitive cancer cells [264, 267]. Therefore, our data suggest that if KHYG-1 cells engineered to overexpress TRAIL were introduced to the immunosuppressive TME of OAC patients with obesity, they might elicit their cytotoxic

activity despite the soluble factors. However, given their modest basal expression of TRAIL, further experiments with TRAILv-KHYG-1 cells would be required to confirm such resilience.

KHYG-1 cells express inherently high levels of NKG2A, and results here show how soluble factors from adipose tissue further increased this expression, while also increasing TIGIT expression. This is in line with previous data from our group that showed that ACM from OAC patients elevated immune checkpoint receptors and their ligands TIGIT, A2aR, PD-L2, and CD160 on the surface of T cells [130]. Combining immune checkpoint inhibitors with NK cell therapies or prior genetic knockout of such immune checkpoint molecules could be necessary to maximise the efficacy of KHYG-1 cell therapy in OAC. Current clinical trials are already evaluating NK cell therapy targeting PD-L1 in gastric and head and neck cancer, and is now in phase II, showing promising results (NCT04847466). Interestingly, TCM from patients without obesity decreased PD-1 expression on KHYG-1 cell markers, but not TCM from patients with obesity, further confirming the striking differences between the soluble TME of OAC patients with or without obesity.

In contrast to blood-derived NK cells from healthy donors, IFN-γ producing KHYG-1 cell levels remained unchanged when treated with ACM or TCM [68, 69]. However, lower frequencies of TNF-α producing KHYG-1 cells were observed following TCM treatment, which seem to be mostly due to reduced serum levels as the 20% M199 control (20% M199 diluted in complete RPMI) seemed to have reduced TNF-α producing KHYG-1 cells as well compared to the non-treated control. Our group has previously shown that nutrient deprivation reduced expression of IL-10 and IFN-γ express by T cells [105], and although the levels of FBS in the results presented here are only reduced by 20% compared to the controls, this could show that reduced nutrient supply, a common feature in solid tumours, could reduce TNF-α expression by KHYG-1 cells and must be considered. IL-10 expression by KHYG-1 cells also seemed to be reduced by lower serum levels present in the media, however reduced expression by KHYG-1 cells treated with ACM and TCM from patients without obesity was not observed. ACM from patients with obesity increased CCR5 expression on KHYG-1 cells, which could have potential adverse effects for this NK cell line therapy in OAC as KHYG-1 cells could be sensitive to the chemotactic cues of MIP-1α in OAC patient VAT [128].

As previously discussed, our research group has focused mainly on NK and T cell trafficking in OAC, and how the soluble chemotactic cues of fractalkine can skew NK cell and T cell migration towards the omentum, at the expense of effective migration towards tumour [69, 127, 129]. Reduced migration of immune cells towards the tumour site has been reported in other cancers and remains a focus of chemokine cell-based therapies. Our group has previously reported that fractalkine is abundantly present in the omentum [129] and that E6130 has potential in restoring NK cell migration towards the tumour site by reducing their movement towards the VAT [68, 69, 127]. Furthermore, even though Eotaxin-3 (CCL26) was shown to bind CX3CR1, our group has investigated CCL26 levels in the omentum, and have found that this chemokine is present at very low levels, suggesting that fractalkine is the main CX3CR1 ligand driver of NK cell migration to the omentum [129]. The KHYG-1 cell line was chosen for this study as it has been previously reported to not express CX3CR1 and to not migrate towards the chemotactic cues of fractalkine, compared to the NK-92 cell line [419]. Thus, using this cell line would evaluate if CX3CR1 deficient NK cells could migrate towards the chemotactic cues of the adipose tissue. The results presented here show that even though KHYG-1 cells express lower levels of CX3CR1 than blood-derived NK cells, they actively migrated towards the chemotactic cues of the soluble adipose tissue microenvironment of OAC patients, at significantly higher levels than towards those of OAC tumour. In line with KHYG-1 expressing low levels of CX3CR1 on their surface, it was unsurprising that the CX3CR1 modulator E6130 was ineffective in reducing their migration towards the ACM, unlike blood-derived NK cells [68, 127]. The abundance of other soluble factors within ACM of OAC patients is likely to recruit KHYG-1 cells and this was next evaluated [39, 110, 128]. Berahovich *et al.* showed that KHYG-1 cells expressed CCR6, CXCR3 and CXCR4, and that they migrated towards the ligands to these receptors [419]. Although the omentum of OAC patients has been shown by our group to have abundant levels of the CCR6 ligand MIP-3α (CCL20), results shown here demonstrate that KHYG-1 cells only express CCR6 at very low levels basally [128]. In contrast, CXCR3 was found to be expressed at much higher levels on KHYG-1 cells compared to blood-derived NK cells. Since we have previously shown that IP-10 (CXCL10), a ligand for CXCR3, is highly expressed in the omentum of OAC patients, we assessed whether this pathway governed KHYG-1 cell migration towards VAT[128]. CXCR3 antagonist AMG487 slightly, but not significantly

reduced KHYG-1 cell migration towards the soluble factors of the omentum. However, OAC TCM supplemented with IP-10 elicited superior ability to recruit KHYG-1 cells compared to TCM alone, therefore confirming the potential of IP-10 to augment KHYG-1 cell migration towards OAC tumour. This might lead to a potential means to improve KHYG-1 migration towards tumour, although these data did not identify an effective way to prevent erroneous KHYG-1 cell migration towards the VAT of OAC patients, which could still present a challenge for efficacy of this treatment in this cohort.

In conclusion, this chapter has highlighted key differences between blood-derived NK cells and the KHYG-1 cell therapy in their phenotypic and functional markers. Moreover, the soluble omentum and tumour tissue microenvironment of OAC patients with or without obesity can change KHYG-1 cell phenotype. Results shown here demonstrate that KHYG-1 cells exhibit multiple markers of NK cell activation and retain some interesting cytotoxic features when treated with ACM or TCM compared to blood-derived NK cells. However, their higher expression of inhibitory markers and immune checkpoint inhibitors remain a concern. Such inhibitory profiles could present a challenge in the treatment of OAC patients and KHYG-1 might require prior engineering to elicit potent anti-tumour activity. Importantly and similar to blood-derived NK cells, KHYG-1 cells migrate towards the soluble chemotactic cues of the omentum at greater levels than the tumour of OAC patients. Our data suggest that supplementing the chemokine profile of OAC tumours might help to overcome this. KHYG-1 cells are easily engineered, and other studies have proven the efficacy of these modified cells, therefore future studies beyond the scope of this research might genetically engineer KHYG-1 cells to home more effectively towards OAC tumour and less towards OAC omentum while exhibiting a less inhibitory phenotype [265, 267, 408, 418]. In summary, the data presented here revealed that KHYG-1 present a similar challenge to blood-derived NK cells in terms of their migratory patterns and might require significant genetic modification or combination therapy to optimise their efficacy in OAC.

6.5 Highlights

- KHYG-1 cells exhibit higher surface expression of NKp30, NKp44, NKG2D, NKG2A and PD-1 compared to healthy donor blood-derived NK cells.
- KHYG-1 cells retain high activation marker expression when cultured in ACM and TCM of OAC patients but also retain high expression of NKG2A and TIGIT.
- KHYG-1 cells express low levels of CX3CR1 and their migration towards OAC ACM cannot be reduced by CX3CR1 modulation with E6130 treatment.
- KHYG-1 cells express high levels of CXCR3 and spiking the OAC soluble tumour microenvironment with IP-10 increases their migration.

Chapter 7 - Discussion

7.1 Discussion

OAC arises in a background of chronic inflammation and is characterised by an aggressive phenotype and poor prognosis, with five-year survival rate of less than 25% [4, 7, 10, 11]. Current response rates to chemo-radiotherapy remain low, at approximately 30%, and most patients present with advanced-stage disease, underscoring the urgent need for novel therapeutic strategies [1, 7, 10, 11]. While immunotherapies have revolutionized cancer treatment and shown considerable promise for OAC, their response rates remain below 25%, highlighting the critical need to enhance their efficacy [51, 54, 313]. A deeper investigation into the TME of OAC is essential to identify new therapeutic targets and develop more effective treatment approaches for patients.

Fractalkine is a pro-inflammatory chemokine with diverse functions extending beyond chemotaxis, and previous studies have demonstrated its direct and indirect roles in promoting tumour growth and metastasis in solid malignancies [173, 189, 191-196, 200, 204, 205, 218, 219, 222, 223, 362, 375, 376]. Targeting fractalkine and its receptor, CX3CR1, has emerged as a promising strategy to mitigate its pro-tumourigenic effects while potentially enhancing immune responses in some instances [192, 194, 196, 197, 222, 362]. However, chemokine-targeted therapies in solid tumours have proven challenging due to several factors including the redundancy of the chemokine system, whereby blocking a single target may be insufficient to achieve therapeutic efficacy [226, 330]. Additionally, such therapies can influence the function of multiple immune cell subsets beyond chemotaxis and affect the biological activity of non-immune cells, highlighting the need to thoroughly explore the non-chemotactic functions of chemokines before therapeutically targeting them in cancer. Previous research by our group has demonstrated that fractalkine is a key mediator of the migration of $CD8^+$ T and NK cells to the omentum in OAC, disrupting their essential functions and hindering their migration toward the tumour site [68, 69, 127]. Based on these findings, we have shown that targeting CX3CR1 on NK cells could enhance their abilities to bypass the omentum and home towards oesophageal tumours, potentially rescuing them from dysfunction and depletion, and ultimately improving anti-tumour immunity in OAC patients [68, 69, 127]. However, the broader biological role of fractalkine in tumourigenic processes in OAC remains unclear. This study aimed to elucidate the role of fractalkine

in OAC tumour growth and progression and assessed whether CX3CR1 modulation can counteract any tumour-promoting effects. Furthermore, while NK cell-based immunotherapies have demonstrated significant potential in cancer treatment, their efficacy in solid tumours remains limited, primarily due to poor infiltration and the immunosuppressive nature of the solid TME [242, 243, 420-423]. Here, the phenotypical and functional characteristics of KHYG-1 cell therapy (previously reported to exhibit strong cytotoxicity) were compared to blood-derived NK cells, to evaluate their potential as a novel immunotherapeutic approach for OAC [255, 256].

This study firstly demonstrated that fractalkine slightly but consistently increases OAC cell viability and proliferation in a panel of different cell lines, including radioresistant and cisplatin resistant cell lines, indicative of fractalkine's pro-tumourigenic role in OAC. To our knowledge, this is the first study to uncover a direct role for fractalkine in OAC tumour cell growth. Previous studies on gastric cancer patients have reported higher expression of fractalkine and CX3CR1 to correlate with cancer cell metastasis, proliferation and survival, while also finding that this pathway could play a role in paclitaxel resistance in gastric cancer cells [189, 214, 424]. Furthermore, the results shown here demonstrated that treatment with recombinant fractalkine increased FLO-1 cell migration towards fractalkine-rich FLO-1^{LM} supernatant, which were used here as a surrogate way of recapitulating the soluble cues of the metastatic liver microenvironment. Primary OAC tumours are inclined to metastasise to sites such as the liver and the omentum, therefore, our data suggest that exposure to fractalkine primes OAC tumour cells for migration towards the fractalkine-rich metastatic site of the liver [354, 355]. This is in line with previous research on prostate cancer cell lines where high levels of dihydrotestosterone increased release of soluble fractalkine in bone cells, and in turn increased prostate cancer cell migration towards the bone marrow [362]. In addition, our data revealed that CX3CR1^{+}FLO-1 cells exhibited higher expression of markers typically associated with epithelial-mesenchymal transition (EMT) such as SLUG and Vimentin and lower E-cadherin, compared to their CX3CR1^{-} counterparts. These data suggest that CX3CR1 expression by OAC tumours could be associated with higher metastatic potential. In addition, CX3CR1^{+}FLO-1 cells displayed higher expression of stem cell like markers CD24 and CD34, suggesting that CX3CR1 expression represents a survival advantage in OAC

tumours. Previous studies in epithelial ovarian cancer have shown that higher expression of CX3CR1 is associated with lower survival for these patients, while CX3CR1 expression in murine models of colorectal cancer, has been associated with tumour cell survival advantage through the fractalkine-CX3CR1 axis, facilitating tumour cell migration, generation of a pro-metastatic niche, and attraction of inhibitory myeloid cells, contributing to immune evasion and resistance to therapies such as anti-PD-1 [219, 376]. Overall, these data reinforce our hypothesis of fractalkine as a driver of tumorigenesis and demonstrate its influence in several hallmarks of cancer such as sustaining proliferative signalling, activating invasion and metastasis and resisting cell death, thus supporting the potential of therapeutically targeting fractalkine [425-427].

To investigate the potential of therapeutically targeting fractalkine in OAC, this study evaluated whether E6130, a CX3CR1 modulator, could attenuate fractalkine-mediated effects on OAC tumours. E6130 has been shown by our group to have potential to rescue NK cells from the chemotactic cues of the omentum in OAC [68, 127]. The next goal of this study was to evaluate if CX3CR1 modulation had additional anti-tumour properties beyond altering NK cell migration in OAC. Considering that E6130 would be administered systematically if used as a treatment in OAC patients, the same dose which effectively reduced NK cell migration to OAC omentum (based on IC50 value 4.9nM) was used in this study [68, 69, 185]. The data presented in this thesis demonstrated firstly that E6130 attenuated fractalkine-induced increases in cell viability and proliferation in OAC cell lines, including radioresistant and cisplatin-resistant OAC cell lines. This is in line with previous studies which showed that CX3CR1 antagonism using JMS-17-2 reduced fractalkine-induced motility, invasion and growth in pancreatic cancer cell lines [203]. Importantly here, these results were validated in *ex vivo* OAC tumour patient samples in which treatment with E6130 induced cytotoxicity and reduced viability in tumour cells, in line with a previous mouse model study of breast cancer which has shown that CX3CR1 antagonism can impair metastasis of circulating tumour cells, by directly reducing tumour growth and proliferation [428]. However, our data revealed that E6130 treatment alone was not sufficient to significantly reduce FLO-1 cell migration towards FLO-1^{LM} supernatant, suggesting that E6130 may have more utility in the impedance of primary tumour growth but not metastasis to the liver. These migration studies were performed

using *in vitro* models and further studies are needed to elucidate whether targeting fractalkine has anti-metastatic effects. Modulation of other chemokines or more than one chemokine pathway could prove more effective. For example, targeting CXCR2 and CXCR4 has previously shown promise in curbing OAC and OSCC invasion and metastasis [227, 228, 234]. Overall, our data show for the first time that E6130 has potential to directly counteract fractalkine's effects on OAC tumour cell viability and proliferation and elicits tumouricidal activity *ex vivo*.

This study focused on evaluating the effects of E6130 on cell viability, proliferation, migration, EMT, and cell cycle distribution in cell lines and assessed the effects of E6130 on patient tumour samples, healthy blood-derived NK cells and blood-derived NK cells from OAC patients. However, a limitation of this study is that it still remains unclear how E6130 reduced cell viability and proliferation in OAC cell lines. Cell cycle distribution was not altered after E6130 or fractalkine treatment, and following 24-hour treatment with E6130, no OAC cell line had modified expression of fractalkine, showing that E6130 does not alter fractalkine secretion. E6130 did not alter surface expression of CX3CR1 by FLO-1 cells, nor healthy or OAC patient derived NK cells. However, it slightly but consistently reduced CX3CR1 expression on intratumoural NK cells from OAC patient tumour samples. Wakita *et al*. showed that E6130 induced reductions in CX3CR1 surface expression in NK cells derived from human peripheral blood, and the study concluded that inhibition of NK cell chemotaxis to fractalkine was regulated this way [185]. They however only treated NK cells for 30 minutes prior to evaluating CX3CR1 expression on their cell surface, therefore, as this study evaluated the effects of E6130 after 24 hours to match timepoint with fractalkine treatment, further timepoints must be investigated to assess the effects of E6130 on CX3CR1 expressing NK cells. A computational study on CX3CR1 and its antagonist and agonist ligands concluded that E6130 has partial or biased agonist activity with CX3CR1, which suggested that it could selectively activate specific pathways downstream of the receptor while avoiding or reducing activation of others, which has been reported in other chemokine receptor antagonists such as CXCR4 antagonist AMD11070 [348, 429]. Interestingly, the data presented in this report also showed that pretreatment with E6130 did not reverse fractalkine-induced endocytosis on NK cells, suggesting that E6130 does not block fractalkine binding to the receptor. As

E6130 is a modulator, and perhaps a partial or biased agonist, it is possible that E6130 could selectively disrupt downstream signalling cascades by binding to the G protein coupled receptor CX3CR1 [185, 429]. Soluble fractalkine binding to CX3CR1 has been shown to activate downstream JAK/STAT and Src-FAK pathways, both shown to regulate cell survival, proliferation and migration, but also the PI3K and MAPK pathways, shown to contribute to proliferation and angiogenesis [173, 192, 193, 217, 430]. Moreover, Fractalkine:CX3CR1 binding can also activate calcium release resulting in chemotaxis [431, 432]. Therefore, E6130 could disrupt fractalkine-induced signalling of one or more of these pathways.

Since our data revealed associations between CX3CR1 expression and EMT phenotype and stemness in FLO-1 cells, the distinct subpopulations of CX3CR1^{+} cells were next investigated i.e. CX3CR1^{low} and CX3CR1^{high}. Previous studies by others have shown that breast and prostate cancer cell lines that are CX3CR1^{high} cells display higher stemness markers, transcriptomic signatures enriched in pluripotency-regulating pathways and metastasis-initiating behaviours in mouse models [361]. In line with these studies, our data showed that CX3CR1^{high}FLO-1 cells drove the higher expression of CD24 and CD34, thus potentially indicating the CX3CR1^{high} expression corresponds with stemness. Next, the independent behaviour of CX3CR1^{-} and CX3CR1^{+} FLO-1 cells were next scrutinized through cell sorting and subsequent functional assays. However, cell sorting into CX3CR1^{-} and CX3CR1^{+} FLO-1 cell populations revealed that FLO-1 cells could only maintain the homogenous CX3CR1^{-} or CX3CR1^{+} phenotype for a short period with the emergence of heterogenous populations of CX3CR1^{-} and CX3CR1^{+} FLO-1 cells in each sorted fraction within several days. Therefore, these data indicate that heterogenous populations of CX3CR1^{-} and CX3CR1^{+} cells are beneficial for FLO-1 cells. From an experimental viewpoint, knockdown/out of CX3CR1 would be warranted to conduct such studies on the individual growth and survival patterns of CX3CR1^{-} and CX3CR1^{+} FLO-1 cells.

The TME is a complex microenvironment that is important to consider when evaluating a new immunotherapy, as it can be shaped by many physiological conditions such as hypoxia, nutrient deprivation and acidosis, which have profound effects on tumour growth, immune cell recruitment, activation, polarisation and cytokine and chemokine

release [318, 321, 324, 325, 327, 331]. Here, moderate acidosis (pH 6.6) increased CX3CR1 surface expression by FLO-1 cells and conferred enhanced susceptibility to fractalkine via increased FLO-1 cell viability, compared to optimal conditions. The physiological conditions of the TME have already been shown to impact the fractalkine:CX3CR1 axis in pancreatic, prostate and ovarian cancer under hypoxia, as the CX3CR1 gene has response elements that can bind to HIF-1α, which upregulates CX3CR1 expression [216, 218, 222]. However, to our knowledge, our data is the first report that acidosis can increase CX3CR1 expression and susceptibility to fractalkine in OAC. Previous research in our group has already shown that acidosis could increase the expression of immune checkpoints on T cells, which could undermine anti-tumour immunity and contribute to disease progression in OAC [106]. As previous research has demonstrated that the physiological condition of acidosis within the TME profoundly impacts tumour growth, especially in solid tumours with pH levels falling between 5.7 and 7.0 [321], the data generated here suggest that fractalkine may be another driver of such processes in OAC [106]. Importantly, E6130 retained its effects under the three physiological conditions of the TME evaluated here (nutrient deprivation, moderate acidosis and hypoxia (0.5%)) as it attenuated fractalkine-induced increases in cell viability in FLO-1 cells. These data suggest that E6130 has potential to attenuate OAC viability and growth under the conditions of the TME and has potential to counteract increased CX3CR1 expression and enhanced susceptibility to fractalkine in OAC tumours.

In the context of OAC, our group has already shown that NK cells and $CD8^+$ T cells preferentially migrate to the visceral adipose tissue (VAT), which contains high levels of fractalkine, where they undergo functional alterations and in the case of NK cells, apoptosis [69, 127, 129]. This hinders their availability to migrate to the oesophageal tumour site and indeed, our previous data found that prevalence of NK cells in OAC tumour negatively correlates with visceral obesity [127]. The results presented here demonstrated that fractalkine is much more abundant in the omentum and the liver of OAC patients compared to tumour tissue, thus reinforcing these findings [127]. One study in gastric cancer has demonstrated that higher fractalkine expression in tumour samples correlated with higher NK cells and $CD8^+$T cell infiltration, while also correlating with better prognosis [187]. However, in the context of OAC, this has not been shown,

and despite higher levels of fractalkine observed in tumours from OAC patients without obesity compared to patients who are overweight or with obesity, the levels of fractalkine in the omentum and liver compartments swamp those of the tumour and should be targeted with therapeutic intent while other chemokine pathways might be exploited to enhance the immune infiltration of OAC tumours [39, 68, 69, 127]. In fact, our group used our novel *ex vivo* model to show that treating NK cells with E6130 or remodelling the TME with RANTES and MIP-1α could redirect NK cells away from the chemotactic cues of the adipose conditioned media (ACM) and towards tumour conditioned media (TCM) [68]. Since E6130 would be administered systemically if it was used in a clinical setting, it was important to investigate its direct effect on tumour cells and its possible effects on the cytokine profile of the OAC TME. In this study, treatment of OAC patient tumour samples with E6130 decreased IFN-γ levels and increased TNF-α, IL-2 and IL-15. IL-2 and IL-15 are important cytokines for NK cell proliferation and activation, and our group has previously shown that fractalkine negatively impacted IL-15-mediated activation of death receptor ligands TRAIL and FasL and adhesion molecule expression by NK cells [69]. Moreover, our previous research has shown that IL-15 is present at very low levels in the TME of OAC, but treatment with IL-15 boosted NK cell migration towards the soluble factors of OAC tumours, therefore, E6130-mediated increases of IL-15 levels could boost activation of NK cells at the tumour site while lessening the deleterious effects of fractalkine [69]. While IL-2 is an important NK cell cytokine, it must also be noted that it supports Treg persistence, which could be an undesirable effect in this context [281, 283]. E6130-mediated decreases in IFN-γ levels at the tumour site could reduce pro-inflammatory effects and contribute to regulating cytokine production in the TME and this is in line with our groups previous results where we found that NK cell production of IFN-γ is significantly increased by fractalkine treatment [127]. E6130-mediated induction of TNF-α in the TME is likely to promote apoptosis of tumour cells suggesting how E6130 might induce OAC tumour cell death [400]. It is important to note that TNF-α can also induce fractalkine expression and vice versa, suggesting that this increase might later lead to more fractalkine production and counteract the effects of E6130 *in vivo* [127, 393, 394]. Further multiplex ELISAs evaluating a broader panel of cytokines, which were beyond the scope of this study, are needed to confirm the broader impact of E6130 on

the cytokine profile of OAC tumours and the effects on immune cell recruitment and activation.

The non-chemotactic role of fractalkine on NK cells has previously been demonstrated by our group as it can induce the conversion of $CX3CR1^{+}CD27^{-}$NK cells to $CX3CR1^{-}CD27^{+}$NK cells and increase their IFN-γ and TNF-α production [127]. Therefore, this study evaluated the effects of E6130 on the phenotype and functionality of healthy NK cells from the peripheral blood, NK cells from the peripheral blood of OAC patients and in intratumoural NK cells from OAC patient tumour samples. There were overall no significant differences found on activating or inhibitory receptor expression or cytokine production by NK cells after E6130 treatment, suggesting that E6130's main effect on NK cells is to reduce their migration towards fractalkine. This would be highly beneficial in the context of OAC as our group has previously shown that circulating $CX3CR1^{+}$ NK cells of OAC patients remain highly cytotoxic, and therefore E6130 would not impair their activation or functionality [68].

Our previous research on NK cell responses in OAC has uncovered important knowledge on the potential of NK cell immunotherapies and the challenges their efficacy might face [39, 68, 69, 127]. The data presented in this study investigated if the NK cell therapy KHYG-1 could be therapeutically applicable in OAC and if it is susceptible to the challenges we reported for blood-derived NK cells in these patients [255]. Firstly, this study demonstrated that KHYG-1 cells actively migrate towards the soluble adipose tissue microenvironment of OAC patients, at significantly higher levels than towards those of OAC tumour, similarly to blood-derived NK cells. It must be noted that KHYG-1 cells exhibit such migratory preferences toward the omentum, despite their lower expression of CX3CR1. Indeed, the results shown here revealed that KHYG-1 cell migration towards ACM cannot be attenuated using E6130, most likely due to their low surface expression of CX3CR1 (reducing their amenability to E6130), but also suggesting that other chemokines in the omentum of OAC patients play a larger role in the recruitment of KHYG-1 cells. Surprisingly, KHYG-1 cells were shown here to express much higher levels of CXCR3 compared to blood-derived NK cells, and as our group has previously shown high expression of its ligand IP-10 (CXCL10) in ACM in OAC patients [110], this chemokine axis was next evaluated to assess if it could potentially be targeted.

KHYG-1 cell migration toward OAC patient-derived ACM could however not significantly be attenuated by pre-treating them with the CXCR3 antagonist AMG487, suggesting that other and/or multiple chemokine pathways must be targeted to counteract KHYG-1 migration towards OAC omentum. Targeting CXCR3 in cancer immunotherapies remains a challenging approach as this receptor has three ligands (CXCL9/MIG, CXCL10/IP-10 and CXCL11/I-TAC), but it has shown some potential in mouse models of melanoma where by inhibition of CXCR3 on NK cells in combination with IL-15 treatment increased their bone marrow homing capacity and contributed to melanoma clearance [433]. Interestingly, the migration of KHYG-1 cells towards the soluble microenvironment of OAC patient tumour could be enhanced by spiking the TCM of OAC patients with IP-10. Therefore, while we did not identify a means by which erroneous KHYG-1 cell migration towards omentum could be targeted, we have identified remodelling the TME with IP-10 as a means through which their homing to OAC tumour can be augmented.

The soluble visceral adipose and tumour tissue microenvironment in OAC patients profoundly alters immune cell phenotype and function, thereby modulating the anti-tumour immune response [39, 60, 68, 69, 71, 110, 124, 126, 127, 129, 130]. Our group previously demonstrated that blood-derived NK cells from healthy donors exhibited reduced expression of activating NK cell receptors when cultured in TCM from OAC patients with obesity, with a specific reduction in NKp30 expression in ACM [68, 69]. Notably, elevated levels of soluble B7-H6, the ligand for NKp30, have been reported in the tumour microenvironment of obese OAC patients. The results presented here suggest that KHYG-1 cells, which were developed from a malignant source, are phenotypically very different from blood-derived NK cells, but show some robustness in the TME as they retain high expression of activating NKRs NKp30, NKp44, NKp46 and NKG2D when cultured with ACM and TCM of OAC patients. However, similarly to blood-derived NK cells, low expression of TRAIL and FasL receptor on KHYG-1 cells were observed in response to the soluble tumour microenvironment, despite previous studies reporting their highly cytotoxic potential [255]. Additionally, the data presented in this study demonstrated that KHYG-1 cells express inherently high levels of inhibitory receptor NKG2A and immune checkpoint receptor PD-1, which could lead to undesirable inhibition of KHYG-1 cells in the OAC TME since HLA-E, PD-L1 and PD-L2 have been

reported to be elevated in OAC [272, 414-417]. Therefore, prior genetic knockout of immune checkpoint receptor or combining immune checkpoint inhibitors could be necessary to maximise their efficacy in OAC. Current clinical trials are already evaluating NK cell therapy targeting PD-L1 in gastric and head and neck cancer showing promising results (NCT04847466). Moreover, other studies have proven the efficacy of genetically modifying KHYG-1 cells to enhance their anti-tumourigenic functions, therefore future studies beyond the scope of this research might genetically engineer KHYG-1 cells to home more effectively towards OAC tumour and less towards OAC omentum while exhibiting a less inhibitory phenotype [265, 267, 408, 418]. As the ultimate goal of this study was to use NK cell therapies in combination with E6130 to boost NK cell migration towards OAC tumours and use E6130 as an anti-tumourigenic compound, combining E6130 with the KHYG-1 cell therapy would not prove beneficial in this context, as E6130 could not prevent KHYG-1 cell migration towards ACM of OAC patients. Therefore, using E6130 alone or in combination with healthy donor blood-derived NK cell therapy could be a better therapeutic strategy in OAC.

In conclusion, this study has uncovered the pro-tumourigenic role of fractalkine in OAC as it was shown to promote cell viability, proliferation and migration of OAC tumour cells. Interestingly, these fractalkine-mediated effects could be mostly reversed by CX3CR1 modulator E6130, which has previously shown efficacy to redirect NK cell migration away from OAC omentum and towards the soluble cues of OAC tumour. Moreover, the tumouricidal activity of E6130 was validated in *ex vivo* OAC patient tumour samples highlighting the anti-cancer therapeutic potential of this drug in OAC. Additionally, these data have uncovered associations between CX3CR1 expression in OAC tumour cells and stemness and metastatic potential suggesting that CX3CR1 expression confers a survival advantage and might hold prognostic utility. However, validation in patient samples would be warranted to confirm and validate this hypothesis. Importantly, E6130 elicited direct non-chemotactic anti-cancer effects on OAC tumours, and didn't detrimentally affect NK cell phenotype and function.

Finally, this study revealed that while KHYG-1 cell therapy has promising features, many hurdles must be overcome for this therapy to be used in the context of OAC and combining E6130 with KHYG-1 cell therapy present no added advantages to KHYG-1

infiltration of OAC tumour, unlike blood-derived NK cells. If E6130 was selected as a combination strategy with NK cell therapy, our data suggest that blood-derived NK cells would be a superior source for therapeutic pairing with E6130.

7.2 Future directions

Here we have demonstrated that fractalkine has a direct pro-tumourigenic role in OAC and enhances several hallmarks of cancer [425-427]. Moreover, CX3CR1^{+} OAC cells express EMT and stem-like markers which could provide them with a survival advantage over their CX3CR1^{-} counterparts. However, one of the limitations of this study was to uncover the differences in viability and growth of CX3CR1^{+} compared to CX3CR1^{-} OAC cells. As cell sorting decreased cell viability of FLO-1 cells, gene knock-out of CX3CR1 and/or overexpression of CX3CR1 on FLO-1 cells could be an alternative way to study biological differences between CX3CR1^{-} and CX3CR1^{+} OAC tumour cells and to assess if overexpression of CX3CR1 can enhance even further cell proliferation and migration, as seen in gastric cancer cell lines [189]. Moreover, this study showed that CX3CR1 modulator E6130 attenuated fractalkine-mediated increases in cell viability and proliferation in OAC cell lines, and reduced viability and increased cytotoxicity in OAC patient tumour samples [68]. However, systemic use of E6130 could elicit unwanted side-effects on other high expressors of CX3CR1, especially immune cells such as monocytes, macrophages, DCs, CD8^{+}T cells and γδ T cells, therefore, further studies are needed to evaluate the off-target effects of E6130 on these immune cells [129, 170].

This study demonstrated some compelling evidence to use E6130 to reduce the detrimental effects of fractalkine, however, it also showed that E6130 alone could not attenuate fractalkine-induced increased migration of FLO-1 cells towards FLO-1^{LM} supernatants, used here as a representative of the soluble cues of the metastatic liver microenvironment [311]. Therefore, further studies investigating combination therapies to target multiple chemokine receptors could be a valid approach in the context of OAC to inhibit metastasis. For example, combining E6130 with a CXCR4 antagonist Plerixafor or BL-8040, which are already in clinical trials for the treatment of oesophageal cancers, could perhaps have added anti-tumourigenic effects (NCT02179970, NCT03281369) [226]. Unpublished data from our group showed that CXCR4 antagonist AMD3100 attenuated OE33 cell migration towards lymph node conditioned media generated from

OAC patient samples, while CXCR4 expression was significantly increased on OE33 cells after 24-hour treatment with liver conditioned media generated from OAC patient samples. As CXCL12 is the sole ligand for CXCR4 and has already been shown to contribute to tumour metastasis in gastric and oesophageal squamous cell carcinoma cells, targeting CXCR4 and CX3CR1 could work synergistically to target OAC tumour metastasis [134, 156].

The next step to evaluate if E6130 has therapeutic potential in OAC would be to investigate its effect *in vivo* in animal models of OAC. A key limitation in OAC research is the absence of obese mouse models that accurately reflect the intricate interactions between obesity, the immune system, and cancer. Fat deposition in mice differs from humans, as their adipose tissue accumulates in fat pads rather than visceral adipose tissue (VAT) depots [434]. Although the mesenteric fat pad is the closest equivalent to human VAT, studies often use perigonadal fat pads due to their accessibility [434]. Another challenge in modelling OAC is the difference in chemokine receptor and ligand expression between mice and humans, which complicates the development of chemokine-based immunotherapies [435, 436]. Moreover, while existing models of the BO-to-OAC progression have been subjected to high-fat diets, accelerating carcinogenesis, the development of BO itself can take up to nine months in these mice models [437]. Patient-Derived Xenografts (PDXs) models have been shown as reliable models for the study of OAC as they retain the tumour's architecture and complexity, however, they remain challenging and time-consuming [438, 439]. However, the development of patient-derived organoids in OAC and BO in recent years has provided an alternative way of investigating the effects of drugs on a dynamic model and has bridged the gap between *in vitro* cell models and PDXs models, which could also be a desirable way of investigating the effects of E6130 [440]. Our previous research on OAC underscores the complexity of visceral obesity in OAC, demonstrating its influence on the omental and tumour microenvironments while exerting systemic effects on NK cells [39, 68, 69, 127]. These findings highlight the necessity of considering obesity status in the design and application of immunotherapies. The next step of this research, which was beyond the scope of this study, would be to generate PDX mouse models of OAC which would use OAC patient blood, tumour and omentum samples to recapitulate the

complexity of the OAC patient i.e. a PDX model with humanized immune system, orthotopically implanted tumour and visceral obesity. Alternative models of OAC have already been explored in our group to address this e.g. our *ex vivo* benchtop model which recapitulates the competing compartments of omentum and tumour in OAC patients and uncovers their simultaneous effects on immune cell migration and chemokine-targeted therapy efficacy [68]. Organ-on-a-chip microfluidic devices have also recently been explored in cancer research to recapitulate physiology and pathophysiology with high fidelity, which in the context of OAC could recapitulate the complexity of the VAT and chemokine system [441].

New immunotherapies are likely to first be tested as 2nd or 3rd line treatment in OAC patients, and as the standard-of-care in OAC usually includes chemo-radiation therapy and surgery, evaluating their impact on any potential immunotherapy is prudent. While this study explored the effects of fractalkine on radioresistant and cisplatin resistant OAC cell lines and found that E6130 seems to retain the same effects seen in non-treatment resistant cell lines, more in-depth analysis is needed to assess each element of chemo-radiation therapy in combination with E6130. Furthermore, our research group has shown that the FLOT regimen increased B7-H6 shedding by OAC cells, however cisplatin resistant OAC cell line supernatants do not significantly impede NK cell functions or degranulation, which is promising for implementing NK cell therapies in OAC [71]. Further research is required to fully assess the effects of chemo-radiation therapy on NK cell therapies and in combination with E6130.

This study uncovered important phenotypical and functional aspects of the KHYG-1 cell therapy. Importantly, it highlighted certain hurdles this cell therapy could face in the harsh TME of OAC and would most likely need to be engineered to resist the chemotactic cues of the VAT. Another alternative to develop NK cell therapies for the treatment of OAC would be to develop cytokine-induced memory-like (CIML) NK cells, derived from healthy donor blood. They exhibit enhanced persistence, proliferation, and cytokine production and could be a strategy for improving the cytotoxicity and memory response of NK cells in immunotherapy settings [291]. A clinical trial is currently evaluating the safety of CIML NK cells with low-dose IL-2 in high-grade ovarian cancer (NCT06321484). As CIML NK cells have been shown to have enhanced cytotoxicity against tumour cells

but retain phenotypic similarities to “conventional” NK cells, their combination with E6130 could ultimately boost NK cell infiltration and killing of tumour while also directly impede tumour growth in OAC and our group is currently exploring this [442, 443].

Chapter 8 - References

References

1. Blot, W.J., S.S. Devesa, and J.F. Fraumeni, Jr., *Continuing climb in rates of esophageal adenocarcinoma: an update.* JAMA, 1993. **270**(11): p. 1320.
2. Tanaka, T., et al., *Outcomes of multimodality therapy for stage IVB esophageal cancer with distant organ metastasis (M1-Org).* Dis Esophagus, 2010. **23**(8): p. 646-51.
3. Oesophageal Cancer Fund. *About Oesophageal Cancer* 2024 [cited 2025 January]; Available from: https://ocf.ie/about-oesophageal-cancer/.
4. National Cancer Registry Ireland. *Cancer in Ireland 1994-2022, Annual Statistical Report of the National Cancer Registry 2025*. 2025 [cited 2025 March]; Available from: https://www.ncri.ie/sites/ncri/files/pubs/NCRI_AnnualStatReport_2024_FINAL_14.pdf.
5. Cancer Research Institute. *Immunotherapy for: Oesophageal cancer*. 2025 January, 2025]; Available from: https://www.cancerresearch.org/cancer-types/esophageal-cancer.
6. Irish Cancer Society. *Oesophageal Cancer*. [cited 2025 January, 21]; Available from: https://www.cancer.ie/cancer-information-and-support/cancer-types/oesophageal-cancer.
7. Oncology, A.S.o.C. *Esophageal Cancer: Statistics*. 2025 January, 2021]; Available from: https://www.cancer.net/cancer-types/esophageal-cancer/statistics#:~:text=Worldwide%2C%20an%20estimated%20604%2C100%20people,diagnosed%20with%20squamous%20cell%20carcinoma.
8. World Health Organization. *The global landscape of esophageal squamous cell carcinoma and esophageal adenocarcinoma incidence and mortality in 2020 and projections to 2040: new estimates from GLOBOCAN 2020*. 2022 [cited 2025 January]; Available from: https://www.iarc.who.int/news-events/the-global-landscape-of-esophageal-squamous-cell-carcinoma-and-esophageal-adenocarcinoma-incidence-and-mortality-in-2020-and-projections-to-2040-new-estimates-from-globocan-2020/.
9. NHS Inform. *Oesophageal Cancer*. 2024 [cited 2025 January]; Available from: https://www.nhsinform.scot/illnesses-and-conditions/cancer/cancer-types-in-adults/oesophageal-cancer#causes-of-oesophageal-cancer)n.
10. American Cancer Society. *Survival Rates for Esophageal Cancer*. 2025 [cited 2025 June, 24]; Available from: https://www.cancer.org/cancer/esophagus-cancer/detection-diagnosis-staging/survival-rates.html.
11. Siegel, R.L., et al., *Cancer statistics, 2025.* CA Cancer J Clin, 2025. **75**(1): p. 10-45.
12. El-Serag, H.B., et al., *Update on the epidemiology of gastro-oesophageal reflux disease: a systematic review.* Gut, 2014. **63**(6): p. 871-80.
13. Hampel, H., N.S. Abraham, and H.B. El-Serag, *Meta-analysis: obesity and the risk for gastroesophageal reflux disease and its complications.* Ann Intern Med, 2005. **143**(3): p. 199-211.
14. Savarino, E., et al., *Advances in the physiological assessment and diagnosis of GERD.* Nat Rev Gastroenterol Hepatol, 2018. **15**(5): p. 323.
15. Valdovinos Diaz, M.A., et al., *Good clinical practice recommendations for the diagnosis and treatment of gastroesophageal reflux disease. An expert review*

from the Asociacion Mexicana de Gastroenterologia. Rev Gastroenterol Mex (Engl Ed), 2024. **89**(1): p. 121-143.
16. Jacobson, B.C., et al., *Body-mass index and symptoms of gastroesophageal reflux in women.* N Engl J Med, 2006. **354**(22): p. 2340-8.
17. Bashir, Y., et al., *Systematic review and meta-analysis on the effect of obesity on recurrence after laparoscopic anti-reflux surgery.* Surgeon, 2019. **17**(2): p. 107-118.
18. Domper Arnal, M.J., A. Ferrandez Arenas, and A. Lanas Arbeloa, *Esophageal cancer: Risk factors, screening and endoscopic treatment in Western and Eastern countries.* World J Gastroenterol, 2015. **21**(26): p. 7933-43.
19. Spechler, S.J., *Barrett's esophagus: Clinical issues.* Gastrointest Endosc Clin N Am, 2011. **21**(1): p. 1-7.
20. Shaheen, N.J., et al., *ACG Clinical Guideline: Diagnosis and Management of Barrett's Esophagus.* Am J Gastroenterol, 2016. **111**(1): p. 30-50; quiz 51.
21. Sawas, T. and D.A. Katzka, *Esophageal adenocarcinoma phenotypes and risk factors.* Curr Opin Gastroenterol, 2022. **38**(4): p. 423-427.
22. Peters, Y., et al., *Barrett oesophagus.* Nat Rev Dis Primers, 2019. **5**(1): p. 35.
23. O'Sullivan, K.E., et al., *The role of inflammation in cancer of the esophagus.* Expert Rev Gastroenterol Hepatol, 2014. **8**(7): p. 749-60.
24. Theron, B.T., et al., *The risk of oesophageal adenocarcinoma in a prospectively recruited Barrett's oesophagus cohort.* United European Gastroenterol J, 2016. **4**(6): p. 754-761.
25. Zellenrath, P.A., et al., *Neoplastic Progression Risk in Females With Barrett's Esophagus: A Systematic Review and Meta-Analysis of Individual Patient Data.* Clin Gastroenterol Hepatol, 2025. **23**(2): p. 225-235 e8.
26. World Health Organization. *Obesity and overweight*. 2024 [cited 2025 January]; Available from: https://www.who.int/news-room/fact-sheets/detail/obesity-and-overweight.
27. Ng, M., et al., *Global, regional, and national prevalence of overweight and obesity in children and adults during 1980-2013: a systematic analysis for the Global Burden of Disease Study 2013.* Lancet, 2014. **384**(9945): p. 766-81.
28. Guh, D.P., et al., *The incidence of co-morbidities related to obesity and overweight: a systematic review and meta-analysis.* BMC Public Health, 2009. **9**: p. 88.
29. Kyrgiou, M., et al., *Adiposity and cancer at major anatomical sites: umbrella review of the literature.* BMJ, 2017. **356**: p. j477.
30. Lysaght, J. and M.J. Conroy, *The multifactorial effect of obesity on the effectiveness and outcomes of cancer therapies.* Nat Rev Endocrinol, 2024. **20**(12): p. 701-714.
31. Wensveen, F.M., et al., *The "Big Bang" in obese fat: Events initiating obesity-induced adipose tissue inflammation.* Eur J Immunol, 2015. **45**(9): p. 2446-56.
32. Shuster, A., et al., *The clinical importance of visceral adiposity: a critical review of methods for visceral adipose tissue analysis.* Br J Radiol, 2012. **85**(1009): p. 1-10.
33. O'Sullivan, J., et al., *Obesity and gastrointestinal cancer: the interrelationship of adipose and tumour microenvironments.* Nat Rev Gastroenterol Hepatol, 2018. **15**(11): p. 699-714.

34. Sihvo, E.I., et al., *Oxidative stress has a role in malignant transformation in Barrett's oesophagus.* Int J Cancer, 2002. **102**(6): p. 551-5.
35. Weisberg, S.P., et al., *Obesity is associated with macrophage accumulation in adipose tissue.* J Clin Invest, 2003. **112**(12): p. 1796-808.
36. Deng, T., et al., *Obesity, Inflammation, and Cancer.* Annu Rev Pathol, 2016. **11**: p. 421-49.
37. Allott, E.H., et al., *MMP9 expression in oesophageal adenocarcinoma is upregulated with visceral obesity and is associated with poor tumour differentiation.* Mol Carcinog, 2013. **52**(2): p. 144-54.
38. Allott, E.H., et al., *Elevated Tumor Expression of PAI-1 and SNAI2 in Obese Esophageal Adenocarcinoma Patients and Impact on Prognosis.* Clin Transl Gastroenterol, 2012. **3**(4): p. e12.
39. Conroy, M.J., et al., *The microenvironment of visceral adipose tissue and liver alter natural killer cell viability and function.* J Leukoc Biol, 2016. **100**(6): p. 1435-1442.
40. Lysaght, J., et al., *Pro-inflammatory and tumour proliferative properties of excess visceral adipose tissue.* Cancer Lett, 2011. **312**(1): p. 62-72.
41. Mongan, A.M., et al., *Visceral Adipose Tissue Modulates Radiosensitivity in Oesophageal Adenocarcinoma.* Int J Med Sci, 2019. **16**(4): p. 519-528.
42. Bolger, J.C., et al., *Advances in the curative management of oesophageal cancer.* Br J Cancer, 2022. **126**(5): p. 706-717.
43. Donohoe, C.L. and J.V. Reynolds, *Neoadjuvant treatment of locally advanced esophageal and junctional cancer: the evidence-base, current key questions and clinical trials.* J Thorac Dis, 2017. **9**(Suppl 8): p. S697-S704.
44. Faron, M., et al., *Individual Participant Data Network Meta-Analysis of Neoadjuvant Chemotherapy or Chemoradiotherapy in Esophageal or Gastroesophageal Junction Carcinoma.* J Clin Oncol, 2023. **41**(28): p. 4535-4547.
45. van Hagen, P., et al., *Preoperative chemoradiotherapy for esophageal or junctional cancer.* N Engl J Med, 2012. **366**(22): p. 2074-84.
46. Leong, T., et al., *TOPGEAR: a randomised phase III trial of perioperative ECF chemotherapy versus preoperative chemoradiation plus perioperative ECF chemotherapy for resectable gastric cancer (an international, intergroup trial of the AGITG/TROG/EORTC/NCIC CTG).* BMC Cancer, 2015. **15**: p. 532.
47. Hoeppner, J., et al., *ESOPEC: prospective randomized controlled multicenter phase III trial comparing perioperative chemotherapy (FLOT protocol) to neoadjuvant chemoradiation (CROSS protocol) in patients with adenocarcinoma of the esophagus (NCT02509286).* BMC Cancer, 2016. **16**: p. 503.
48. Puhr, H.C., M. Preusser, and A. Ilhan-Mutlu, *Immunotherapy for Esophageal Cancers: What Is Practice Changing in 2021?* Cancers (Basel), 2021. **13**(18).
49. Shah, M.A., et al., *KEYNOTE-975 study design: a Phase III study of definitive chemoradiotherapy plus pembrolizumab in patients with esophageal carcinoma.* Future Oncol, 2021. **17**(10): p. 1143-1153.
50. Sun, J.M., et al., *Pembrolizumab plus chemotherapy versus chemotherapy alone for first-line treatment of advanced oesophageal cancer (KEYNOTE-590): a randomised, placebo-controlled, phase 3 study.* Lancet, 2021. **398**(10302): p. 759-771.
51. Kelly, R.J., et al., *Adjuvant Nivolumab in Resected Esophageal or Gastroesophageal Junction Cancer.* N Engl J Med, 2021. **384**(13): p. 1191-1203.

52. Shah, M.A., et al., *Immunotherapy and Targeted Therapy for Advanced Gastroesophageal Cancer: ASCO Guideline.* J Clin Oncol, 2023. **41**(7): p. 1470-1491.
53. Janjigian, Y.Y., et al., *First-Line Nivolumab Plus Chemotherapy for Advanced Gastric, Gastroesophageal Junction, and Esophageal Adenocarcinoma: 3-Year Follow-Up of the Phase III CheckMate 649 Trial.* J Clin Oncol, 2024. **42**(17): p. 2012-2020.
54. Lynch, E., A.G. Duffy, and R.J. Kelly, *Immune Checkpoint Inhibitors: Changing the Treatment Landscape in Esophagogastric Adenocarcinoma.* Pharmaceuticals (Basel), 2023. **16**(1).
55. Shitara, K., et al., *Zolbetuximab in Gastric or Gastroesophageal Junction Adenocarcinoma.* N Engl J Med, 2024. **391**(12): p. 1159-1162.
56. Shitara, K., et al., *Zolbetuximab plus mFOLFOX6 in patients with CLDN18.2-positive, HER2-negative, untreated, locally advanced unresectable or metastatic gastric or gastro-oesophageal junction adenocarcinoma (SPOTLIGHT): a multicentre, randomised, double-blind, phase 3 trial.* Lancet, 2023. **401**(10389): p. 1655-1668.
57. Shah, M.A., et al., *Zolbetuximab plus CAPOX in CLDN18.2-positive gastric or gastroesophageal junction adenocarcinoma: the randomized, phase 3 GLOW trial.* Nat Med, 2023. **29**(8): p. 2133-2141.
58. van Sandick, J.W., et al., *Lymphocyte subsets and T(h)1/T(h)2 immune responses in patients with adenocarcinoma of the oesophagus or oesophagogastric junction: relation to pTNM stage and clinical outcome.* Cancer Immunol Immunother, 2003. **52**(10): p. 617-24.
59. Fitzgerald, R.C., et al., *Diversity in the oesophageal phenotypic response to gastro-oesophageal reflux: immunological determinants.* Gut, 2002. **50**(4): p. 451-9.
60. Kavanagh, M.E., et al., *Impact of the inflammatory microenvironment on T-cell phenotype in the progression from reflux oesophagitis to Barrett oesophagus and oesophageal adenocarcinoma.* Cancer Lett, 2016. **370**(1): p. 117-24.
61. Vivier, E., et al., *Functions of natural killer cells.* Nat Immunol, 2008. **9**(5): p. 503-10.
62. Lv, L., et al., *The accumulation and prognosis value of tumor infiltrating IL-17 producing cells in esophageal squamous cell carcinoma.* PLoS One, 2011. **6**(3): p. e18219.
63. Lu, L., et al., *IL-17A promotes immune cell recruitment in human esophageal cancers and the infiltrating dendritic cells represent a positive prognostic marker for patient survival.* J Immunother, 2013. **36**(8): p. 451-8.
64. Tumino, N., et al., *The tumor microenvironment drives NK cell metabolic dysfunction leading to impaired antitumor activity.* Int J Cancer, 2023. **152**(8): p. 1698-1706.
65. Dean, I., et al., *Rapid functional impairment of natural killer cells following tumor entry limits anti-tumor immunity.* Nat Commun, 2024. **15**(1): p. 683.
66. Wang, J., et al., *The prognostic value of B7-H6 protein expression in human oral squamous cell carcinoma.* J Oral Pathol Med, 2017. **46**(9): p. 766-772.
67. Cui, K., et al., *Innate Immune Cells in the Esophageal Tumor Microenvironment.* Front Immunol, 2021. **12**: p. 654731.

68. Mylod, E., et al., *Real-time ex vivo monitoring of NK cell migration toward obesity-associated oesophageal adenocarcinoma following modulation of CX3CR1.* Sci Rep, 2024. **14**(1): p. 4017.
69. Mylod, E., et al., *The Omentum in Obesity-Associated Cancer: A Hindrance to Effective Natural Killer Cell Migration towards Tumour Which Can Be Overcome by CX3CR1 Antagonism.* Cancers (Basel), 2021. **14**(1).
70. Buckley, A.M., et al., *Characterisation of an Isogenic Model of Cisplatin Resistance in Oesophageal Adenocarcinoma Cells.* Pharmaceuticals (Basel), 2019. **12**(1).
71. Mylod, E., et al., *Investigating the susceptibility of treatment-resistant oesophageal tumours to natural killer cell-mediated responses.* Clin Exp Med, 2022.
72. Souza, R.F., et al., *Gastroesophageal reflux might cause esophagitis through a cytokine-mediated mechanism rather than caustic acid injury.* Gastroenterology, 2009. **137**(5): p. 1776-84.
73. Ku, G.Y., *The Current Status of Immunotherapies in Esophagogastric Cancer.* Surg Oncol Clin N Am, 2017. **26**(2): p. 277-292.
74. Ma, Y., et al., *Dendritic cells in the cancer microenvironment.* J Cancer, 2013. **4**(1): p. 36-44.
75. Conroy, M.J., et al., *A study of the immune infiltrate and patient outcomes in esophageal cancer.* Carcinogenesis, 2021. **42**(3): p. 395-404.
76. Davern, M., et al., *FLOT and CROSS chemotherapy regimens alter the frequency of CD27(+) and CD69(+) T cells in oesophagogastric adenocarcinomas: implications for combination with immunotherapy.* J Cancer Res Clin Oncol, 2023. **149**(7): p. 3753-3774.
77. Han, P., et al., *Esophageal Microenvironment: From Precursor Microenvironment to Premetastatic Niche.* Cancer Manag Res, 2020. **12**: p. 5857-5879.
78. Underwood, T.J., et al., *Cancer-associated fibroblasts predict poor outcome and promote periostin-dependent invasion in oesophageal adenocarcinoma.* J Pathol, 2015. **235**(3): p. 466-77.
79. Gabitass, R.F., et al., *Elevated myeloid-derived suppressor cells in pancreatic, esophageal and gastric cancer are an independent prognostic factor and are associated with significant elevation of the Th2 cytokine interleukin-13.* Cancer Immunol Immunother, 2011. **60**(10): p. 1419-30.
80. Lin, E.W., et al., *The tumor microenvironment in esophageal cancer.* Oncogene, 2016. **35**(41): p. 5337-5349.
81. Umansky, V., et al., *The Role of Myeloid-Derived Suppressor Cells (MDSC) in Cancer Progression.* Vaccines (Basel), 2016. **4**(4).
82. Hegde, S., A.M. Leader, and M. Merad, *MDSC: Markers, development, states, and unaddressed complexity.* Immunity, 2021. **54**(5): p. 875-884.
83. Karakasheva, T.A., et al., *CD38-Expressing Myeloid-Derived Suppressor Cells Promote Tumor Growth in a Murine Model of Esophageal Cancer.* Cancer Res, 2015. **75**(19): p. 4074-85.
84. Milano, F., et al., *Expression pattern of immune suppressive cytokines and growth factors in oesophageal adenocarcinoma reveal a tumour immune escape-promoting microenvironment.* Scand J Immunol, 2008. **68**(6): p. 616-23.
85. Hashemi Goradel, N., et al., *Cyclooxygenase-2 in cancer: A review.* J Cell Physiol, 2019. **234**(5): p. 5683-5699.

86. Morris, C.D., et al., *Cyclooxygenase-2 expression in the Barrett's metaplasia-dysplasia-adenocarcinoma sequence.* Am J Gastroenterol, 2001. **96**(4): p. 990-6.
87. Shitara, K. and H. Nishikawa, *Regulatory T cells: a potential target in cancer immunotherapy.* Ann N Y Acad Sci, 2018. **1417**(1): p. 104-115.
88. Wang, G., et al., *FOXP3 expression in esophageal cancer cells is associated with poor prognosis in esophageal cancer.* Hepatogastroenterology, 2012. **59**(119): p. 2186-91.
89. Karstens, K.F., et al., *Anti-inflammatory microenvironment of esophageal adenocarcinomas negatively impacts survival.* Cancer Immunol Immunother, 2020. **69**(6): p. 1043-1056.
90. Huang, C. and Z.X. Fu, *Localization of IL-17+Foxp3+ T cells in esophageal cancer.* Immunol Invest, 2011. **40**(4): p. 400-12.
91. Derks, S., et al., *Epithelial PD-L2 Expression Marks Barrett's Esophagus and Esophageal Adenocarcinoma.* Cancer Immunol Res, 2015. **3**(10): p. 1123-1129.
92. Zheng, Y., et al., *Immune suppressive landscape in the human esophageal squamous cell carcinoma microenvironment.* Nat Commun, 2020. **11**(1): p. 6268.
93. Davern, M., et al., *Cooperation between chemotherapy and immune checkpoint blockade to enhance anti-tumour T cell immunity in oesophageal adenocarcinoma.* Transl Oncol, 2022. **20**: p. 101406.
94. Zheng, Y., et al., *TNF-alpha-induced Tim-3 expression marks the dysfunction of infiltrating natural killer cells in human esophageal cancer.* J Transl Med, 2019. **17**(1): p. 165.
95. Liu, Y., et al., *Increased expression of programmed cell death protein 1 on NK cells inhibits NK-cell-mediated anti-tumor function and indicates poor prognosis in digestive cancers.* Oncogene, 2017. **36**(44): p. 6143-6153.
96. Loke, P. and J.P. Allison, *PD-L1 and PD-L2 are differentially regulated by Th1 and Th2 cells.* Proc Natl Acad Sci U S A, 2003. **100**(9): p. 5336-41.
97. Gebauer, F., et al., *Lymphocyte activation gene-3 (LAG3) mRNA and protein expression on tumour infiltrating lymphocytes (TILs) in oesophageal adenocarcinoma.* J Cancer Res Clin Oncol, 2020. **146**(9): p. 2319-2327.
98. Lonie, J.M., A.P. Barbour, and R. Dolcetti, *Understanding the immuno-biology of oesophageal adenocarcinoma: Towards improved therapeutic approaches.* Cancer Treat Rev, 2021. **98**: p. 102219.
99. Infantino, V., et al., *Cancer Cell Metabolism in Hypoxia: Role of HIF-1 as Key Regulator and Therapeutic Target.* Int J Mol Sci, 2021. **22**(11).
100. Sethi, N., et al., *Mutant p53 induces a hypoxia transcriptional program in gastric and esophageal adenocarcinoma.* JCI Insight, 2019. **4**(15).
101. Ling, F.C., et al., *HIF-1alpha protein expression is associated with the environmental inflammatory reaction in Barrett's metaplasia.* Dis Esophagus, 2009. **22**(8): p. 694-9.
102. Sormendi, S. and B. Wielockx, *Hypoxia Pathway Proteins As Central Mediators of Metabolism in the Tumor Cells and Their Microenvironment.* Front Immunol, 2018. **9**: p. 40.
103. Kolosenko, I., et al., *Therapeutic implications of tumor interstitial acidification.* Semin Cancer Biol, 2017. **43**: p. 119-133.
104. Driessen, A., et al., *Expression of carbonic anhydrase IX (CA IX), a hypoxia-related protein, rather than vascular-endothelial growth factor (VEGF), a pro-angiogenic*

factor, correlates with an extremely poor prognosis in esophageal and gastric adenocarcinomas. Ann Surg, 2006. **243**(3): p. 334-40.
105. Davern, M., et al., *Nutrient deprivation and hypoxia alter T cell immune checkpoint expression: potential impact for immunotherapy.* J Cancer Res Clin Oncol, 2023. **149**(8): p. 5377-5395.
106. Davern, M., et al., *Acidosis significantly alters immune checkpoint expression profiles of T cells from oesophageal adenocarcinoma patients.* Cancer Immunol Immunother, 2023. **72**(1): p. 55-71.
107. Howard, J.M., et al., *Associations between leptin and adiponectin receptor upregulation, visceral obesity and tumour stage in oesophageal and junctional adenocarcinoma.* Br J Surg, 2010. **97**(7): p. 1020-7.
108. Garcia, J.M., et al., *Circulating inflammatory cytokines and adipokines are associated with increased risk of Barrett's esophagus: a case-control study.* Clin Gastroenterol Hepatol, 2014. **12**(2): p. 229-238 e3.
109. Duggan, C., et al., *Association between markers of obesity and progression from Barrett's esophagus to esophageal adenocarcinoma.* Clin Gastroenterol Hepatol, 2013. **11**(8): p. 934-43.
110. Kavanagh, M.E., et al., *Altered T Cell Migratory Capacity in the Progression from Barrett Oesophagus to Oesophageal Adenocarcinoma.* Cancer Microenviron, 2019. **12**(1): p. 57-66.
111. Jenkins, G.J., et al., *The bile acid deoxycholic acid (DCA) at neutral pH activates NF-kappaB and induces IL-8 expression in oesophageal cells in vitro.* Carcinogenesis, 2004. **25**(3): p. 317-23.
112. Deans, D.A., et al., *Elevated tumour interleukin-1beta is associated with systemic inflammation: A marker of reduced survival in gastro-oesophageal cancer.* Br J Cancer, 2006. **95**(11): p. 1568-75.
113. Yang, H., et al., *Tocopherols inhibit esophageal carcinogenesis through attenuating NF-kappaB activation and CXCR3-mediated inflammation.* Oncogene, 2018. **37**(29): p. 3909-3923.
114. Yang, H., et al., *Obesity increases the production of proinflammatory mediators from adipose tissue T cells and compromises TCR repertoire diversity: implications for systemic inflammation and insulin resistance.* J Immunol, 2010. **185**(3): p. 1836-45.
115. Mathis, D., *Immunological goings-on in visceral adipose tissue.* Cell Metab, 2013. **17**(6): p. 851-859.
116. Sena, L.A., et al., *Mitochondria are required for antigen-specific T cell activation through reactive oxygen species signaling.* Immunity, 2013. **38**(2): p. 225-36.
117. Cadenas, E. and K.J. Davies, *Mitochondrial free radical generation, oxidative stress, and aging.* Free Radic Biol Med, 2000. **29**(3-4): p. 222-30.
118. Wetscher, G.J., et al., *Reflux esophagitis in humans is mediated by oxygen-derived free radicals.* Am J Surg, 1995. **170**(6): p. 552-6; discussion 556-7.
119. Zhang, H.Y., et al., *In benign Barrett's epithelial cells, acid exposure generates reactive oxygen species that cause DNA double-strand breaks.* Cancer Res, 2009. **69**(23): p. 9083-9.
120. Sundaresan, M., et al., *Requirement for generation of H2O2 for platelet-derived growth factor signal transduction.* Science, 1995. **270**(5234): p. 296-9.

121. Bae, Y.S., et al., *Epidermal growth factor (EGF)-induced generation of hydrogen peroxide. Role in EGF receptor-mediated tyrosine phosphorylation.* J Biol Chem, 1997. **272**(1): p. 217-21.
122. Singh, S., et al., *Central adiposity is associated with increased risk of esophageal inflammation, metaplasia, and adenocarcinoma: a systematic review and meta-analysis.* Clin Gastroenterol Hepatol, 2013. **11**(11): p. 1399-1412 e7.
123. Beddy, P., et al., *Association of visceral adiposity with oesophageal and junctional adenocarcinomas.* Br J Surg, 2010. **97**(7): p. 1028-34.
124. Lysaght, J., et al., *T lymphocyte activation in visceral adipose tissue of patients with oesophageal adenocarcinoma.* Br J Surg, 2011. **98**(7): p. 964-74.
125. Zhang, Y., et al., *Inflamed macrophage microvesicles induce insulin resistance in human adipocytes.* Nutr Metab (Lond), 2015. **12**: p. 21.
126. Conroy, M.J., et al., *Parallel Profiles of Inflammatory and Effector Memory T Cells in Visceral Fat and Liver of Obesity-Associated Cancer Patients.* Inflammation, 2016. **39**(5): p. 1729-36.
127. Mylod, E., et al., *Fractalkine Elicits Chemotactic, Phenotypic, and Functional Effects on CX3CR1(+)CD27(-) NK Cells in Obesity-Associated Cancer.* J Immunol, 2021. **207**(4): p. 1200-1210.
128. Conroy, M.J., et al., *CCR1 antagonism attenuates T cell trafficking to omentum and liver in obesity-associated cancer.* Immunol Cell Biol, 2016. **94**(6): p. 531-7.
129. Conroy, M.J., et al., *Identifying a Novel Role for Fractalkine (CX3CL1) in Memory CD8(+) T Cell Accumulation in the Omentum of Obesity-Associated Cancer Patients.* Front Immunol, 2018. **9**: p. 1867.
130. Davern, M., et al., *Visceral adipose tissue secretome from early and late-stage oesophageal cancer patients differentially affects effector and regulatory T cells.* J Cancer Res Clin Oncol, 2023. **149**(9): p. 6583-6599.
131. Luster, A.D., *Chemokines--chemotactic cytokines that mediate inflammation.* N Engl J Med, 1998. **338**(7): p. 436-45.
132. da Silva, P.H.R., et al., *Chemokines and the extracellular matrix: Set of targets for tumor development and treatment.* Cytokine, 2021. **144**: p. 155548.
133. Balkwill, F., *Cancer and the chemokine network.* Nat Rev Cancer, 2004. **4**(7): p. 540-50.
134. Chow, M.T. and A.D. Luster, *Chemokines in cancer.* Cancer Immunol Res, 2014. **2**(12): p. 1125-31.
135. Zlotnik, A., A.M. Burkhardt, and B. Homey, *Homeostatic chemokine receptors and organ-specific metastasis.* Nat Rev Immunol, 2011. **11**(9): p. 597-606.
136. Nibbs, R.J. and G.J. Graham, *Immune regulation by atypical chemokine receptors.* Nat Rev Immunol, 2013. **13**(11): p. 815-29.
137. Hannan, N.J., et al., *The chemokines, CX3CL1, CCL14, and CCL4, promote human trophoblast migration at the feto-maternal interface.* Biol Reprod, 2006. **74**(5): p. 896-904.
138. Stumm, R.K., et al., *A dual role for the SDF-1/CXCR4 chemokine receptor system in adult brain: isoform-selective regulation of SDF-1 expression modulates CXCR4-dependent neuronal plasticity and cerebral leukocyte recruitment after focal ischemia.* J Neurosci, 2002. **22**(14): p. 5865-78.

139. Stumm, R. and V. Hollt, *CXC chemokine receptor 4 regulates neuronal migration and axonal pathfinding in the developing nervous system: implications for neuronal regeneration in the adult brain.* J Mol Endocrinol, 2007. **38**(3): p. 377-82.
140. McGrath, K.E., et al., *Embryonic expression and function of the chemokine SDF-1 and its receptor, CXCR4.* Dev Biol, 1999. **213**(2): p. 442-56.
141. Strydom, N. and S.M. Rankin, *Regulation of circulating neutrophil numbers under homeostasis and in disease.* J Innate Immun, 2013. **5**(4): p. 304-14.
142. Inokuma, D., et al., *CTACK/CCL27 accelerates skin regeneration via accumulation of bone marrow-derived keratinocytes.* Stem Cells, 2006. **24**(12): p. 2810-6.
143. Griffith, J.W., C.L. Sokol, and A.D. Luster, *Chemokines and chemokine receptors: positioning cells for host defense and immunity.* Annu Rev Immunol, 2014. **32**: p. 659-702.
144. Vergunst, C.E. and P.P. Tak, *Chemokines: their role in rheumatoid arthritis.* Curr Rheumatol Rep, 2005. **7**(5): p. 382-8.
145. Chatterjee, A., et al., *Chemokines and chemokine receptors in susceptibility to HIV-1 infection and progression to AIDS.* Dis Markers, 2012. **32**(3): p. 143-51.
146. Deshmane, S.L., et al., *Monocyte chemoattractant protein-1 (MCP-1): an overview.* J Interferon Cytokine Res, 2009. **29**(6): p. 313-26.
147. Russo, R.C., et al., *The CXCL8/IL-8 chemokine family and its receptors in inflammatory diseases.* Expert Rev Clin Immunol, 2014. **10**(5): p. 593-619.
148. Groom, J.R. and A.D. Luster, *CXCR3 in T cell function.* Exp Cell Res, 2011. **317**(5): p. 620-31.
149. Wendel, M., et al., *Natural killer cell accumulation in tumors is dependent on IFN-gamma and CXCR3 ligands.* Cancer Res, 2008. **68**(20): p. 8437-45.
150. Bai, Y. and Q. Sun, *Macrophage recruitment in obese adipose tissue.* Obes Rev, 2015. **16**(2): p. 127-36.
151. Wu, H., et al., *T-cell accumulation and regulated on activation, normal T cell expressed and secreted upregulation in adipose tissue in obesity.* Circulation, 2007. **115**(8): p. 1029-38.
152. Karin, N., *Chemokines in the Landscape of Cancer Immunotherapy: How They and Their Receptors Can Be Used to Turn Cold Tumors into Hot Ones?* Cancers (Basel), 2021. **13**(24).
153. Murphy, P.M., *Chemokines and the molecular basis of cancer metastasis.* N Engl J Med, 2001. **345**(11): p. 833-5.
154. Sun, X., et al., *CXCL12 / CXCR4 / CXCR7 chemokine axis and cancer progression.* Cancer Metastasis Rev, 2010. **29**(4): p. 709-22.
155. Hermann, P.C., et al., *Distinct populations of cancer stem cells determine tumor growth and metastatic activity in human pancreatic cancer.* Cell Stem Cell, 2007. **1**(3): p. 313-23.
156. Sugihara, H., et al., *Cancer-associated fibroblast-derived CXCL12 causes tumor progression in adenocarcinoma of the esophagogastric junction.* Med Oncol, 2015. **32**(6): p. 618.
157. Gabrilovich, D.I. and S. Nagaraj, *Myeloid-derived suppressor cells as regulators of the immune system.* Nat Rev Immunol, 2009. **9**(3): p. 162-74.
158. Pollard, J.W., *Tumour-educated macrophages promote tumour progression and metastasis.* Nat Rev Cancer, 2004. **4**(1): p. 71-8.

159. Wang, J.M., et al., *Purification and identification of chemokines potentially involved in kidney-specific metastasis by a murine lymphoma variant: induction of migration and NFkappaB activation.* Int J Cancer, 1998. **75**(6): p. 900-7.
160. Xu, W., et al., *CCL2-SQSTM1 positive feedback loop suppresses autophagy to promote chemoresistance in gastric cancer.* Int J Biol Sci, 2018. **14**(9): p. 1054-1066.
161. Burrack, A.L., et al., *Cxcr3 constrains pancreatic cancer dissemination through instructing T cell fate.* Cancer Immunol Immunother, 2022.
162. Cannon, A., et al., *Contribution of CXCR3-mediated signaling in the metastatic cascade of solid malignancies.* Biochim Biophys Acta Rev Cancer, 2021. **1876**(2): p. 188628.
163. Zohar, Y., et al., *CXCL11-dependent induction of FOXP3-negative regulatory T cells suppresses autoimmune encephalomyelitis.* J Clin Invest, 2014. **124**(5): p. 2009-22.
164. Halama, N., et al., *Tumoral Immune Cell Exploitation in Colorectal Cancer Metastases Can Be Targeted Effectively by Anti-CCR5 Therapy in Cancer Patients.* Cancer Cell, 2016. **29**(4): p. 587-601.
165. Long, H., et al., *Autocrine CCL5 signaling promotes invasion and migration of CD133+ ovarian cancer stem-like cells via NF-kappaB-mediated MMP-9 upregulation.* Stem Cells, 2012. **30**(10): p. 2309-19.
166. Kranjc, M.K., et al., *Cytokine CCL5 and receptor CCR5 axis in glioblastoma multiforme.* Radiol Oncol, 2019. **53**(4): p. 397-406.
167. Davern, M., et al., *Analysing the Combined Effects of Radiotherapy and Chemokine Receptor 5 Antagonism: Complementary Approaches to Promote T Cell Function and Migration in Oesophageal Adenocarcinoma.* Biomedicines, 2024. **12**(4).
168. Bogacka, J., et al., *CC Chemokine Receptor 4 (CCR4) as a Possible New Target for Therapy.* Int J Mol Sci, 2022. **23**(24).
169. Bazan, J.F., et al., *A new class of membrane-bound chemokine with a CX3C motif.* Nature, 1997. **385**(6617): p. 640-4.
170. Lee, M., et al., *Tissue-specific Role of CX(3)CR1 Expressing Immune Cells and Their Relationships with Human Disease.* Immune Netw, 2018. **18**(1): p. e5.
171. Tsou, C.L., C.A. Haskell, and I.F. Charo, *Tumor necrosis factor-alpha-converting enzyme mediates the inducible cleavage of fractalkine.* J Biol Chem, 2001. **276**(48): p. 44622-6.
172. Imai, T., et al., *Identification and molecular characterization of fractalkine receptor CX3CR1, which mediates both leukocyte migration and adhesion.* Cell, 1997. **91**(4): p. 521-30.
173. Conroy, M.J. and J. Lysaght, *CX3CL1 Signaling in the Tumor Microenvironment.* Adv Exp Med Biol, 2020. **1231**: p. 1-12.
174. Rodriguez, C., et al., *Fractalkine in Health and Disease.* Int J Mol Sci, 2024. **25**(15).
175. Nakayama, T., et al., *Eotaxin-3/CC chemokine ligand 26 is a functional ligand for CX3CR1.* J Immunol, 2010. **185**(11): p. 6472-9.
176. El-Shazly, A.E., et al., *Novel cooperation between CX3CL1 and CCL26 inducing NK cell chemotaxis via CX3CR1: a possible mechanism for NK cell infiltration of the allergic nasal tissue.* Clin Exp Allergy, 2013. **43**(3): p. 322-31.

177. Moon, H.G., et al., *CX(3)CR(1)(+) Macrophage Facilitates the Resolution of Allergic Lung Inflammation via Interacting CCL26.* Am J Respir Crit Care Med, 2023. **207**(11): p. 1451-1463.
178. Chiu, D.K., et al., *Hypoxia induces myeloid-derived suppressor cell recruitment to hepatocellular carcinoma through chemokine (C-C motif) ligand 26.* Hepatology, 2016. **64**(3): p. 797-813.
179. Yang, X.P., et al., *Fractalkine upregulates intercellular adhesion molecule-1 in endothelial cells through CX3CR1 and the Jak Stat5 pathway.* Circ Res, 2007. **101**(10): p. 1001-8.
180. Zhuang, Q., et al., *Crosstalk between the CX3CL1/CX3CR1 Axis and Inflammatory Signaling Pathways in Tissue Injury.* Curr Protein Pept Sci, 2019. **20**(8): p. 844-854.
181. Zhuang, Q., K. Cheng, and Y. Ming, *CX3CL1/CX3CR1 Axis, as the Therapeutic Potential in Renal Diseases: Friend or Foe?* Curr Gene Ther, 2017. **17**(6): p. 442-452.
182. Mendiola, A.S., et al., *Defective fractalkine-CX3CR1 signaling aggravates neuroinflammation and affects recovery from cuprizone-induced demyelination.* J Neurochem, 2022. **162**(5): p. 430-443.
183. Muraoka, S., et al., *CX3CL1/fractalkine regulates the differentiation of human peripheral blood monocytes and monocyte-derived dendritic cells into osteoclasts.* Cytokine, 2021. **146**: p. 155652.
184. Gong, Q., et al., *Fractalkine aggravates LPS-induced macrophage activation and acute kidney injury via Wnt/beta-catenin signalling pathway.* J Cell Mol Med, 2021. **25**(14): p. 6963-6975.
185. Wakita, H., et al., *E6130, a Novel CX3C Chemokine Receptor 1 (CX3CR1) Modulator, Attenuates Mucosal Inflammation and Reduces CX3CR1(+) Leukocyte Trafficking in Mice with Colitis.* Mol Pharmacol, 2017. **92**(5): p. 502-509.
186. White, G.E. and D.R. Greaves, *Fractalkine: a survivor's guide: chemokines as antiapoptotic mediators.* Arterioscler Thromb Vasc Biol, 2012. **32**(3): p. 589-94.
187. Hyakudomi, M., et al., *Increased expression of fractalkine is correlated with a better prognosis and an increased number of both CD8+ T cells and natural killer cells in gastric adenocarcinoma.* Ann Surg Oncol, 2008. **15**(6): p. 1775-82.
188. Ohta, M., et al., *The high expression of Fractalkine results in a better prognosis for colorectal cancer patients.* Int J Oncol, 2005. **26**(1): p. 41-7.
189. Wei, L.M., et al., *Overexpression of CX3CR1 is associated with cellular metastasis, proliferation and survival in gastric cancer.* Oncol Rep, 2015. **33**(2): p. 615-24.
190. Park, M.H., J.S. Lee, and J.H. Yoon, *High expression of CX3CL1 by tumor cells correlates with a good prognosis and increased tumor-infiltrating CD8+ T cells, natural killer cells, and dendritic cells in breast carcinoma.* J Surg Oncol, 2012. **106**(4): p. 386-92.
191. Tsang, J.Y., et al., *CX3CL1 expression is associated with poor outcome in breast cancer patients.* Breast Cancer Res Treat, 2013. **140**(3): p. 495-504.
192. Liu, P., et al., *CX3CL1/fractalkine enhances prostate cancer spinal metastasis by activating the Src/FAK pathway.* Int J Oncol, 2018. **53**(4): p. 1544-1556.
193. Tang, J., et al., *CX3CL1 increases invasiveness and metastasis by promoting epithelial-to-mesenchymal transition through the TACE/TGF-alpha/EGFR pathway in hypoxic androgen-independent prostate cancer cells.* Oncol Rep, 2016. **35**(2): p. 1153-62.

194. Wang, H., et al., *Fractalkine/CX3CR1 induces apoptosis resistance and proliferation through the activation of the AKT/NF-kappaB cascade in pancreatic cancer cells.* Cell Biochem Funct, 2017. **35**(6): p. 315-326.
195. Liu, W., et al., *CX3CL1 promotes lung cancer cell migration and invasion via the Src/focal adhesion kinase signaling pathway.* Oncol Rep, 2019. **41**(3): p. 1911-1917.
196. Schmall, A., et al., *Macrophage and cancer cell cross-talk via CCR2 and CX3CR1 is a fundamental mechanism driving lung cancer.* Am J Respir Crit Care Med, 2015. **191**(4): p. 437-47.
197. Okuma, A., et al., *p16(Ink4a) and p21(Cip1/Waf1) promote tumour growth by enhancing myeloid-derived suppressor cells chemotaxis.* Nat Commun, 2017. **8**(1): p. 2050.
198. Castriconi, R., et al., *Neuroblastoma-derived TGF-beta1 modulates the chemokine receptor repertoire of human resting NK cells.* J Immunol, 2013. **190**(10): p. 5321-8.
199. Liu, C., et al., *CX3CL1 and CX3CR1 in the GL261 murine model of glioma: CX3CR1 deficiency does not impact tumor growth or infiltration of microglia and lymphocytes.* J Neuroimmunol, 2008. **198**(1-2): p. 98-105.
200. Su, Y.C., et al., *Differential impact of CX3CL1 on lung cancer prognosis in smokers and non-smokers.* Mol Carcinog, 2018. **57**(5): p. 629-639.
201. Seitz, S., et al., *The chemokine CX3CL1 promotes intraperitoneal tumour growth despite enhanced T-cell recruitment in ovarian cancer.* Neoplasia, 2025. **60**: p. 101130.
202. Xu, X., et al., *High expression of CX3CL1/CX3CR1 axis predicts a poor prognosis of pancreatic ductal adenocarcinoma.* J Gastrointest Surg, 2012. **16**(8): p. 1493-8.
203. Stout, M.C., et al., *Inhibition of CX(3)CR1 reduces cell motility and viability in pancreatic adenocarcinoma epithelial cells.* Biochem Biophys Res Commun, 2018. **495**(3): p. 2264-2269.
204. Geismann, C., et al., *TRAIL/NF-kappaB/CX3CL1 Mediated Onco-Immuno Crosstalk Leading to TRAIL Resistance of Pancreatic Cancer Cell Lines.* Int J Mol Sci, 2018. **19**(6).
205. Ren, H., et al., *The CX3CL1/CX3CR1 reprograms glucose metabolism through HIF-1 pathway in pancreatic adenocarcinoma.* J Cell Biochem, 2013. **114**(11): p. 2603-11.
206. Shah, R., et al., *Fractalkine is a novel human adipochemokine associated with type 2 diabetes.* Diabetes, 2011. **60**(5): p. 1512-8.
207. Siddiqui, I., et al., *Enhanced recruitment of genetically modified CX3CR1-positive human T cells into Fractalkine/CX3CL1 expressing tumors: importance of the chemokine gradient.* J Immunother Cancer, 2016. **4**: p. 21.
208. Erreni, M., et al., *The Fractalkine-Receptor Axis Improves Human Colorectal Cancer Prognosis by Limiting Tumor Metastatic Dissemination.* J Immunol, 2016. **196**(2): p. 902-14.
209. Zheng, J., et al., *Chemokine receptor CX3CR1 contributes to macrophage survival in tumor metastasis.* Mol Cancer, 2013. **12**(1): p. 141.
210. Olsen, R.S., et al., *Circulating inflammatory factors associated with worse long-term prognosis in colorectal cancer.* World J Gastroenterol, 2017. **23**(34): p. 6212-6219.

211. Liu, J., et al., *Increased CX3CL1 mRNA expression level is a positive prognostic factor in patients with lung adenocarcinoma.* Oncol Lett, 2019. **17**(6): p. 4877-4890.
212. Tang, L., et al., *Gene therapy with CX3CL1/Fractalkine induces antitumor immunity to regress effectively mouse hepatocellular carcinoma.* Gene Ther, 2007. **14**(16): p. 1226-34.
213. Matsubara, T., et al., *Fractalkine-CX3CR1 axis regulates tumor cell cycle and deteriorates prognosis after radical resection for hepatocellular carcinoma.* J Surg Oncol, 2007. **95**(3): p. 241-9.
214. Liu, X., et al., *CX3CL1 and its receptor CX3CR1 interact with RhoA signaling to induce paclitaxel resistance in gastric cancer.* Heliyon, 2024. **10**(7): p. e29100.
215. Marchica, V., et al., *Bone Marrow CX3CL1/Fractalkine is a New Player of the Pro-Angiogenic Microenvironment in Multiple Myeloma Patients.* Cancers (Basel), 2019. **11**(3).
216. Zhao, T., et al., *Hypoxia-inducible factor-1alpha regulates chemotactic migration of pancreatic ductal adenocarcinoma cells through directly transactivating the CX3CR1 gene.* PLoS One, 2012. **7**(8): p. e43399.
217. Huang, L., et al., *Fractalkine/CX3CR1 axis modulated the development of pancreatic ductal adenocarcinoma via JAK/STAT signaling pathway.* Biochem Biophys Res Commun, 2017. **493**(4): p. 1510-1517.
218. Singh, S.K., M.K. Mishra, and R. Singh, *Hypoxia-inducible factor-1alpha induces CX3CR1 expression and promotes the epithelial to mesenchymal transition (EMT) in ovarian cancer cells.* J Ovarian Res, 2019. **12**(1): p. 42.
219. Shao, D., et al., *CX3CR1 is a potential biomarker of immune microenvironment and prognosis in epithelial ovarian cancer.* Medicine (Baltimore), 2024. **103**(3): p. e36891.
220. Ferretti, E., et al., *A novel role of the CX3CR1/CX3CL1 system in the cross-talk between chronic lymphocytic leukemia cells and tumor microenvironment.* Leukemia, 2011. **25**(8): p. 1268-77.
221. Yao, X., et al., *Expression of CX3CR1 associates with cellular migration, metastasis, and prognosis in human clear cell renal cell carcinoma.* Urol Oncol, 2014. **32**(2): p. 162-70.
222. Xiao, L.J., et al., *Hypoxia increases CX3CR1 expression via HIF-1 and NF-kappaB in androgen-independent prostate cancer cells.* Int J Oncol, 2012. **41**(5): p. 1827-36.
223. Tang, J., et al., *Upregulation of fractalkine contributes to the proliferative response of prostate cancer cells to hypoxia via promoting the G1/S phase transition.* Mol Med Rep, 2015. **12**(6): p. 7907-14.
224. Bule, P., et al., *Chemokine-Directed Tumor Microenvironment Modulation in Cancer Immunotherapy.* Int J Mol Sci, 2021. **22**(18).
225. Drouillard, D., B.T. Craig, and M.B. Dwinell, *Physiology of chemokines in the cancer microenvironment.* Am J Physiol Cell Physiol, 2023. **324**(1): p. C167-C182.
226. Nagarsheth, N., M.S. Wicha, and W. Zou, *Chemokines in the cancer microenvironment and their relevance in cancer immunotherapy.* Nat Rev Immunol, 2017. **17**(9): p. 559-572.
227. Drenckhan, A., et al., *Effective inhibition of metastases and primary tumor growth with CTCE-9908 in esophageal cancer.* J Surg Res, 2013. **182**(2): p. 250-6.

228. Uchi, Y., et al., *CXCL12 expression promotes esophageal squamous cell carcinoma proliferation and worsens the prognosis.* BMC Cancer, 2016. **16**: p. 514.
229. Halama, N., et al., *Tumoral Immune Cell Exploitation in Colorectal Cancer Metastases Can Be Targeted Effectively by Anti-CCR5 Therapy in Cancer Patients.* Cancer Cell, 2016. **29**(4): p. 587-601.
230. Sandhu, S.K., et al., *A first-in-human, first-in-class, phase I study of carlumab (CNTO 888), a human monoclonal antibody against CC-chemokine ligand 2 in patients with solid tumors.* Cancer Chemother Pharmacol, 2013. **71**(4): p. 1041-50.
231. Pienta, K.J., et al., *Phase 2 study of carlumab (CNTO 888), a human monoclonal antibody against CC-chemokine ligand 2 (CCL2), in metastatic castration-resistant prostate cancer.* Invest New Drugs, 2013. **31**(3): p. 760-8.
232. Bonapace, L., et al., *Cessation of CCL2 inhibition accelerates breast cancer metastasis by promoting angiogenesis.* Nature, 2014. **515**(7525): p. 130-3.
233. Wang, B., et al., *A growth-related oncogene/CXC chemokine receptor 2 autocrine loop contributes to cellular proliferation in esophageal cancer.* Cancer Res, 2006. **66**(6): p. 3071-7.
234. Wu, K., et al., *Silencing of CXCR2 and CXCR7 protects against esophageal cancer.* Am J Transl Res, 2016. **8**(8): p. 3398-408.
235. Yang, L., et al., *Blockade of CCR5-mediated myeloid derived suppressor cell accumulation enhances anti-PD1 efficacy in gastric cancer.* Immunopharmacol Immunotoxicol, 2018. **40**(1): p. 91-97.
236. Jiao, X., et al., *Recent Advances Targeting CCR5 for Cancer and Its Role in Immuno-Oncology.* Cancer Res, 2019. **79**(19): p. 4801-4807.
237. Kochenderfer, J.N., et al., *Eradication of B-lineage cells and regression of lymphoma in a patient treated with autologous T cells genetically engineered to recognize CD19.* Blood, 2010. **116**(20): p. 4099-102.
238. Weber, E.W., M.V. Maus, and C.L. Mackall, *The Emerging Landscape of Immune Cell Therapies.* Cell, 2020. **181**(1): p. 46-62.
239. Vivier, E., et al., *Innate Lymphoid Cells: 10 Years On.* Cell, 2018. **174**(5): p. 1054-1066.
240. Malmberg, K.J., et al., *Natural killer cell-mediated immunosurveillance of human cancer.* Semin Immunol, 2017. **31**: p. 20-29.
241. Melaiu, O., et al., *Influence of the Tumor Microenvironment on NK Cell Function in Solid Tumors.* Front Immunol, 2019. **10**: p. 3038.
242. Mylod, E., J. Lysaght, and M.J. Conroy, *Natural killer cell therapy: A new frontier for obesity-associated cancer.* Cancer Lett, 2022. **535**: p. 215620.
243. Nersesian, S., et al., *NK cell infiltration is associated with improved overall survival in solid cancers: A systematic review and meta-analysis.* Transl Oncol, 2021. **14**(1): p. 100930.
244. Wang, J. and S. Matosevic, *NT5E/CD73 as Correlative Factor of Patient Survival and Natural Killer Cell Infiltration in Glioblastoma.* J Clin Med, 2019. **8**(10).
245. Daher, M., et al., *CAR-NK cells: the next wave of cellular therapy for cancer.* Clin Transl Immunology, 2021. **10**(4): p. e1274.
246. Wang, D., et al., *A phase 1 study of a novel fully human BCMA-targeting CAR (CT103A) in patients with relapsed/refractory multiple myeloma.* Blood, 2021. **137**(21): p. 2890-2901.

247. Xu, J., et al., *Exploratory trial of a biepitopic CAR T-targeting B cell maturation antigen in relapsed/refractory multiple myeloma.* Proc Natl Acad Sci U S A, 2019. **116**(19): p. 9543-9551.
248. Zhao, W.H., et al., *A phase 1, open-label study of LCAR-B38M, a chimeric antigen receptor T cell therapy directed against B cell maturation antigen, in patients with relapsed or refractory multiple myeloma.* J Hematol Oncol, 2018. **11**(1): p. 141.
249. Zhang, Y., et al., *Phase I clinical trial of EGFR-specific CAR-T cells generated by the piggyBac transposon system in advanced relapsed/refractory non-small cell lung cancer patients.* J Cancer Res Clin Oncol, 2021. **147**(12): p. 3725-3734.
250. Wang, J., et al., *Chemokine Receptors CCR6 and PD1 Blocking scFv E27 Enhances Anti-EGFR CAR-T Therapeutic Efficacy in a Preclinical Model of Human Non-Small Cell Lung Carcinoma.* Int J Mol Sci, 2023. **24**(6).
251. Wu, X. and S. Matosevic, *Gene-edited and CAR-NK cells: Opportunities and challenges with engineering of NK cells for immunotherapy.* Mol Ther Oncolytics, 2022. **27**: p. 224-238.
252. Klingemann, H., L. Boissel, and F. Toneguzzo, *Natural Killer Cells for Immunotherapy - Advantages of the NK-92 Cell Line over Blood NK Cells.* Front Immunol, 2016. **7**: p. 91.
253. Tam, Y.K., et al., *Ex vivo expansion of the highly cytotoxic human natural killer-92 cell-line under current good manufacturing practice conditions for clinical adoptive cellular immunotherapy.* Cytotherapy, 2003. **5**(3): p. 259-72.
254. Gong, J.H., G. Maki, and H.G. Klingemann, *Characterization of a human cell line (NK-92) with phenotypical and functional characteristics of activated natural killer cells.* Leukemia, 1994. **8**(4): p. 652-8.
255. Suck, G., et al., *KHYG-1, a model for the study of enhanced natural killer cell cytotoxicity.* Exp Hematol, 2005. **33**(10): p. 1160-71.
256. Yagita, M., et al., *A novel natural killer cell line (KHYG-1) from a patient with aggressive natural killer cell leukemia carrying a p53 point mutation.* Leukemia, 2000. **14**(5): p. 922-30.
257. Klingemann, H.G., E. Wong, and G. Maki, *A cytotoxic NK-cell line (NK-92) for ex vivo purging of leukemia from blood.* Biol Blood Marrow Transplant, 1996. **2**(2): p. 68-75.
258. Rossi, F., et al., *Next Generation Natural Killer Cells for Cancer Immunotherapy.* Front Immunol, 2022. **13**: p. 886429.
259. Wu, X. and S. Huang, *HER2-specific chimeric antigen receptor-engineered natural killer cells combined with apatinib for the treatment of gastric cancer.* Bull Cancer, 2019. **106**(11): p. 946-958.
260. Stroes, C.I., et al., *Tumor immune microenvironmental characteristics in Human Epidermal Growth Factor-2 (HER2) positive esophageal adenocarcinoma: A comparative analysis and biomarker study.* Transl Oncol, 2024. **49**: p. 102079.
261. Xiao, L., et al., *Adoptive Transfer of NKG2D CAR mRNA-Engineered Natural Killer Cells in Colorectal Cancer Patients.* Mol Ther, 2019. **27**(6): p. 1114-1125.
262. Li, Y., et al., *Human iPSC-Derived Natural Killer Cells Engineered with Chimeric Antigen Receptors Enhance Anti-tumor Activity.* Cell Stem Cell, 2018. **23**(2): p. 181-192 e5.
263. Walczak, H., et al., *Tumoricidal activity of tumor necrosis factor-related apoptosis-inducing ligand in vivo.* Nat Med, 1999. **5**(2): p. 157-63.

264. Song, X., et al., *Secretory TRAIL-Armed Natural Killer Cell-Based Therapy: In Vitro and In Vivo Colorectal Peritoneal Carcinomatosis Xenograft.* Mol Cancer Ther, 2016. **15**(7): p. 1591-601.
265. Kim, M., et al., *Folate receptor 1 (FOLR1) targeted chimeric antigen receptor (CAR) T cells for the treatment of gastric cancer.* PLoS One, 2018. **13**(6): p. e0198347.
266. Kang, C.H., et al., *Development of Antigen-specific Chimeric Antigen Receptor KHYG-1 Cells for Glioblastoma.* Anticancer Res, 2021. **41**(4): p. 1811-1819.
267. Sheedy, A.M., et al., *NK cell line modified to express a potent, DR5 specific variant of TRAIL, show enhanced cytotoxicity in ovarian cancer models.* Heliyon, 2024. **10**(15): p. e34976.
268. Hsu, J., et al., *Contribution of NK cells to immunotherapy mediated by PD-1/PD-L1 blockade.* J Clin Invest, 2018. **128**(10): p. 4654-4668.
269. Arianfar, E., et al., *Suppression of CD56(bright) NK cells in breast cancer patients is associated with the PD-1 and TGF-betaRII expression.* Clin Transl Oncol, 2023. **25**(3): p. 841-851.
270. Nie, J., et al., *Addition of Low-Dose Decitabine to Anti-PD-1 Antibody Camrelizumab in Relapsed/Refractory Classical Hodgkin Lymphoma.* J Clin Oncol, 2019. **37**(17): p. 1479-1489.
271. Zhang, Q., et al., *Blockade of the checkpoint receptor TIGIT prevents NK cell exhaustion and elicits potent anti-tumor immunity.* Nat Immunol, 2018. **19**(7): p. 723-732.
272. Sun, C., et al., *High NKG2A expression contributes to NK cell exhaustion and predicts a poor prognosis of patients with liver cancer.* Oncoimmunology, 2017. **6**(1): p. e1264562.
273. Morinaga, T., et al., *Evaluation of HLA-E Expression Combined with Natural Killer Cell Status as a Prognostic Factor for Advanced Gastric Cancer.* Ann Surg Oncol, 2022. **29**(8): p. 4951-4960.
274. Hiraoka, N., et al., *Expression of classical human leukocyte antigen class I antigens, HLA-E and HLA-G, is adversely prognostic in pancreatic cancer patients.* Cancer Sci, 2020. **111**(8): p. 3057-3070.
275. Guo, Z.Y., et al., *Predictive value of HLA-G and HLA-E in the prognosis of colorectal cancer patients.* Cell Immunol, 2015. **293**(1): p. 10-6.
276. Gooden, M., et al., *HLA-E expression by gynecological cancers restrains tumor-infiltrating CD8(+) T lymphocytes.* Proc Natl Acad Sci U S A, 2011. **108**(26): p. 10656-61.
277. Bossard, C., et al., *HLA-E/beta2 microglobulin overexpression in colorectal cancer is associated with recruitment of inhibitory immune cells and tumor progression.* Int J Cancer, 2012. **131**(4): p. 855-63.
278. Tinker, A.V., et al., *Dose-Ranging and Cohort-Expansion Study of Monalizumab (IPH2201) in Patients with Advanced Gynecologic Malignancies: A Trial of the Canadian Cancer Trials Group (CCTG): IND221.* Clin Cancer Res, 2019. **25**(20): p. 6052-6060.
279. Andre, P., et al., *Anti-NKG2A mAb Is a Checkpoint Inhibitor that Promotes Anti-tumor Immunity by Unleashing Both T and NK Cells.* Cell, 2018. **175**(7): p. 1731-1743 e13.
280. Patel, S.P., et al., *Phase 1/2 study of monalizumab plus durvalumab in patients with advanced solid tumors.* J Immunother Cancer, 2024. **12**(2).

281. Yang, Y. and A. Lundqvist, *Immunomodulatory Effects of IL-2 and IL-15; Implications for Cancer Immunotherapy.* Cancers (Basel), 2020. **12**(12).
282. Sharma, R. and A. Das, *IL-2 mediates NK cell proliferation but not hyperactivity.* Immunol Res, 2018. **66**(1): p. 151-157.
283. Waldmann, T.A., *The biology of interleukin-2 and interleukin-15: implications for cancer therapy and vaccine design.* Nat Rev Immunol, 2006. **6**(8): p. 595-601.
284. Vial, T. and J. Descotes, *Clinical toxicity of interleukin-2.* Drug Saf, 1992. **7**(6): p. 417-33.
285. Simon, A.D., et al., *Elevated plasma levels of interleukin-2 and soluble IL-2 receptor in ischemic heart disease.* Clin Cardiol, 2001. **24**(3): p. 253-6.
286. Yshii, L., et al., *Astrocyte-targeted gene delivery of interleukin 2 specifically increases brain-resident regulatory T cell numbers and protects against pathological neuroinflammation.* Nat Immunol, 2022. **23**(6): p. 878-891.
287. Buchbinder, E.I., et al., *Therapy with high-dose Interleukin-2 (HD IL-2) in metastatic melanoma and renal cell carcinoma following PD1 or PDL1 inhibition.* J Immunother Cancer, 2019. **7**(1): p. 49.
288. Tam, Y.K., et al., *Characterization of genetically altered, interleukin 2-independent natural killer cell lines suitable for adoptive cellular immunotherapy.* Hum Gene Ther, 1999. **10**(8): p. 1359-73.
289. Delehedde, C., et al., *Enhancing natural killer cells proliferation and cytotoxicity using imidazole-based lipid nanoparticles encapsulating interleukin-2 mRNA.* Mol Ther Nucleic Acids, 2024. **35**(3): p. 102263.
290. Miller, J.S., et al., *A First-in-Human Phase I Study of Subcutaneous Outpatient Recombinant Human IL15 (rhIL15) in Adults with Advanced Solid Tumors.* Clin Cancer Res, 2018. **24**(7): p. 1525-1535.
291. Gang, M., et al., *CAR-modified memory-like NK cells exhibit potent responses to NK-resistant lymphomas.* Blood, 2020. **136**(20): p. 2308-2318.
292. Cortez, V.S., et al., *SMAD4 impedes the conversion of NK cells into ILC1-like cells by curtailing non-canonical TGF-beta signaling.* Nat Immunol, 2017. **18**(9): p. 995-1003.
293. Kremer, V., et al., *Correction to: Genetic engineering of human NK cells to express CXCR2 improves migration to renal cell carcinoma.* J Immunother Cancer, 2017. **5**(1): p. 88.
294. Levy, E., et al., *Enhanced Bone Marrow Homing of Natural Killer Cells Following mRNA Transfection With Gain-of-Function Variant CXCR4(R334X).* Front Immunol, 2019. **10**: p. 1262.
295. Carlsten, M., et al., *Efficient mRNA-Based Genetic Engineering of Human NK Cells with High-Affinity CD16 and CCR7 Augments Rituximab-Induced ADCC against Lymphoma and Targets NK Cell Migration toward the Lymph Node-Associated Chemokine CCL19.* Front Immunol, 2016. **7**: p. 105.
296. Wennerberg, E., et al., *CXCL10-induced migration of adoptively transferred human natural killer cells toward solid tumors causes regression of tumor growth in vivo.* Cancer Immunol Immunother, 2015. **64**(2): p. 225-35.
297. Ng, Y.Y., J.C.K. Tay, and S. Wang, *CXCR1 Expression to Improve Anti-Cancer Efficacy of Intravenously Injected CAR-NK Cells in Mice with Peritoneal Xenografts.* Mol Ther Oncolytics, 2020. **16**: p. 75-85.

298. Feigl, F.F., et al., *Efficient Redirection of NK Cells by Genetic Modification with Chemokine Receptors CCR4 and CCR2B.* Int J Mol Sci, 2023. **24**(4).
299. Kim, K.S., et al., *Cationic Nanoparticle-Mediated Activation of Natural Killer Cells for Effective Cancer Immunotherapy.* ACS Appl Mater Interfaces, 2020. **12**(51): p. 56731-56740.
300. Somanchi, S.S., et al., *Engineering lymph node homing of ex vivo-expanded human natural killer cells via trogocytosis of the chemokine receptor CCR7.* Blood, 2012. **119**(22): p. 5164-72.
301. Li, F., et al., *CCL5-armed oncolytic virus augments CCR5-engineered NK cell infiltration and antitumor efficiency.* J Immunother Cancer, 2020. **8**(1).
302. Lee, J., et al., *An Antibody Designed to Improve Adoptive NK-Cell Therapy Inhibits Pancreatic Cancer Progression in a Murine Model.* Cancer Immunol Res, 2019. **7**(2): p. 219-229.
303. Moon, E.K., et al., *Intra-tumoral delivery of CXCL11 via a vaccinia virus, but not by modified T cells, enhances the efficacy of adoptive T cell therapy and vaccines.* Oncoimmunology, 2018. **7**(3): p. e1395997.
304. Perez Del Rio, E., et al., *CCL21-loaded 3D hydrogels for T cell expansion and differentiation.* Biomaterials, 2020. **259**: p. 120313.
305. O'Hara, M.H., et al., *Safety and Pharmacokinetics of CXCR4 Peptide Antagonist, LY2510924, in Combination with Durvalumab in Advanced Refractory Solid Tumors.* J Pancreat Cancer, 2020. **6**(1): p. 21-31.
306. Qin, G., et al., *Metformin blocks myeloid-derived suppressor cell accumulation through AMPK-DACH1-CXCL1 axis.* Oncoimmunology, 2018. **7**(7): p. e1442167.
307. He, D. and S. Zhang, *UNBS5162 inhibits the proliferation of esophageal cancer squamous cells via the PI3K/AKT signaling pathway.* Mol Med Rep, 2018. **17**(1): p. 549-555.
308. Melenhorst, J.J., et al., *Author Correction: Decade-long leukaemia remissions with persistence of CD4(+) CAR T cells.* Nature, 2022. **612**(7941): p. E22.
309. Lynam-Lennon, N., et al., *Alterations in DNA repair efficiency are involved in the radioresistance of esophageal adenocarcinoma.* Radiat Res, 2010. **174**(6): p. 703-11.
310. Lynam-Lennon, N., et al., *MicroRNA-17 is downregulated in esophageal adenocarcinoma cancer stem-like cells and promotes a radioresistant phenotype.* Oncotarget, 2017. **8**(7): p. 11400-11413.
311. Liu, D.S., et al., *Novel metastatic models of esophageal adenocarcinoma derived from FLO-1 cells highlight the importance of E-cadherin in cancer metastasis.* Oncotarget, 2016. **7**(50): p. 83342-83358.
312. Siegel, R.L., et al., *Cancer statistics, 2023.* CA Cancer J Clin, 2023. **73**(1): p. 17-48.
313. Kelly, R.J., *Immunotherapy for Esophageal and Gastric Cancer.* Am Soc Clin Oncol Educ Book, 2017. **37**: p. 292-300.
314. Mundhara, N. and P. Sadhukhan, *Cracking the Codes behind Cancer Cells' Immune Evasion.* Int J Mol Sci, 2024. **25**(16).
315. Liu, Y., et al., *Drug resistance and tumor immune microenvironment: An overview of current understandings (Review).* Int J Oncol, 2024. **65**(4).
316. Li, Z., et al., *Tumor microenvironment as a complex milieu driving cancer progression: a mini review.* Clin Transl Oncol, 2024.

317. Bakshi, H.A., et al., *Cellular signaling in the hypoxic cancer microenvironment: Implications for drug resistance and therapeutic targeting.* Cell Signal, 2024. **113**: p. 110911.
318. King, R., et al., *Hypoxia and its impact on the tumour microenvironment of gastroesophageal cancers.* World J Gastrointest Oncol, 2021. **13**(5): p. 312-331.
319. Facciabene, A., et al., *Tumour hypoxia promotes tolerance and angiogenesis via CCL28 and T(reg) cells.* Nature, 2011. **475**(7355): p. 226-30.
320. Singer, K., et al., *Immunometabolism in cancer at a glance.* Dis Model Mech, 2018. **11**(8).
321. Erra Diaz, F., E. Dantas, and J. Geffner, *Unravelling the Interplay between Extracellular Acidosis and Immune Cells.* Mediators Inflamm, 2018. **2018**: p. 1218297.
322. Ashby, B.S., *pH studies in human malignant tumours.* Lancet, 1966. **2**(7458): p. 312-5.
323. Vaupel, P., F. Kallinowski, and P. Okunieff, *Blood flow, oxygen and nutrient supply, and metabolic microenvironment of human tumors: a review.* Cancer Res, 1989. **49**(23): p. 6449-65.
324. Ibrahim-Hashim, A. and V. Estrella, *Acidosis and cancer: from mechanism to neutralization.* Cancer Metastasis Rev, 2019. **38**(1-2): p. 149-155.
325. Aki, S., et al., *Cancer metabolism within tumor microenvironments.* Biochim Biophys Acta Gen Subj, 2023. **1867**(5): p. 130330.
326. Kato, M., et al., *Acidic extracellular pH drives accumulation of N1-acetylspermidine and recruitment of protumor neutrophils.* PNAS Nexus, 2023. **2**(10): p. pgad306.
327. Damgaci, S., et al., *Hypoxia and acidosis: immune suppressors and therapeutic targets.* Immunology, 2018. **154**(3): p. 354-362.
328. Xu, J., et al., *Advances in Research on the Effects and Mechanisms of Chemokines and Their Receptors in Cancer.* Front Pharmacol, 2022. **13**: p. 920779.
329. Guan, M., et al., *Chemokine systems in oncology: From microenvironment modulation to nanocarrier innovations.* Int J Biol Macromol, 2024. **268**(Pt 1): p. 131679.
330. Mollica Poeta, V., et al., *Chemokines and Chemokine Receptors: New Targets for Cancer Immunotherapy.* Front Immunol, 2019. **10**: p. 379.
331. Puschel, F., et al., *Starvation and antimetabolic therapy promote cytokine release and recruitment of immune cells.* Proc Natl Acad Sci U S A, 2020. **117**(18): p. 9932-9941.
332. Ahmadiankia, N., M. Bagheri, and M. Fazli, *Nutrient Deprivation Modulates the Metastatic Potential of Breast Cancer Cells.* Rep Biochem Mol Biol, 2019. **8**(2): p. 139-146.
333. Worsley, C.M., R.B. Veale, and E.S. Mayne, *The effect of acute acid exposure on immunomodulatory protein secretion, cell survival, and cell cycle progression in tumour cell lines.* Cytokine, 2023. **162**: p. 156118.
334. Wu, Q., et al., *Hypoxia-inducible factors: master regulators of hypoxic tumor immune escape.* J Hematol Oncol, 2022. **15**(1): p. 77.
335. Li, R.U., K. Tang, and Q. Li, *Pan-cancer Bioinformatics Analysis of the Double-edged Role of Hypoxia-inducible Factor 1alpha (HIF-1alpha) in Human Cancer.* Cancer Diagn Progn, 2022. **2**(2): p. 263-278.

336. Wu, X., et al., *CXCR4 promotes the growth and metastasis of esophageal squamous cell carcinoma as a critical downstream mediator of HIF-1alpha.* Cancer Sci, 2022. **113**(3): p. 926-939.
337. Roy, I., et al., *Pancreatic Cancer Cell Migration and Metastasis Is Regulated by Chemokine-Biased Agonism and Bioenergetic Signaling.* Cancer Res, 2015. **75**(17): p. 3529-42.
338. Qian, B.Z., et al., *CCL2 recruits inflammatory monocytes to facilitate breast-tumour metastasis.* Nature, 2011. **475**(7355): p. 222-5.
339. Pradelli, E., et al., *Antagonism of chemokine receptor CXCR3 inhibits osteosarcoma metastasis to lungs.* Int J Cancer, 2009. **125**(11): p. 2586-94.
340. Mishra, A., et al., *An updated review on the role of the CXCL8-CXCR1/2 axis in the progression and metastasis of breast cancer.* Mol Biol Rep, 2021. **48**(9): p. 6551-6561.
341. Li, J.Y., et al., *The chemokine receptor CCR4 promotes tumor growth and lung metastasis in breast cancer.* Breast Cancer Res Treat, 2012. **131**(3): p. 837-48.
342. Mylod, E., *Harnessing natural killer cell-mediated immune responses in obesity-associated cancer*, in *Surgery*. 2023, Trinity College Dublin: TARA.
343. Veldkamp, C.T., et al., *Structural basis of CXCR4 sulfotyrosine recognition by the chemokine SDF-1/CXCL12.* Sci Signal, 2008. **1**(37): p. ra4.
344. Smith, J.M., et al., *CXCL12 activation of CXCR4 regulates mucosal host defense through stimulation of epithelial cell migration and promotion of intestinal barrier integrity.* Am J Physiol Gastrointest Liver Physiol, 2005. **288**(2): p. G316-26.
345. Gerlach, C., et al., *The Chemokine Receptor CX3CR1 Defines Three Antigen-Experienced CD8 T Cell Subsets with Distinct Roles in Immune Surveillance and Homeostasis.* Immunity, 2016. **45**(6): p. 1270-1284.
346. Chandrasekar, B., et al., *Fractalkine (CX3CL1) stimulated by nuclear factor kappaB (NF-kappaB)-dependent inflammatory signals induces aortic smooth muscle cell proliferation through an autocrine pathway.* Biochem J, 2003. **373**(Pt 2): p. 547-58.
347. Bertini, R., et al., *Noncompetitive allosteric inhibitors of the inflammatory chemokine receptors CXCR1 and CXCR2: prevention of reperfusion injury.* Proc Natl Acad Sci U S A, 2004. **101**(32): p. 11791-6.
348. Jorgensen, A.S., et al., *Biased action of the CXCR4-targeting drug plerixafor is essential for its superior hematopoietic stem cell mobilization.* Commun Biol, 2021. **4**(1): p. 569.
349. Uva, P., et al., *Comparative Membranome expression analysis in primary tumors and derived cell lines.* PLoS One, 2010. **5**(7): p. e11742.
350. Zheng, X., et al., *Inhibition of ADAM17 reduces hypoxia-induced brain tumor cell invasiveness.* Cancer Sci, 2007. **98**(5): p. 674-84.
351. Wang, X.J., C.W. Feng, and M. Li, *ADAM17 mediates hypoxia-induced drug resistance in hepatocellular carcinoma cells through activation of EGFR/PI3K/Akt pathway.* Mol Cell Biochem, 2013. **380**(1-2): p. 57-66.
352. Szalad, A., et al., *Transcription factor Sp1 induces ADAM17 and contributes to tumor cell invasiveness under hypoxia.* J Exp Clin Cancer Res, 2009. **28**(1): p. 129.
353. Barsoum, I.B., et al., *Hypoxia induces escape from innate immunity in cancer cells via increased expression of ADAM10: role of nitric oxide.* Cancer Res, 2011. **71**(24): p. 7433-41.

354. Verstegen, M.H., et al., *Metastatic pattern in esophageal and gastric cancer: Influenced by site and histology.* World J Gastroenterol, 2020. **26**(39): p. 6037-6046.
355. Wu, S.G., et al., *Patterns of Distant Metastasis Between Histological Types in Esophageal Cancer.* Front Oncol, 2018. **8**: p. 302.
356. Liu, W., et al., *CX3CL1: a potential chemokine widely involved in the process spinal metastases.* Oncotarget, 2017. **8**(9): p. 15213-15219.
357. Tomizawa, Y., T.T. Wu, and K.K. Wang, *Epithelial mesenchymal transition and cancer stem cells in esophageal adenocarcinoma originating from Barrett's esophagus.* Oncol Lett, 2012. **3**(5): p. 1059-1063.
358. Jethwa, P., et al., *Overexpression of Slug is associated with malignant progression of esophageal adenocarcinoma.* World J Gastroenterol, 2008. **14**(7): p. 1044-52.
359. Yang, J., et al., *Author Correction: Guidelines and definitions for research on epithelial-mesenchymal transition.* Nat Rev Mol Cell Biol, 2021. **22**(12): p. 834.
360. Brungs, D., et al., *Expression of cancer stem cell markers is prognostic in metastatic gastroesophageal adenocarcinoma.* Pathology, 2019. **51**(5): p. 474-480.
361. DiNatale, A., et al., *Subsets of cancer cells expressing CX3CR1 are endowed with metastasis-initiating properties and resistance to chemotherapy.* Oncogene, 2022. **41**(9): p. 1337-1351.
362. Jamieson, W.L., et al., *CX3CR1 is expressed by prostate epithelial cells and androgens regulate the levels of CX3CL1/fractalkine in the bone marrow: potential role in prostate cancer bone tropism.* Cancer Res, 2008. **68**(6): p. 1715-22.
363. Pandur, E., et al., *Modulatory Effects of Fractalkine on Inflammatory Response and Iron Metabolism of Lipopolysaccharide and Lipoteichoic Acid-Activated THP-1 Macrophages.* Int J Mol Sci, 2022. **23**(5).
364. Evan, G.I. and K.H. Vousden, *Proliferation, cell cycle and apoptosis in cancer.* Nature, 2001. **411**(6835): p. 342-8.
365. Feitelson, M.A., et al., *Sustained proliferation in cancer: Mechanisms and novel therapeutic targets.* Semin Cancer Biol, 2015. **35 Suppl**(Suppl): p. S25-S54.
366. Chen, S., et al., *Impact of Detachment Methods on M2 Macrophage Phenotype and Function.* J Immunol Methods, 2015. **426**: p. 56-61.
367. Quan, Y., et al., *Impact of cell dissociation on identification of breast cancer stem cells.* Cancer Biomark, 2012. **12**(3): p. 125-33.
368. Jager, L.D., et al., *Effect of enzymatic and mechanical methods of dissociation on neural progenitor cells derived from induced pluripotent stem cells.* Adv Med Sci, 2016. **61**(1): p. 78-84.
369. Keysar, S.B. and A. Jimeno, *More than markers: biological significance of cancer stem cell-defining molecules.* Mol Cancer Ther, 2010. **9**(9): p. 2450-7.
370. Kapoor, S., S.P. Shenoy, and B. Bose, *CD34 cells in somatic, regenerative and cancer stem cells: Developmental biology, cell therapy, and omics big data perspective.* J Cell Biochem, 2020. **121**(5-6): p. 3058-3069.
371. Lyons, V.J., A. Helms, and D. Pappas, *The effect of protein expression on cancer cell capture using the Human Transferrin Receptor (CD71) as an affinity ligand.* Anal Chim Acta, 2019. **1076**: p. 154-161.

372. Park, E., et al., *The role of CD98 heavy chain in cancer development.* Histol Histopathol, 2024. **39**(12): p. 1557-1564.
373. Berger, A.C., et al., *Complete response to neoadjuvant chemoradiotherapy in esophageal carcinoma is associated with significantly improved survival.* J Clin Oncol, 2005. **23**(19): p. 4330-7.
374. Wu, X., et al., *Upregulation of extracellular matrix metalloproteinase inducer promotes hypoxia-induced epithelial-mesenchymal transition in esophageal cancer.* Mol Med Rep, 2015. **12**(5): p. 7419-24.
375. Tardaguila, M., et al., *CX3CL1 promotes breast cancer via transactivation of the EGF pathway.* Cancer Res, 2013. **73**(14): p. 4461-73.
376. Chaudhri, A., et al., *The CX3CL1-CX3CR1 chemokine axis can contribute to tumor immune evasion and blockade with a novel CX3CR1 monoclonal antibody enhances response to anti-PD-1 immunotherapy.* Front Immunol, 2023. **14**: p. 1237715.
377. Sano, A., et al., *CD24 expression is a novel prognostic factor in esophageal squamous cell carcinoma.* Ann Surg Oncol, 2009. **16**(2): p. 506-14.
378. Kristiansen, G., et al., *CD24 expression is a new prognostic marker in breast cancer.* Clin Cancer Res, 2003. **9**(13): p. 4906-13.
379. Kristiansen, G., et al., *CD24 is an independent prognostic marker of survival in nonsmall cell lung cancer patients.* Br J Cancer, 2003. **88**(2): p. 231-6.
380. Kristiansen, G., et al., *CD24 expression is a significant predictor of PSA relapse and poor prognosis in low grade or organ confined prostate cancer.* Prostate, 2004. **58**(2): p. 183-92.
381. Kristiansen, G., et al., *CD24 is expressed in ovarian cancer and is a new independent prognostic marker of patient survival.* Am J Pathol, 2002. **161**(4): p. 1215-21.
382. Kraus, S., et al., *Predictive Levels of CD24 in Peripheral Blood Leukocytes for the Early Detection of Colorectal Adenomas and Adenocarcinomas.* Dis Markers, 2015. **2015**: p. 916098.
383. Chou, Y.Y., et al., *Cytoplasmic CD24 expression is a novel prognostic factor in diffuse-type gastric adenocarcinoma.* Ann Surg Oncol, 2007. **14**(10): p. 2748-58.
384. Wu, J.X., et al., *Clinicopathological and prognostic significance of CD24 overexpression in patients with gastric cancer: a meta-analysis.* PLoS One, 2014. **9**(12): p. e114746.
385. Jiao, X.L., et al., *Downregulation of CD24 inhibits invasive growth, facilitates apoptosis and enhances chemosensitivity in gastric cancer AGS cells.* Eur Rev Med Pharmacol Sci, 2013. **17**(13): p. 1709-15.
386. Fujikuni, N., et al., *Hypoxia-mediated CD24 expression is correlated with gastric cancer aggressiveness by promoting cell migration and invasion.* Cancer Sci, 2014. **105**(11): p. 1411-20.
387. Jimenez, P., et al., *CD24 Expression Is Increased in 5-Fluorouracil-Treated Esophageal Adenocarcinoma Cells.* Front Pharmacol, 2017. **8**: p. 321.
388. Trevellin, E., et al., *Prognostic value of stem cell markers in esophageal and esophagogastric junction cancer: a meta-analysis.* J Cancer, 2020. **11**(14): p. 4240-4249.

389. Carraro, A., et al., *Esophageal adenocarcinoma microenvironment: Peritumoral adipose tissue effects associated with chemoresistance.* Cancer Sci, 2017. **108**(12): p. 2393-2404.
390. Lauby-Secretan, B., et al., *Body Fatness and Cancer--Viewpoint of the IARC Working Group.* N Engl J Med, 2016. **375**(8): p. 794-8.
391. Mandard, A.M., et al., *Pathologic assessment of tumor regression after preoperative chemoradiotherapy of esophageal carcinoma. Clinicopathologic correlations.* Cancer, 1994. **73**(11): p. 2680-6.
392. Dworak, O., L. Keilholz, and A. Hoffmann, *Pathological features of rectal cancer after preoperative radiochemotherapy.* Int J Colorectal Dis, 1997. **12**(1): p. 19-23.
393. Chen, Y.M., et al., *Tumor necrosis factor-alpha stimulates fractalkine production by mesangial cells and regulates monocyte transmigration: down-regulation by cAMP.* Kidney Int, 2003. **63**(2): p. 474-86.
394. Ahn, S.Y., et al., *Tumor necrosis factor-alpha induces fractalkine expression preferentially in arterial endothelial cells and mithramycin A suppresses TNF-alpha-induced fractalkine expression.* Am J Pathol, 2004. **164**(5): p. 1663-72.
395. Melo, A.M., et al., *Mucosal-Associated Invariant T Cells Display Diminished Effector Capacity in Oesophageal Adenocarcinoma.* Front Immunol, 2019. **10**: p. 1580.
396. Andre, N.D., et al., *Measurement of cytotoxic activity in experimental cancer.* J Clin Lab Anal, 2004. **18**(1): p. 27-30.
397. Rossin, A., G. Miloro, and A.O. Hueber, *TRAIL and FasL Functions in Cancer and Autoimmune Diseases: Towards an Increasing Complexity.* Cancers (Basel), 2019. **11**(5).
398. Bennett, M.W., et al., *The Fas counterattack in vivo: apoptotic depletion of tumor-infiltrating lymphocytes associated with Fas ligand expression by human esophageal carcinoma.* J Immunol, 1998. **160**(11): p. 5669-75.
399. Lee, S.H., et al., *Expression of FasL by tumor cells does not abrogate anti-tumor CTL function.* Immunol Lett, 2004. **91**(2-3): p. 119-26.
400. Balkwill, F., *Tumour necrosis factor and cancer.* Nat Rev Cancer, 2009. **9**(5): p. 361-71.
401. Becknell, B. and M.A. Caligiuri, *Interleukin-2, interleukin-15, and their roles in human natural killer cells.* Adv Immunol, 2005. **86**: p. 209-39.
402. Zhang, S., et al., *Prognostic Significance of Tumor-Infiltrating Natural Killer Cells in Solid Tumors: A Systematic Review and Meta-Analysis.* Front Immunol, 2020. **11**: p. 1242.
403. Xu, B., et al., *Prognostic value of tumor infiltrating NK cells and macrophages in stage II+III esophageal cancer patients.* Oncotarget, 2016. **7**(46): p. 74904-74916.
404. Imai, K., et al., *Natural cytotoxic activity of peripheral-blood lymphocytes and cancer incidence: an 11-year follow-up study of a general population.* Lancet, 2000. **356**(9244): p. 1795-9.
405. Ishigami, S., et al., *Prognostic value of intratumoral natural killer cells in gastric carcinoma.* Cancer, 2000. **88**(3): p. 577-83.
406. Klingemann, H., *Are natural killer cells superior CAR drivers?* Oncoimmunology, 2014. **3**: p. e28147.

407. Li, Y., K. Rezvani, and H. Rafei, *Next-generation chimeric antigen receptors for T- and natural killer-cell therapies against cancer.* Immunol Rev, 2023. **320**(1): p. 217-235.
408. Sarkar, S., et al., *The CD38(low) natural killer cell line KHYG1 transiently expressing CD16(F158V) in combination with daratumumab targets multiple myeloma cells with minimal effector NK cell fratricide.* Cancer Immunol Immunother, 2020. **69**(3): p. 421-434.
409. O'Donovan, C., et al., *Chemokine-targeted therapies: An opportunity to remodel immune profiles in gastro-oesophageal tumours.* Cancer Lett, 2021. **521**: p. 224-236.
410. Zhang, C., et al., *Chimeric Antigen Receptor-Engineered NK-92 Cells: An Off-the-Shelf Cellular Therapeutic for Targeted Elimination of Cancer Cells and Induction of Protective Antitumor Immunity.* Front Immunol, 2017. **8**: p. 533.
411. Nagler, A., et al., *Comparative studies of human FcRIII-positive and negative natural killer cells.* J Immunol, 1989. **143**(10): p. 3183-91.
412. Cooper, M.A., T.A. Fehniger, and M.A. Caligiuri, *The biology of human natural killer-cell subsets.* Trends Immunol, 2001. **22**(11): p. 633-40.
413. Seki, T., et al., *NK Cells Can Preferentially Target Prostate Cancer Stem-like Cells via the TRAIL/DR5 Signaling Pathway.* Biomolecules, 2021. **11**(11).
414. Keir, M.E., et al., *PD-1 and its ligands in tolerance and immunity.* Annu Rev Immunol, 2008. **26**: p. 677-704.
415. Fassan, M., et al., *PD-L1 expression in gastroesophageal dysplastic lesions.* Virchows Arch, 2020. **477**(1): p. 151-156.
416. Rodriguez-Garcia, G.J., et al., *Cancer Cell Small Molecule Secretome Induces the Immune Checkpoint NKG2A and Dysfunction of Human CD8+ T Cells.* Immunohorizons, 2024. **8**(6): p. 464-477.
417. Fisher, J.G., L.V. Graham, and M.D. Blunt, *Strategies to disrupt NKG2A:HLA-E interactions for improved anti-cancer immunity.* Oncotarget, 2024. **15**: p. 501-503.
418. Murakami, T., et al., *Novel Human NK Cell Line Carrying CAR Targeting EGFRvIII Induces Antitumor Effects in Glioblastoma Cells.* Anticancer Res, 2018. **38**(9): p. 5049-5056.
419. Berahovich, R.D., et al., *Evidence for NK cell subsets based on chemokine receptor expression.* J Immunol, 2006. **177**(11): p. 7833-40.
420. Nayyar, G., Y. Chu, and M.S. Cairo, *Overcoming Resistance to Natural Killer Cell Based Immunotherapies for Solid Tumors.* Front Oncol, 2019. **9**: p. 51.
421. Chiossone, L., et al., *Natural killer cells and other innate lymphoid cells in cancer.* Nat Rev Immunol, 2018. **18**(11): p. 671-688.
422. Andrea, A.E., et al., *Advances in CAR-T Cell Genetic Engineering Strategies to Overcome Hurdles in Solid Tumors Treatment.* Front Immunol, 2022. **13**: p. 830292.
423. Tong, L., et al., *NK cells and solid tumors: therapeutic potential and persisting obstacles.* Mol Cancer, 2022. **21**(1): p. 206.
424. Su, J., et al., *Lactate/GPR81 recruits regulatory T cells by modulating CX3CL1 to promote immune resistance in a highly glycolytic gastric cancer.* Oncoimmunology, 2024. **13**(1): p. 2320951.

425. Swanton, C., et al., *Embracing cancer complexity: Hallmarks of systemic disease.* Cell, 2024. **187**(7): p. 1589-1616.
426. Hanahan, D. and R.A. Weinberg, *The hallmarks of cancer.* Cell, 2000. **100**(1): p. 57-70.
427. Hanahan, D., *Hallmarks of Cancer: New Dimensions.* Cancer Discov, 2022. **12**(1): p. 31-46.
428. Qian, C., et al., *Impeding Circulating Tumor Cell Reseeding Decelerates Metastatic Progression and Potentiates Chemotherapy.* Mol Cancer Res, 2018. **16**(12): p. 1844-1854.
429. Goode-Romero, G. and L. Dominguez, *Computational study of the conformational ensemble of CX3C chemokine receptor 1 (CX3CR1) and its interactions with antagonist and agonist ligands.* J Mol Graph Model, 2022. **117**: p. 108278.
430. Lee, S.J., et al., *Fractalkine stimulates angiogenesis by activating the Raf-1/MEK/ERK- and PI3K/Akt/eNOS-dependent signal pathways.* Am J Physiol Heart Circ Physiol, 2006. **291**(6): p. H2836-46.
431. Maciejewski-Lenoir, D., et al., *Characterization of fractalkine in rat brain cells: migratory and activation signals for CX3CR-1-expressing microglia.* J Immunol, 1999. **163**(3): p. 1628-35.
432. Korbecki, J., et al., *Fractalkine/CX3CL1 in Neoplastic Processes.* Int J Mol Sci, 2020. **21**(10).
433. Bonanni, V., et al., *Targeting of CXCR3 improves anti-myeloma efficacy of adoptively transferred activated natural killer cells.* J Immunother Cancer, 2019. **7**(1): p. 290.
434. Chusyd, D.E., et al., *Relationships between Rodent White Adipose Fat Pads and Human White Adipose Fat Depots.* Front Nutr, 2016. **3**: p. 10.
435. Chen, J., et al., *The development and improvement of immunodeficient mice and humanized immune system mouse models.* Front Immunol, 2022. **13**: p. 1007579.
436. Fahimi, F., et al., *Human CXCR1 knock-in mice infer functional expression of a murine ortholog.* J Leukoc Biol, 2023. **114**(4): p. 373-380.
437. Munch, N.S., et al., *High-Fat Diet Accelerates Carcinogenesis in a Mouse Model of Barrett's Esophagus via Interleukin 8 and Alterations to the Gut Microbiome.* Gastroenterology, 2019. **157**(2): p. 492-506 e2.
438. Bhat, N., et al., *Esophageal adenocarcinoma models: a closer look.* Front Mol Biosci, 2024. **11**: p. 1440670.
439. Liang, F., et al., *Patient-derived tumor models: a suitable tool for preclinical studies on esophageal cancer.* Cancer Gene Ther, 2023. **30**(11): p. 1443-1455.
440. Milne, J.V., E.H. Mustafa, and N.J. Clemons, *Modelling esophageal adenocarcinoma and Barrett's esophagus with patient-derived organoids.* Front Mol Biosci, 2024. **11**: p. 1382070.
441. Ingber, D.E., *Human organs-on-chips for disease modelling, drug development and personalized medicine.* Nat Rev Genet, 2022. **23**(8): p. 467-491.
442. Terren, I., et al., *Cytokine-Induced Memory-Like NK Cells: From the Basics to Clinical Applications.* Front Immunol, 2022. **13**: p. 884648.
443. Arellano-Ballestero, H., et al., *Proteomic and phenotypic characteristics of memory-like natural killer cells for cancer immunotherapy.* J Immunother Cancer, 2024. **12**(7).